Performance Evaluation of Rubberized Geopolymer Concrete and Fly Ash Based Geopolymer Mortar

BY

Salmabanu Luhar

2013RCE9511

DEPARTMENT OF CIVIL ENGINEERING,

MALAVIYA NATIONAL INSTITUTE OF TECHNOLOGY

JAIPUR-302017

DECEMBER 2017

Performance Evaluation of Rubberized Geopolymer Concrete and Fly Ash Based Geopolymer Mortar

Submitted in partial fulfillment of the requirements

For the degree of

Doctor of Philosophy in Civil Engineering

Structural Engineering

By

Salmabanu Luhar

2013RCE9511

DEPARTMENT OF CIVIL ENGINEERING,

MALAVIYA NATIONAL INSTITUTE OF TECHNOLOGY

JAIPUR-302017

DECEMBER 2017

Dedicated to My Family Especially to Janab Ismailbhai Luhar (My beloved Father) and My Teachers

DECLARATION

This is to certify that

a. The thesis entitled **"Performance Evaluation of Rubberized Geopolymer Concrete and Fly Ash Based Geopolymer Mortar"** comprises my original work towards the Degree of **Doctor of Philosophy** in Civil Engineering (Structural Engineering) at Malaviya National Institute of Technology and has not been submitted elsewhere for a degree.

b. Due acknowledgement has been made in the text to all other material used.

Salmabanu Luhar
2013RCE9511

CERTIFICATE OF SUPERVISOR

This is to certify that the thesis entitled **"Performance Evaluation of Rubberized Geopolymer Concrete and Fly Ash Based Geopolymer Mortar"** submitted by **Ms. Salmabanu Luhar** (2013RCE9511) towards the partial fulfilment of the requirement for the Degree of **Doctor of Philosophy** in Civil Engineering (Structural Engineering) at Malaviya National Institute of Technology, Jaipur, is the record of work carried out by her under my supervision and guidance. In my opinion, the submitted work has reached the level required for being accepted for examination. The results embodied in this thesis, to the best of my knowledge, have not been submitted to any other university or institution for the award of any degree or diploma.

Signature of Supervisor
Dr. Sandeep Chaudhary
Associate Professor,
Department of Civil Engineering,
Malaviya National Institute of Technology, Jaipur.

Abstract

The construction and infrastructure industries are currently experiencing strong growth. Consequently, the demand for concrete as an essential construction material has also amplified significantly. An exponential usage of concrete around the globe is second only to water. Ordinary Portland Cement is a predominant ingredient of conventional concrete which is in huge demand at present. The present production process of OPC is not only highly energy intensive next to steel and aluminium but also associated with an emission of deleterious gases like Carbon Dioxide, Nitrogen Oxide, and Sulphur Trioxide into the atmosphere contributing to global climate change and acid rains. This scenario has inspired researchers to develop sustainable, user and eco-friendly alternative binder to OPC that offer excellent strength, durability and fire resistance properties. Nowadays, Geopolymer is a novel inorganic binding material produced by a geopolymerization reaction which is drawing the attention of construction industry.

The huge volumes of fly ash (as a residue by product from mainly thermal power stations) and waste rubber tyres across the globe have generated a gigantic dilemma of their safe disposal. Both of them are not effectively used so far, and a large part of them is disposed of in landfills. The highly complex chemical structure of waste rubber tyres makes recycling a challenging task, and their disposal in the vicinity of populated areas creates health and environmental hazards. On the other hand, accessibility of fine aggregate i.e. river sand is also becoming a hindrance in rapid construction activities. Recently, many countries have imposed curbs on the utilization of river sand as fine aggregate due to environmental concerns. The problem of lack of fine aggregate is coupled with carbon dioxide emissions in the production of cement used for concrete.

This research work establishes the viability of using waste rubber tyre fibers as partial replacement of river sand in geopolymer concrete with 90% less CO_2 emission than OPC for addressing the above-stated problems. To date, to the best of the knowledge

of the author, there is no comprehensive study available on the strength, durability, elevated temperature behaviour and microstructure behaviour of rubberised Geopolymer concrete and fly ash based geopolymer mortar.

This research work investigates the compressive strength, split tensile strength, flexural strength, modulus of elasticity, pull off strength of rubberized Geopolymer Concrete for strength characterisation. Water permeability, carbonation, drying shrinkage, sulfate resistance, acid resistance, salt attack resistance, abrasion resistant, water sorptivity, chloride ion migration properties and corrosion resistance have been evaluated for durability characterization of rubberized Geopolymer Concrete.

The fire resistance of fly ash-based geopolymer concrete is established, and rubberized geopolymers are exposed to elevated temperatures to investigate the thermal effects on density, visual surface appearance, compressive strength, and microstructural characteristics.

Carbonation and strength studies related to geopolymer mortar are conducted using advanced analytical techniques such as X-ray diffractometry and scanning electron microscopy. The influence of the aggregate-to-binder ratio and curing temperature on the carbonation of the mortar is investigated.

Preliminary studies have been carried out for the feasibility of replacing fly ash by rice husk ash in geopolymer mortar along with using seawater and sea sand instead of normal water and fine aggregate. The effect of sea water and sea sand has also been investigated on the behaviour of fly ash based geopolymer concrete.

The results reported in this research indicate that, compared with conventional OPC concrete, the rubberized and control geopolymer concretes have excellent strength, water permeability, sulfate resistance, salt resistance, corrosion, sorptivity, chloride diffusion, carbonation resistance, and shrinkage properties. Geopolymer concrete also exhibit better resistance against surface cracking when exposed to elevated tempera-

tures.

Concisely, the results of the present research study are expected to bring the engineering community more closely towards sustainable construction by addressing three fold problem such as safe disposal of fly ash and waste rubber tyres, lack of river sand as fine aggregate for concrete and carbon dioxide emissions due to conventional cement production.

The results of the research study can be helpful not only in sustainable construction but also in value added utilization of three profuse wastes such as, (i) Waste rubber tyres, (ii) Fly ash and; (iii) Rice husk ash.

Ultimately, it can be concluded that the rubberized and control geopolymer concretes offer definite, tangible advantages over OPC concrete in terms of strength and durability properties.

Acknowledgement

I am eternally grateful to **Almightly**, the Mostgracious Merciful and Most Compassionate, for giving me the strength, wisdom, perseverance, and enthusiasm to complete this venture.

First and foremost, I would like to express my sincere gratitude to my supervisor **Dr. Sandeep Chaudhary**, Department of the Civil Engineering and in-charge of the Concrete Technology Laboratory; for the continuous support of my research, for his patience, motivation, enthusiasm and immense knowledge. His guidance helped me in all the time of research and writing of this thesis.

Besides my supervisor, I would like to thank the Head of Civil engineering Department, **Dr. Gunwant Sharma**, **Prof. Udaykumar R Yaragatti**, Director and rest of **DPGC committee** for providing all kind of required support during my research.

I express my sincere thanks to my DREC committee members, **Dr. Ravindra Nagar, Dr. Rajesh Gupta and Dr. Sandeep Shrivastava** for his critical evaluation and creative suggestions.

I gratefully acknowledge the financial support for this research by the **Department of Science and Technology**, New Delhi, under the Women Scientist scheme-A (sanction number SR/WOS-A/ET-1016/ 2015). I also very thankful to **Material Research Centre and Concrete Technology Laboratory** at Malaviya National Institute of Technology, Jaipur for extending experimental facilities support for this study.

I owe special thanks to my respective teachers **Dr. Paresh Patel, Dr. Urmil Dave** and **Dr. S. P. Purohit**, Department of Civil Engineering, Institute of Technology, Nirma University, Ahmedabad, who changed my whole aspect on my learning, I wouldn't be where I am today without them. Their continual kind words of encour-

agement and motivation very useful throughout my carreer.

I would like to take this opportunity to say warm thanks to **Dr. Trilok Gupta, Dr. Kashyap Patel, Dr. Blessen Skariah Thomas, Mrs. Priya, Mr. Sudarshan Kore, Mr. K I Syed Ahmed Kabeer** and **Ms. Kanika Tomar** for their advices and help in carrying out the experiments and thesis work.

I would like to thank **Mr. Sita Ram Jat**, Laboratory Assistant, Concrete technology laboratory, MNIT, for his assistance during testing. I also thankful to **Mr. Pukharaj** and **Mr. Sapan Gaur**, helpers, Concrete technology laboratory, MNIT, for their help during casting.

I also would like to express my wholehearted thanks to my beloved **Late Grandparents**, especially to **My Late Grandfather, Janab Gafurbhai Maulabax Luhar**, without whose foresight towards the knowledge our family would not had reached the ocean of education. I feel extremely thankful to **My Family**, especially to **My parents**, for their support they provided me throughout my entire life. Because of their unconditional love and prayers, I have the chance to complete this research.

This acknowledgement will remain unfinished without mentioning a name of my beloved father **Mr.Ismailbhai Luhar**. He is a person who achieved an ostentatious success in the field of knowledge and passed on the same to all decendents and fulfilled the dream of my paternal grandparents ! Words are powerless to express my gratitude towards him. I can only say, I love you “PAPA” from bottom of my heart so please accept my vehment Protestations of gratitude. Your generosity overwhelm me and your thoughtfulness put me on cloud nine !

Last but not the least, I sincerely thank all who, directly or indirectly, have lent their helping hand in this venture.

- Ms. Salmabanu Luhar

Abbreviation, Notation, and Nomenclature

GPC	Geopolymer Concrete
FA	Fly Ash
RHA	Rice Husk Ash
OPC	Ordinary Portland Cement
CO_2	Carbon Dioxide
NaOH	Sodium Hydroxide
Na_2SiO_3	Sodium Silicate
Na_2SO_4	Sodium Sulfate
H_2SO_4	Sulfuric Acid
SEM	Scanning Electron Microscopy
XRD	X-ray Diffraction
TGA	Thermogravimetric Analysis
FTIR	Fourier Transform Infrared Spectroscopy Analysis

Contents

List of Figures

List of Tables

Chapter 1

Introduction and Literature Review

1.1 Prelude

Concrete is a heterogeneous, man-made construction material that has been widely employed for civil infrastructure since its use was revolutionized by the ancient Romans. Presently, its usage in the construction industry is second only to water across the globe. Such extensive use is testament to its properties of strength, mouldability, and the ability to customize various characteristics. The burgeoning global population and massive worldwide development of industry and infrastructure has resulted in demand for prodigious quantities of concrete. In addition, as horizontal expansions become restricted, vertical growth has accelerated, further boosting demand [1]. It is estimated that more than a ton of concrete is produced each year for every person in the world [2].

Concrete is typically prepared by mixing ordinary Portland cement (OPC) with sand, crushed rocks, and water [3]. Thus, the increase in demand for concrete has, in turn, resulted in strong demand for OPC, a primary binder of concrete. Worldwide, the production of OPC was reported to be around 4100 million metric tons in 2016 [4]. In India alone, the production of OPC reached approximately 368 million tons in 2016 [5].

India is already the second-largest producer of cement, accounting for around 6.7% of global output.Unfortunately, the present production process for OPC is expensive, highly energy intensive, user-hostile, and non-eco-friendly. It emits significant quantities of carbon dioxide, a primary greenhouse gas, into the atmosphere during the decomposition of limestone and fossil fuels. The process emits not only carbon dioxide, but also sulphur trioxide and nitrogen oxide, which are strongly linked to climate change and acid rain [6]. Furthermore, the natural and restricted resource of mineral coal is used to obtain the high energy needed for OPC processing. The production of OPC by this process yields nearly the same amount of carbon dioxide through the calcination of limestone. Carbon dioxide is thought to be responsible for approximately 65% of the global warming effect. The cement industry alone is responsible for about 6% of this [7], and Provis et al. [8] reported that the predictions of the International Energy Agency indicate this will rise to around 9–10% of total world carbon dioxide emissions by 2050.

$$5CaCO_3 + 2SiO_2 => (3CaO, SiO_2)(2CaO, SiO_2) + 5CO_2(emission) \qquad (1.1)$$

A simplified formula for the emissions states that each ton of OPC yield is equivalent to one ton of CO_2 being emitted into the atmosphere.

The European Communities Commission, seeking to limit carbon dioxide emissions linked to global warming, recommended in 1991 that member states adopt a new energy and fuel tax [9]. No energy efficiency measures are capable of mitigating its effects, with greenhouse gases being a significant factor in global climate change. This is a matter of great concern to environmentalists, and should act as a red flag to communities across the planet [10]. Analogous to OPC, there has been a tremendous increase in the demand for natural sand because of the escalating demand for concrete. This is a great concern to the environment on account of the excessive exploitation of restricted natural resources. The cost of natural sand has risen as a result of the need for transportation from distant sources and legislative restrictions on exploration.

These factors have combined to bring about considerable research into feasible alternative binding materials [10]. However, note that feasible alternatives, i.e. supplementary cementing materials, must be sustainable, relatively cheap, and inherently environmentally friendly. Parallel to kaolinitic materials, an alkaline activation of inorganic wastes such as fly ash, slag, mining waste, rice husk ash, and silica fume provides the possibility of synthesizing low-cost eco- and user-friendly structural materials that are analogous to cement.

Fly ash is a fine-grained, powdery, pulverized fuel ash produced as a residue from burning pulverized coal in electric power generation plants. It consists of the remnants of clays, sands, and organic matter present in the parent coal, along with high alumina and silica contents. Fly ash is a pozzolanic material found in abundance as an industrial waste by-product, and is therefore relatively low-cost compared with materials such as metakaolin while offering superior mechanical strength and durability ref [11–13]. Though global coal ash production totals more than 390 million tons per year, only 15% is currently utilized, resulting in significant amounts going to landfill ref [14, 15] as shown in Figure 1.1. A systematic use of this by-product is needed to overcome this problem. In India, the production of fly ash was estimated to be 184 million ton in 2015 [16]. Each million tons of fly ash that replace OPC help to conserve one million tons of limestone, 0.25 million tons of coal, and more than 80 million units of power, notwithstanding the abatement of 1.5 million tons of carbon dioxide being emitted into the atmosphere [17]. In addition, the appropriate usage of one ton of fly ash earns one carbon-credit, which has a redemption value of US$10–20. Therefore, monetary benefits are also possible through carbon-credit trade [18]. Hence, the use of fly ash in concrete production has attracted researchers and engineers on account of its suitability and global ubiquity as a discarded residue.

Figure 1.1: Disposal of fly ash at site [18]

1.2 Geopolymer Technology

In 1978, the French scientist **Joseph Davidovits** [19] reported that alternative binders could be produced, under high alkaline conditions, by an exothermic polymeric chemical reaction of an alkaline liquid with silicon and aluminium in a source material of geological or industrial origin. Davidovits termed the resulting material a "geopolymer", i.e. a mineral polymer resulting from geochemistry or geosynthesis of mostly rock-forming mineral materials or industrial wastes. The advantage of geopolymers is that, unlike for OPC, high-energy and high-temperature reactions are no longer essential.

The word geopolymer implies a geological origin, and the products of geopolymerization [19] can effectively be thought of as synthetic rock. This process of geopolymerization takes place by alkaline activation, i.e. dissolution at high pH, atmospheric pressures, and at low temperatures (from room temperature to 100°C), and thus consumes a very low amount of energy as compared to OPC production (up to 60% less) [20], making it approximately 10-30% cheaper than OPC. In spite of their precise

mouldability and very high surface smoothness and precision, geopolymers range from 4–7 on the Mohs hardness scale. Geopolymers are three-dimensional silico-aluminates that are amorphous to semi-crystalline in form, and are non-flammable and incombustible "plastic-like materials". This group of inorganic binders possesses Si-O-Si polymer system bonding, similar to zeolites and ceramics. They are polymers, therefore they transform, polycondense, and adopt a shape swiftly at low temperatures, i.e. a few hours at 30°C, a few minutes at 85°C, and just a few seconds in microwave ovens.

The earth's crust contains at least 55% Siloxo-Sialates and Sialates and 12% pure quartz or silica. Synthetic minerals are analogous to those that form the lithosphere. Geosynthesis is frequently manifested in nature, with silicon and aluminium atoms combining to form building blocks that are chemically and structurally comparable to those binding natural rocks. Nowadays, novel geopolymer concrete is gaining attention in the construction industry as it does not require OPC as a binder. Moreover, it is an eco- and user-friendly material with multiple benefits and excellent as well as entirely different characteristics that indicate it could be a superior alternative binder to OPC. Geopolymers have numerous industrial applications on account of their sustainability under aggressive environmental conditions. Potential benefits such as self-binding for concrete, augmented durability, improved performance, low cost, reduced environmental impact, low energy consumption, environmental and user friendliness, fire and weather resistance, and exceptional hardness as well as entirely peculiar physical, mechanical, optical, and thermal characteristics signal the possible replacement of OPC by geopolymer concrete in the future. They are candidate materials for the immobilization of industrial and mining wastes, and are analogous to thermosetting organic resins, but remain stable up to 1000–1200°C. Fly ash-based geopolymeric cement has attracted intensive research worldwide because its production generates 90% less CO_2 than that of OPC. Put simply, this means that nine times more cement for infrastructure and building applications can be manufactured for the same CO_2 emissions [21]. This proves that geopolymer technology is capable of reducing CO_2 emissions into the atmosphere from OPC production and the aggregate industries by about 80% [22], ameliorating the process of global climate change. The

development of geopolymer technology therefore resolves a major concern regarding global warming and reduces the problem of waste disposal. Health hazards related to fly ash residues have motivated researchers to develop a new type of sustainable, user- and eco-friendly material that is heat, fire, and weather resistant, namely **"Fly ash-based Geopolymer Concrete"**.

1.2.1 Chemistry and Terminology of Geopolymer

In 1978, the French scientist **Joseph Davidovits** [23] first introduced the term "geopolymer" to represent a broad range of materials characterized by networks of inorganic molecules. These are inorganic alumina-silicate polymers that are synthesized from predominantly silicon (Si) and aluminium (Al) of geological origin. Thus, these mineral polymers are the product of geochemistry. The chemical composition of this group of mineral binders is similar to that of zeolites, but their microstructure is amorphous. A synthesis process of Si and Al atoms results in building blocks that are chemically and structurally comparable to those binding natural rocks. The term "poly (Sialate)" was also suggested for the chemical designation of geopolymers based on silico-aluminates ref [24–27].Three-dimensional Poly Silicon-Oxo-Aluminate (Sialate) is a chain and ring of polymers with Si^{4+} and Al^{3+} in IV-fold coordination with oxygen, and ranges from amorphous to semi-crystalline with the empirical formula:

$$Mn(-(SiO_2)_z - AlO_2)_n.wH_2O \tag{1.2}$$

where z is 1, 2, ... 32, the "-" symbol indicates the presence of a bond, M is a monovalent cation such as sodium or potassium, and n is the degree of polycondensation or polymerization. Three types of Poly Sialates were distinguished by Davidovits [24]–[27]. They are the Poly (Sialate) type (-Si-O-Al-O-), the Poly (Sialate-Siloxo) type (-Si-O-Al-Si-O-), and the Poly (Sialate-DiSiloxo) type (-Si-O-Al-Si-O-Si-O-), as shown in Figures 1.2 and 1.3.

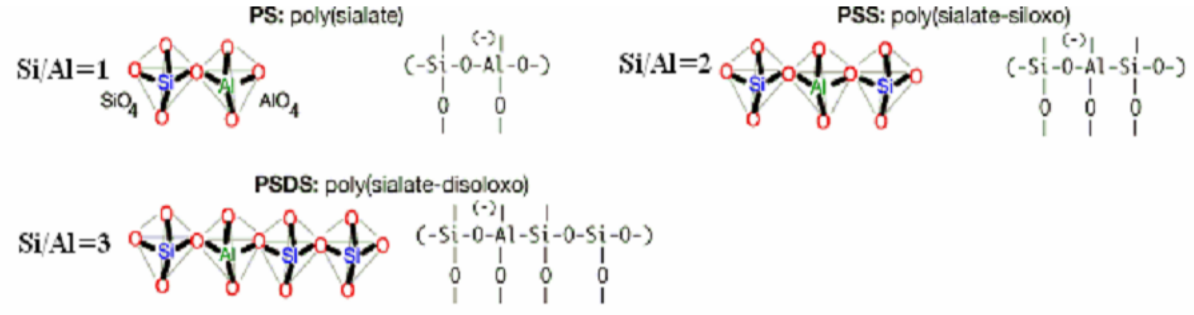

Figure 1.2: Three basic forms of geopolymers [28]

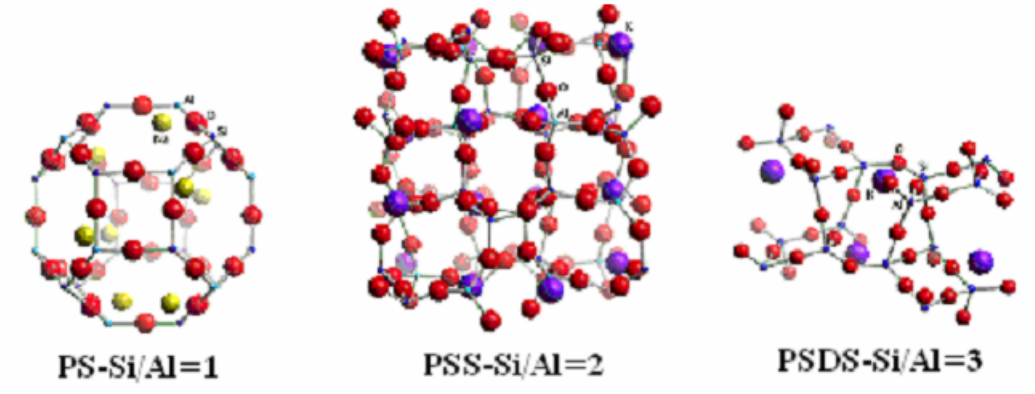

Figure 1.3: Polymeric structures from polymerisation of monomers [28]

In the process of geopolymerization, a chemical reaction of alumino-silicate oxides (Si_2O_5, Al_2O_2) with alkali polysilicates produces polymeric Si-O-Al bonds. An illustration of polycondensation by alkali into poly (Sialate-Siloxo) is shown in Figure 1.4

The equation of Figure 1.4 shows that, there is loss of water during the geopolymerization process. There is further loss of water occurred during curing period. This leads to porosity in the polymer matrix. The pores are however discontinuous. This improves the properties of geopolymer. It can be said that water does not have important role in the geopolymerization. The water just helps in fresh properties only. The role of water in geopolymer is thus different from its role in OPC concrete.

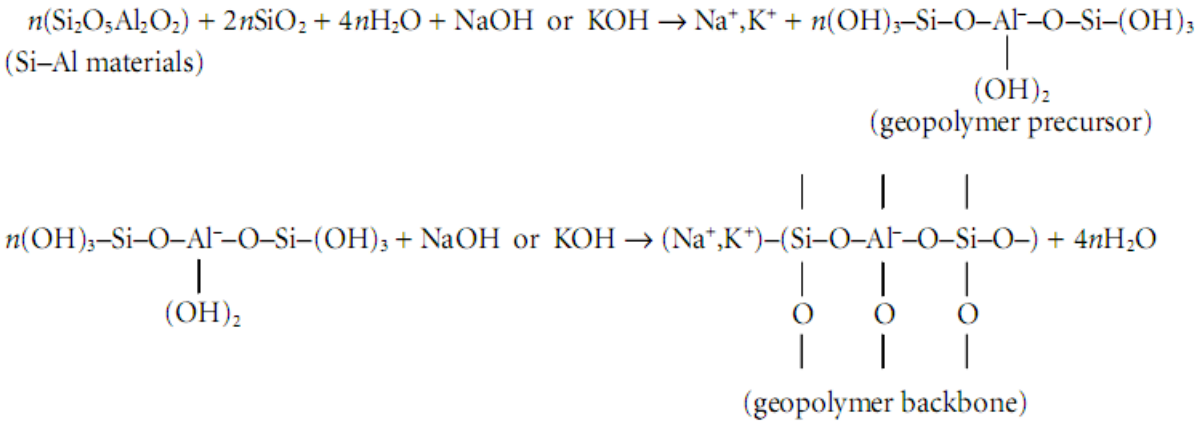

Figure 1.4: Formation of geopolymer material [28]

1.2.2 Constituents of Geopolymers

The source materials and alkaline liquids are the main constituents of geopolymers. These are used together with aggregates to produce a geopolymer concrete.

Source Materials and Alkaline Liquids

The manufacturing of a geopolymer requires source materials that are rich in silica and alumina. Kaolinite, clays, andalousite, spinel, micas, slag, fly ash, silica fume, rice husk ash, and red mud can be used as source materials. The main factors in selecting the source material are availability, type of application, user demands, and cost. Soluble alkali metals, which usually have a sodium or potassium base, are needed to form alkaline liquids.

Davidovits [29, 30] produced a geopolymer through the polymerization of a kaolinite source material with alkali (NaOH, KOH) in 1972. The performance of this calcined kaolinite is superior to that of other natural source materials used to manufacture geopolymers.

Calcined source materials such as calcined kaolin, fly ash, and slag exhibit higher compressive strength than non-calcined materials, e.g. mine tailings, kaolin clay, and

natural minerals. Barbosa *et al.* [31] and Xu and Daventer [32] reported that calcined (i.e. fly ash) and non-calcined materials (i.e. kaolinite or kaolin clay and albite) could be combined to increase the compressive strength and reduce the reaction time. Fly ash is preferable to other source materials because of its bulk availability, comparatively low-cost, and high reactivity due to having a finer particle size.

A study of 16 natural Si-Al minerals that covered the ring, chain, sheet, and framework crystal structure groups as well as feldspar, clay, garnet, mica, sodalite, and zeolite mineral groups has been conducted by Xu and Deventer [32]. This study examined potential sources for geopolymer synthesis with sodium or potassium hydroxide as alkaline liquids.

A potential use of waste such as fly ash, mine tailing, building waste, and contaminated soil with immobilized toxic metals was identified by Van Jaarsveld *et al.* [33]. Palomo *et al.* [34] used sodium silicate with sodium hydroxide and potassium silicate with potassium hydroxide as an alkaline solution, and found that the type of alkaline liquid affects the mechanical strength of geopolymer concrete. In this case, the highest compressive strength is given by the combination of sodium silicate and sodium hydroxide. Cheng and Chiu [35] used granulated blast furnace slag and metakaolinite as source materials with sodium silicate and potassium hydroxide as an alkaline liquid to make fire-resistant geopolymer concrete.

The properties of geopolymers vary according to the origin, particle size, and morphology of the fly ash, as well as with the alkali, metal, and amorphous content [33]. Fernandez and Palomo [36] explained that fly ash with characteristics such as low calcium content, high vitreous phase content, 80–90% particle sizes less than 45 μm, less than 5% unburned material, 40–50% reactive silica content, and less than 10% Fe_2O_3 content results in the optimal binding properties. Significant quantities of calcium can interfere with the polymerization setting rate resulting from an alteration of the microstructure [37]. Thus, fly ash with a low calcium content is preferable for making geopolymer concrete.

1.2.3 Applications of Geopolymers

Geopolymers have a vast range of applications in automobiles, aerospace, non-ferrous foundries and metallurgy, plastic industries, and civil engineering. The discovery of a new class of inorganic materials that act as advanced mineral binders, i.e. geopolymer resins and cement as well as geopolymer concretes, has resulted in broad scientific interest and multiple developments ref [38–40]. The inventor of geopolymers, **Joseph Davidovits**, has classified various applications on the basis of the silicon and aluminium atomic ratio (see Table 1.1). Here, a low Si:Al atomic ratio of 1, 2, or 3 represents a 3D network that is very rigid, whereas Si:Al atomic ratios above 15 indicate a polymeric character.

Table 1.1: Applications of geopolymeric materials based on Si:Al atomic ratio [41]

Si:Al ratio	Applications
1	Bricks, ceramics, fire protection
2	Low CO_2 cements, concrete, radioactive and toxic waste encapsulation
3	Heat resistance composites, foundry equipments, fibre glass composites
>3	Sealants for industry
20-35	Fire-resistant and heat-resistant fibre composites

The above table indicates that many civil engineering applications require low Si:Al atomic ratios.

- Geopolymer behaves similarly to zeolitic materials, which are known for their ability to absorb toxic chemical waste. Owing to this property, one potential field for the application of geopolymeric materials is in toxic waste management [41]. Comrie *et al.* [42] recommended geopolymite 50 (a registered trademark of Cordi-Geopolymere SA) for applications of geopolymer technology in toxic waste management.

- As geopolymers provide excellent adhesion to both concrete surfaces and inter-laminar fabrics, they are useful for strengthening concrete structural elements. A study has reported the results of using geopolymer in place of organic polymer for fastening carbon fabrics to the surface of reinforced concrete beams [43].

- Geopolymer technology has been used to develop sewer pipeline products, masonry units, high-performance fibre-reinforced laminates, railway sleepers, building products including fire and chemical-resistant wall panels, coatings, and repair materials [44, 45].

- Since 1972, geopolymer applications developed in Europe and the USA have covered fire-resistant wood panels, high-tech resin systems, insulated panels and walls, fireproof high-tech applications, aircraft, automobile, interiors, decorative stone art, fire-resistant and fireproof composites for infrastructure repair, foamed geopolymer panels for thermal insulation, geopolymer cement and concrete, low-energy ceramic tiles, thermal shock refraction and refractory items [46].

1.3 Rubberized Cement Concrete

Each year, a vast number of discarded rubber tyres are accumulated across the world, but their disposal in landfill is increasingly unacceptable on environmental grounds as shown in 1.5. More than 300 million tyres per year are discarded in the USA, with a further 180 million in the European Union. About 600,000 tonnes of scrap tyres are reported to have been dumped in landfill, creating yet another problem similar to fly ash. In addition, there are 128 million old tyres stockpiled in the USA [47]; such stockpiles create air, water, health and soil pollution problems, and are not only fire hazards but also provide a breeding ground for rats, mice, and mosquitoes [48, 49]. Rubber tyres are of limited use for recycling because of their highly complex chemical structure. The burning of tyres is not only impractical but also expensive and environmentally destructive. Moreover, burning is prohibited in some countries because of the unacceptable smell and enormous amounts of dark smoke carrying toxic gases.

The automobile industry is the main driver of the number of rubber tyres. The number of tyres in circulation is likely to increase as the amount of traffic on roads continues to rise. Consequently, millions of tyres are discarded every year, and this

waste is not biodegradable in ambient conditions. To reduce air, water, and soil pollution, serious health and fire hazards, and aesthetic inconveniences, it is highly necessary to utilize the bulk rubber tyre waste by some other means. The aim, at this juncture, is to use the waste tyres to build a geopolymeric matrix and, thus, obtain a technically valuable composite material. This will prove to be the most viable, sustainable, technically suitable, legally sound, cost-effective, eco-friendly, publicly acceptable, and systematic solution to the dilemma.

Figure 1.5: Rubber tyre waste at site [49]

Currently, waste rubber tyres are being used in concrete as a partial replacement for fine aggregate. Rubberized concrete not only solves the problem of the accumulation of tyres, but also saves natural resources [48]. Though a number of experimental studies are available and encouraging results have been reported, rubberized cement concrete is still in the early stages of practical application. Rubberized cement concrete has been used in foundations, sidewalks, parking lots, and tennis courts in the state of Arizona, USA [48]. Further, waste rubber tyres are being used in rubberized asphalt concrete in many parts of the world [48].

1.3.1 Rubberized Fly ash-based Geopolymer Concrete

Investigations into the use of fly ash and rubber tyre waste in rubberized fly ash-based geopolymer concrete are likely to increase, as this offers an environmentally sustainable option of using industrial waste to form useful material. Research and industry groups are excited about this new direction of research into concrete made from industrial by-products that would otherwise cause disposal problems.

The manufacture of rubberized fly ash-based geopolymer concrete uses ordinary concrete technologies. The largest volume of aggregates in OPC concrete occupies about 75–80% by mass, and this remains the same in the case of geopolymer concrete. In this case, fly ash is used as a binder in place of Portland or other hydraulic cement, and natural sand is partially replaced by rubber tyre fibres. Fly ash (containing silica and alumina) reacts with an alkaline liquid (combination of sodium silicate and sodium hydroxide solutions) in a polymerization reaction to form a geopolymer paste that binds the non-reacted materials (aggregates and rubber tyre fibres). The resulting product is rubberized fly ash-based geopolymer concrete.

1.3.2 Advantages of Geopolymer Concrete and Rubberized Geopolymer Concrete

- The raw material resources of any pozzolanic compound or source of silicate and alumina silicate, which are soluble in an alkaline solution, are available in abundance. This suffices as a source of geopolymer production [6, 50].
- The energy consumption of geopolymer manufacturing is low. A low temperature of 600–800°C is suitable for the thermal processing of natural alumina silicates. The process requires 60% less energy than OPC processing, and emits far less carbon dioxide [6, 50].
- Short curing periods at room temperature will result in similar strength to OPC concrete [6, 50].
- The preparation of geopolymers is simple because they can be synthesized

directly by mixing alumina silicate reactive materials and high alkaline solutions [35, 36].

- Geopolymer concrete or mortar suffers little loss of function over thousands of years against weathering. This shows its excellent durability [6, 50].
- Geopolymer cement suffers 80% less shrinkage than Portland cement [6, 50].
- Geopolymer concrete does not lose functionality, even at 1000–1200°C, proving its low thermal conductivity and suggesting higher resistance to fire [6, 45, 50].
- The rubber fibres have good tensile strength, which leads to increased flexural strength of geopolymer concrete.
- Rubberized geopolymer concrete can be effectively used for pedestrian driveways, residential buildings, and because of its light weight in partition walls.

1.4 Research Significance

The assimilation of the latest technology with continuous technological upgrading is ongoing in the conventional concrete industry. The primary binder of an ordinary conventional cement contributes nearly 7% of global carbon dioxide emissions during its production, making it a non-eco-friendly industry [6, 50]. The production of cement is highly energy-intensive and consumes non-renewable natural resources such as limestone, natural sand, and coal. There is a growing demand for new construction materials that have low greenhouse gas emissions associated with their manufacture. Geopolymer concrete is the best solution to these problems because of its contribution to reducing global anthropogenic CO_2 which, in turn, may reduce the effects of climate change and because it is a sustainable building material. Geopolymer concrete can be manufactured using industrial waste as one of its constituents. It generates 90% less CO_2 than OPC production, and is therefore relatively eco-friendly. It has unique properties such as early strength, low shrinkage, good sulfate and corrosion resistance, making it a viable alternative solution to conventional cement concrete.

In addition, the use of rubber tyre fibres as an aggregate in geopolymer concrete results in a new type of concrete with acceptable properties under varied conditions. The use of waste material in the geopolymer concrete offers an amicable disposal method, facilitating an effective use of solid waste, minimizing the accumulation of tyres, and reducing the consumption of natural resources. Further, the use of this waste will produce a sustainable construction material.

This work establishes the viability of using rubber tyre fibres in concrete in future construction activities. To date, there is no information available regarding the durability of geopolymer concrete incorporating rubber tyre fibres. This research is expected to fill this gap and provide confidence to users, field engineers, and researchers that these wastes can be used in geopolymer concrete. Geopolymer concrete offers a time saving, cost saving (10–30%), eco- and user-friendly, sustainable option, with the conservation of non-renewable natural resources such as coal and natural sand from excessive exploitation and a reduction in hazardous rubber tyre waste and fly ash in landfill. Additional benefits of developing effective rubberized geopolymer concrete include reduced energy consumption (60% less in cement production), carbon credits to the Indian economy, the removal of OPC from the process, self-autoclave curing, the ability of the resulting concrete to withstand severe freeze/thaw conditions, fire resistance, and reduced CO_2 emissions.

1.5 Hiatus in the Research Area

Geopolymer concrete has not been studied in detail. There have been some efforts to use waste rubber tyre fibres in the Portland cement concrete industry, but never, to the best of the author's knowledge, as a partial replacement for natural sand in a geopolymer concrete. Enormous efforts have been observed from various publications towards durability and strength properties of geopolymer concrete [184]– [192]. Therefore, there is a strong need for an extensive study of the strength and durability properties of geopolymer concrete incorporating waste rubber tyre fibres as a partial replacement for fine aggregates, as this will contribute to the identification, develop-

ment, and promotion of viable products. This research work will contribute to filling this hiatus in the current knowledge base.

Investigations into the use of fly ash-based geopolymer concrete have accelerated since 2000 under the impetus of finding an environmentally sustainable option of using industrial waste to form useful materials. Research and industry groups are excited about the prospect of concrete made from industrial byproducts, which would obviate the need to dispose of these materials.

1.6 Literature Review

A number of studies have investigated different properties of rubberized cement concrete, but no studies are available on rubberized geopolymer concrete. A summary of the previous literature based on the properties of rubberized cement concrete is presented in Table 1.2, and the literature examining the properties of geopolymer concrete is listed in Table 1.3.

To the best of the author's knowledge, no studies have analysed the effect of various factors on the properties of rubberized geopolymer concrete using the Taguchi method. Therefore, the effect of various factors on the compressive strength of rubberized geopolymer concrete, which is a highly sustainable replacement for OPC, has been studied in this research. The factors considered are the curing time, curing temperature, Na_2SiO_3/NaOH ratio, alkaline liquid/fly ash ratio, superplasticizer, rest period, water content, and NaOH concentration. Experimentally, it is very difficult to consider the separate effects of these factors on the compressive strength of concrete. Therefore, the Taguchi method is used to evaluate the effect of these factors on the compressive strength of rubberized geopolymer concrete. Thereby, it is possible to determine the optimal value of these parameters for the composition of rubberized geopolymer concrete. The analysis of variance (ANOVA) method is used to rank the impact of each factor on the rubberized geopolymer concrete and produce the optimal mix proportion. One of the major advantages of the Taguchi method over other

experimental designs is that it minimizes the number of experiments, which reduces the experimental cost. Previous literature on the Taguchi method applied to concrete and geopolymers is summarized in Table 1.3.

Table 1.2: Existing literature on the properties of rubberized cement concrete

Studies	Test Conducted	Material	Paper	Observations
Strength studies	Compressive strength	Crumb rubber	Khatib and Bayomy [51]	A significant decrease in compressive strength of concrete on replacement of fine aggregate by crumb rubber. The reduction was attributed to the presence of softer rubber particles than the surrounding cement matrix and insufficient bonding between rubber particles and cement paste, which results in rubber particles acting like voids.
			Guneyisi *et al.* [52]	Systematic decrease in the compressive strength of concrete on replacement of aggregate by crumb rubber. The compressive strength increased on inclusion of silica fume. The increase was attributed to the filling of voids by silica fume.
			Reda Taha *et al.* [53]	Decrease in compressive strength on replacement of fine aggregates by crumb rubber for 0.7 water to cement ratio. They observed more than 67% reduction in compressive strength full replacement of fine aggregates by crumb rubber.
			Batayneh *et al.* [54]	Decrease in compressive strength following up to 100% replacement of fine aggregate by crumb rubber for w/c ratio 0.55. More than 90% reduction in compressive strength on 100% replacement. The reduction was attributed to weak aggregate paste bond and substitution with a softer, less dense crumb rubber compared with the harder dense natural aggregate.
			Son *et al.* [55]	A 22% reduction in compressive strength on partial replacement of aggregate by crumb rubber

Studies	Test Conducted	Material	Paper	Observations
Strength studies	Compressive strength	Crumb rubber	Ozbay *et al.* [56]	A significant decrease in compressive strength of reported a decrease in compressive strength following up to 25% replacement of fine aggregate by crumb rubber for w/c ratio 0.4. More than 26% reduction in compressive strength on 25% replacement.
			Grinys *et al.* [57]	Decrease in compressive strength following up to 30% replacement of sand by crumb rubber for w/c ratio 0.35. More than 85% reduction in compressive strength on 30% replacement. The reduction was attributed to presence of more elastic and weaker rubber particles as compared to surrounding cement matrix, and replacement of higher density material with low density material.
			Xue and Shinozuka [58]	Decrease in compressive strength following up to 20% replacement of coarse aggregate by . crumb rubber More than 47% reduction in compressive strength on 20% replacement.
			Onuaguluchi *et al.* [59]	Decrease in compressive strength on replacement of up to 15% fine aggregate by crumb rubber for w/c ratio 0.47. More than 40% reduction in compressive strength on 15% replacement.

Studies	Test Conducted	Material	Paper	Observations
Strength studies	Compressive strength	Rubber tyre chips	Khatib and Bayomy [51]	A significant decrease in compressive strength of concrete on replacement of coarse aggregate by rubber tyre chips.
			Li *et al.* [60]	Decrease in the compressive strength of concrete on replacement of 15% of volume of coarse aggregate by rubber tyre chips.
			Guneyisi *et al.* [52]	Decrease in the compressive strength of concrete on replacement of aggregate by rubber tyre chips.
			Ganjian *et al.* [61]	23% decrease in the compressive strength of concrete on 10% replacement of coarse aggregates by rubber chips. This strength reduction resulted from poor bonding between rubber aggregate and cement paste and non-uniform distribution of rubber particles in the concrete.
			Reda Taha *et al.* [53]	More than 78% reduction in compressive strength on full replacement of coarse aggregate by rubber chips.
	Flexural strength	Rubber aggregate	Benazzouk *et al.* [62]	Higher flexural strength of cement matrix on inclusion of rubber aggregate
			Turatsinze and Garros [63]	Decrease in flexural strength following up to 25% replacement of coarse aggregate by rubber aggregate for w/c ratio 0.4. They observed more than 42% reduction in flexural strength on 25% replacement of coarse aggregate by rubber aggregate. The reduction was attributed to poor mechanical behaviour of rubber aggregate concrete.
			Turki *et al.* [64]	Decrease in flexural strength following up to 50% replacement of fine aggregate by rubber aggregate for w/c ratio 0.5. They observed more than 72% reduction in flexural strength on 50% replacement of fine aggregate by rubber aggregate. The reduction was attributed to the low density of rubber.

Studies	Test Conducted	Material	Paper	Observations
Strength studies	Flexural strength	Rubber aggregate	Najim *et al.* [65]	Decrease in flexural strength on replacement of coarse aggregate and fine aggregate by rubber aggregate. More than 39% reduction in flexural strength on 15% replacement.
			Su *et al.* [66]	Decrease in flexural strength following up to 20% replacement of fine aggregate by rubber aggregate for 0.37 w/c ratio. More than 12% reduction in flexural strength on 20% replacement of fine aggregate by rubber aggregate.
		Rubber chip	Ganjian *et al.* [61]	Decrease in flexural strength on replacement of coarse aggregate by chipped rubber and cement by ground rubber for w/c ratio 0.5. More than 37% reduction in flexural strength on 10% replacement of coarse aggregate by chipped rubber. The reduction was attributed to weak bonding between rubber aggregates and the cement paste.
			Gesog'lu *et al.* [67]	Decrease in flexural strength on replacement of coarse aggregate by tyre chips and fine aggregate by crumb and fine crumb rubber for w/c ratio 0.27. More than 81% reduction in flexural strength on 10% replacement of coarse aggregate by tyre chips and 10% replacement of fine aggregates by fine crumb rubber. Reduction in flexural strength was attributed to weak interface bond.
		Crumb rubber	Grinys *et al.* [57]	Decrease in flexural strength following up to 30% replacement of sand by crumb rubber for ratio 0.35. w/c They observed more than 72% reduction in flexural strength on 30% replacement of sand by crumb rubber.

Studies	Test Conducted	Material	Paper	Observations
Durability studies	Abrasion resistance	Crumb rubber	Ozbay *et al.* [56]	Abrasion resistance has been reported on replacement of up to 25% fine aggregates by crumb rubber for a single 0.4 w/c ratio in cement mortar. More than 20% increase in depth of wear on 25% replacement of fine aggregates by crumb rubber.
			Sukontasukkul and Chaikaew [68]	Increase in weight loss due to abrasion on replacement of coarse aggregates and fine aggregates by crumb rubber. More than 90% increase in weight loss on 20% replacement of fine aggregates by crumb rubber.
			Gesog'lu *et al.* [67]	Decrease in depth of wear on replacement of coarse aggregate by tyre chips and fine aggregate by crumb and fine crumb rubber for w/c ratio 0.27. More than 81% reduction in depth of wear on 20% replacement of aggregate by rubber particles. The reduction was attributed to the ability of the rubber particles to hold the paste together.
	Water permeability	Chipped rubber	Ganjian *et al.* [61]	The effect of replacement of coarse aggregate by chipped rubber and cement by ground rubber on the water permeability for w/c ratio 0.5. More than 150% increase in water permeability depth on 10% replacement of coarse aggregate and 114% increase on 10% replacement of cement. This increase in water permeability was attributed to the reduction in bonding between particles in the modified concrete.
		Granulated rubber particles	Bjegovic *et al.* [69]	Increase in water permeability on replacement of up to total of 15% volume of aggregate by granulated, shredded, and small rubber particles. Increase in water permeability was attributed to higher amount of air voids entrapped around the rubber surface.

Studies	Test Conducted	Material	Paper	Observations
Durability studies	Water permeability	Granulated rubber particles	Su *et al.* [70]	Increase in water permeability following up to 20% replacement of fine aggregate granulated rubber aggregate for w/c ratio 0.37. More than 215% increase in depth of water permeability on 20% replacement of FA by granulated rubber aggregate. Increase in water permeability was attributed to increased porosity of rubber concrete.
	Shrinkage	Rubber Aggregate	Turatsinze and Garros [71]	Decrease in restrained shrinkage cracking of self- compacting concrete on up to 25% replacement of coarse aggregate by rubber aggregate for 0.4 w/c ratio.The improved resistance to cracking was attributed to the enhanced strain capacity.
			Bravo and Brito [72]	Increase in total shrinkage on replacement of natural aggregate by tyre rubber aggregate for single 0.35 w/c ratio. However, the drying shrinkage was not found to be affected by use of rubber aggregate.
			Nguyen *et al.* [73]	Increase in restrained shrinkage on replacement of fine aggregate (0–30%) by rubber aggregate for a single 0.47 w/c ratio in mortar. The replacement was found to delay the shrinkage cracking.
		Crumb rubber	Sukontasukkul and Tiamlom [74]	Increase in drying shrinkage on up to 30% replacement of FA by crumb rubber for single 0.47 w/c ratio. Increase in drying shrinkage was attributed to the decrease in internal restraint and more flexible material.
		Rubber powder	Yung *et al.* [75]	Increase in drying shrinkage on replacement of fine aggregate (0–20%) by rubber powder for 0.35 w/c ratio. More than 95% increase in drying shrinkage on 20% replacement of fine aggregate by rubber powder. The minor deformation capability of rubber powder was cited as the reason for the increase in drying shrinkage.

Studies	Test Conducted	Material	Paper	Observations
Durability studies	Shrinkage	Rubber particles	Uygunoglu and Topcu [76]	Up to 50% sand aggregate was replaced by scrap rubber particles and the drying shrinkage was found to increase with an increase in rubber content. The increase was attributed to the increase in porosity of the mix due to the rubber particles.
			Bravo and Brito [72]	Increase in carbonation depth on replacement of natural aggregate (0–15%) by tyre rubber aggregate for 0.35 w/c ratio. More than 56% increase in carbonation depth was observed on 15% replacement of natural aggregate by rubber aggregate. The increase in carbonation depth was attributed to the greater water demand of the rubber content to maintain workability and the greater void volume between the rubber aggregate and the cement paste.
	Corrosion and chloride diffusion	Rubber ash	Al-Akhras and Smadi [77]	Rubberized mortar, containing tyre rubber ash as partial replacement of sand for a 0.65 w/c ratio . It was stated that the filling of the voids by the rubber ash prevented the diffusion of chloride.
		Rubber aggregate	Bravo and Brito [72]	No trends of variation in chloride-ion penetration on replacement of natural aggregate (0–15%) by tyre rubber aggregate for 0.35 w/c ratio. Decrease in chloride-ion penetration on replacement of natural aggregate by rubber up to 5% aggregate and subsequent increase for higher replacement ratios.

Studies	Test Conducted	Material	Paper	Observations
Durability studies	Corrosion and chloride diffusion	Crumb rubber	Gesoglu and Guneyisi [67]	Decrease in the penetration of chloride ions on partial replacement of fine aggregate by crumb rubber. The chloride ion permeability increased by up to 59% on 25% replacement of total aggregate by rubber. The increase in permeability was found to be controlled by the addition of silica fume.
			Dong *et al.* [78]	Increase in chloride-ion penetration on replacement of FA by crumb rubber. More than 40% increase in chloride-ion penetration on 10% replacement of natural aggregate by crumb rubber and more than 20% increase on 30% replacement. Increase in voids at the interface of cement paste and rubber aggregates was given as the reason for the increase in chloride-ion penetration.
			Onuaguluchi *et al.* [59]	An uneven trend in chloride-ion penetration on replacement of FA by crumb rubber for a 0.47 w/c ratio. Decrease of 18%, 25%, and 12% in chloride-ion penetration on 5%, 10%, and 15% replacement of fine aggregate by crumb rubber.
	Acid resistance	Rubber waste	Azevedo *et al.* [79]	Increase in mass loss, caused by sulphuric acid attack, on partial replacement of sand (0–15%) by rubber waste for a 0.35 w/c ratio. More than 35% increase in mass loss was reported on 15% replacement of sand by rubber waste. The acid resistance of rubberized concrete was found to be better than that of a control mix following the addition of fly ash and metakaolin.
		Rubber shred	Raghavan *et al.* [80]	Little effect of an alkaline environment on rubber shreds was observed. It was therefore assumed that the rubber shreds would not be affected by the alkaline environment in the mortar.

Table 1.3: Existing literature on properties of geopolymer concrete

Studies	Paper	Test Conducted	Observations
Strength studies	Hardjito *et al.* [81] Lloyd *et al.* [82] Panias *et al.* [83] Sofi *et al.* [84] Rangan *et al.* [85]	Compressive strength	Fly ash-based geopolymer composites exhibited high early compressive strength compared to cement concrete. Higher temperature and higher sodium hydroxide concentration gives highest compressive strength. There is no significant reduction in compressive strength with concrete age.
	Sofi *et al.* [84]	Flexural strength	The flexural strength determines the tensile properties of concrete under internal or external loading. The flexural strength of geopolymer concrete is higher than that of cement concrete, which exhibits a decreasing rate of crack propagation due to corrosion of embedded steel bars in the concrete.
	Sofi *et al.* [84]	Split tensile strength	The split tensile strength of geopolymer concrete decreased as the proportion of rubber tyre waste increased. However, the strength is higher than that of cement concrete because of good bonding between the geopolymer paste and aggregates.
	Sofi *et al.* [84] Fernande *et al.* [86] Neville [87] Hardjito et al. [88]	Modulus of Elasticity	The modulus of elasticity of geopolymer concrete is dependent on the modulus of elasticity of the aggregate, as well as the microstructure and modulus of elasticity of the geopolymer paste. Geopolymer concrete exhibits good bonding between the geopolymer paste and aggregates. However, geopolymer concrete has a higher modulus of elasticity than cement concrete.

Studies	Paper	Test Conducted	Observations
Durability studies	Bakharev [89] Wallah *et al.* [39] Thokchom *et al.* [90]	Sulfate resistance	Geopolymer concrete exhibits excellent performance against sulfates. Significant changes in mass and compressive strength have been observed in geopolymer concrete, as compared to cement concrete, as a result of alkaline liquid enhancing the stability of the geopolymeric structure. Increased alkaline content in the geopolymer mixture can increase the performance of geopolymer concrete against sulfates.
	Cheema *et al.* [91]	Water permeability	The coefficient of water permeability is low in geopolymer concrete as compared to cement concrete. As the alkaline ratio increases, the water permeability of geopolymer concrete decreases.
	Adam *et al.* [92] Thokchom *et al.* [90] Mishra *et al.* [93]	Sorptivity	As the alkaline liquid ratio increased from 0.75 to 1.25, the sorptivity of geopolymer concrete decreased. An increase in Na_2O content in geopolymer concrete decreased the sorptivity.
	Song *et al.* [94] Sathia *et al.* [95]	Water absorption	The water absorption of geopolymer concrete is lower than in cement concrete.
	Bharkdev [96] Song *et al.* [97]	Acid resistance	The degradation of mass and compressive strength of specimens after immersion in acid solution is less than observed in cement concrete specimens under an acidic environment.
	Adam *et al.* [92] Roy [98]	Carbonation	The carbonation performance of geopolymer concrete is good compared to that of cement concrete.
	Monita et al. [99]	Corrosion	The corrosion of steel reinforcement embedded in geopolymer concrete is similar to that of steel embedded in cement concrete.
	Monita et al. [99]	Chloride ion penetration	The chloride-ion penetration of fly ash geopolymer was higher than for OPC concrete.
	Wallah and Rangan [6]	Shrinkage	Geopolymer concrete has very little drying shrinkage compared to that of OPC concrete.

Studies	Paper	Test Conducted	Observations
Elevated temperature studies	Rashad and Zeedan [100]	Residual strength of alkali activated fly ash paste at different temperatures	Sodium silicate is more resistant to degradation caused by exposure to elevated temperatures than Portland cement specimens. The compressive strength and thermal shock resistance decreased.
	Kong and Sanjayan [101]	Residual thermal damage of geopolymer composites	Geopolymer strength increased by approximately 53% after exposure to elevated temperatures. Aggregate expanded with temperature. At 800°C, expansion reached approximately 1.5–2.5%.
	Kong and Sanjayan [102]	Compressive strength of geopolymer paste	Aggregates larger than 10 mm show higher strength at both ambient and elevated temperatures.
	Zhu Pan et al. [103]	Compressive strength of geopolymer mortar	The compressive strength of geopolymer mortar decreases in some cases and increases in others after exposure to high temperatures.
	Ranjbar et al. [104]	Compressive strength, density and TGA of fuel ash-based geopolymer mortar	Palm oil fuel ash and fly ash used as source materials. Geopolymer mortar accelerated micropore formation at elevated temperatures.
	Kong et al. [105]	Compressive strength of fly ash and metakaolin	The compressive strength of fly ash-based geopolymer concrete increased beyond 800°C, but the strength of the metakaolin-based geopolymer concrete decreased at the same temperature.
	Zhu Pan et al. [106]	Compressive strength and transient creep of geopolymer and OPC composites	At 550°C, the strength of the geopolymer paste increased whereas the OPC paste exhibited little change.

Studies	Paper	Test Conducted	Observations
Elevated temperature studies	Hussain *et al.* [107]	Mass loss, compressive strength of blended ash geopolymer concrete	The geopolymer concrete gives better compressive strength compared to OPC concrete at elevated temperatures.
	Kong *et al.* [105]	Compressive strength of metakaolin-based geopolymers	The Si:Al ratio has a significant influence on material degradation after exposure to elevated temperatures. A high Si:Al ratio (1.5) produces less strength loss due to elevated temperatures.
	Bakharev [108]	Compressive strength, XRD and SEM of fly ash-based geopolymer	The thermal stability of fly ash-based geopolymer materials was investigated in the range 800–1200°C. When using potassium silicate, compressive strength increased upon heating before decreasing at temperatures greater than 1000°C.
	Omar *et al.* [109]	Compressive strength of lightweight geopolymer paste, mortar, and concrete	Excellent mechanical and microstructural properties of the unexposed geopolymers. The deterioration of the geopolymer properties starts at a temperature of 800°C.
	Sun *et al.* [110]	Compressive strength, TGA, SEM and FTIR analysis of geopolymer paste	Ceramic waste used as source material. The synthesized geopolymer paste showed a 28-day compressive strength of 71.1 MPa before exposure and 75.6 MPa after thermal treatment at 1000°C.

Studies	Paper	Observations
Sea water and Sea sand Studies	Shinde and Kadam [111]	The untreated sea sand affects compressive strength in geopolymer concrete same as cement concrete but treated sea sand gives similar results as river sand concrete.
	Akram *et al.* [112]	Geopolymeric Materials have astrong potential place of conventional concrete due to unique salt resistance properties.
	Limeira *et al.* [113]	The use of dredged marine sand in substitution of river sand in concrete is maintained or accessible pores.
	Karthikeyan and Nagarajan [114]	Salt content present in sea sand must be eliminated before used in concrete because it contains chloride iron which may corrode steel.
	Karthikeyan and Nagarajan [115]	Sea sand in concrete with micro silica results in higher compressive, split and flexural strength than the conventional concrete.
	Liu *et al.* [116]	Chloride ion which is present in sea sand has some beneficial effect on the carbonation resistance of concrete.
	Katano *et al.* [117]	The permeability coefficient of sea water and unwashed sea sand concrete becomes small compared with that of concrete made using tap water.
	Ming *et al.* [118]	Compressive strength and elastic modulus of marine sand sea water concrete cured in sea water decrease than that of ordinary concrete cured in fresh water.
	Huiguang *et al.* [119]	The mud and clay content of sea sand is lower than that of river sand the fewer clay particles attached to the sea sand surface increase bonding between cement and aggregate.
	Nishida *et al.* [120]	The introduction of blast furnace slag might contribute significantly to the corrosion resistance of steel bar.
	Mohammed *et al.* [121]	No significant difference observed in compressive strength for concrete mixed with sea water and tap water after 20 years of exposure.
	Sun *et al.* [122]	The chloride ion content of sea sand can improve compressive strength.

Studies	Paper	Observations
Taguchi studies	Olivia and Nikraz [123]	Effect of parameters such as aggregate content alkaline solution to fly ash ratio,, sodium silicate to sodium hydroxide ratio, and curing method on fly ash-based geopolymer concrete using the Taguchi method. They reported the maximum compressive strength of 55 MPa at 28 days with higher tensile and flexural strength, but less expansion and drying shrinkage. They confirmed that geopolymer concrete is durable and is a possible alternative to OPC concrete.
	Nazari *et al.* [124]	Taguchi method was used to design compressive strength of OPC-based geopolymer concrete. They investigated the effect of factors such as NaOH concentration, sodium silicate to NaOH ratio, alkaline activator to cement ratio, curing temperature, curing time, and additional water content on compressive strength of OPC-based geopolymer concrete. Using ANOVA techniques, they concluded that the specimen with an NaOH concentration of 14M, Na_2SiO_3 to NaOH ratio of 1.0, and alkaline activator to cement ratio of 0.42 cured at room temperature for 28 days acquired the highest compressive strength.
	Nazari *et al.* [125]	Taguchi L32 array was used and gene expression programming (GEP) model was developed to predict the compressive strength of OPC-based geopolymer concrete.
	Mijarsh *et al.* [126]	Optimized factors by L25 Taguchi orthogonal array in their study. They divided six factors into two parts, wherein the first part included $Ca(OH)_2$, silica fume, $Al_2(OH)_3$,and additive materials and the second part included NaOH concentration, sodium silicate to NaOH ratio, alkaline activator to solid material ratio, and alkaline activators. The binding phase consists of N-A-S-H (Na_2O- Al_2O_3- SiO_2-H_2O) gel and C-S-H gel.
	Bagheri and Nazari [127]	Developed class C fly ash-based geopolymer concrete with granulated blast furnace slag aggregate. They considered four factors, namely the total aggregate content, NaOH concentration, curing time, and curing temperature.They reported that highest compressive strength was achieved with 12M NaOH concentration, 90°C curing temperature, 16 h curing time, and 30% aggregate content.
	Richi *et al.* [128]	Used Taguchi method and ANOVA to determine the optimum curing time, curing temperature, and NaOH concentration of fly ash- and rice husk ash-based geopolymer concrete. They achieved optimum strength on the 7th day by applying light and medium concentrations of NaOH for all specimens.

1.7 Objectives of Study

The main purpose of this study is to develop a fly ash-based geopolymer concrete containing waste rubber tyre fibres.

- To produce fly ash-based rubberized geopolymer concrete using the optimal combination of fly ash and rubber tyre fibres.

- To study the effect of various parameters such as alkaline liquid to fly ash ratio, rest period, curing temperature, curing time, concentration of NaOH solution, alkaline liquid ratio, addition of superplasticizer, and addition of water content on compressive strength for selected concrete mixes. To develop a mix design process on the basis of the selected parameters using the Taguchi method for fly ash-based rubberized geopolymer concrete.

- To study the compressive strength, flexural strength, split tensile strength, modulus of elasticity, and pull-off strength of fly ash-based geopolymer concrete having different rubber tyre fibre contents as a partial replacement for natural sand. The results will be compared with a control fly ash-based geopolymer concrete.

- To study durability properties such as water permeability, abrasion resistance, carbonation, shrinkage, corrosion, sorptivity, resistance to acid attack, salt attack, and sulfate attack with respect to rubber tyre fibre content and compare the results with a control fly ash-based geopolymer concrete.

- To study corrosion resistance and chloride diffusion in geopolymer concrete and compare the results with rubberized geopolymer concrete.

- To study the effect of control and rubberized geopolymer concrete at elevated temperatures.

- To examine the compressive strength and carbonation properties of geopolymer mortar.

- To study the effect of sea water and sea sand on strngth properties of rice husk based geopolymer mortar and fly ash based geopolymer concrete.

1.8 Layout of Report

This thesis is organized into seven chapters.

Chapter 1 introduces geopolymer technology and describes the need for a comprehensive study on the properties of geopolymer concrete and rubberized geopolymer concrete. This chapter gives an overview of the applications and advantages of geopolymers, the objectives of the study, and the scope of work. This chapter also includes a literature review based on previous research into the strength and durability of rubberized cement concrete, geopolymer concrete, and Taguchi method as applied to concrete. A brief description of the chemistry and constituents of geopolymer concrete is also given.

Chapter 2 describes the experimental programme. The materials used to produce geopolymer concrete and rubberized geopolymer concrete and the test procedure used are reported in this chapter. This chapter also describes the Taguchi experimental design method used to determine the effect of different parameters on compressive strength.

Chapter 3 presents the experimental results for mechanical properties including the compressive strength, split tensile strength, flexural strength, and modulus of elasticity for geopolymer concrete and the control concrete at different ages. This chapter also reports durability properties such as water permeability, abrasion resistance, carbonation, shrinkage, corrosion, sorptivity, resistance to acid attack, salt attack, and sulfate attack with respect to rubber tyre fibre content and compares the results with a control fly ash-based geopolymer concrete. Corrosion resistance and chloride diffusion in geopolymer concrete is also examined, and the results compared with those for rubberized geopolymer concrete.

Chapter 4 systematically examines the fire resistance of fly ash-based geopolymer concrete and establishes a comparison with the fire resistance of rubberized geopolymer exposed to elevated temperatures (200°C, 400°C, 600°C, and 800°C) to investigate the thermal effects on density, visual surface appearance, compressive strength, and microstructural characteristics. The experimental methods used to study the control and rubberized geopolymer concretes includes X-ray diffraction (XRD), thermogravimetric analysis (TGA), and Fourier transform infrared spectroscopy (FTIR).

Chapter 5 describes carbonation and strength studies related to geopolymer mortar. This chapter focuses on the effect of mix composition parameters and process parameters on the performance of the alkali activated geopolymer mortar. Further carbonation of the mortar and the effect on its morphology are also discussed.

Chapter 6 analyses the effect of sea water and sea sand on strength properties of rice husk based geopolymer mortar and fly ash based geopolymer concrete.

Chapter 7 summarizes this study, presents some concluding remarks, and outlines the future scope of work on the basis of the research conducted here.

Chapter 2

Experimental Programme

2.1 Prelude

This chapter describes an experimental programme for measuring the strength and durability properties of a control fly ash-based geopolymer concrete and rubberized fly ash-based geopolymer concrete according to the objectives determined in the previous chapter. This chapter also provide a characterization of the relevant materials, and describes a parameter study using the Taguchi method as well as a mix design for geopolymer concrete and OPC concrete.

The entire experimental study is divided into five parts. In the first part, a preliminary investigation examines the material characteristics, mix design, and the effect of different parameters on the compressive strength of geopolymer concrete using the Taguchi method. The second part looks at strength and durability properties using the optimum combination of parameters. Strength and durability properties include compressive strength, flexural strength, split tensile strength, pull-off strength, abrasion resistance, modulus of elasticity, and water permeability, as well as sulfate, acid, salt, shrinkage, corrosion, and chloride diffusion resistance, sorptivity, and carbonation. These properties are studied in control and rubberized geopolymer concrete samples, and the results compared with OPC concrete. The third part includes the effect of elevated temperatures on the control and rubberized geopolymer concrete.

Carbonation and strength studies of fly ash based geopolymer mortar is conducted in fourth part. Finally, the fifth part examines the effect of sea water and sea sand on strength properties of rice husk based geopolymer mortar and fly ash based geopolymer concrete.

2.2 Material Characterization

The two most important materials for producing geopolymer composites (mortar and concrete) are the source material, such as fly ash, and the alkaline solution.

2.2.1 Fly Ash

Class F low-calcium fly ash (procured from Dirk India Pvt. Ltd, Nasik, Pune, India) was used as the source material for making fly ash-based geopolymer composites. The chemical properties of fly ash are presented in Table 2.1. Silica, magnesium oxide, sulfur trioxide, and sodium oxide are present in fly ash up to permissible limits as per IS:3812 [129]. It can be seen from the loss of ignition value (LOI) that the fly ash contains a very small percentage of carbon. The total percentage of SiO_2 + Al_2O_3 + Fe_2O_3 is 92.26%, which is greater than the 70% limit prescribed in IS:3812 [129].

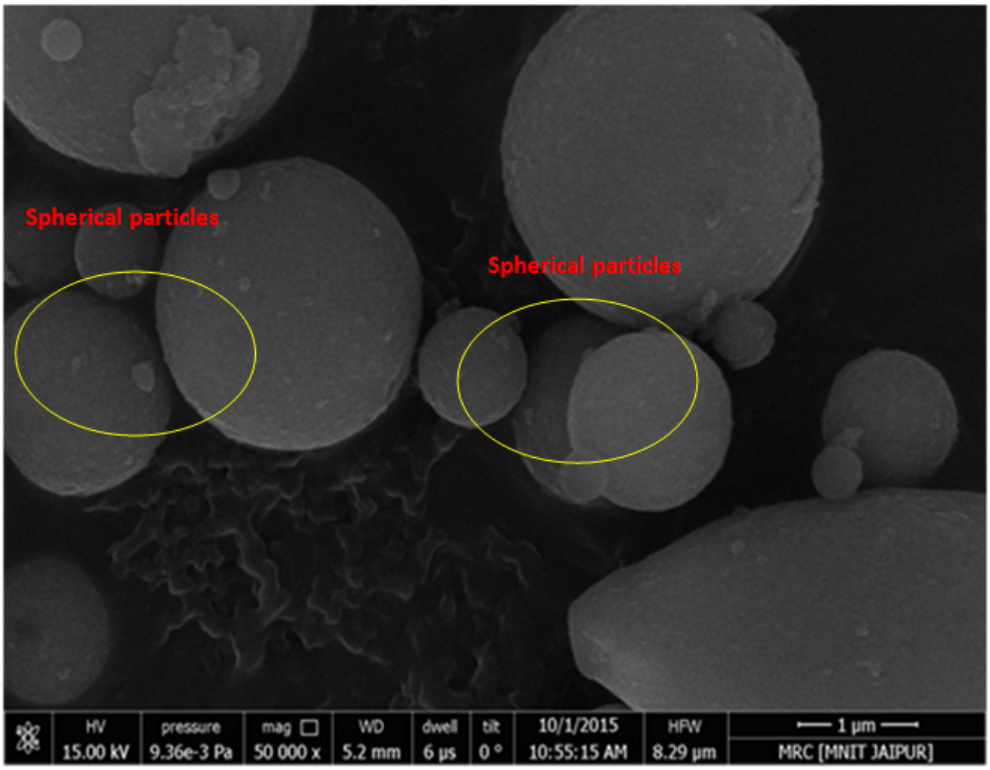

Figure 2.1: SEM view of fly ash (50000x)

The LOI value is very low because of the small amount of carbon present in the fly ash. The fly ash contains less than 10% calcium. Hence, according to ASTM C618-03 [130], it is said to be low calcium class F-type fly ash. The colour of the fly ash is dark grey, and its specific area is 428 m^2/kg. The fineness of the fly ash can be described by stating that 95% passes through a 45 μm sieve. Figures 2.1 and 2.2 show scanning electron microscopy (SEM) images of the fly ash at 50000x and 10000x. Fly ash is composed of spherical particles, as shown in Figure 2.1. These small glass spheres improve the fluidity and workability of fresh geopolymer concrete. The size of fly ash particles varies from 0.01 to 1000 μm. The fineness of fly ash particles increase the surface area and improve the particle packing in the binder paste which in turn contributes to its pozzolanic reactivity.

Figure 2.3 presents XRD images of fly ash at an angle of 2θ. The XRD analysis of fly ash reveals the presence of mullite, magnetite, hematite, and quartz. Ca, Si, Al, and C are present in the fly ash, as per the EDS analysis illustrated in Figure 2.4.

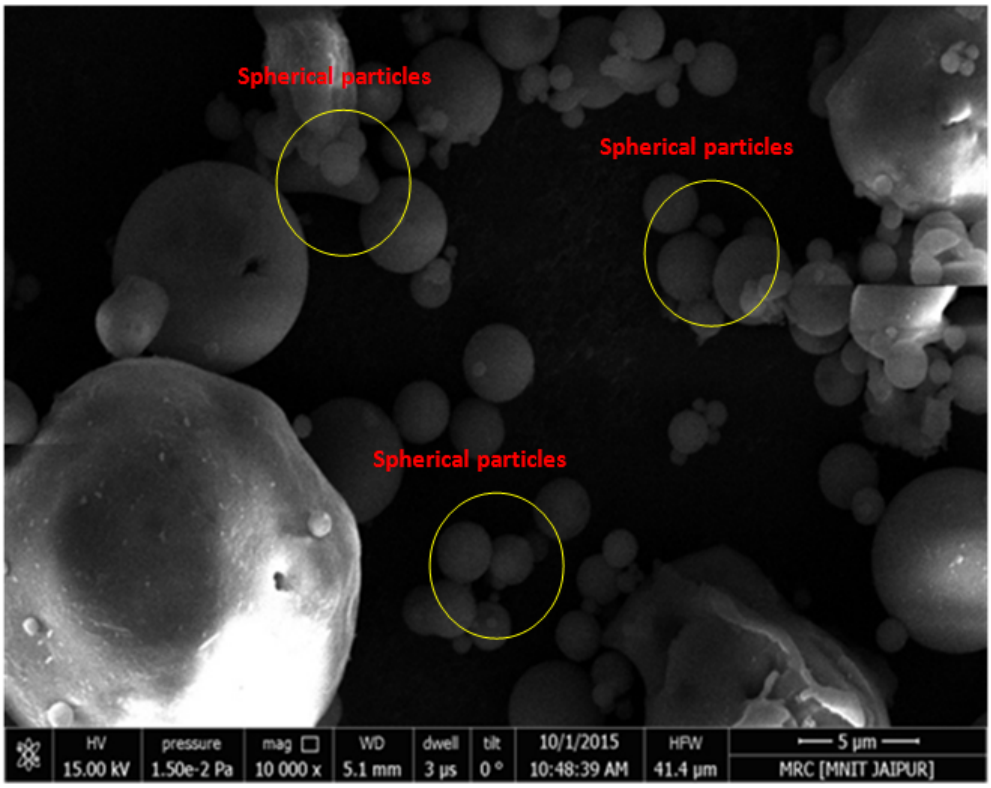

Figure 2.2: SEM view of fly ash (10000x)

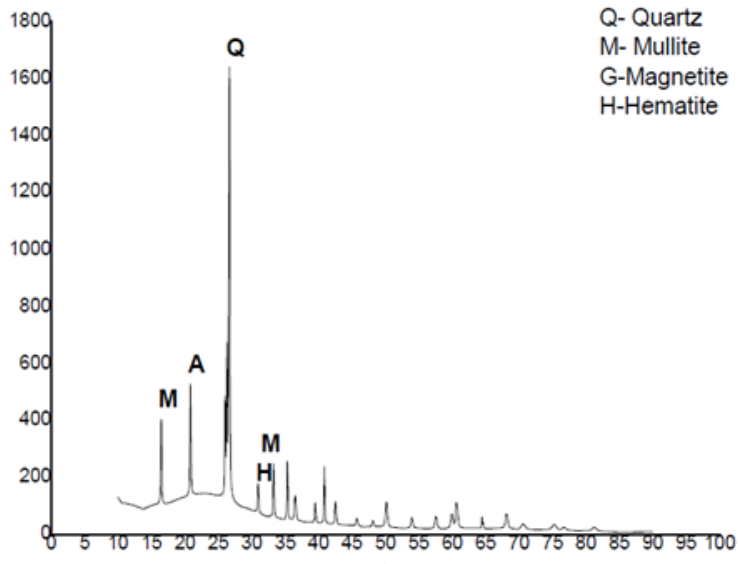

Figure 2.3: XRD analysis of fly ash

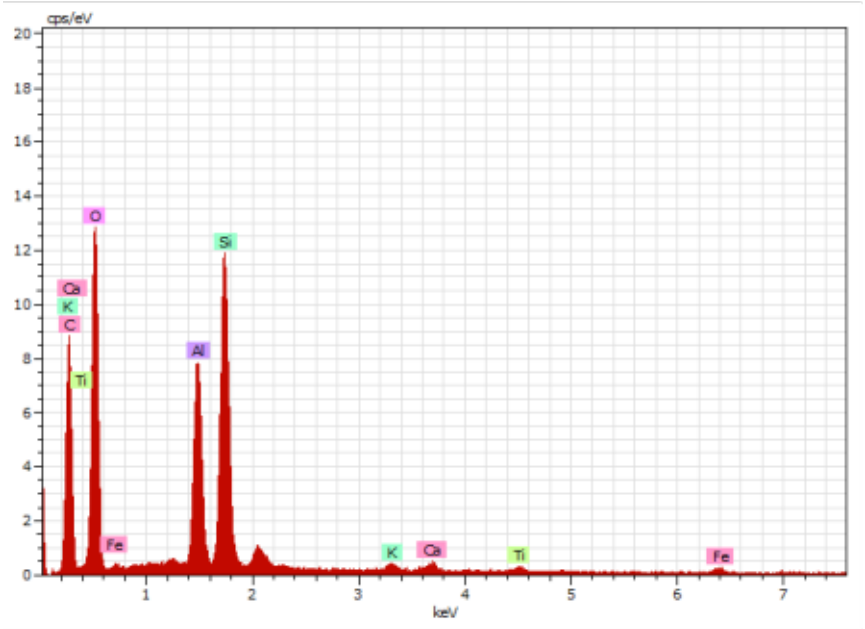

Figure 2.4: EDS analysis of fly ash

Table 2.1: Properties of fly ash

Sr. No.	Particulars	Unit	Fly ash Properties	Specification (IS:3812-1981) [129])
1	Colour	-	Dark grey	-
2	Loss on ignition (max)	%	0.94	5
3	SiO_2 + Al_2O_3 + Fe_2O_3	%	92.26	70 min. by mass
4	SiO_2	%	58.88	35 min. by mass
5	SO_3	%	0.74	3 max. by mass
6	Na_2O	%	0.5	1.5 max. by mass
7	MgO	%	1.64	5 max. by mass
8	Total Chlorides	%	0.025	0.05 max. by mass

2.2.2 Alkaline Solution

An alkaline solution was prepared by mixing sodium hydroxide liquid and sodium silicate solution.

- **Peculiarity of Sodium Hydroxide (NaOH)**

  Sodium Hydroxide (NaOH) is the most commonly used hydroxide activator in geopolymer synthesis, as it is readily available and is cheaper than other alkali hydroxides. Its low viscosity is an additional advantage as an activator. Therefore, NaOH flakes with 98% purity and a laboratory-grade reagent were used in this study.

  The NaOH solution was prepared by dissolving NaOH flakes into the water. The concentration of NaOH is expressed in terms of molarity, M. A concentration of 14M was achieved by dissolving 404 g of NaOH flakes in 1 L of water. The properties of the NaOH are given in Table 2.2.

Table 2.2: Properties of Sodium Hydroxide flakes

Properties	Value
NaOH (purity) (%)	98.0
Chloride (%)	1.0
Silicate (%)	0.015
(Na_2CO_3)(%)	0.015
Nitrate (NO_3)(%)	0.0055

- **Peculiarity of Sodium Silicate ($\mathbf{Na_2SiO_3}$)**

  A water glass form of sodium silicate was used for the current research. The properties of sodium silicate are listed in Table 2.3.

Table 2.3: Properties of Sodium Silicate solution

Properties	Value
Na_2O (%)	17.76
SiO_2 (%)	34.00
Water (%)	46.44
SiO_2/Na_2O	2.10
Specific gravity (g/cc)	1.48

2.2.3 Aggregates

Natural sand with a maximum particle size of 4.75 mm was used as a fine aggregate. Crushed basalt rock of 20 mm and 10 mm diameter was used as a coarse aggregate. Tests for fine and coarse aggregates were conducted as per the provisions of IS:2386-1963 [131] and IS:383-1970 [132], respectively. The physical properties of the river sand, sea sand and coarse aggregates are listed in Table 2.4. Sea sand obtained from the coast of Vapi (Gujarat) was used to produce the rice husk based geopolymer mortar and fly ash based geopolymer concrete. XRD analysis of the sand is illustrated in Figure 2.5. Potassium aluminium silicate, sodium silicate, silicon oxide, and manganese rhodium silicon were present in river sand and sea sand, as shown in Figures 2.5 and 2.6. The particle size distribution of Sea sand is shown in Figure 2.7.

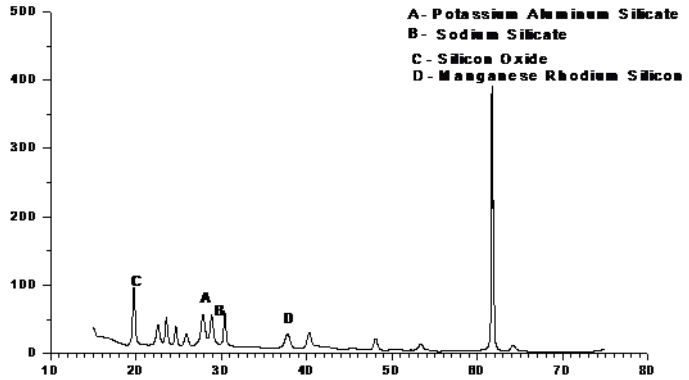

Figure 2.5: XRD analysis of sand

Table 2.4: Properties of the River Sand, Sea Sand, and Coarse Aggregate

Sr No.	Properties	River Sand	Sea Sand	Coarse Aggregate
1	Specific gravity	2.6	2.3	2.67
2	Water absorption (%)	0.8	0.95	0.5
3	Moisture content (%)	0.15	0.21	Nil
4	Fineness modulus	2.5	2.6	–
5	Zone	II	II	–

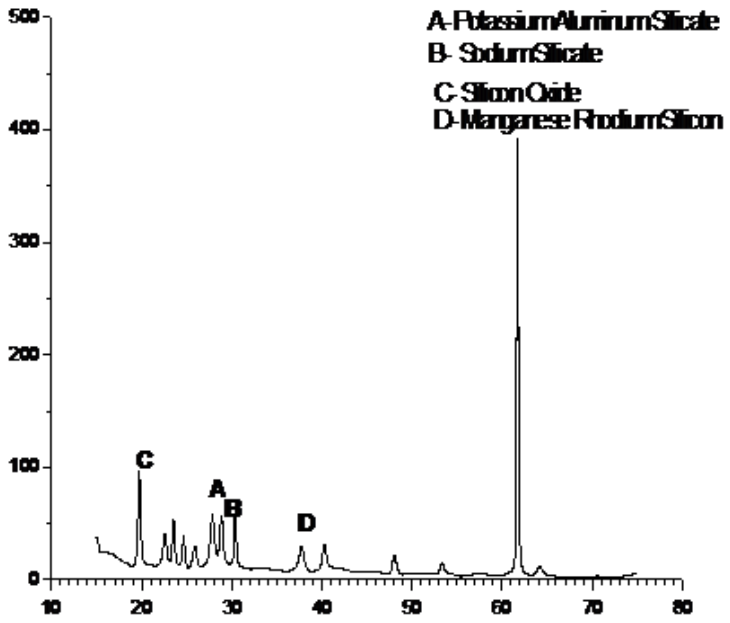

Figure 2.6: XRD analysis of sea sand

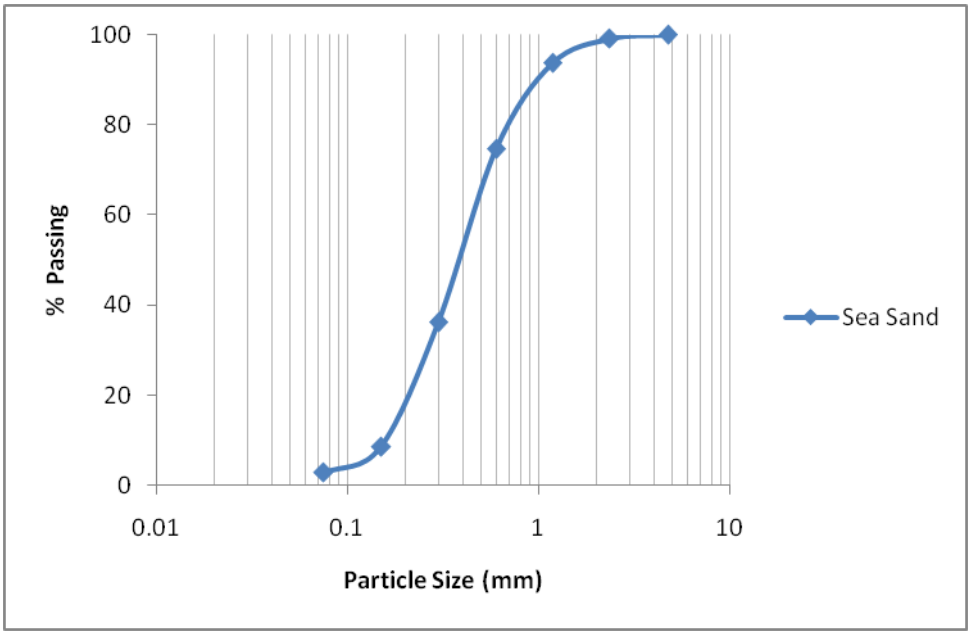

Figure 2.7: Particle size analysis of Sea Sand

2.2.4 Rubber Tyre Fibres

Rubber tyre fibres obtained from the mechanical grinding of rubber tyre waste were used as a partial replacement of the fine aggregates, as shown in Figure 2.8. These rubber tyre fibres were approximately 2–4 mm wide and up to 22 mm long, with a specific gravity of 1.09. Rubber fibres replaced 10%, 20% and 30% by weight of the fine aggregate. The particle size of the rubber tyre fibres is within Zone II, as per IS:383-1970 [132], as shown in Figure 2.9.

Figure 2.8: Rubber tyre fibres

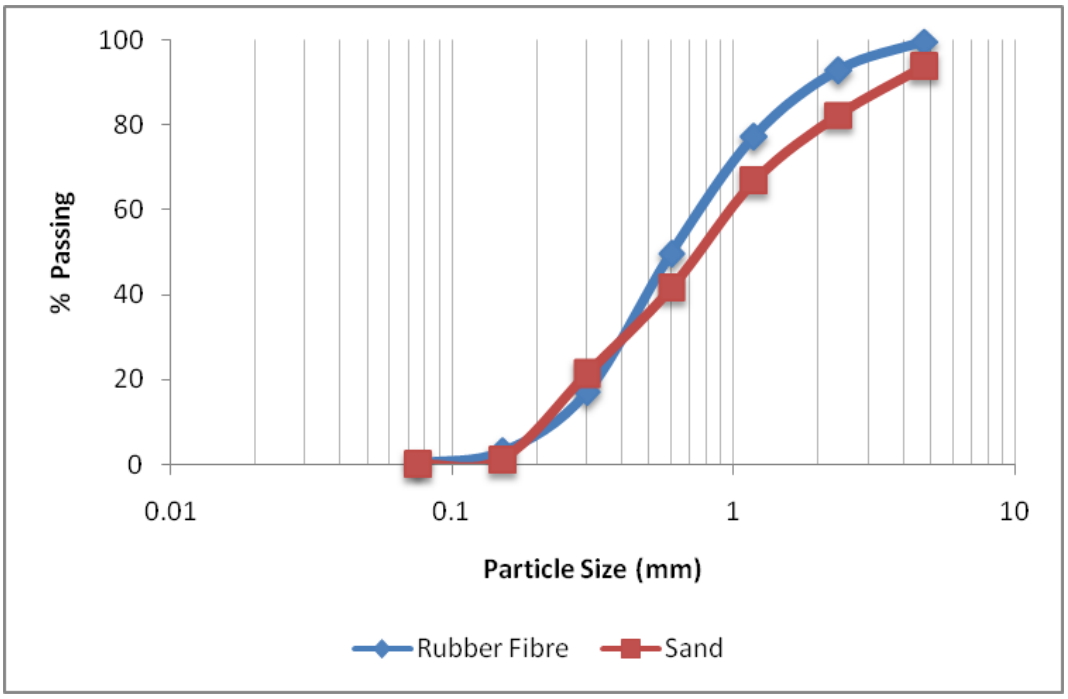

Figure 2.9: Particle size analysis of sand and rubber fibres

2.2.5 Superplasticizer

It was observed that any increase in rubber fibre content in the geopolymer concrete mix leads to a reduction in the slump value of the geopolymer concrete. Therefore, to achieve the desired slump value, naphthalene sulfonate-based superplasticizer was used as an admixture. This superplasticizer has a relative density of 1.26 ± 0.02 at 25°C, pH>6, and a chloride ion content of less than 0.2%.

2.2.6 Ordinary Portland Cement

OPC 43 grade "Binani cement conforming to IS-4031-1989 [133] was used to prepare cement concrete specimens. The properties of this cement are listed in Table 2.5.

Table 2.5: Properties of the Cement

Sr No.	Properties	Results
1	Fineness (percentage retained by 90 μm sieve)	0.9%
2	Setting Time	
	Initial	112 min
	Final	250 min
3	Soundness	5 mm
4	Specific Gravity	3.13
5	Compressive Strength	
	3 days	25.4 MPa
	7 days	36.24 MPa
	28 days	46.0 MPa

2.3 Process of Manufacturing Geopolymer Composites

Geopolymer mortar was produced by mixing fly ash and sand with alkaline solution. The mixture was dark grey in colour and homogenous in nature. An alkaline liquid to fly ash ratio of 0.4, water to fly ash ratio of 0.35, and fly ash to sand ratio of 1.0 were considered in manufacturing geopolymer mortar for the present study. The steps involved in the manufacture of geopolymer mortar are illustrated in Figure 2.10.

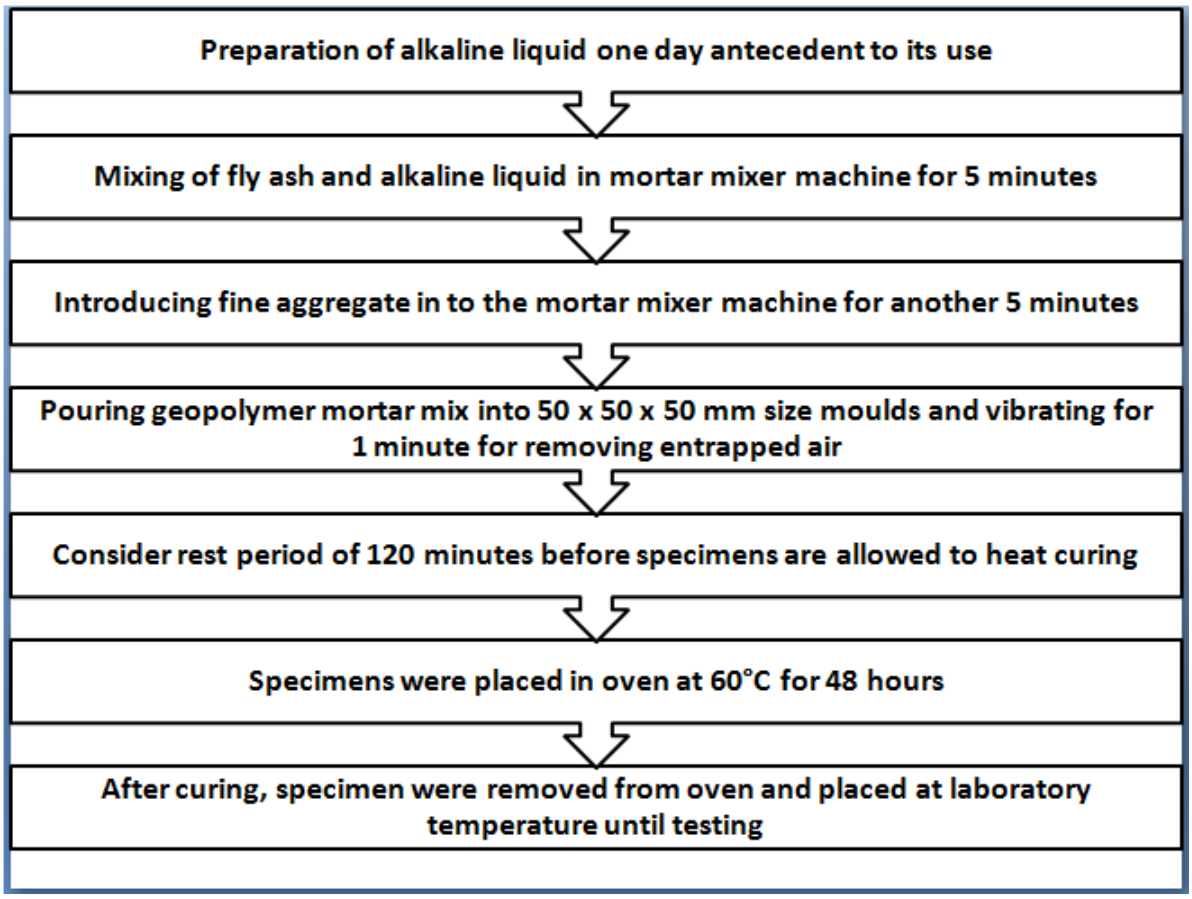

Figure 2.10: Steps involved in the manufacture of geopolymer mortar

The main difference between mixing geopolymer concrete and OPC concrete is the binder material. In the manufacturing of geopolymer concrete, fly ash that is rich in silicon and aluminium oxides reacts with the alkaline solution to produce geopolymeric bonds between the aggregates and other unreacted materials. In the mix design of geopolymer concrete, the total aggregates constituted 75% by mass of the concrete, which is similar to OPC concrete, i.e. 75–80%. Fine aggregates made up 35% of the total aggregate. The density of geopolymer concrete was similar to that of OPC concrete, i.e. 2500 kg/m^3. The mass of fly ash, sodium silicate, and sodium hydroxide required in the mix was calculated using parameters such as the alkaline solution

to fly ash ratio. To manufacture rubberized geopolymer concrete, locally available waste rubber tyre fibre particles were used to replace 10%, 20%, and 30% of the fine aggregates. The steps involved in manufacturing geopolymer concrete are shown in Figure 2.11.

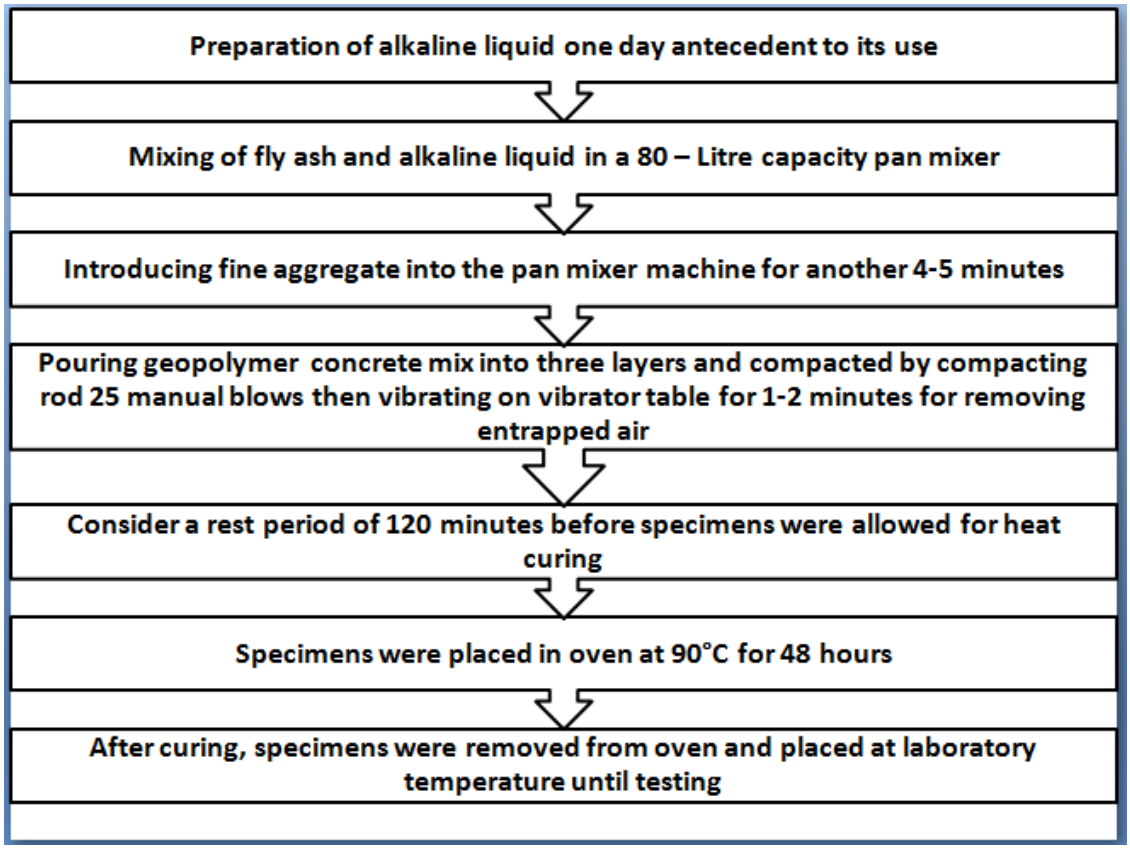

Figure 2.11: Steps involved in the manufacture of geopolymer concrete

2.3.1 Testing Procedure

Various strength, durability, and non-destructive tests were performed as per Indian standards and ASTM codes (see Table 2.6).

Table 2.6: Type of Test

Properties	Test	Testing Age (days)	Code
Fresh concrete properties	Slump	–	IS:1199-1959 [134]
	Compaction Factor	–	IS:1199-1959 [134]
Strength Properties	Compressive Strength	3, 7, 28, 90, 365	IS:516-1959 [135]
	Split Tensile Strength	28, 90, 365	IS:5816-1999 [136]
	Flexural strength	28, 90, 365	IS:516-1959 [135]
	Pull-off Strength	28	ASTM 1583-04 [137]
	Modulus of Elasticity	28	IS:516-1959 [135]
Durability Properties	Water Permeability	28	DIN-1048 [138]
	Shrinkage	7, 14, 21, 28, 35, 49	–
		63, 77, 91, 180, 365	–
	Sorptivity	28, 90, 365	ASTM C 1585-04 [139]
	Carbonation resistance	14, 21, 28, 35, 42, 56, 90	CPC-18 RILEM [140]
	Salt attack resistance	7, 28, 84, 162, 356	–
	Sulfate attack resistance	7, 28, 84, 162, 356	–
	Acid attack resistance	7, 28, 84, 162, 365	–
	Corrosion resistance	30, 60, 90, 120, 150	ASTM G 109 [141]
		180, 210, 240, 270, 300, 330, 360	ASTM C 876-15 [142]
	Chloride diffusion	28	ASTMC-1556 [143]
	Abrasion resistance	28	IS:1237-1980 [144]
Microstructural properties	SEM, FTIR, XRD	–	–

2.4 Fresh Properties

The workability of fresh concrete depends on factors such as stability, compactness, placement, and finishing. These aspects can be individually measured, but there is no method that can measure the workability of concrete in terms of all necessary aspects. Slump and compaction factor tests were conducted to study the fresh properties of the concrete. These tests to determine the fresh properties of concrete were carried out according to IS:1199-1959 [134] specifications.

2.4.1 Slump Flow Test

The slump is the vertical settlement of unsupported fresh concrete, flowing to the sides and sinking in height. It is an indication of the consistency or workability of cement concrete and provides an idea of the amount of water needed for concrete to be used for different applications. The concrete will be considered workable if it has no segregation or bleeding and can be easily mixed, placed, compacted, and finished. The workability of control OPC concrete having slump value 100 mm, whereas the workability of control geopolymer concrete is stickey stiff type with a slump value of 250 mm as observed in this study.

2.4.2 Compaction Factor Test

The basis of the compaction factor test lies in the definition that workability is a property of the concrete that determines the amount of work required to produce full compaction. In this test, one has to apply a standard amount of work to a standard quantity of concrete and measure the resulting compaction.

2.5 Strength Properties

After heat curing of the geopolymer specimen, strength properties were appraised according to Indian standards. Comprehensive details of the testing program are described below.

2.5.1 Compressive Strength Test

As per IS:516-1959 [135], cube specimens of size 100 mm were cast for compressive strength tests. All test specimens were finished with a steel trowel after casting. The specimens were covered with sheets soon after finishing to minimize the moisture loss. After a period of 48 h, the covers were taken and the geopolymer specimens stored at room temperature until the test. The OPC specimens were prepared and cured as conventinal method. Compressive strength tests were carried out after 3, 7, 28, 90, and 365 days. An automated compression testing machine (CTM) was used to test all specimens, as shown in Figure 2.12. Specimens were placed in the CTM such that the load was applied gradually at a rate of 140 kg/cm^2/min on smooth surfaces until the ultimate load resistance was reached. The average of three specimen values was considered to be the compressive strength. The compressive strength was calculated as a ratio of ultimate load resistance to the cross-sectional area of the specimen.

$$Compressive\ Strength(N/mm^2) = \frac{P \times 10^3}{A} \tag{2.1}$$

where

P = Failure load of cube (kN)

A = Area of cube (100 x 100) (mm^2)

Figure 2.12: Compression testing machine

2.5.2 Split Tensile Strength Test

This test was first developed in Brazil in 1943. The split tensile strength was measured as per IS:5816-1999 [136]. This test was used to determine the tensile strength of geopolymer concrete. Strength was measured 28, 90, and 365 days after the specimens were cast. Cylindrical specimens of 150 mm diameter and 300 mm height were used for the test. The test was performed by placing a cylindrical specimen horizontally between load surfaces in the CTM. A gradual load was applied along the longer face of the specimen, as demonstrated in Figure 2.13, until the specimen failed. The average of three tests was considered to be the split tensile strength of that particular specimen type. The split tensile strength was calculated as:

$$Split\ Tensile\ Strength(N/mm^2) = \frac{2 \times P \times 10^3}{\Pi \times L \times d} \tag{2.2}$$

where

P = Failure load of cylinder (kN)

L = Height of specimen (300 mm)

d = Diameter of specimen (150 mm)

Figure 2.13: Testing of split tensile strength

2.5.3 Flexural Strength Test

Flexural strength tests were performed as per IS:516-1959 [135] specifications. The three-point loading method was adopted, whereby the bearing surfaces of the supporting and loading rollers were cleaned and loose sand or other material was removed from the surface of the specimen. Specimens of size 100 x 100 x 500 mm were used for this test, as per IS:516-1959 [135] specifications. The test specimen beam was placed in such a way that the load was applied on the uppermost surface of the beam along two lines 13.3 cm apart. The axis of the specimen was aligned with the axis of the loading device. A gradual load was applied at a rate of 180 kg/cm^2/min until the specimen failed. The average of three specimens was considered as the flexural strength of that concrete type. The test setup used for this test is shown in Figure 2.14. The flexural strength of the beam specimens was calculated as:

Figure 2.14: Testing of flexural strength

$$Flexural\ Strength(N/mm^2) = \frac{P \times 10^3 \times L}{b \times d^2} \tag{2.3}$$

where

P = Failure load of beam (kN)

L = Span of beam (400 mm)

b = Width of beam (100 mm)

d = Depth of specimen (100 mm)

2.5.4 Modulus of Elasticity Test

The slope of the stress-strain curve with a proportional limit of the material is known as the modulus of elasticity. Tests were performed at CTAE, Udaipur as per IS:516-1959 [135] specifications. Cylindrical specimens of 150 mm diameter and 300 mm height were used for this test. A cylindrical specimen was placed vertically between two frames of a compressometer, as shown in Figure 2.15. Spacers were used to hold the frames in the proper position. A dial gauge was attached to the compressometer to show the change in length of the specimen when subjected to a compressive load. The compressive load was applied gradually to the test specimen at a rate of 140 kg/cm^2/min over three loading-unloading cycles. The average of three cycles was used to calculate the modulus of elasticity according to the following formula.

$$Es = \frac{(\sigma 2 - \sigma 1)}{(\epsilon - 0.000050)} \tag{2.4}$$

where

$\sigma 2$ = Stress corresponding to 40% of ultimate load

$\sigma 1$ = Stress corresponding to longitudinal strain

ϵ = Longitudinal strain produced by stress $\sigma 2$

Figure 2.15: Testing the modulus of elasticity

2.5.5 Pull-off Strength Test

The pull-off test determines the tensile strength of concrete near to the prepared surface or cover zone of the concrete. In this test, 50 mm diameter steel discs were bonded to the concrete surface with the help of epoxy adhesive material one day prior to testing. The test setup is illustrated in Figure 2.16. The force required to pull off the concrete surface was recorded as the pull-off load. The pull-off strength was calculated as the pull-off load per unit area. The average of three specimens was considered to be the pull-off strength of the specimen.

Figure 2.16: Pull-off test setup

2.6 Durability Properties

The durability of concrete is defined as its ability to resist weathering, abrasion, chemical attachment, or any other process of deterioration.

2.6.1 Water Permeability Test

Permeability is defined as the ability of a fluid to pass through concrete. It is the most important parameter of durability. Tests were performed as per DIN 1048-1991 [138]. Concrete cubes of size 150 x 150 x 150 mm were dried in a drying chamber for 14 days. The depth of water penetration inside the concrete under sustained pressure was determined from this test. The test setup is shown in Figure 2.17. A sustained pressure of 5 bars (0.5 N/mm^2) was applied in the vertical plane along the mould-filled direction for 3 days. After 3 days, the depth of penetration was measured by splitting the cube in half. The average of three cubes was considered as the depth of penetration.

Figure 2.17: DIN 1048 water permeability test setup

2.6.2 Carbonation Test

Carbonation is the progressive neutralization of the alkali in the concrete cover by acidic gases from external sources (mainly carbon dioxide from the atmosphere). This method of testing consists of determining the depth of the carbonated layer on the surface of hardened concrete by means of an indicator. To perform an accelerated carbonation test, cubes of 100 x 100 x 100 mm were split into four prisms of size 50 x 50 x 100 mm. Each prism specimen was allowed to dry in a drying chamber for 2 weeks until a constant weight was achieved. After drying, two coats of epoxy paint were applied on the longitudinal side of the specimens to resist the penetration of carbon dioxide, leaving the top and bottom sides of each specimen to be penetrated by carbon dioxide. After specimen preparation, the specimens were kept in a carbonation chamber, as shown in Figure 2.18. The carbonation chamber maintains a level of 5% carbon dioxide, relative humidity of 50 ± 5%, and a temperature of 25 ± 1°C. The depth of carbonation was measured after 14, 21, 28, 35, 42, 56 and 90 days of CO_2 exposure. The depth of carbonation was measured by splitting the specimens in half and instantly spraying a phenolphthalein indicator over the broken surface. This

indicator was prepared by mixing 1% phenolphthalein in 70% ethyl alcohol. After spraying the indicator, the depth of carbonation was measured from the top and bottom face of the specimen. The average of three specimen readings was considered to be the depth of carbonation of that mix.

Figure 2.18: Carbonation chamber setup

2.6.3 Drying Shrinkage Test

This test examined the effect of rubber tyre fibre replacement on the shrinkage of geopolymer concrete and cement concrete. Three prisms of size 75 x 75 x 285 mm were cast for each mix. After curing, Demec studs were pasted 212 ± 1 mm apart on the top surface of each specimen, as demonstrated in Figure 2.19. Shrinkage strain was measured using a mechanical strain gauge 3 days after casting. The next shrinkage strain measurement was taken 4 days after casting, and this was considered to be the first day shrinkage measurement of the specimen. Measurements were taken every day in the first week, once a week up to the fourth week, once every two weeks up to the twelfth week, and then once every four weeks. The gauge has a minimum resolution of 0.002 mm. Specimens were kept in a laboratory room where the temperature was

maintained at 25°C and the relative humidity was 50–60%.

Figure 2.19: Shrinkage specimen with studs

2.6.4 Sulfate Resistance Test

The sulfate resistance of the control geopolymer concrete and cement concrete was examined by means of the change in mass and residual compressive strength. To measure the change in mass and residual compressive strength, 100 x 100 x 100 mm cubes were cast. After curing, each specimen was weighed to give an initial weight. Seven days after curing, the specimens were immersed in a 5% concentration of sodium sulfate solution, as shown in Figure 2.20. The volume of sodium sulfate was calculated on the basis of the volume of sulfate solution to the volume of the specimen (4:1 ratio). The solution was replaced every month to maintain its concentration. The change in mass, change in length, and residual compressive strength were measured after 7, 28, 84, 162, and 365 days exposure. After exposure, the residual compressive strength was determined by testing the specimens in the saturated surface dry (SSD) condition. To measure the change in mass, specimens were removed from the solution, wiped properly, and their weight was measured. The specimens were then returned to soak in the sulfate solution. The change in length was measured using a mechanical strain gauge.

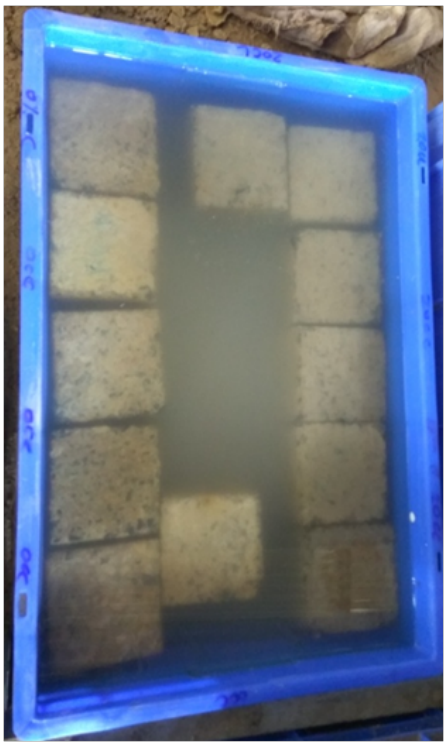

Figure 2.20: Specimen immersed in sulfate solution

2.6.5 Acid Resistance Test

Resistance against acid was evaluated using geopolymer and cement concrete specimens of size 100 x 100 x 100 mm. Solutions of 3%, 5% and 10% concentration sulfuric acid were prepared to examine the effect of acid attack on the specimens, as shown in Figure 2.21. Seven days after casting, the initial weight or dry weight of the specimens was measured, and then the specimens were soaked in solution for 7, 28, 84, 162, and 365 days. At every selected exposure period, the change in mass and residual compressive strength was measured. To maintain the pH level, the solution was stirred every week and replaced every month. The volume of solution was determined on the basis of the volume of solution to the volume of the specimen (4:1 ratio). After selected exposure periods, the specimens were removed from solution and wiped to remove solution from their surface. The weight of the specimens was measured in SSD condition and the residual compressive strength was tested. The average of three specimens was considered to be the residual compressive strength

after acid exposure.

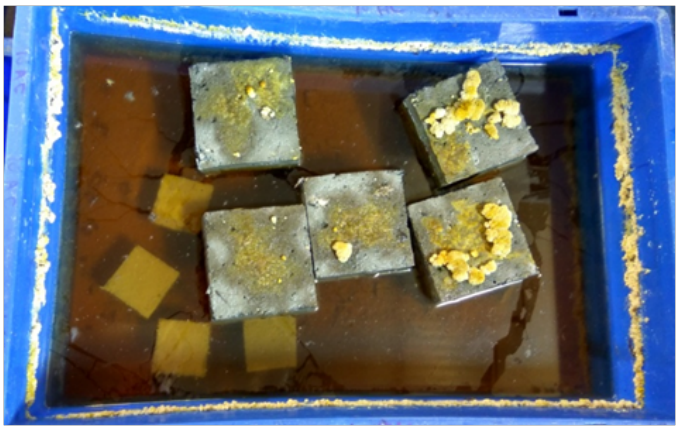

Figure 2.21: Specimens immersed in sulfuric acid

2.6.6 Salt Attack Resistance Test

Salt attack resistance was measured using 100 x 100 x 100 mm cubes for 7, 28, 84, 162, and 365 days exposure periods. A solution was prepared with a 5% concentration of sodium chloride, as shown in Figure 2.22. After curing, the specimens were weighed to determine their initial weight. The specimens were then immersed in solution for a selected exposure period. The change in mass and residual compressive strength was determined from this test. For the change in mass, specimens were removed from solution, wiped, and weighed. For the change in compressive strength, the specimens were tested in SSD condition. The average of three specimens was considered to be the residual compressive strength after exposure.

Figure 2.22: Specimens immersed in salt solution

2.6.7 Abrasion Resistance Test

This test was conducted as per IS:1237-1980 [144] specifications on 100 x 100 x 100 mm specimens. Abrasion resistance refers to the depth of wear. Figure 2.23 shows the arrangement of this test. Firstly, specimens were dried at 110 ± 5°C for 24 h in a drying chamber and weighed to the nearest 0.1 g to give W_1. Twenty g of abrasive aluminium powder was evenly spread over the grinding path of the disc on an abrasion testing machine. The specimen was fixed in a holding device under a 300 N load. The grinding disc was then put in motion at 30 revolutions per minute and the abrasive powder was continuously spread over the grinding path. After every 22 revolutions, the disc was stopped, the abrasive powder was removed from the grinding path, and a fresh 20 g of abrasive powder was placed in the path. At every 22 revolutions, the specimen was turned about the vertical axis by 90°. This process was repeated nine times, thereby giving a total of 220 revolutions. After the abrasion test, the specimen was reweighed to the nearest 0.1 g. Thus, the depth of wear was determined as

$$T = \frac{W_1 - W_2 \times V_1}{W_1 \times A} \tag{2.5}$$

where

T = Average loss of thickness (mm)

W_1 = Initial weight of the specimen (g)

W_2 = Mass of specimen after abrasion (g)

V_1= Initial volume of the specimen (mm^3)

A = Surface area of the specimen (mm^2)

Figure 2.23: Abrasion testing machine

2.6.8 Water Sorptivity Test

Water sorptivity tests were carried out to determine the rate of absorption (sorptivity) of water through the capillary suction of concrete. The tests were performed as per ASTM C1585-04 [139] specifications. Specimens of 100 ± 6 mm diameter and 50 ± 3 mm height were used for this test. In this test, specimens were placed in a dessicator at a temperature of 50 ± 2 °C. To control the relative humidity, potassium bromide solution was placed in the bottom of the dessicator in such a way that the test specimens could not contact the solution. Each specimen was placed in the dessicator for 3 days. After 3 days, the specimen was placed inside a sealable container to prevent contact with free air. A separate container was used for each specimen. The container was stored at 23 ± 2°C for at least 15 days prior to the sorptivity procedure. Specimens were removed from storage and their mass was recorded before sealing. The bottom and side surfaces of each specimen were sealed with a sealing material, as shown in Figure 2.24. The mass of each sealed specimen was measured and this was recorded as the initial mass for the water sorptivity calculations. The bars were placed as support at the bottom of a pan. The pan was filled with distilled water to a level of 1–3 mm above the top of the support bars. A timing device was started and placed immediately at the test surface of the specimen on the support device. The time and date of initial contact with water were recorded. The mass was recorded at intervals of 60 s, 5 min, 10 min, 20 min, 30 min, 60 min, and then every hour up to 6 h and once a day up to 7 days. One final reading was taken on day 9. To weigh the specimens, they were taken from the tray, excess water removed, and their dry surface placed on an electronic pan balance. The absorbing surface was not touched, and the specimen was returned to the tray within 15 s.

Figure 2.24: Sorptivity test

2.6.9 Chloride Ion Migration Test

This test examined the resistance of the concrete samples against chloride ion penetration. Concrete cores of 60 mm diameter and 150 mm height were used in this test. Each core was cut to a thickness of 40 mm with the help of a cutting saw machine. The side and ends of the specimen were covered with silicon sealant and masking tape, respectively. The specimen was then fitted with a rubber gasket and masking tape applied to the top and bottom before being immersed in distilled water. As shown in Figure 2.25, the chloride cell consisted of two parts: an upstream part acting as the anode was filled with 3% concentration of sodium chloride solution, whereas a downstream part was filled with distilled water to act as the cathode. The specimen was placed between migration cells and a potential difference of 30 V DC was applied. The chloride ion concentration was examined in the upstream cell using a titration method. Similarly, in the downward part, the chloride ion concentration was calculated every 4 h until the steady state condition was reached. Titration was done by taking 20 ml samples of solution from the downstream cell and adding potassium chromate indicator. Silver nitrate solution (0.0141 N) was then slowly added to

the flask until the solution had a reddish tinge, and the volume of silver nitrate was recorded. The chloride ion concentration in the downstream cell was calculated as The steady state chloride diffusion coefficient D_{ssm} was evaluated as

$$D_{ssm} = \frac{R \times T \times L \times J}{Z \times F \times \Delta E \times C_1} \tag{2.6}$$

where

T = Average value of initial and final temperatures in anolyte solution (K)

R = Gas constant = 8.314 J/(K.mol^{-1})

L = Thickness of the specimen (mm)

Z = Absolute value of ion valence (for chloride, Z=1)

F = Faraday constant = $9.648x10^4$ J/(V.mol)

J = Chloride flux j (mol/cm^{2}s)

C_1 = Chloride ions activity

E = Absolute potential difference between the upstream solution and downstream solution measured using two reference electrodes.

Figure 2.25: Chloride migration setup

2.6.10 Corrosion Test

To study the resistance of concrete to steel corrosion, a chloride-induced corrosion method was used. To examine the corrosion induced by embedded steel in concrete, we used a macro-cell corrosion method and a half-cell potential method. In these methods, 12 mm diameter thermomechanically treated reinforcements of length 350 mm were first cleaned using a wire brush. Then, 70 mm at each end of the bar was coated with epoxy paint to prevent corrosion of that portion of the bar outside the specimen. Specimens of 250 x 205 x 135 mm with a ponding well of 15 mm at the top were cast, as shown in Figure 2.26. The bars were arranged such that 350 mm of their length was within the specimen, with one bar centrally placed at the top and two bars placed with 30 mm cover at the bottom, such that the middle portion of the bars (210 mm length) was exposed to corrosion and 70 mm protruded from each side of the concrete specimen. The top bars acted as the anode and the bottom bars acted as the cathode. Before casting the corrosion specimens, the reinforcement bars were weighed properly. After curing, the bottom and side faces of the specimens were coated with epoxy paint. Specimens were kept in a temperature- and humidity-controlled room. The electrical connection between the anode and cathode was ensured by means of a soldered wire. A 100 mm resistor was connected between the top and bottom bars. The 15 mm depression at the top of each specimen was filled with a 3% concentration of sodium chloride solution, and the specimens were subjected to alternate wetting and drying cycles for up to 2 weeks.

The macro-cell corrosion test was used to measure the potential difference between the anode and cathode bars across the resistor with the help of a voltmeter. The test was conducted as per ASTM G 109 [141]. An initial reading was taken 7 days after ponding the sodium chloride over the specimen. To take a reading, the common terminal of the voltmeter was connected with the bottom bars. A negative voltage corresponds to a positive galvanic current, that is, the top bar is the anode. Readings were taken every month over a period of 12 months. The macro-cell current was calculated as

$$I_j = \frac{V_j}{100} \tag{2.7}$$

where

I_j = Macro-cell current

V_j = Measured voltage across 100 Ω resistor

Half-cell potential measurements were taken at the top steel bar according to the reference copper-copper sulfate electrode (CSE) by placing it in the ponding with 3% concentrated sodium chloride solution. Before taking the reading, the top and bottom bars were disconnected and the current was allowed to stabilize. The potential reading was taken once every month with the help of a voltmeter. ASTM C 876 [142] provides guidelines on the probability of corrosion based on the potential difference values with respect to CSE. If potentials over an area are above −200 mV, there is a probability of greater than 90% that no reinforcing steel corrosion is occurring in that area at the time of measurement. If the potentials over an area are in the range −200 to −350 mV, then corrosion of the reinforcing steel in that area is uncertain. If potentials over an area are less than −350 mV, then there is a greater than 90% probability that reinforcing steel corrosion is occurring in that area at the time of measurement.

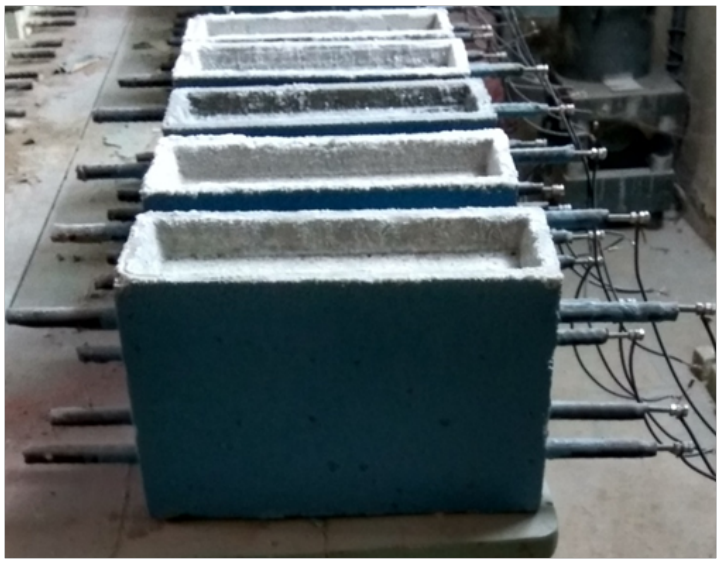

Figure 2.26: Corrosion test specimen

2.7 Taguchi Experimental Design Method

The aim of this study was to determine the effect of different factors on the compressive strength of rubberized geopolymer concrete. In the present study, eight factors were examined using the Taguchi DOE method: curing time, curing temperature, Na_2SiO_3/NaOH ratio, alkaline liquid/fly ash ratio, plasticizer, rest period, water content, and NaOH concentration. Each factor was considered at three levels. Table 2.7 lists the factors and the levels of each factor.

Table 2.7: Factors and their levels

Factors	Level-I	Level-II	Level-III
Factor-A Alkaline liquid/ Fly ash ratio	0.3	0.35	0.4
Factor-B Na_2SiO_3/NaOH	1.5	2.0	2.5
Factor-C NaOH concentration (M)	10M	12M	14M
Factor-D Curing temperature (°C)	60	75	90
Factor-E Curing time (hr)	24	48	72
Factor-F Water content (%)	15	20	25
Factor-G Rest period (Days)	0	1	2
Factor-H Plasticizer (%)	2	3	4

In this study, Taguchi orthogonal arrays, L_{27} (3^{13}), were used in a full factorial design [145]. Orthogonal arrays for a total of 27 mixes of rubberized geopolymer concrete are given in Table 2.8. Primary tests were conducted to specify the range of each factor. The variables of each of the mixes are presented in Table 2.9. A total of 27 trial mixes of rubberized geopolymer concrete (T-1 to T-27) were used to evaluate the compressive strength of various parameter combinations. The rubberized geopolymer was produced by replacement of fine aggregate with 10% rubber fiber. The tests were carried out on three standard cube specimens per mix. Table 2.10 presents the mix proportions for the trial variables.

Table 2.8: Properties of Taguchi orthogonal arrays (L_{27})

Trial Mixes	Factor-A	Factor-B	Factor-C	Factor-D	Factor-E	Factor-F	Factor-G	Factor-H	Compressive strength (N/mm2)	S/N ratio
T-1	1	1	1	1	1	1	1	1	34.85	30.84406
T-2	1	1	1	1	2	2	2	2	36.00	31.12605
T-3	1	1	1	1	3	3	3	3	33.11	30.39918
T-4	1	2	2	2	1	1	1	2	43.71	32.81162
T-5	1	2	2	2	2	2	2	3	42.59	32.58615
T-6	1	2	2	2	3	3	3	1	44.00	32.86905
T-7	1	3	3	3	1	1	1	3	51.26	34.19557
T-8	1	3	3	3	2	2	2	1	59.08	35.42881
T-9	1	3	3	3	3	3	3	2	53.18	34.51497
T-10	2	1	2	3	1	2	3	1	48.83	33.77373
T-11	2	1	2	3	2	3	1	2	49.00	33.80392
T-12	2	1	2	3	3	1	2	3	46.11	33.2759
T-13	2	2	3	1	1	2	3	2	41.35	32.32951
’ T-14	2	2	3	1	2	3	1	3	42.00	32.46499
T-15	2	2	3	1	3	1	2	1	43.11	32.69156
T-16	2	3	1	2	1	2	3	3	41.35	32.32951
T-17	2	3	1	2	2	3	1	1	46.11	33.2759
T-18	2	3	1	2	3	1	2	2	45.59	33.17739
T-19	3	1	3	2	1	3	2	1	41.18	32.29373
T-20	3	1	3	2	2	1	3	2	42.26	32.51859
T-21	3	1	3	2	3	2	1	3	43.00	32.66937
T-22	3	2	1	3	1	3	2	2	45.63	33.18501
T-23	3	2	1	3	2	1	3	3	44.00	32.86905
T-24	3	2	1	3	3	2	1	1	43.11	32.69156
T-25	3	3	2	1	1	3	2	3	44.63	32.99254
T-26	3	3	2	1	2	1	3	1	45.00	33.06425
T-27	3	3	2	1	3	2	1	2	43.83	32.83543

Table 2.9: Factors and variables of trials

Trial Mixes	Ratio of Alkaline Liquid /Fly Ash Factor-A	Ratio of Na_2SiO_3 / NaOH Factor-B	NaOH Concentration (M) Factor-C	Curing Temperature (°C) Factor-D	Curing Time (h) Factor-E	Water Content (%) Factor-F	Rest Period (days) Factor-G	Plasticizer (%) Factor-H
T-1	0.3	1.5	10	60	24	15	0	2
T-2	0.3	1.5	10	60	48	20	1	3
T-3	0.3	1.5	10	60	72	25	2	4
T-4	0.3	2	12	75	24	15	0	3
T-5	0.3	2	12	75	48	20	1	4
T-6	0.3	2	12	75	72	25	2	2
T-7	0.3	2.5	14	90	24	15	0	4
T-8	0.3	2.5	14	90	48	20	1	2
T-9	0.3	2.5	14	90	72	25	2	3
T-10	0.35	1.5	10	60	24	20	2	2
T-11	0.35	1.5	10	60	48	25	0	3
T-12	0.35	1.5	10	60	72	15	1	4
T-13	0.35	2	12	75	24	20	2	3
T-14	0.35	2	12	75	48	25	0	4
T-15	0.35	2	12	75	72	15	1	2
T-16	0.35	2.5	14	90	24	20	2	4
T-17	0.35	2.5	14	90	48	25	0	2
T-18	0.35	2.5	14	90	72	15	1	3
T-19	0.4	1.5	10	60	24	20	1	2
T-20	0.4	1.5	10	60	48	25	2	3
T-21	0.4	1.5	10	60	72	15	0	4
T-22	0.4	2	12	75	24	25	1	3
T-23	0.4	2	12	75	48	15	2	4
T-24	0.4	2	12	75	72	20	0	2
T-25	0.4	2.5	14	90	24	25	1	4
T-26	0.4	2.5	14	90	48	15	2	2
T-27	0.4	2.5	14	90	72	20	0	3

Table 2.10: Mix proportions for variables of trials (per m^3)

Trial Mixes	Fly Ash	Aggregate			Rubber Fibre	NaOH	Sodium Silicate	Extra Water	Super-Plasticizer
		20 mm	10 mm	Fine Sand					
	(kg)	(kg)	(kg)	(kg)	(kg)	(kg)	(kg)	(kg)	(kg)
T-1	480.77	731.25	487.5	656.25	26.83	57.69	86.54	72.12	9.62
T-2	480.77	731.25	487.5	656.25	26.83	57.69	86.54	96.15	14.42
T-3	480.77	731.25	487.5	656.25	26.83	57.69	86.54	120.19	19.23
T-4	480.77	731.25	487.5	656.25	26.83	57.69	96.15	72.12	19.42
T-5	480.77	731.25	487.5	656.25	26.83	48.08	96.15	96.15	19.23
T-6	480.77	731.25	487.5	656.25	26.83	48.08	96.15	120.19	9.62
T-7	480.77	731.25	487.5	656.25	26.83	41.21	103.02	72.12	19.23
T-8	480.77	731.25	487.5	656.25	26.83	41.21	103.02	96.15	9.62
T-9	480.77	731.25	487.5	656.25	26.83	41.21	103.02	120.19	14.42
T-10	462.96	731.25	487.5	656.25	26.83	64.81	97.22	92.59	9.26
T-11	462.96	731.25	487.5	656.25	26.83	64.81	97.22	115.74	13.89
T-12	462.96	731.25	487.5	656.25	26.83	64.81	97.22	69.44	18.52
T-13	462.96	731.25	487.5	656.25	26.83	54.01	108.02	92.59	13.89
T-14	462.96	731.25	487.5	656.25	26.83	54.01	108.02	115.74	18.52
T-15	462.96	731.25	487.5	656.25	26.83	54.01	108.02	69.44	9.26
T-16	462.96	731.25	487.5	656.25	26.83	46.3	115.74	92.59	18.52
T-17	462.96	731.25	487.5	656.25	26.83	46.3	115.74	115.74	9.26
T-18	462.96	731.25	487.5	656.25	26.83	46.3	115.74	92.59	13.89
T-19	446.43	731.25	487.5	656.25	26.83	71.43	107.14	111.61	8.93
T-20	446.43	731.25	487.5	656.25	26.83	71.43	107.14	66.96	13.39
T-21	446.43	731.25	487.5	656.25	26.83	71.43	107.14	89.29	17.86
T-22	446.43	731.25	487.5	656.25	26.83	59.52	119.05	111.61	13.39
T-23	446.43	731.25	487.5	656.25	26.83	59.52	119.05	66.96	17.86
T-24	446.43	731.25	487.5	656.25	26.83	59.52	119.05	89.29	8.93
T-25	446.43	731.25	487.5	656.25	26.83	51.02	127.55	111.61	17.86
T-26	446.43	731.25	487.5	656.25	26.83	51.02	127.55	66.96	8.93
T-27	446.43	731.25	487.5	656.25	26.83	51.02	127.55	89.29	13.39

2.7.1 Results and Analysis

In the present study, the results of three runs were used to select the optimum level. To determine the importance of the control factor on the compressive strength of rubberized geopolymer concrete, the signal-to-noise ratio (S/N ratio) was analysed. There are three types of S/N ratio in the Taguchi method:

1. Lower is better,

2. Normal is better,

3. Higher is better.

As the target of this study is to achieve the highest compressive strength, the third type (higher is better) was used. According to this type,

$$S/N Ratio = -10 \log \left(1/N \times \sum_{i=1}^{n} \times 1/Y_i^2\right) \tag{2.8}$$

where n is the number of repetitions under the same experimental conditions and Y represents the results of measurement, i.e. Y is the compressive strength of the fly ash-based geopolymer paste.

Figure 2.27 shows the average compressive strength of 27 trial mixes of rubberized geopolymer concrete at age 7 days. The highest compressive strength of 59.08 MPa was achieved by mix T-8, which has an alkaline liquid to fly ash ratio of 0.3, sodium hydroxide to sodium silicate ratio of 2.5, NaOH concentration of 14M, curing temperature of 90°C, curing time of 48 h, water content of 20%, rest period of 1 day, and 2% superplasticizer. The increase in compressive strength indicates an increase in the rate of geopolymerization reaction. ANOVA results show that the curing temperature has a significant effect on the compressive strength of geopolymer concrete. This is because heat is the primary component in the completion of the geopolymerization process.

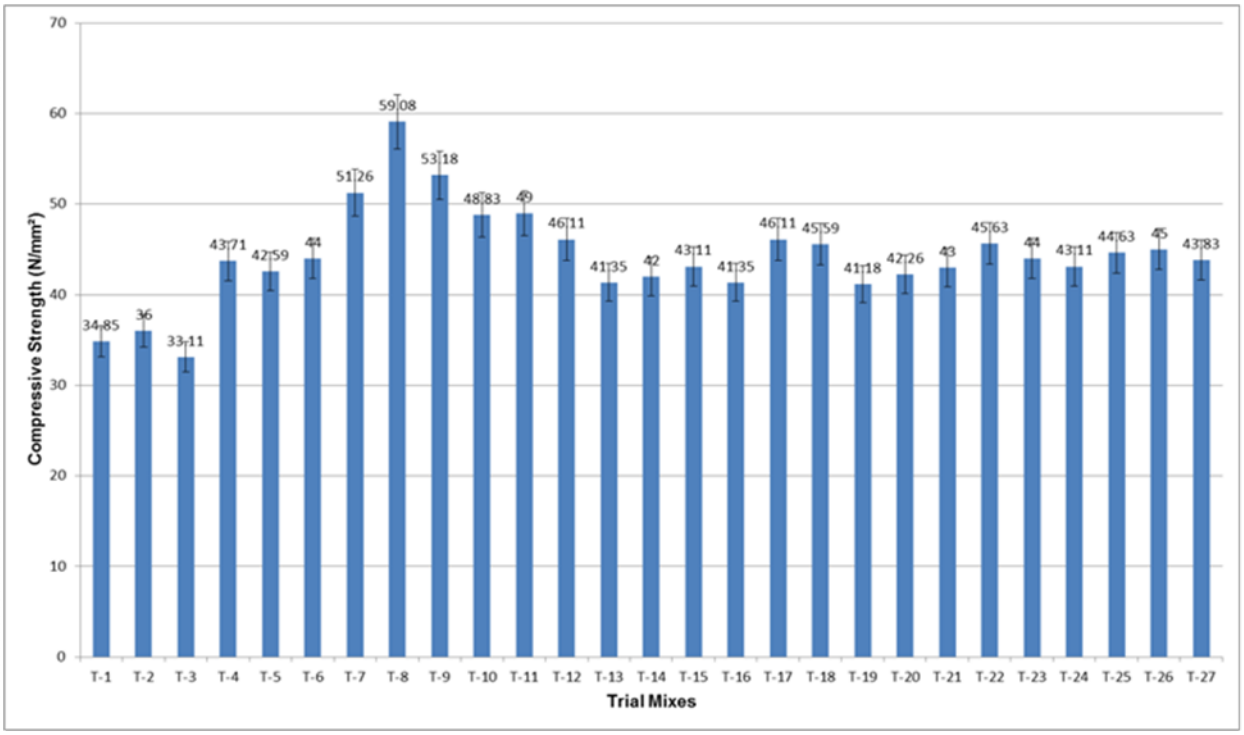

Figure 2.27: Compressive strength of rubberized geopolymer concrete for each trial mix (bars indicate standard deviation)

Table 2.8 gives the S/N ratios for each trial mix, calculated on the condition that larger is better. The maximum S/N ratio is given by mix T-8, which indicates that this mix has the highest compressive strength among all the rubberized geopolymer concrete mixes considered. The effect of each factor on the compressive strength of rubberized geopolymer concrete is calculate by Taguchi software (shown 2.28). An increase in the alkaline solution to fly ash ratio (factor-A) from 0.3 to 0.4 marginal change in the compressive strength of concrete observed. Increases in the sodium silicate to sodium hydroxide ratio (factor-B), NaOH concentration (factor-C), and curing temperature (factor-D) also increase the compressive strength of rubberized geopolymer concrete. The curing time (factor-E) was increased up to 72 h, and it was found that any increase beyond 48 h reduces the strength. This is because water evaporates from the specimen surface. A limited water content is required in rubber-

ized geopolymer concrete, because water is expelled during the reaction of the alkaline solution and source material. A water content (factor- F) of up to 25% was found to help in producing dense concrete without any loss of strength. It was further observed that the addition of up to 3% superplasticizer (factor-H) increased the compressive strength of geopolymer concrete.

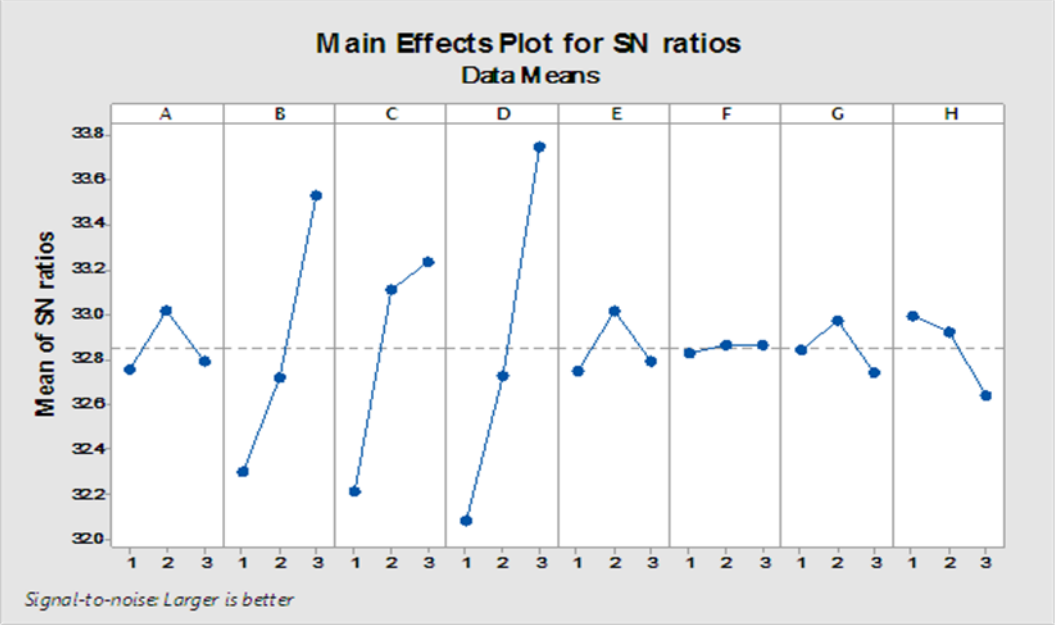

Figure 2.28: Effect of each factor on compressive strength of rubberized geopolymer concrete

From the ANOVA reported in Table 2.11, it is clear that the main contributing factors are the sodium silicate to sodium hydroxide ratio, NaOH concentration, and curing temperature. The ranking of all eight factors is given in Table 2.12.

Table 2.11: ANOVA for means

Source	DF	Seq SS	Adj SS	Adj MS	F	P
A	2	6.497	6.497	3.249	1.14	0.358
B	2	184.218	184.218	92.109	32.33	0.000
C	2	136.827	136.827	68.414	24.02	0.000
D	2	334.713	334.713	167.356	58.75	0.000
E	2	11.171	11.171	5.586	1.96	0.191
F	2	0.717	0.717	0.358	0.13	0.883
G	2	6.725	6.725	3.362	1.18	0.347
H	2	17.595	17.595	8.797	3.09	0.090
Residual Error	10	28.488	28.488	2.849		
Total	26	726.950				

In this Table 2.11, DF denotes degrees of freedom, SS denotes the sum of squares, and P denotes the percentage.

Table 2.13 indicates the optimum value of each factor that gives the highest compressive strength according to the Taguchi method. These results prove that the Taguchi method is suitable for determining the maximum compressive strength for rubberized geopolymer concrete. The results of Taguchi method have been compared with experimental results and there is good agreement between results.

Table 2.12: Parameters rank as per ANOVA method

Levels	Factor-A	Factor- B	Factor-C	Factor-D	Factor-E	Factor-F	Factor-G	Factor-H
1	32.75	32.30	32.21	32.08	32.75	32.83	32.84	32.99
2	33.01	32.72	33.11	32.73	33.02	32.86	32.97	32.92
3	32.79	33.53	33.23	33.75	32.79	32.87	32.74	32.64
Delta	0.26	1.23	1.02	1.67	0.26	0.04	0.23	0.35
Rank	6	2	3	1	5	8	7	4

Table 2.13: Selected parameter values using the Taguchi method and ANOVA

Trial Mixes	Ratio of Alkaline Liquid /Fly Ash Factor-A	Ratio of Na_2SiO_3 / NaOH Factor-B	NaOH Concentration (M) Factor-C	Curing Temperature (°C) Factor-D	Curing Time (h) Factor-E	Water Content (%) Factor-F	Rest Period (days) Factor-G	Plasticizer (%) Factor-H
Optimum Value	0.3	2.5	14	90	48	20	1	2

2.8 Conclusion

The material characterization of fly ash, sodium silicate, sodium hydroxide, cement, fine aggregate (river sand and sea sand), and rubber fibres was investigated by carrying out experiments for specific gravity, particle size analysis, water absorption, moisture content, and fineness. The microstructural behaviour of fly ash, river sand, and sea sand was examined by SEM and XRD. The following conclusions can be drawn from the results in this chapter.

1. The specific gravity of rubber fibre is lower than that of fine aggregate. Thus, the density of rubberized geopolymer concrete is expected to be lower than that of the control geopolymer concrete.

2. Rubber fibres have a high carbon content, which helps to produce softer geopolymer concrete. Therefore, the compressive strength of rubberized geopolymer concrete is expected to be lower than that of the control geopolymer concrete.

3. The particle size distribution of rubber fibre particles and river sand particles conform to the Zone II requirements of the Indian Standards for fine aggregates.

4. The Taguchi method was used to determine the effect of the curing time, curing temperature, Na_2SiO_3/NaOH ratio, alkaline liquid/fly ash ratio, plasticizer, rest period, water content, and NaOH concentration. The main contributing factors were found to be the sodium silicate to sodium hydroxide ratio, NaOH concentration, and curing temperature.

Chapter 3

Strength and Durability Properties

3.1 Prelude

This chapter describes the mix design process developed for rubberized geopolymer concrete and the control geopolymer concrete based on the optimal parameters identified by a preliminary investigation. This chapter also investigates the mechanical and durability properties of compressive strength, flexural strength, split tensile strength, pull-off strength, abrasion resistance, modulus of elasticity, permeability, resistance to sulfate, acid, salt, shrinkage, corrosion, and chloride diffusion, and sorptivity and carbonation studies of control and rubberized geopolymer concrete. The results are compared with the values obtained for OPC concrete.

3.2 Mix Design Proportioning

3.2.1 OPC Concrete Mix Design

The proportions for the OPC concrete mix were calculated based on IS 10262-2009 [146]. The volume of aggregate used in the OPC concrete was in the range 75–80% by mass. The fine aggregate was taken as 35% of the total aggregate. The mixture proportion of OPC concrete is listed in Table 3.1. Waste rubber tyre fibres were used in concrete as a partial replacement for the fine aggregate. The mixture proportions of OPC concrete are similar to those of the geopolymer concrete mixture, except for

the water content (see Table 3.1).

3.2.2 Geopolymer Concrete Mix Design

The geopolymer concrete mix design was finalized, according to the past studies of Rangan [147], by considering parameters such as NaOH concentration, alkaline liquid ratio, alkaline liquid to fly ash ratio, aggregate content, and water content. The main difference between geopolymer concrete mix design and OPC concrete mix design is the binding material. In geopolymer concrete, a source material such as fly ash, which is rich in silica and alumina, reacts with an alkaline liquid to form geopolymeric bonds between the aggregates, geopolymer paste, and other unreacted materials that make up geopolymer concrete [148]. In geopolymer concrete, the aggregate was taken as 75–78% of the entire mix by mass. This value is similar to that used in OPC concrete. Fine aggregate constituted 35% of the total aggregate. The average density of the geopolymer concrete was similar to that of OPC concrete, i.e. 2500 kg/m^3 [149].

3.2.3 Concrete Mix Proportioning for Geopolymer Concrete

The following constituents were derived from Taguchi method for mix design of each mix:

- Ratio of alkaline liquid to fly ash by mass: 0.4
- Ratio of sodium silicate to sodium hydroxide: 2.5
- Concentration of sodium hydroxide solution: 14 M
- Admixture dosage: 2%
- Additional water content: 5%
- Curing temperature: 90°C
- Curing time: 48 h
- Rest period: 1 day

- **Design of geopolymer concrete**

a. Density:

From a literature survey it was found that the density of fly ash-based geopolymer concrete varies from 2300–2500 kg/m^3. Therefore, the density of the geopolymer concrete is assumed to be 2500 kg/m^3.

b. Aggregates:

The combined mass of the aggregates was selected to be 75% of the mass of the concrete.

Total aggregate = 0.75 x 2500 = 1875 kg/m^3

Fine aggregate was assumed to make up 35% of the total mass of aggregate.

Fine aggregate = 0.35 x 1875 = 656 kg/m^3

For rubberized geopolymer concrete, 10%, 20%, and 30% of the fine aggregate was replaced by rubber tyre fibres.

Coarse aggregate = 1875 - 656 = 1218 kg/m^3

We assume a composition of 60% of 20 mm aggregate and 40% of 10 mm aggregate by mass.

20 mm aggregate = 1218 x 0.6 = 731 kg/m^3

10 mm aggregate = 1218 - 731 = 487 kg/m^3

c. Fly ash:

Mass of fly ash and alkaline liquid = 2500 - 1875 = 625 kg/m^3

Ratio of alkaline solution to fly ash is 0.4.

Mass of fly ash = 625/(0.4+1) = 446 kg/m^3

d. Alkaline liquid:

Mass of alkaline liquid = 625 - 446 = 179 kg/m^3

Ratio of sodium silicate solution to sodium hydroxide solution = 2.5

Mass of sodium hydroxide solution = 179/(2.5+1) = 51 kg/m^3

Mass of sodium silicate solution = 179 - 51 = 128 kg/m^3

e. Extra water:

It has been observed that 5% extra water is essential to achieve the required workability of the geopolymer concrete.

Extra water = 446 x 0.05 = 22.3 kg/m^3.

f. Superplasticizer:

Naphthalene sulfonate-based superplasticizer of about 2% of the mass of fly ash was used for the mix design.

Superplasticizer = 446 x 0.02 = 8.93 kg/m^3

Based on this mix design process, the final mass of the constituents was calculated as described in Table 3.1.

Table 3.1: Mix design proportion (per m^3)

Mixes	Fly Ash	Cement	Aggregate			Rubber Fibre	NaOH	Sodium Silicate	Extra Water	Super-Plasticizer
	(kg)	(kg)	20 mm (kg)	10 mm (kg)	Fine Sand (kg)	(kg)	(kg)	(kg)	(kg)	(kg)
GP-0	446.43	–	731.25	487.5	656.25	0.0	51.02	127.55	22.32	8.93
GP-10	446.43	–	731.25	487.5	629.35	26.9	51.02	127.55	22.32	8.93
GP-20	446.43	–	731.25	487.5	602.55	53.80	51.02	127.55	22.32	8.93
GP-30	446.43	–	731.25	487.5	575.64	80.71	51.02	127.55	22.32	8.93
CC-0	–	446.43	731.25	487.5	656.25	0.0	–	–	160.71	8.93
CC-10	–	446.43	731.25	487.5	629.35	26.9	–	–	160.71	8.93
CC-20	–	446.43	731.25	487.5	602.55	53.80	–	–	160.71	8.93
CC-30	–	446.43	731.25	487.5	575.64	80.71	–	–	160.71	8.93

3.3 Compressive Strength Test

The compressive strength of geopolymer concrete measured at 3, 7, 28, 90, and 365 days is shown in Figure 3.1. It can be seen that, as the percentage of waste rubber tyre increases from 0-30%, the compressive strength decreases at all ages. In geopolymer concrete, a fast geopolymerization process takes place due to a chemical reaction between the alkaline solution and source material, resulting in 95% compressive strength gain in only 7 days [39, 50, 88]. After 28 days, the compressive strength of geopolymer concrete varies from 30–54 MPa depending on the rubber fibre content. The compressive strength depends on the geopolymeric mechanism developed in the geopolymer paste. After 365 days, the compressive strength had only increased marginally because of the speed of the polymerization process. This is because of the chemical reduction of the geopolymer gel with age and the development of a crystalline structure [148,151]. The compressive strength of geopolymer concrete depends on factors such as NaOH concentration, alkaline liquid ratio, curing temperature, and aggregate content. From past studies, it is clear that increasing each of these factors will increase the compressive strength of the geopolymer concrete [147, 151].

Figure 3.2 shows the compressive strength of OPC concrete measured at 28, 90, and 365 days. The compressive strength of OPC concrete depends on the hydration mechanism of cement paste [150]. The hydration process is a long, continuous process whereby the pores of the concrete gradually fill, resulting in strength gains over the course of a year [150]. The compressive strength of OPC concrete decreases when waste rubber fibres are introduced. The compressive strength of OPC concrete is less than that of geopolymer concrete.

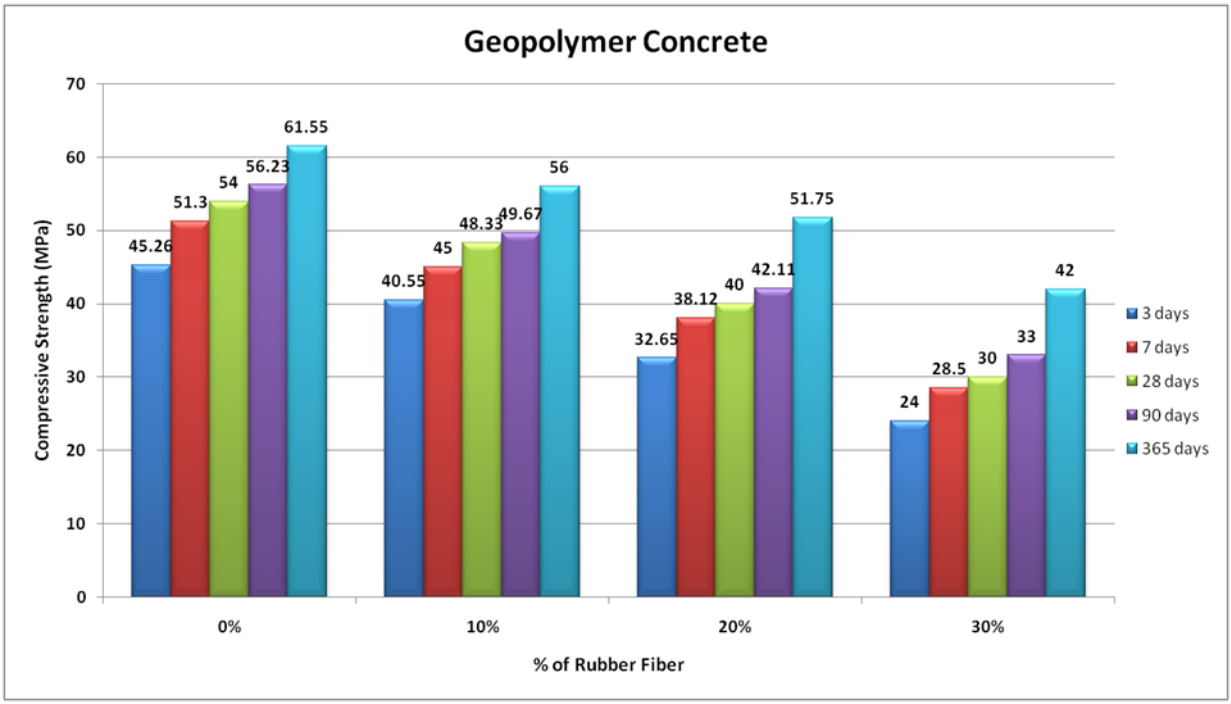

Figure 3.1: Compressive strength of geopolymer concrete

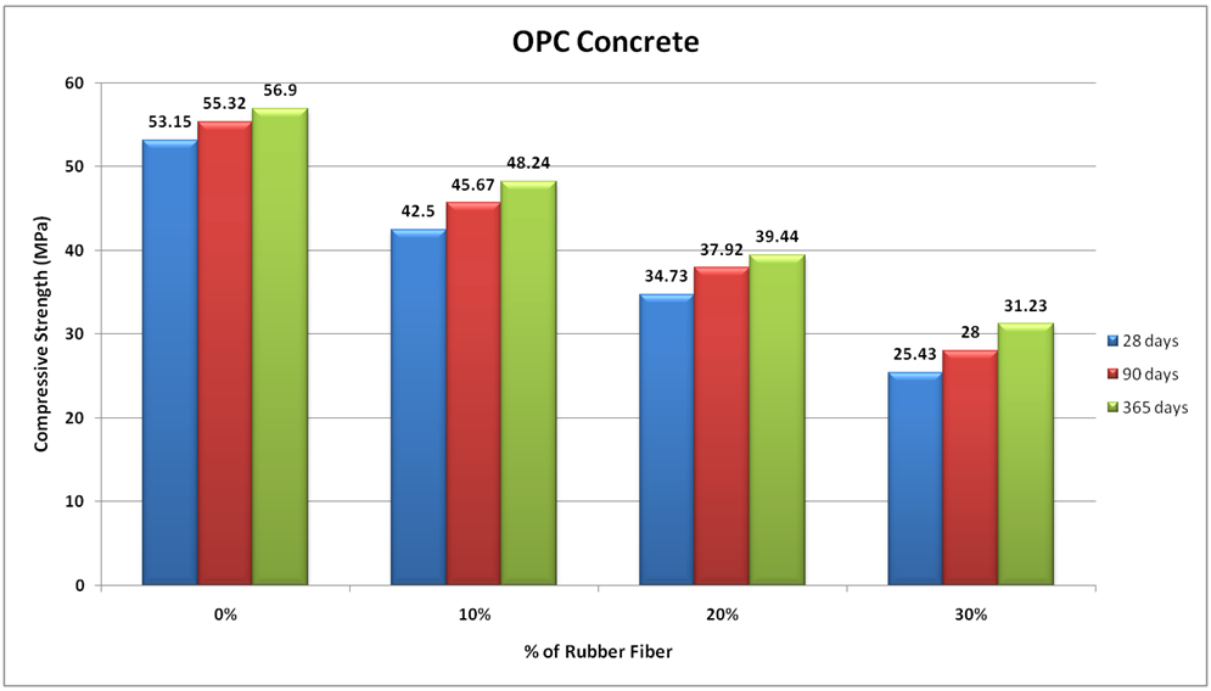

Figure 3.2: Compressive strength of OPC concrete

3.4 Split Tensile Strength Test

Figures 3.3 and 3.4 show the split tensile strength of geopolymer concrete and OPC concrete after 28, 90, and 365 days. The split tensile strength of all mixes is ranges from 5.34–5.49 MPa after 365 days. The geopolymer concrete exhibits higher tensile strength than OPC concrete because of the good bonding between the geopolymer paste and aggregate. Similar observations have been reported in past studies [148, 151, 154]. The highest split tensile strength was found in the 30% rubber fibre mix after 365 days, and the lowest tensile strength was found in the control geopolymer concrete after 28 days. A gradual increase in split tensile strength can be observed as the rubber fibre content increases from 0–30%. Similar results have been reported in previous study [152]. In geopolymer concrete, there is a high level of geopolymeric bonding between the geopolymer paste and aggregate; therefore, during testing, when the cylinder was broken in half, none of the aggregate was pulled out, unlike for the OPC concrete. This is a result of the chemical bonding between the alkaline liquid and aggregate [155].

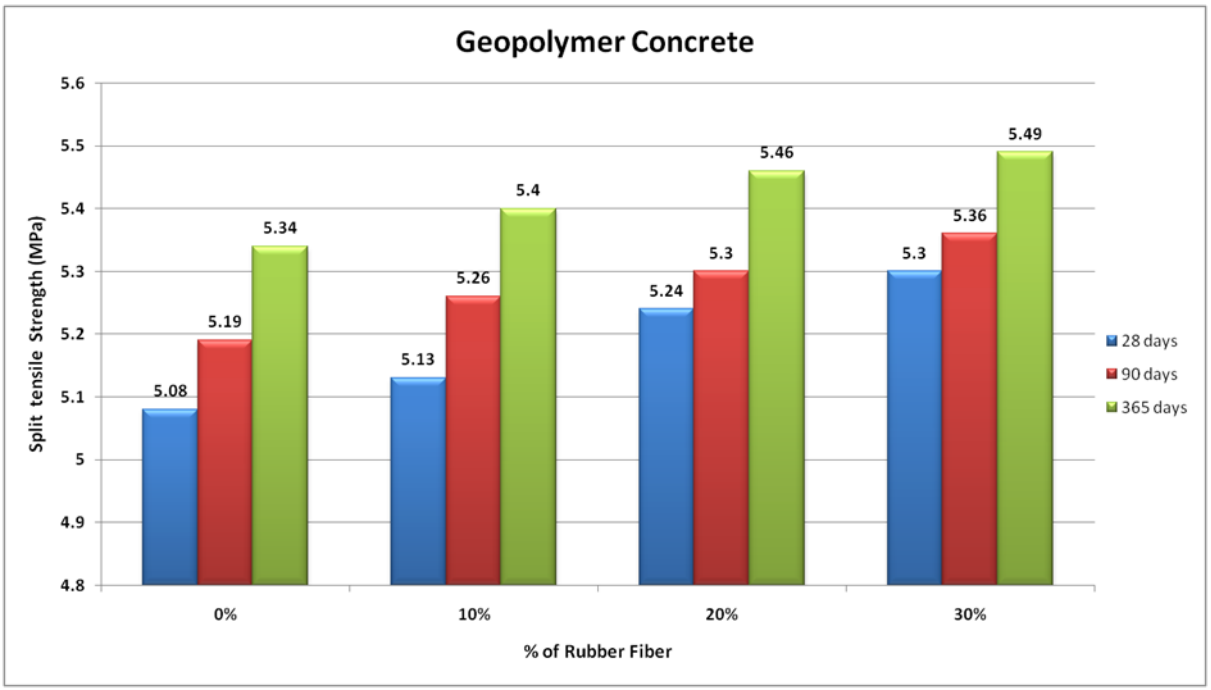

Figure 3.3: Split tensile strength of geopolymer concrete

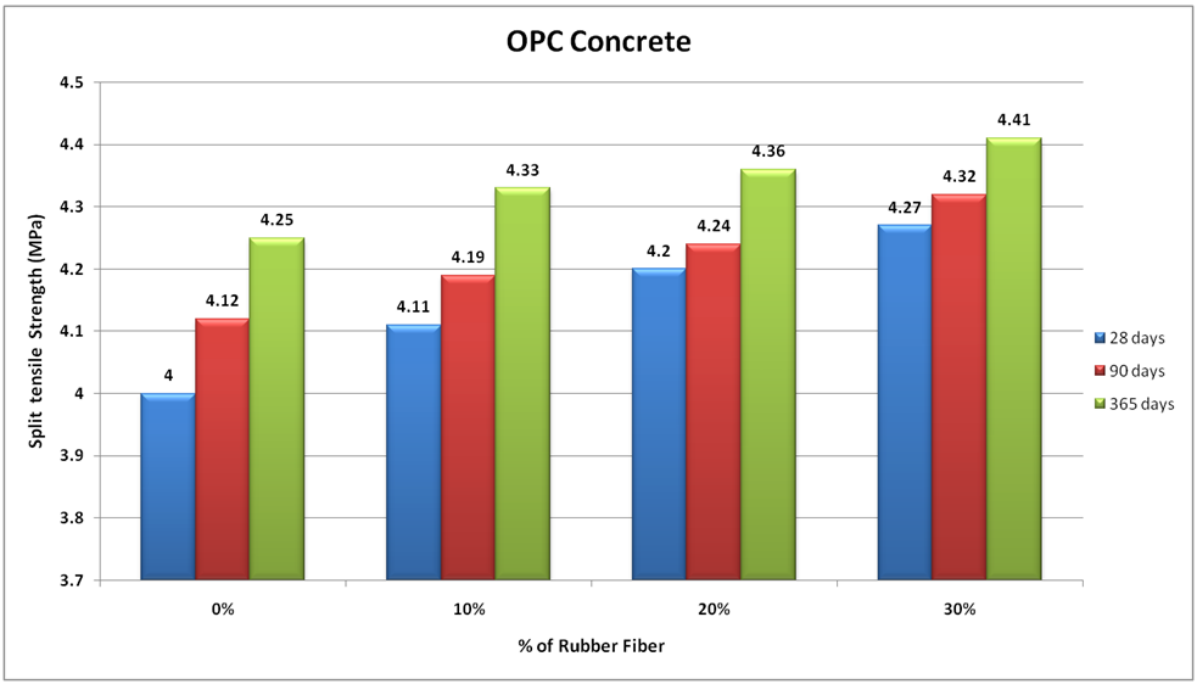

Figure 3.4: Split tensile strength of OPC concrete

3.5 Flexural Strength Test

Figures 3.5 and 3.6 show the average flexural strength of the geopolymer concrete and OPC concrete. The flexural strength of the geopolymer concrete varies from 6.45–9.97 MPa, whereas that for OPC concrete varies from 5.35–6.86 MPa. The flexural strength increases with age in all mixtures. This proves that the flexural strength of geopolymer concrete is higher than that of OPC concrete. Similar evidence has been reported in previous research [151, 153]. The tension properties of geopolymer concrete, such as flexural and tensile strength, are superior to those of OPC concrete because of the better bonding between the geopolymeric paste and aggregate. The flexural strength also increases with percentage of rubber fibres for both OPC and geopolymer concrete.

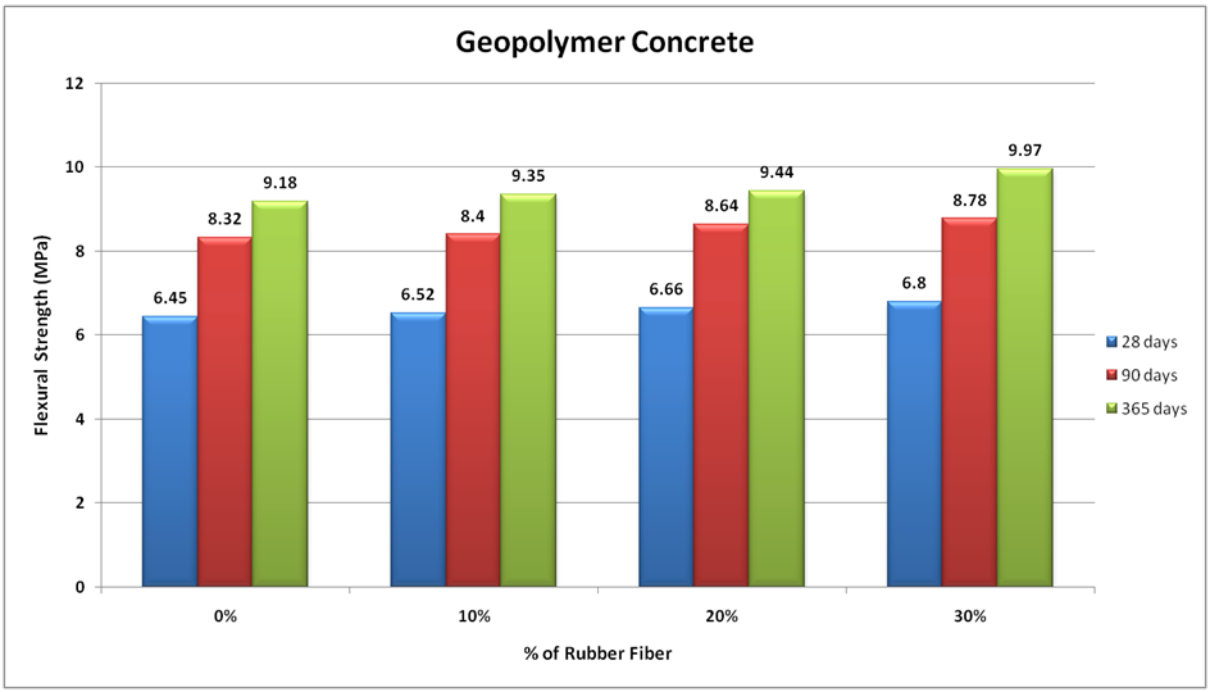

Figure 3.5: Flexural strength of geopolymer concrete

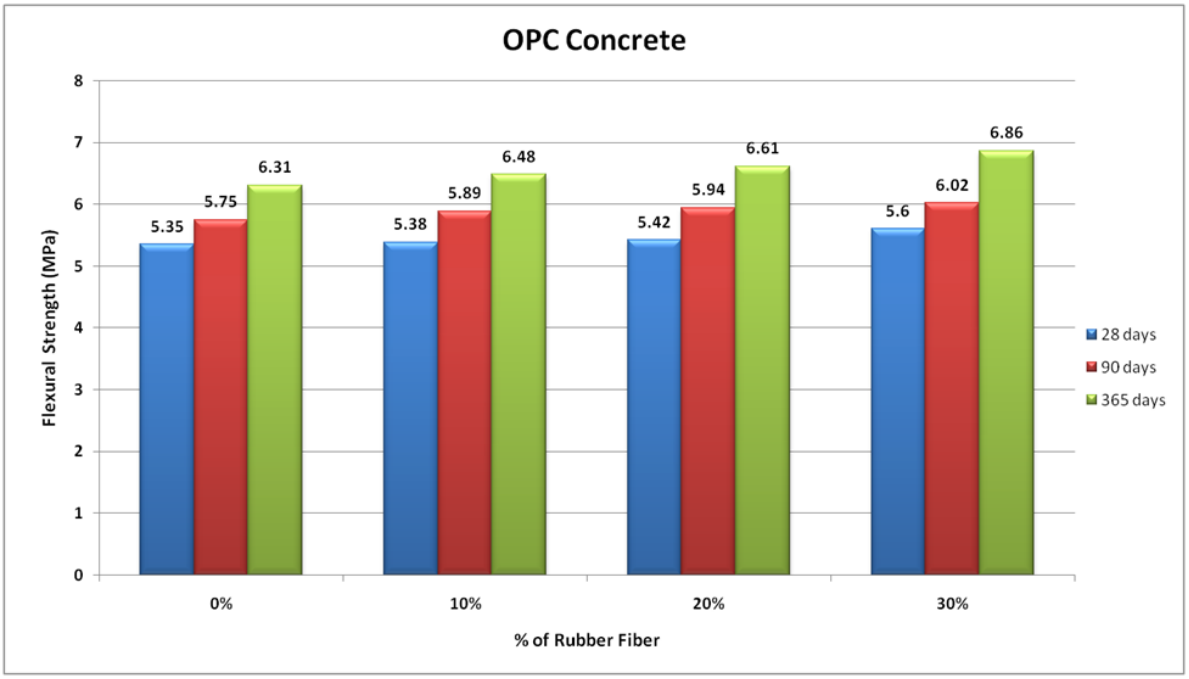

Figure 3.6: Flexural strength of OPC concrete

3.6 Modulus of Elasticity Test

The average modulus of elasticity of the geopolymer concrete and OPC concrete was measured after 28 days. The modulus of elasticity of the geopolymer concrete varied from 20–31.5 GPa, and that for OPC concrete ranged from 18–27.5 GPa (see Figure 3.7). It can be seen that, in all the mixes, the modulus of elasticity decreases as the rubber fibre content increases. The modulus of elasticity of geopolymer concrete depends on the geopolymeric microstructure, and is independent of the aggregate and source materials. An increase in the rubber fibre content decreases the homogeneity of the geopolymer and OPC concrete, resulting in a decrease in the modulus of elasticity. Similar observations have been made in previous studies [152]. The modulus of elasticity of the geopolymer concrete and OPC concrete decrease by 36.34% and 34.54%, respectively, as the rubber fibre content increases from 0–30%.

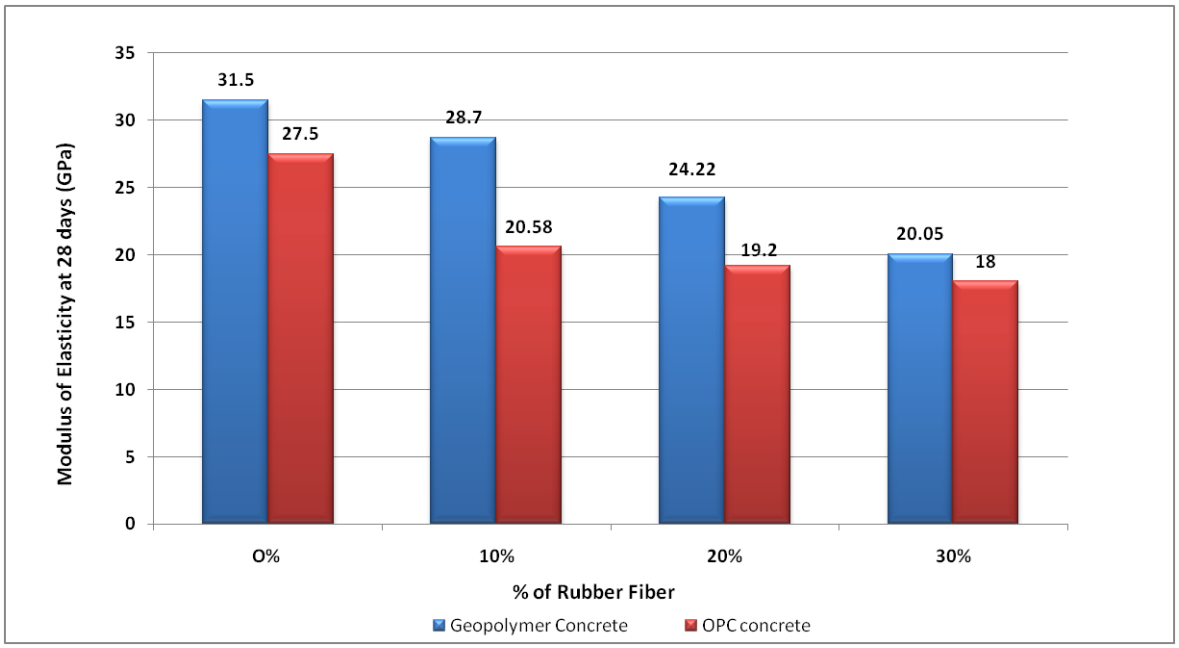

Figure 3.7: Modulus of elasticity of OPC and geopolymer concrete

3.7 Pull-off Test

The average pull-off strength was measured after 28 days, and the results are shown in Figure 3.8. As the compressive strength increases, the pull-off strength increases. It can be seen that the pull-off strength decreases when rubber fibres are introduced to the mix. The results show geopolymer concrete has better pull-off strength than OPC concrete. Both rubber fibre geopolymer and OPC concrete exhibit poor pull-off strength performance, because there is less bonding between the paste and aggregate, which results in a weaker surface layer than in the control geopolymer and control OPC concrete. The pull-off strength of geopolymer concrete decreases from 13.46% to 21.15% and then by 32.69% as the rubber fibre content increases to 10%, 20%, and 30%, respectively; the pull-off strength of the OPC concrete reduces from 2.38% to 21.42% and then 26.19%, respectively.

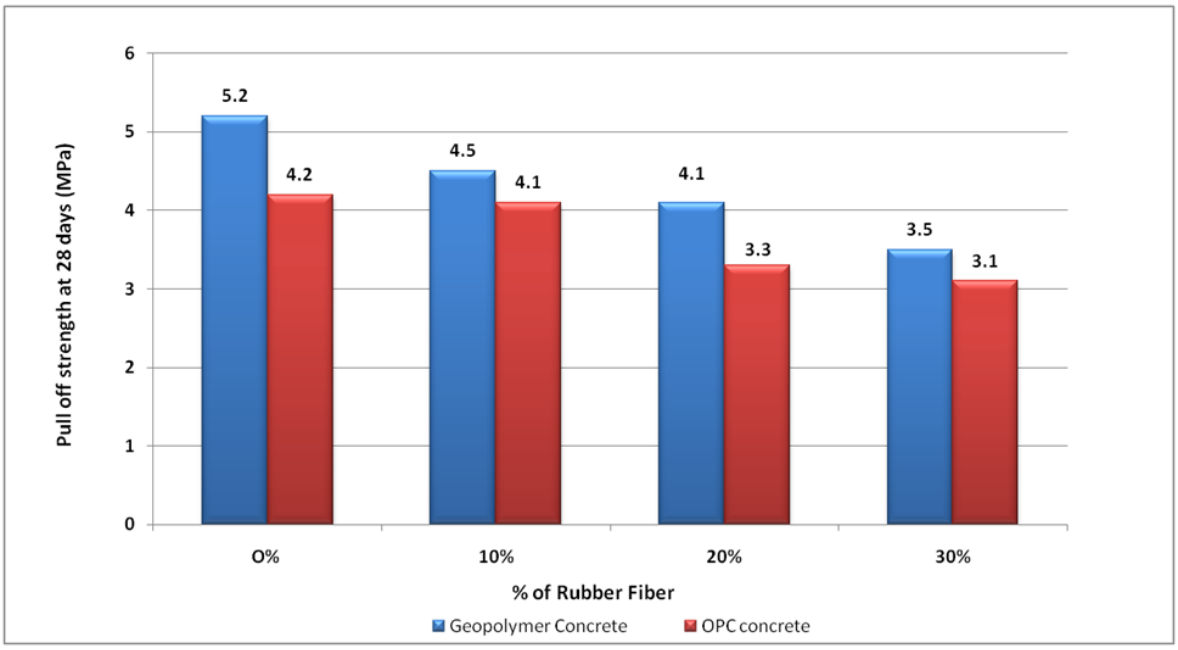

Figure 3.8: Pull-off strength of OPC and geopolymer concrete

3.8 Abrasion Resistance Test

The abrasion resistance test was carried out at 28 days age according to IS 1237-2009 [144]. Abrasion resistance was measured in terms of depth of wear. Figure 3.9 shows that the abrasion resistance increases as more rubber fibres are added to the mix. As per IS 1237-2009 [144], the permissible depth of wear for general purpose tiles and heavy-duty floor tiles is 4.0 mm and 2.5 mm, respectively. From the figure, it is evident that the maximum depth of wear occurs when there are no rubber fibres in the mix. In all mixes, the depth of wear is within permissible limits. It can be concluded that rubber tyre fibres could be used with fly ash or cement to make general purpose and heavy-duty floor tiles.

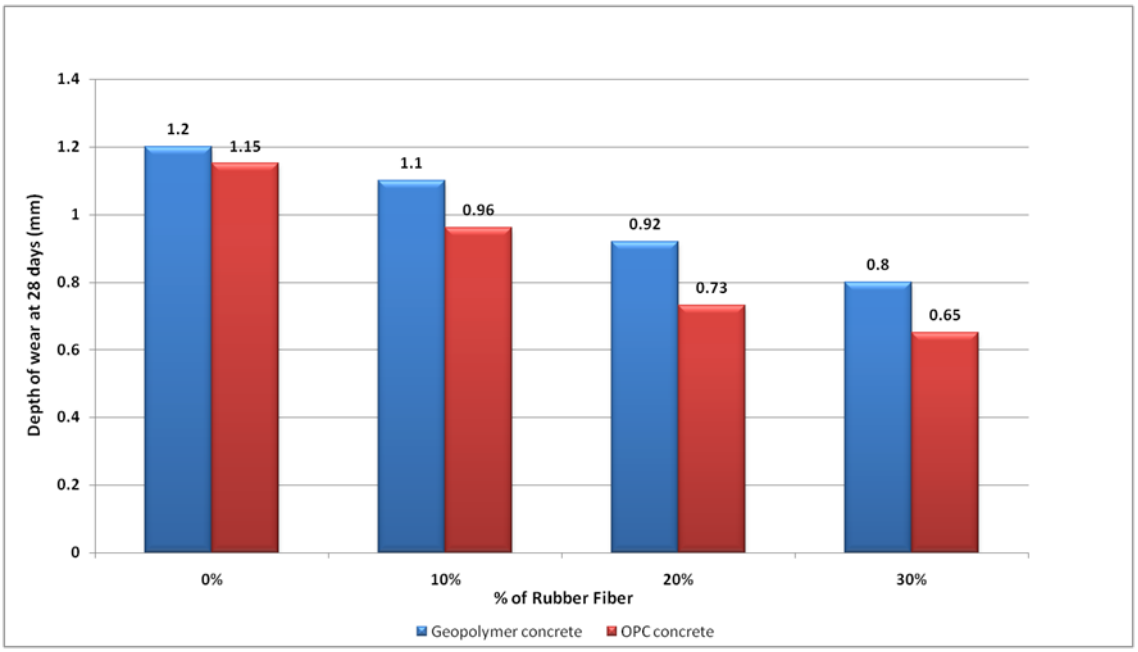

Figure 3.9: Depth of wear for OPC and geopolymer concrete

3.9 Water Permeability Test

The water permeability test was carried out according to DIN-1048 [138]. Permeability was evaluated in terms of the depth of water penetration. Figure 3.10 shows the variation in water penetration depth with respect to rubber fibre content. The water penetration depth increases as the rubber fibre content is increased. The water penetration is lower in geopolymer concrete than in OPC concrete. Similar results have been reported in previous study [151]. The continuous chemical reaction between fly ash and alkaline solution results in a change in porosity and creates denser pores in geopolymer concrete [148, 151]. However, a detailed examination found that the variations were very small in the case of geopolymer concrete. Minimum and maximum water penetration values of 31.2 mm and 35.7 mm occur in the geopolymer concrete. The increase in penetration depth can be attributed to the increase in porosity of the concrete, which is evident at higher replacement levels of rubber fibres. In OPC concrete, the minimum and maximum water penetration is 38.03 mm and 42.8 mm, respectively. It is evident that the development of pores is dependent on the alkaline solution, aggregate, and source materials. Unlike the OPC concrete, which undergoes a hydration process, the pores in the geopolymer are filled by alumino-silicates. This lower permeability of geopolymer concrete has led to it being referred to as "excellent" concrete [151, 156].

3.10 Sorptivity Test

Sorptivity measures the transport properties of concrete by which water passes through capillary pores into the concrete. Figures 3.11 and 3.12 illustrate the sorptivity index of geopolymer concrete and OPC concrete. From Figure 3.11, it can be concluded that the geopolymer concrete has lower sorptivity (0.09–0.164 mm/min$^{0.5}$) than OPC concrete (0.113-0.203 mm/min$^{0.5}$) after 28 days. A similar observation was recorded in previous research [92]. The limit of the sorptivity index is below 0.200 mm/min$^{0.5}$, which is the recommended value for concrete according to previous research [92]. The control geopolymer concrete has a sorptivity index of 0.09 mm/min$^{0.5}$ after 28 days.

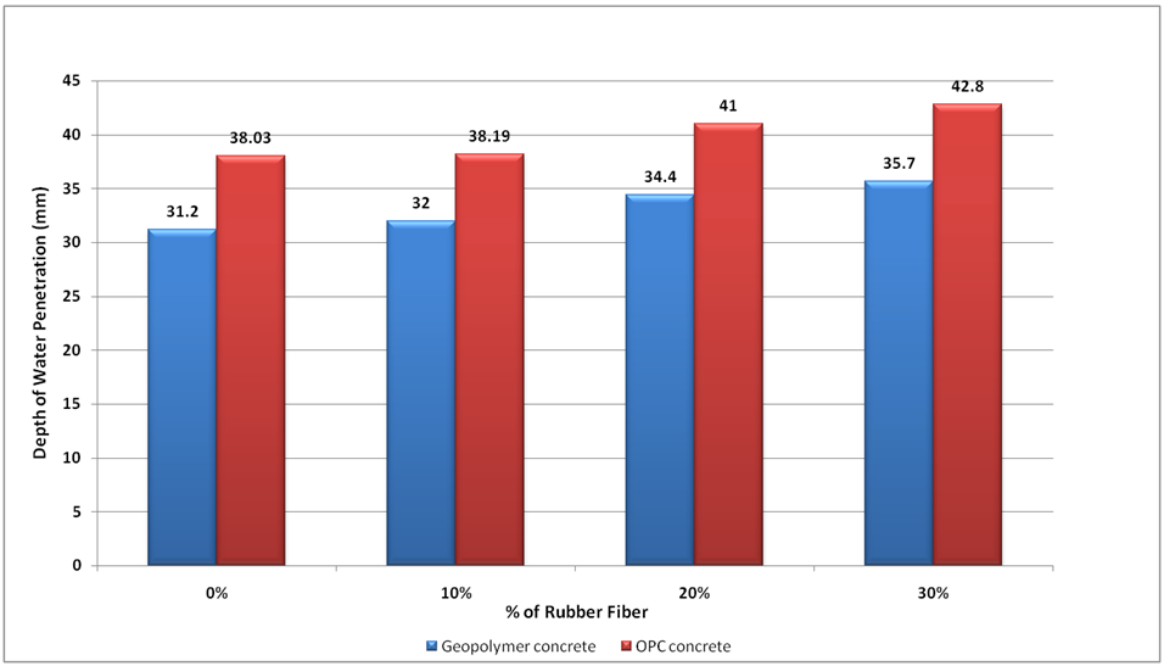

Figure 3.10: Water permeability of geopolymer and OPC concrete

This fact indicates that few capillary pores exist following the effective reaction between the alkaline solution and source material, whereas capillary pores persist in the OPC concrete to enable the hydration of the cement. Also as the percentage of rubber fiber is increased, the sorptivity index is also increased for both the concrete (geopolymer and OPC). Hence, geopolymer concrete has fewer capillary pores than OPC concrete. This results in a slower rate of sorptivity into the geopolymer concrete compared with OPC concrete.

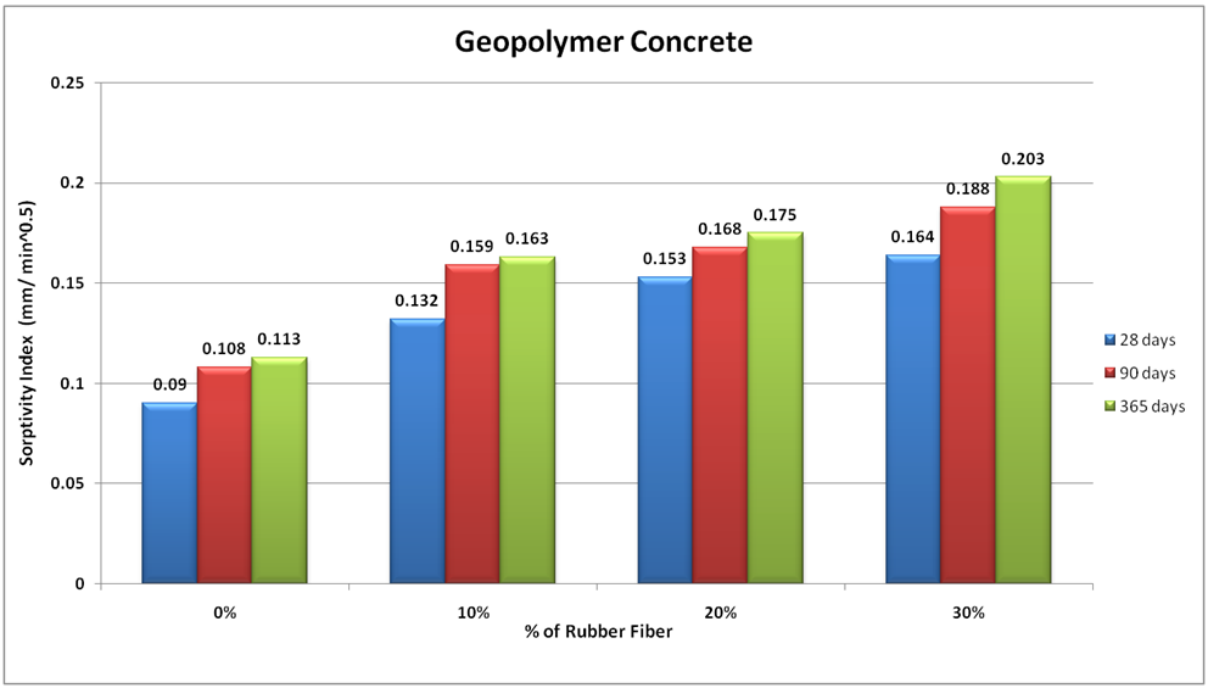

Figure 3.11: Sorptivity of geopolymer concrete

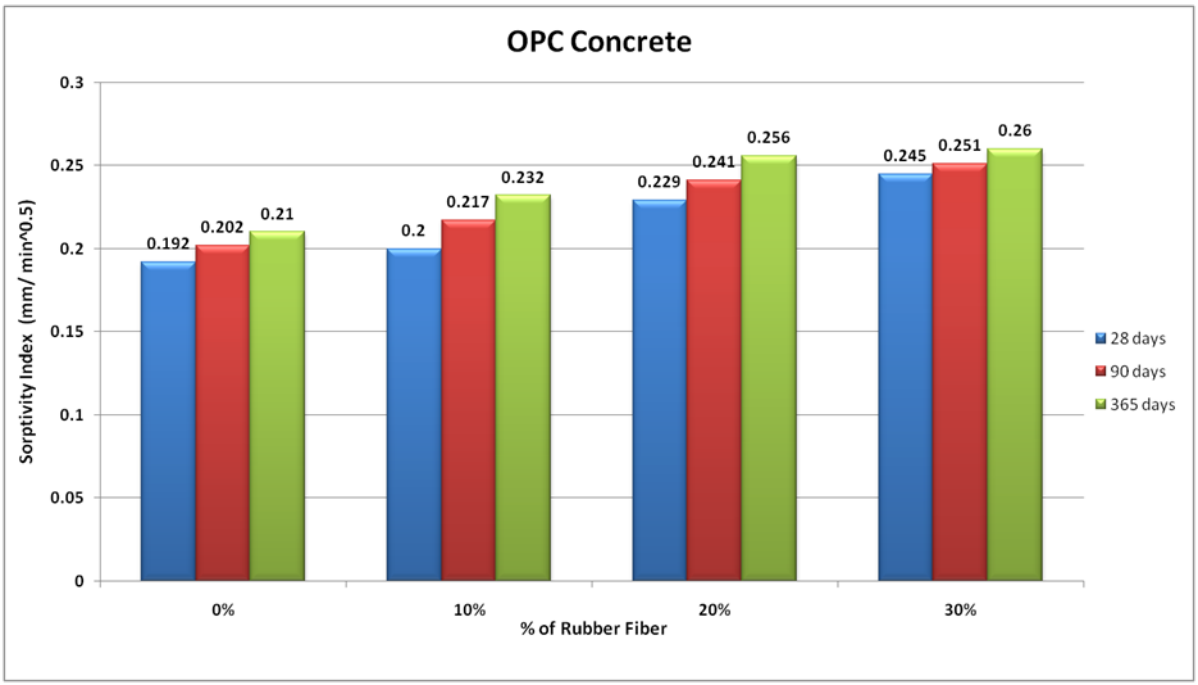

Figure 3.12: Sorptivity of OPC concrete

3.11 Sulfate Resistance Test

The sulfate resistance test was conducted on the geopolymer concrete and OPC concrete. The test was performed by soaking the specimen in 5% Na_2SO_4 (sodium sulfate) solution. The sulfate resistance was evaluated based on changes in physical appearance, mass, length, and compressive strength after exposure periods of 7, 28, 84, 162 and 365 days. For comparison, specimens were also soaked in distilled water.

The **physical appearance** of the geopolymer specimens after one year exposure is shown in Figure 3.13. After exposure to sodium sulfate for up to one year, no changes were observed in the geopolymer specimens. These specimens did not exhibit any change in shape, and no cracking or spalling; in contrast, the OPC concrete specimen had expanded and suffered from frequent random cracking. Figure 3.13 shows that the physical appearance of the geopolymer specimen soaked in 5% sodium sulfate solution was also unchanged. Similar observations have been reported in previous research [85].

Figure 3.13: Physical appearance of geopolymer and OPC concrete

Figure 3.14 illustrates the **change in mass** of geopolymer concrete specimens after exposure to sodium sulfate for up to one year. It can be seen that there has been no significant change in mass in the geopolymer specimen, whereas the mass of the OPC concrete specimen has increase intially due to absorption of sodium sulphate solution and degradation of mass observed due to effect of sodium sulphate solution shown in Figure 3.15. A significant increase in mass was observed in the geopolymer specimen as a result of the absorption of liquid through geopolymer specimens. The absorption of liquid by the geopolymer specimens increased their mass by 1.3%, compared with an increase in mass of 3.0–3.5% in the OPC specimens.

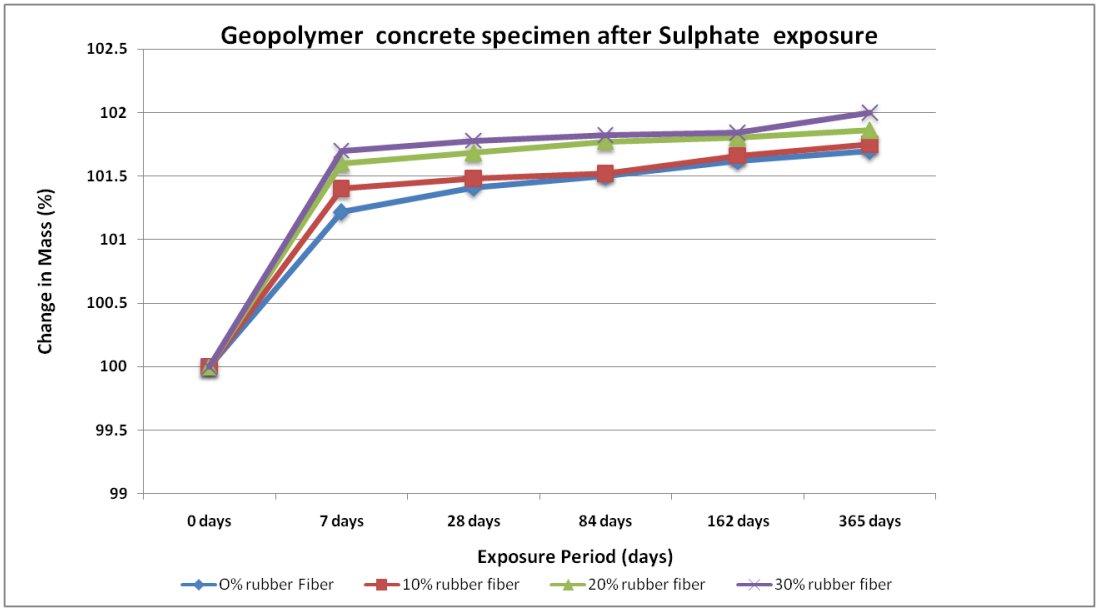

Figure 3.14: Change in mass of geopolymer specimens after sodium sulfate exposure

The **change in compressive strength** of the geopolymer concrete and OPC concrete specimens after exposure to sodium sulfate is illustrated in Figures 3.16 and 3.17. The compressive strength of each specimen was measured under the SSD condition after exposure. A significant change in compressive strength was observed in the geopolymer specimens with exposure, whereas the OPC concrete specimens show reduced compressive strength. The reduced compressive strength in OPC concrete is due to the formation of ettringite and expansive gypsum, which result in cracking, expansion, and spalling. Similar results have been observed in past research [85],

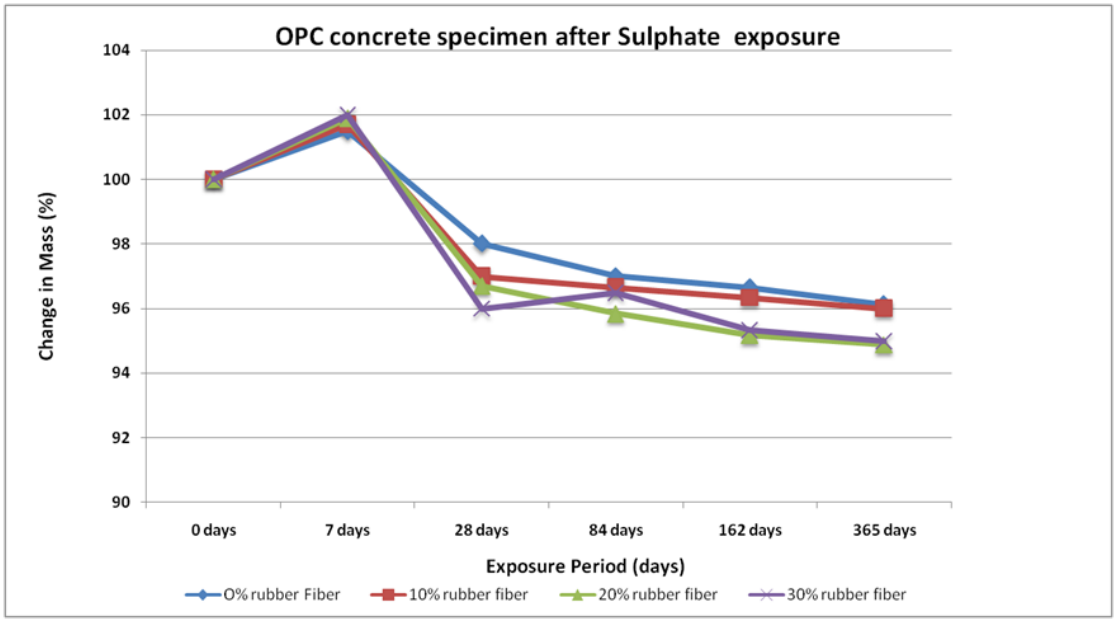

Figure 3.15: Change in mass of OPC specimens after sodium sulfate exposure

ref [157–163]. In geopolymer concrete, the geopolymerization process occurs in place of hydration, meaning that there is generally no formation of gypsum and ettringite. The high alkali content improves the resistance of geopolymers against sulfate exposure, as confirmed by previous research [85]. These test results clearly show the superior resistance of geopolymer concrete against sulfates over that of OPC concrete.

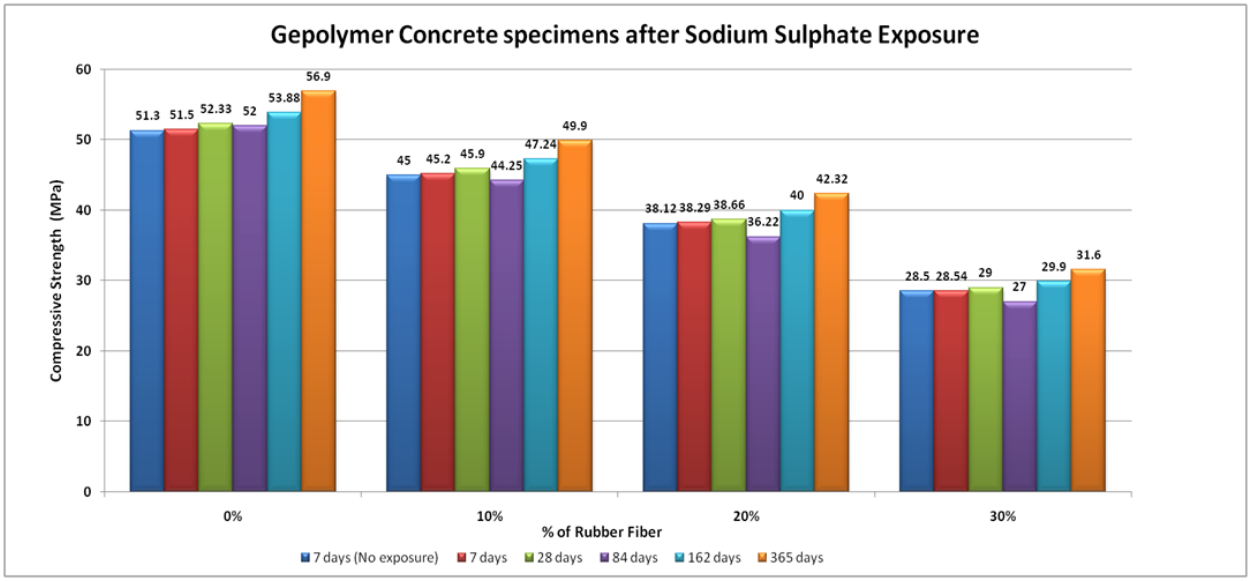

Figure 3.16: Change in compressive strength of geopolymer concrete specimens after sodium sulfate exposure

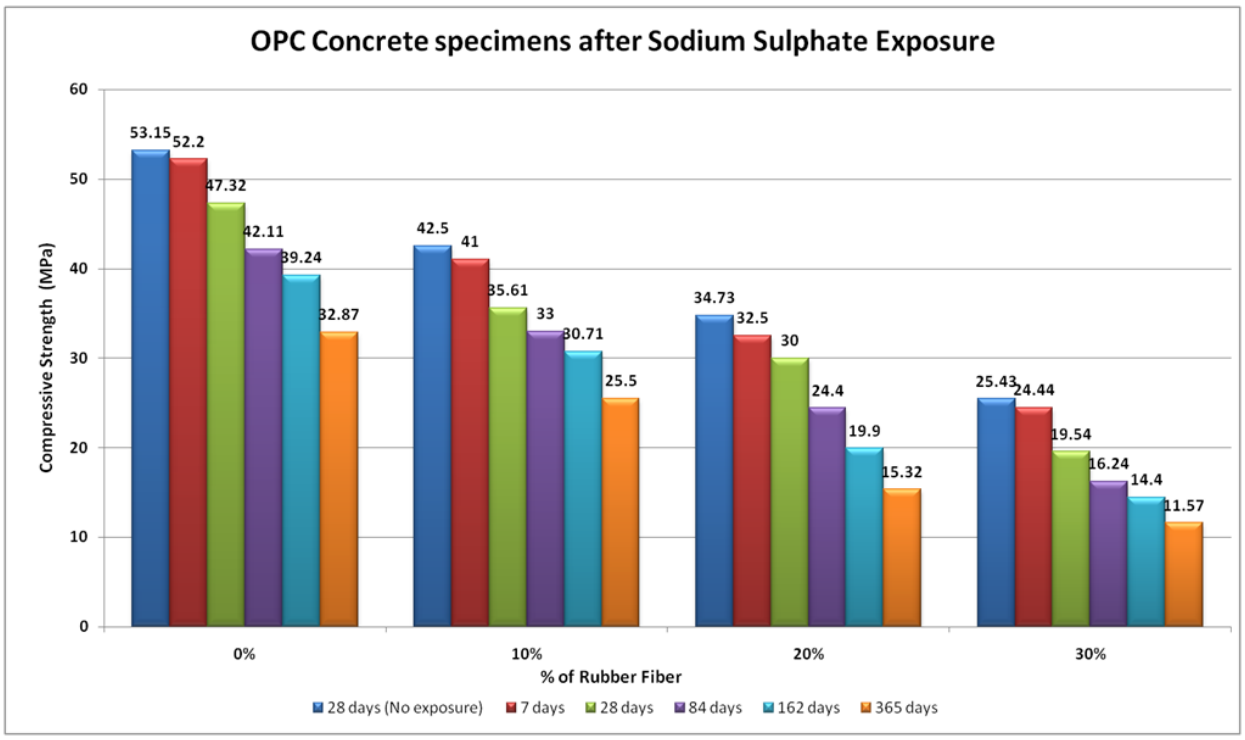

Figure 3.17: Change in compressive strength of OPC concrete specimens after sodium sulfate exposure

3.12 Acid Resistance Test

The acid resistance test was conducted on the geopolymer concrete and OPC concrete specimens by soaking them in 3%, 5%, and 10% concentrations of sulfuric acid for 7, 28, 84, 162, and 365 days. This test demonstrates the behaviour of geopolymer concrete and OPC concrete in terms of physical appearance, change in mass, and change in compressive strength after exposure to sulfuric acid.

Figure 3.18 shows the **physical appearance** of the geopolymer specimens after one year exposure period. It is evident that the specimens of all mixtures undergo erosion after exposure to acid. The damage to the concrete surface increases as the sulfuric acid becomes stronger. The erosion of the OPC concrete specimens is greater than that of the geopolymer concrete.

Figure 3.18: Physical appearances of specimens after sulphuric acid exposure

Figures 3.19 and 3.20 show the **change in mass** of both types of concrete after 5% acid exposure for up to 365 days. It can be seen that the geopolymer concrete specimens gain some weight during the first week of exposure, because they absorb the liquid over this period. From this point on, the mass of all specimens decreases as a result of acid exposure. It can be seen that the percentage of mass loss increases with the exposure period. In geopolymer concrete, the results for the first week show that the mass of the specimens increased by 0.98–1.15% for all concentrations, then decreased over the remaining exposure period. In the OPC concrete, the mass of the specimen increased by 1.8–2.5% in the first week, and then decreased. The OPC concrete specimens lost more mass than the geopolymer concrete specimens. This result agrees with previous research [23, 44, 85, 94, 96].

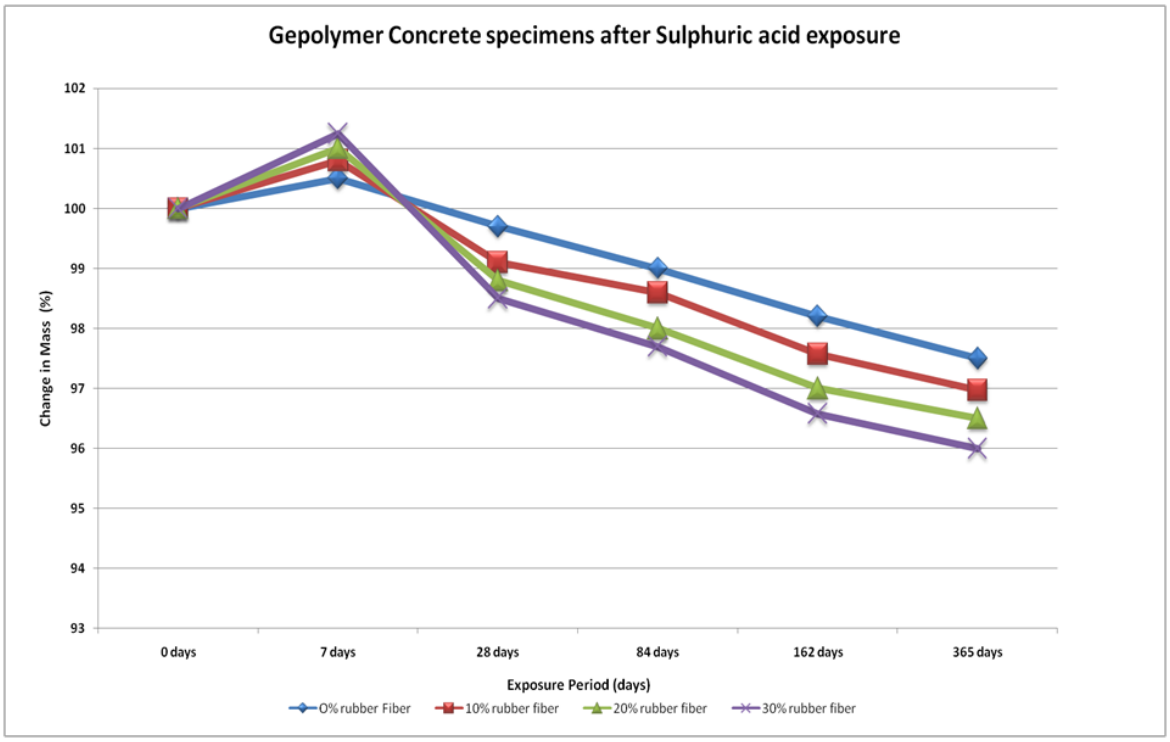

Figure 3.19: Change in mass of geopolymer specimen after sulfuric acid exposure

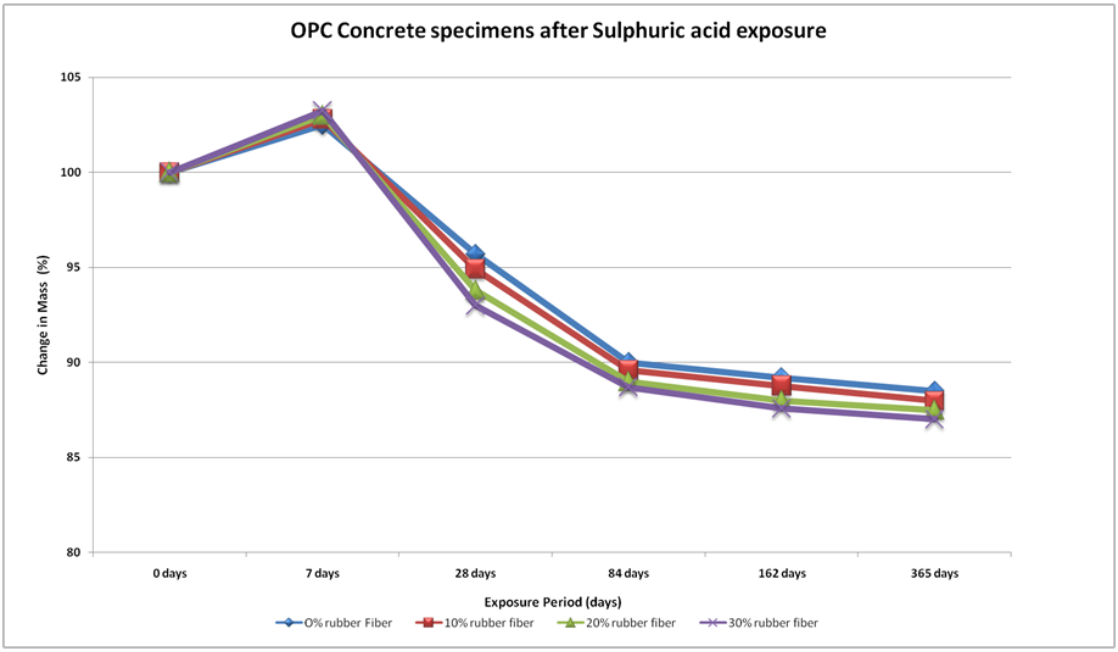

Figure 3.20: Change in mass of OPC concrete specimen after sulfuric acid exposure

Figures 3.21–3.26 show the **change in compressive strength** of the geopolymer concrete and OPC concrete specimens after each exposure period. These results can be compared with the compressive strength of specimens that were not subjected to acid exposure.

From Figures 3.21–3.26, it can be seen that the compressive strength is reduced on exposure to sulfuric acid. The change in compressive strength depends on the concentration of sulfuric acid and the period of exposure. Increases in the period of exposure and concentration of sulfuric acid enhance the degradation in compressive strength of all mixes. The rate of reduction of compressive strength is highest following the one year exposure period. In the control geopolymer concrete, the 3%, 5%, and 10% concentrations of sulfuric acid result in compressive strengths of 32.14, 30.78, and 17.65 MPa, respectively, after 365 days, whereas for the control OPC concrete, the respective strengths are 29.23, 26.00, and 13.89 MPa. This shows that the geopolymer concrete is more resistant to sulfuric acid than OPC concrete. In geopolymer concrete, the source material contains relatively little calcium, which is

the major factor in increasing resistance against acid [85, 94, 96]. In all mixes, it was found that higher concentrations of sulfuric acid result in greater deterioration, resulting in greater loss of strength. In the geopolymer specimens, this deterioration is due to the formation of zeolite and the depolymerization of alumino-silicate. Similar results have been confirmed by previous research [85, 96]. These results also prove that geopolymer and OPC concrete containing rubber fibres increase the porosity of the concrete, which causes a greater reduction in compressive strength.

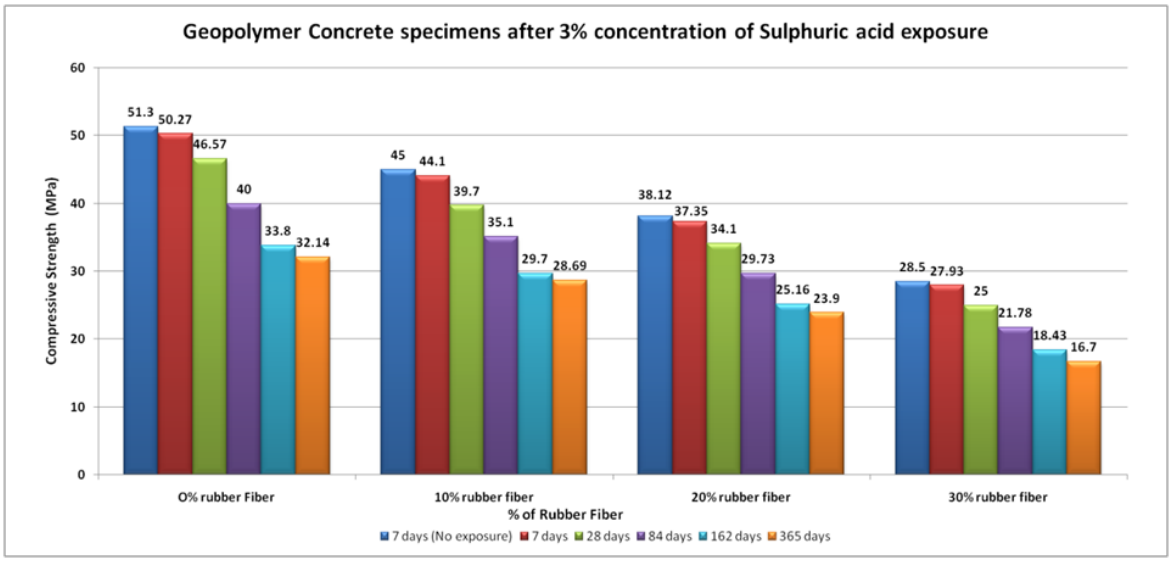

Figure 3.21: Change in compressive strength of geopolymer specimens after exposure to 3% sulfuric acid

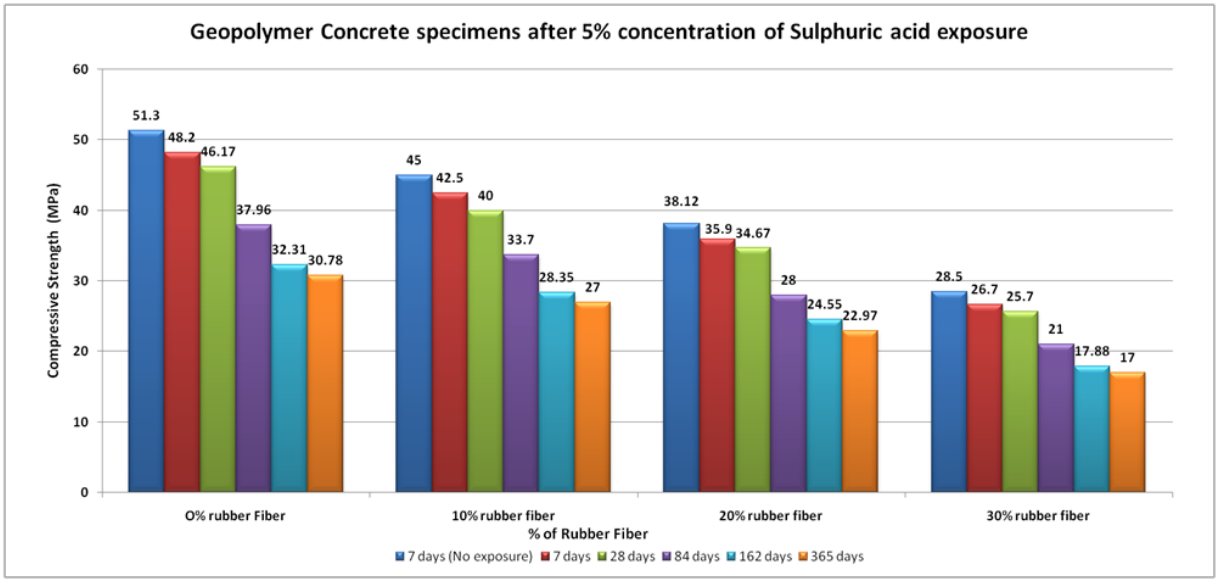

Figure 3.22: Change in compressive strength of geopolymer specimens after exposure to 5% sulfuric acid

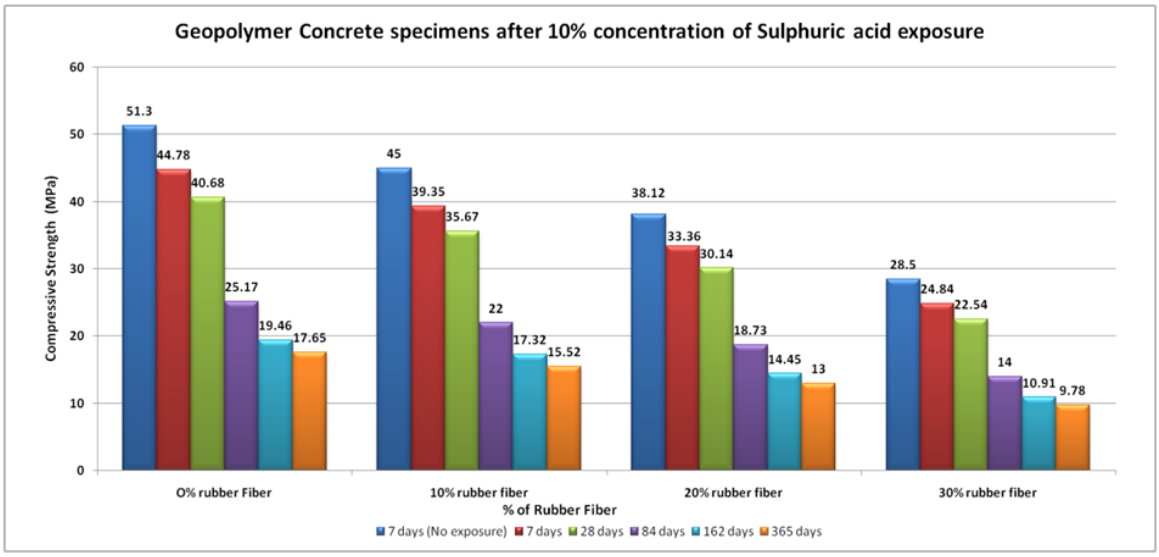

Figure 3.23: Change in compressive strength of geopolymer specimens after exposure to 10% sulfuric acid

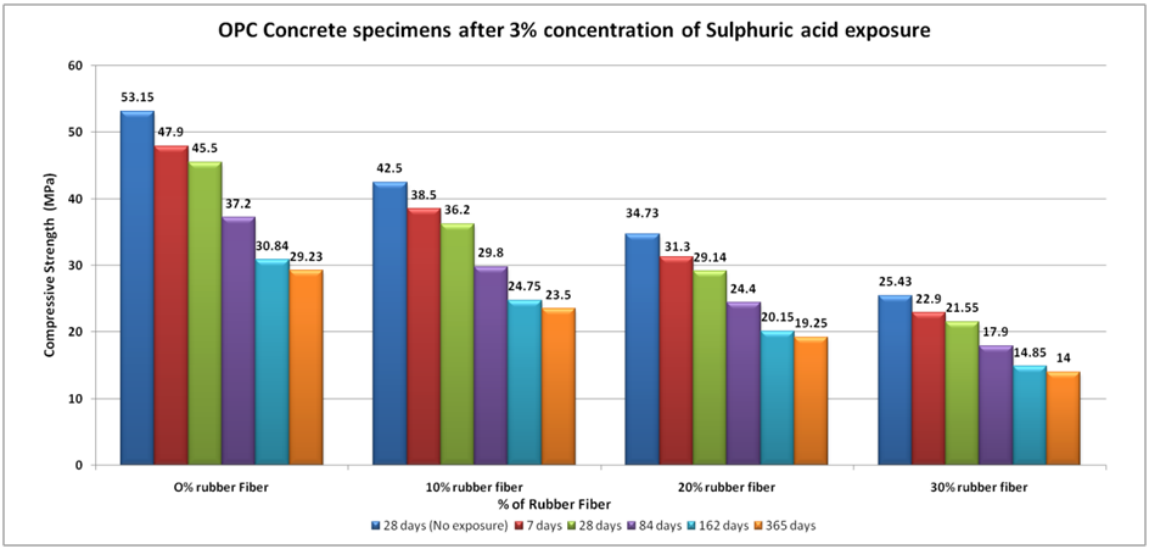

Figure 3.24: Change in compressive strength of OPC specimens after exposure to 3% sulfuric acid

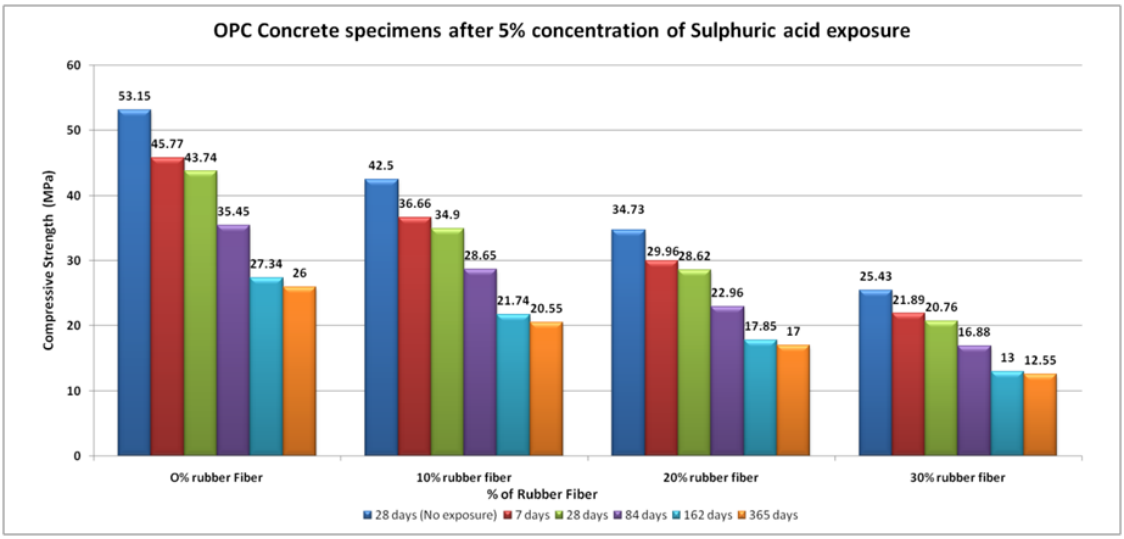

Figure 3.25: Change in compressive strength of OPC specimens after exposure to 5% sulfuric acid

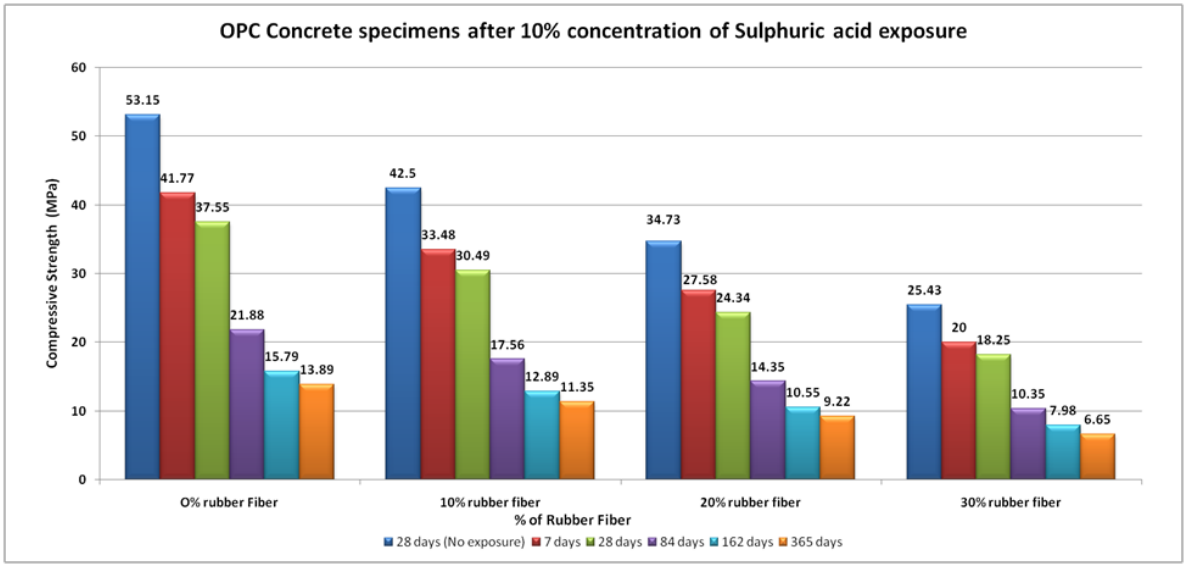

Figure 3.26: Change in compressive strength of OPC specimens after exposure to 10% sulfuric acid

3.13 Chloride Diffusion Test

The steady state chloride ion migration test was performed for the geopolymer and OPC concrete specimens, and the coefficients of chloride diffusion are presented in Figure 3.27. From this figure, it can be seen that the geopolymer concrete has lower chloride diffusion coefficients than the OPC concrete. The chloride diffusion coefficients increase with the rubber fibre content in both types of concrete. The minimum chloride diffusion coefficients for geopolymer concrete and OPC concrete are 1.0 x 10^{-12} and 1.5 x 10^{-12}, respectively, and the maximum chloride diffusion coefficients are 1.2 x 10^{-12} and 1.7 x 10^{-12}, respectively. These values are similar to those reported in a previous study [152].

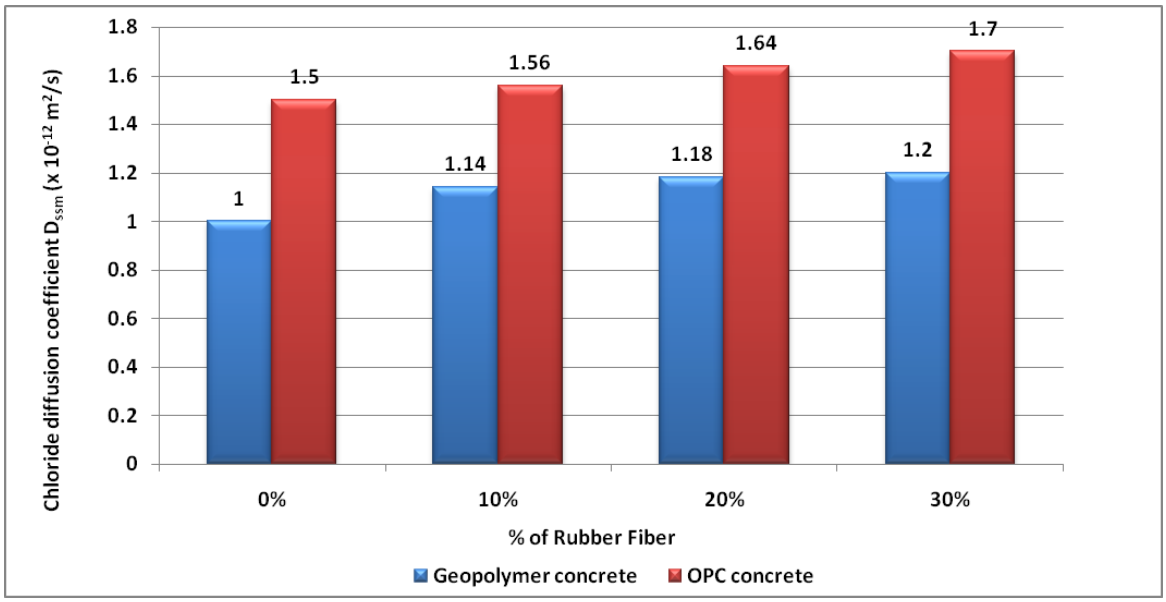

Figure 3.27: Chloride diffusion coefficient of geopolymer and OPC concrete

3.14 Corrosion Resistance Test

3.14.1 Macrocell current mesurements

The Macrocell current was measured according to ASTM G109 [141] with the 100-Ohm resistance. The positive macrocell current indicate that corrosion is in progress. A minimum value of 10 μA is considered to ensure the presence of sufficient corrosion. Figure 3.28 shows that, the macrocell current of geopolymer concrete specimen was less than 10 μA, up to the age of 9 months for control as well as rubberized geopolymer concrete. Whereas, more than 10 μA macrocell current was recorded at 10^{th} , 11^{th} and 12^{th} month for all mixes.

The variation of macrocell current with time for geopolymer concrete and OPC concrete is shown in Figures 3.28 and 3.29. The macrocell current for rubberized concrete mixes was more than that for the control concrete at all the ages. For OPC concrete, current exceeded 10 μA at 8^{th} month to 12^{th} month for all mixes. The maximum anodic current for control mix was measured as 11.2 μA, 13.4 μA, 17.1 μA and 19.3 μA at 12^{th} month for geopolymer concrete whereas the maximum current for OPC concrete was measured as 15.3 μA, 18.9 μA , 15.8 μA and 22.1 μA . From the above results, it can be shown that the inclusion of waste rubber fiber increases the probability of early initiation of corrosion in both type of concrete.

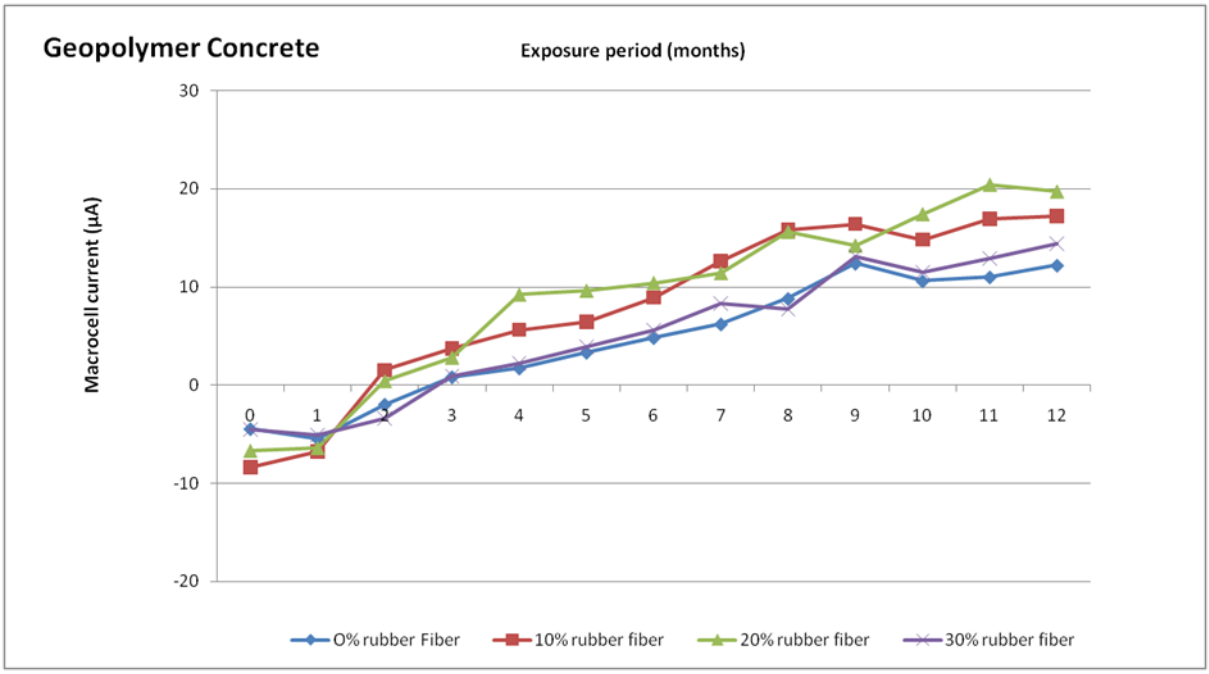

Figure 3.28: Macrocell current of geopolymer concrete

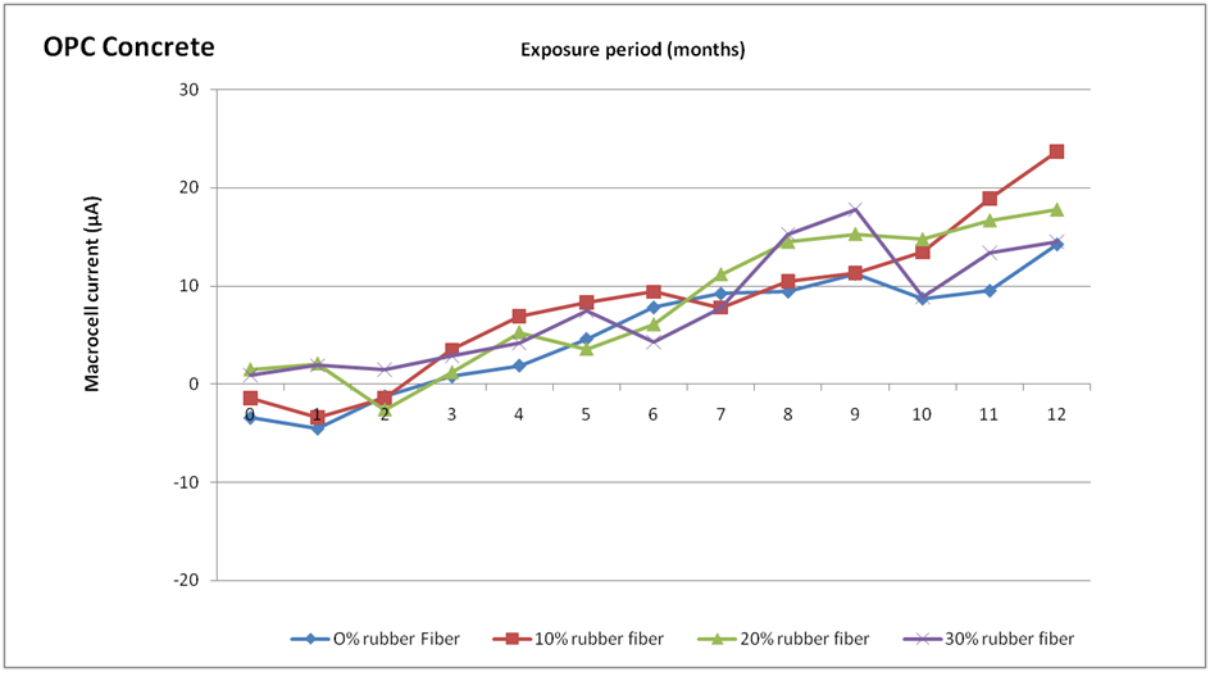

Figure 3.29: Macrocell current of OPC concrete

3.14.2 Half-cell potential measurements

The half-cell potential was measured as according to ASTM C876 [142] between top bar and reference electrode. The results of half-cell potential readings for geopolymer concrete and OPC concrete are shown in Figures 3.30 and 3.31. According to ASTM standard, when potentials are more negative than -350 mV, there is more than 90% probability that corrosion in reinforcing steel bars will occur. For geopolymer concrete, the potential was less negative than -350 mV up to 9^{th} months shown whereas for OPC concrete , the potential was less negative than -350 mV up to 8^{th} months as shown in Figures 3.30 and 3.31.

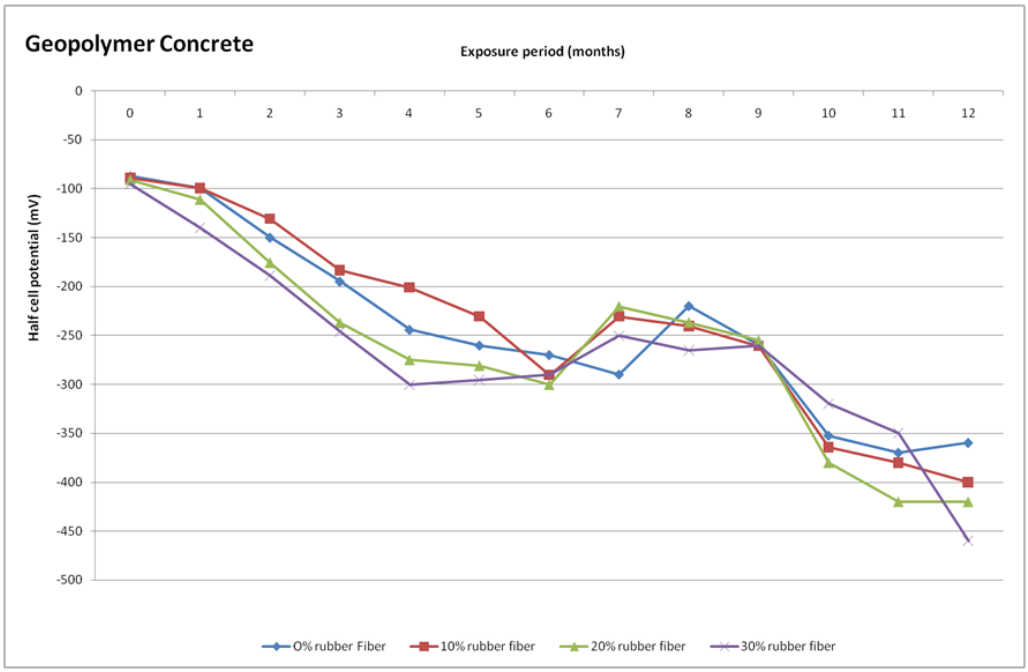

Figure 3.30: Half-cell potential mesurement of geopolymer concrete

Figure 3.31: Half-cell potential mesurement of OPC concrete

The variation of half-cell potential for geopolymer and OPC concrete is shown in Figure 3.31. The half cell potential of waste rubber fiber concrete was higher than that for the control mix at the ages. More negative than -350 mV potential was recorded at 10^{th} month to 12^{th} month in geopolymer concrete whereas, OPC concrete the potential became more negative than -350 mV at 9^{th} month to 12^{th} month. The maximum potential was measured as -360mV, -400 mV and -420, and -460 mV for geopolymer concrete at 12^{th} month whereas the maximum potential for OPC concrete at 12^{th} month was measured as -400 mV, -455 mV, -482 mV and -500 mV. It is observed from the above results that the geopolymer concrete decreases the probability of early initiation of corrosion compare than OPC concrete.

3.15 Drying Shrinkage Test

The drying shrinkage with time for geopolymer concrete and OPC concrete is shown in Figures 3.32 and 3.33 From the figure it can be seen that geopolymer concrete undergoes low drying shrinkage compare with OPC concrete. The low drying shrinkage associated with its finer pore structure leads to low diffusibility and considerably slows down rate of drying shrinkage. In the geopolymerization process water is expelled which results less amount of water present in the micro pores of geopolymer concrete. This Results in low drying shrinkage. The shrinkage strain is fluctuating with time due to moisture movement from the environment to concrete and vice versa which develops reversible shrinkage and swelling of concrete. It can be observed that the drying shrinkage increased with the increase in the rubber fiber content as well as increase in time for both the cases. The increase in porosity due to rubber particles leads to increase in the rate of shrinkage.

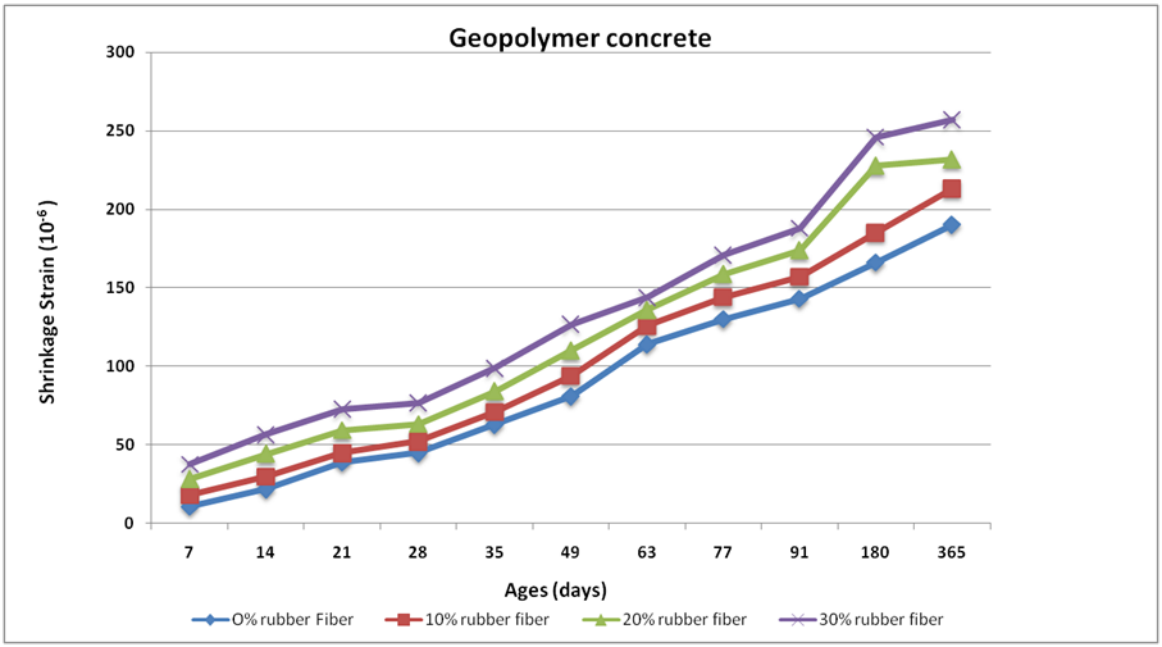

Figure 3.32: Drying shrinkage of geopolymer concrete specimen

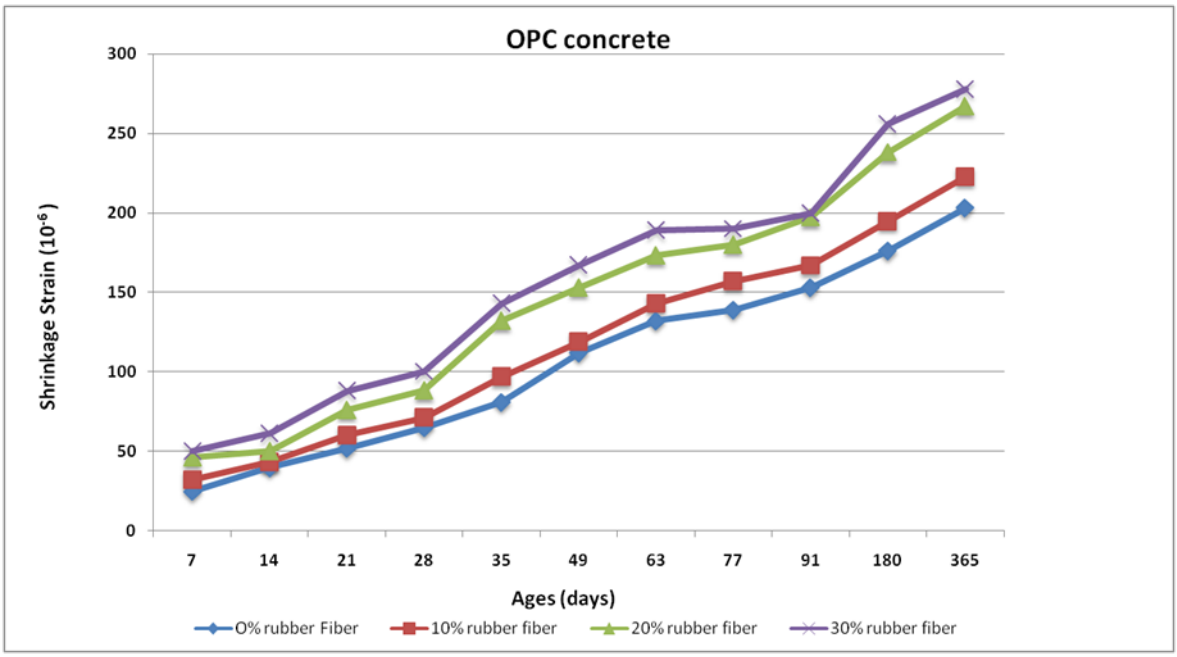

Figure 3.33: Drying shrinkage of OPC concrete specimen

3.16 Carbonation Resistance Test

The depth of carbonation measured for geopolymer and OPC concrete is shown in Figures 3.34 and 3.35 for 14, 21, 28, 35, 42, 56 and 90 days duration (5% CO_2 exposure). It can be observed that the carbonation depth increased with the increase of CO_2 exposure duration and replacement level for all the mixes. It is observed from the present study that the carbonation depth for large replacement level (30%) and high CO_2 concentration (5% for 90 days) was less than the minimum cover required (15 mm) for both the concrete. The carbonation depth for any replacement level of fine aggregate by rubber fiber decreased with increase in rubber content. The increase in carbonation depth may be due to increase in water absorption and water permeability as earlier observed in the present research. A maximum carbonation depth of 8.0 mm was observed for geopolymer concrete with 30% replacement level of fine aggregate whereas at the same replacement level, carbonation depth of 9.0 mm was observed for OPC concrete at 90 days exposure.

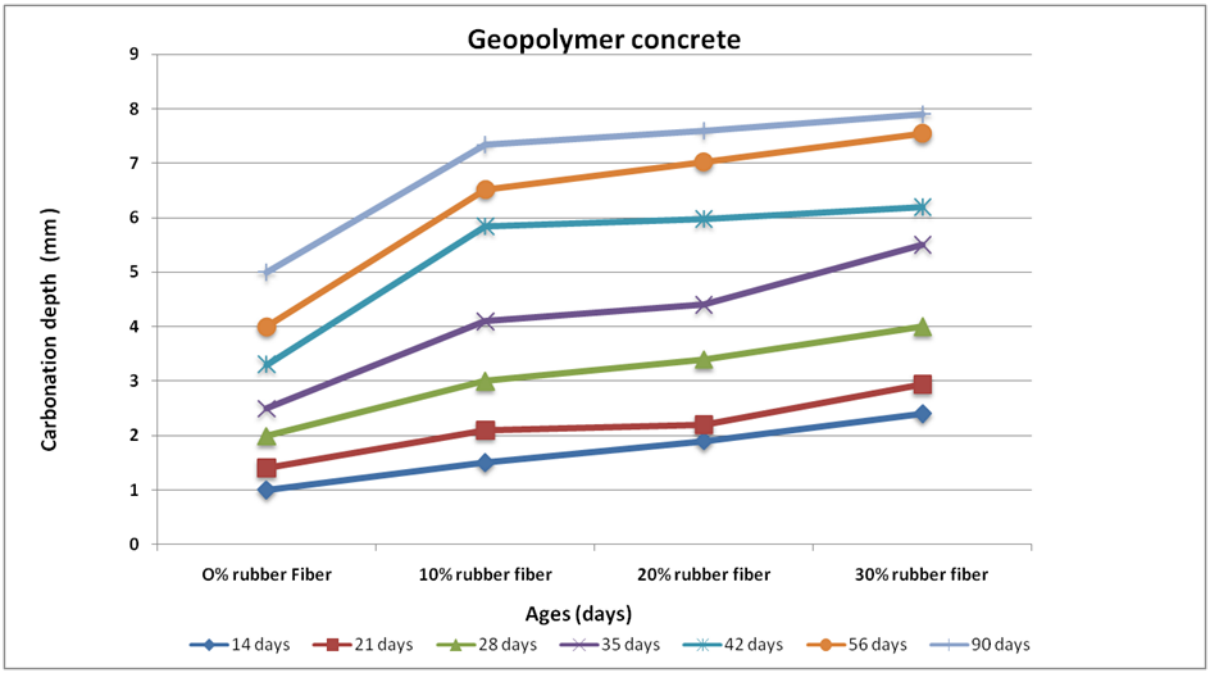

Figure 3.34: Carbonation depth of geopolymer concrete specimen

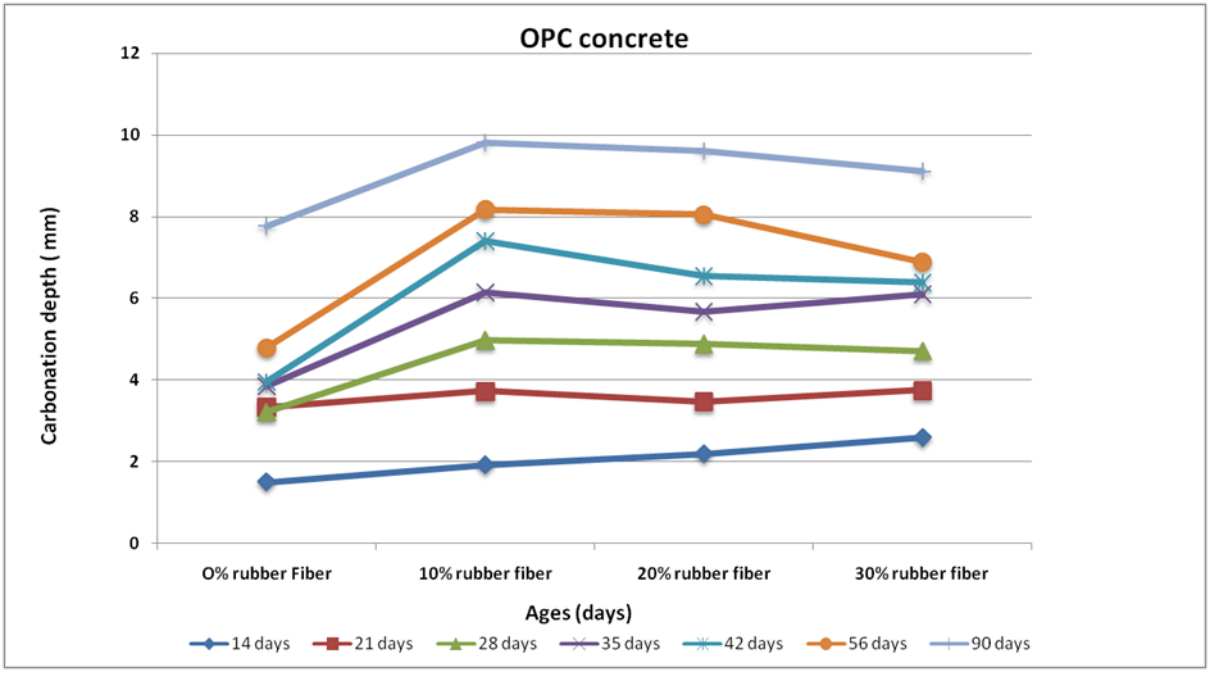

Figure 3.35: Carbonation depth of OPC concrete specimen

3.17 Salt Resistance Test

Salt resistance test was conducted on geopolymer concrete and OPC concrete. The test was performed by soaking the specimen in 5% NaCl (Sodium chloride) solution. The salt resistance was evaluated based on change in compressive strength after exposure of 7, 28, 84, 162, and 365 days. Compressive strength of geopolymer concrete and OPC concrete after exposure to sodium chloride is shown in Figures 3.36 and 3.37, respectively. Compressive strength of specimens was taken under saturated surface dry condition after exposure and results compared with the specimens with no exposure. No significant change was observed in the compressive strength of geopolymer concrete on exposure to salty solution. There was however some reduction in the compressive strength of the rubberized geopolymer concrete on exposure to salt after replacement of more than 10%. There was significant reduction in the compressive strength on exposure to salty solution for control OPC concrete as well as rubberized concrete. The results clearly show the excellent resistance of geopolymer concrete (both control as well as rubberized) against the OPC concrete (both rubberized as well as geopolymer).

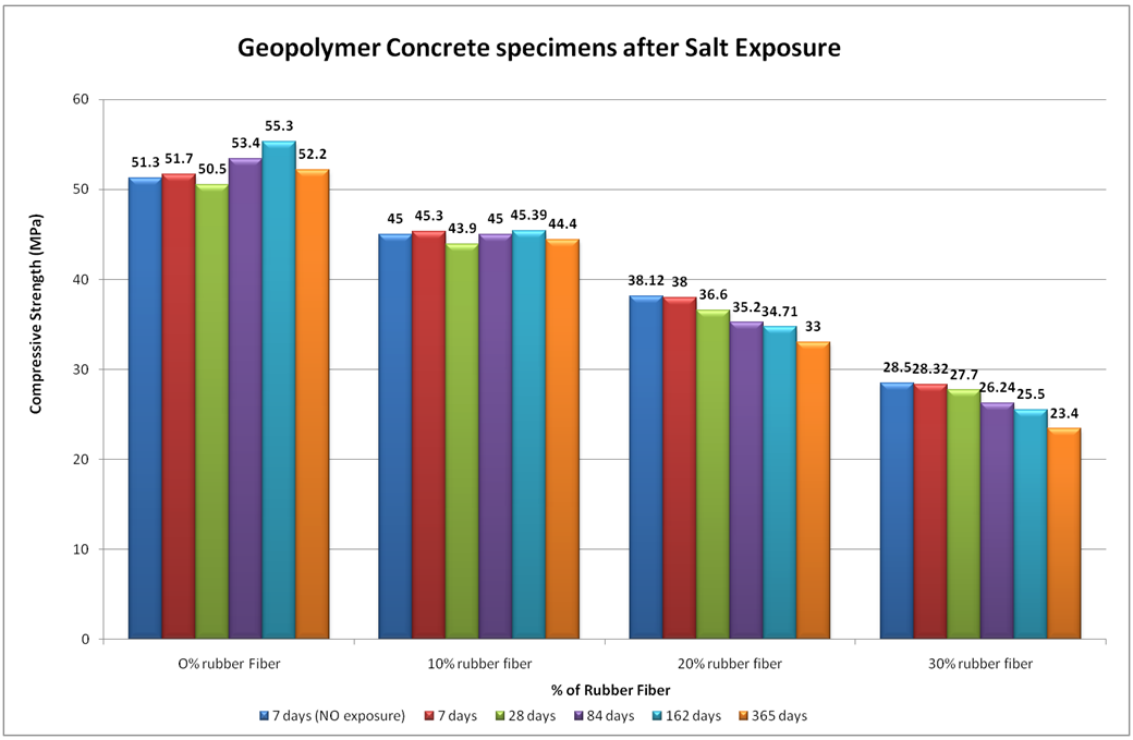

Figure 3.36: Salt Resistance of geopolymer concrete specimen

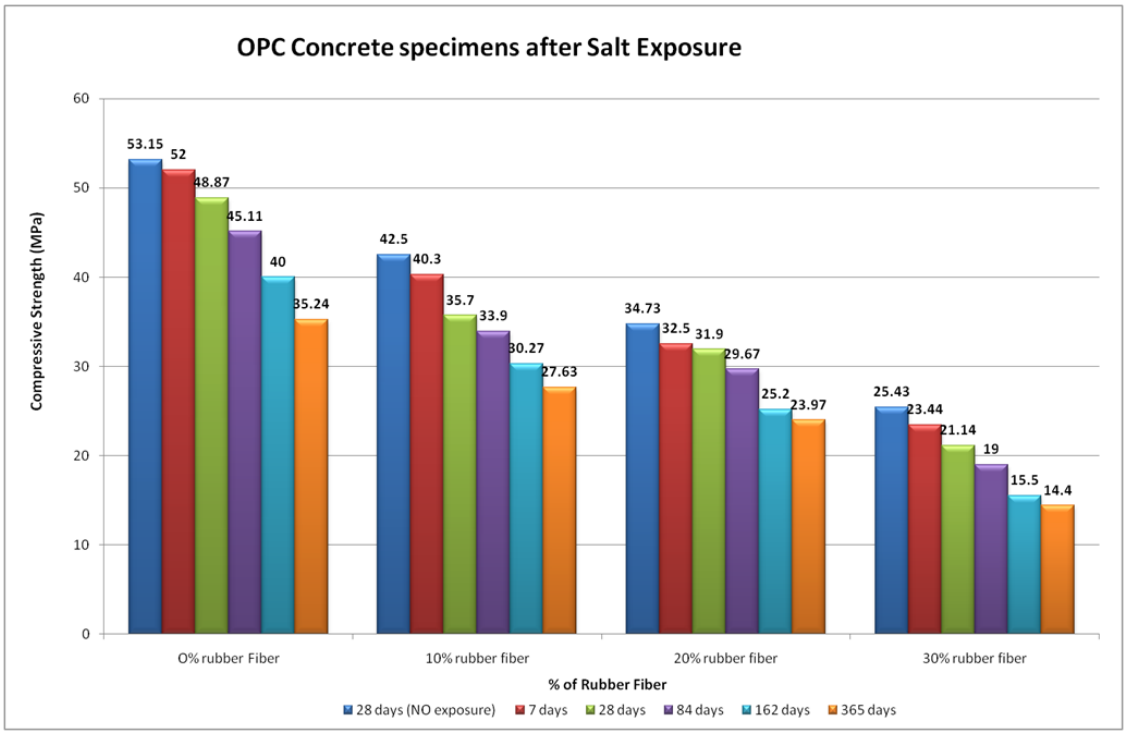

Figure 3.37: Salt Resistance of OPC concrete specimen

3.18 Conclusion

From the results reported in this chapter, the following conclusions can be drawn:

1. As the percentage of waste rubber fibers increases, the compressive strength decreases at all ages. Geopolymer concrete gain 95% compressive strength only in 7 days. The compressive strength of OPC concrete is less than that of geopolymer concrete.

2. The geopolymer concrete exhibits higher tensile strength than OPC concrete because of the good bonding between the geopolymer paste and aggregate.

3. The tension properties of rubberized geopolymer concrete, such as flexural and tensile strength, are increased as the percentage of rubber fibers increased. The maximum Flexural strength was observed in 30% replacement of sand by fibers. This is because of the fibers which provide a better bridge between propagated cracks.

4. It can be seen that, in all the mixes, the modulus of elasticity decreases as the rubber fibre content increases. The modulus of elasticity of the geopolymer concrete and OPC concrete decreased by 36.34% and 34.54%, respectively, as the rubber fibre content increases from 0–30%.

5. It can be seen that the pull off strength decreases when rubber fibres are introduced to the mix. The results show geopolymer concrete has better pull off strength than OPC concrete.

6. It is evident that the maximum depth of wear occurs when there are no rubber fibres in the mix. In all mixes, the depth of wear is within permissible limits. It can be concluded that rubber tyre fibres could be used with fly ash or cement to make general purpose and heavy-duty floor tiles.

7. The water penetration depth increases as the rubber fibre content is increased. The water penetration depth is lower in geopolymer concrete than in OPC concrete. The increase in penetration depth can be attributed to the increase in porosity of the concrete, which is evident at higher replacement levels of rubber fibres.

8. After exposure to sodium sulfate for up to one year, no physical changes were observed in the geopolymer specimens. These specimens did not exhibit any change in shape, and no cracking or spalling, in contrast, the OPC concrete specimen had expanded and suffered from frequent random cracking. A significant change in compressive strength was observed in the geopolymer specimens after exposure, whereas the OPC concrete specimens show reduced compressive strength.

9. The specimens of all mixtures undergo erosion after exposure to acid. The damage to the concrete surface increases as the sulfuric acid becomes stronger. It was found that higher concentrations of sulfuric acid result in greater deterioration, resulting in greater loss of strength.

10. It can be seen that the geopolymer concrete has lower chloride diffusion coefficients than the OPC concrete. The chloride diffusion coefficients increase with the rubber fibre content in both types of concrete.

11. The macrocell current for rubberized concrete mixes was more than that for the control concrete at all the ages. For OPC concrete, current exceeded 10 μA at 8^{th} month to 12^{th} month for all mixes. It can be stated that the inclusion of waste rubber fiber increases the probability of early initiation of corrosion in both type of concrete.

12. The half cell potential of waste rubber fiber geopolymer and OPC concrete was higher than that for the control geopolymer and OPC concrete mix. More negative than -350 mV potential was recorded at 10^{th} month to 12^{th} month in rubberized geopolymer concrete whereas, rubberized OPC concrete the potential became more negative than -350 mV at 9^{th} month to 12^{th} month.

13. The drying shrinkage increased with the increase in the rubber fiber content as well as increase in time for both the cases. The increase in porosity due to rubber particles which lead to decrease the rate of shrinkage.

14. The carbonation depth for any replacement level of fine aggregate by rubber fiber decreased with increase in rubber content. A maximum carbonation depth of

8.0 mm was observed for geopolymer concrete with 30% replacement level of fine aggregate whereas at the same replacement level, carbonation depth of 9.0 mm was observed for OPC concrete at 90 days exposure.

Chapter 4

Thermal Properties

4.1 Prelude

Fire has been crucial in the development of human society, and remains an important part of human civilization. However, fire constitutes a significant threat to life and property in urban and rural areas. It can be extremely dangerous in sites such as high-rise buildings, tunnels, nuclear reactors, pressurized vessels, storage tanks for flammable fuels, and gasification and liquation vessels. Fires or elevated temperatures represent extreme conditions that any structure may be exposed to during its service life. Conventional OPC concrete can only withstand regular fires. Therefore, fire resistance is a critical parameter in the reinforced concrete structural systems widely used in high-rise buildings.

As concrete is a heterogeneous material, an increase in temperature influences both the aggregate and the cement paste. Further, the behaviour of concrete at high temperatures depends on its composition and the properties of its individual components. The loss of strength in OPC paste exceeds 50% on exposure to 400–500°C. This is because of the dehydroxylation of hydroxide and the continuous dehydration of calcium silicate hydrate (CSH), which starts at 105°C. This problem has compelled researchers to explore the possibility of tweaking the chemical composition and ingredients of concrete. A significant number of studies have looked at the feasibility

of using industrial by-products in concrete.

Owing to the associated risk of fires, along with environmental and health hazards, 38 states of the USA have banned the dumping of unprocessed whole tyres. Akin to fly ash, the disposal of rubber tyres in the vicinity of populated areas raises grave health and environmental concerns. Therefore, the systematic recycling of these wastes may help to address societal challenges. Geopolymer concrete is a recently developed concrete that is easy to make and offers superior performance and a lower carbon footprint than conventional OPC concrete.

Geopolymers have demonstrated superb physical, mechanical, optical, and thermal attributes, and their manufacture requires relatively little energy (up to 60% less than OPC), which makes them an attractive alternative to conventional OPC concrete.

Geopolymer concrete exhibits excellent stability at high temperatures, little shrinkage, autoclave curing, freeze/thaw and thermal stability, as well as acid and fire resistance. Additionally, the enhanced polymerization causes an increase in the amorphous content, which in turn increases the strength of fly ash-based geopolymer concrete. It also offers significant cost savings compared to conventional concrete (in the range 10–30%). Moreover, the production of geopolymer cement emits 90% less CO_2 than the production of OPC. This implies that, in developing countries, infrastructure and building applications will create far lower CO_2 emissions.

This chapter presents a systematic study of the fire resistance of fly ash-based geopolymer concrete, and then establishes a comparison with the fire resistance of rubberized geopolymers. In this study, rubber tyre fibres were used to replace 10% of the natural sand to give rubberized geopolymer concrete. This concrete was exposed to elevated temperatures (200°C, 400°C, 600°C, and 800°C) to investigate the thermal effects on density, visual surface appearance, compressive strength, and microstructural characteristics. The experimental methods used to study the control and rubberized geopolymer concrete include XRD, TGA, and FTIR. The pozzolanic material used

was fly ash incorporating rubber tyre fibres along with an alkaline solution of sodium hydroxide and sodium silicate for geopolymerization.

4.2 Preparation of Geopolymer Concrete

Rubberized geopolymer concrete was composed using a 14M NaOH concentration, sodium silicate-to-sodium hydroxide ratio of 2.5, fly ash-to-alkaline solution ratio of 0.4, 10% extra water content, 20% relative content of superplasticizer, curing time of 48 h, curing temperature of $90°C$, 10% rubber fibre content, and 75% total aggregate content.

Fly ash, rubber fibres, and aggregates were initially dry mixed in a pan mixer for 5 min. Thereafter, alkaline solution, extra water, and superplasticizer were added and mixed for another 6 min. The mixture was then poured into cubic moulds (100 x 100 x 100 mm) in three layers. Each layer was compacted with a tamping rod and then placed on a vibrating table for 10–12 s to expel air bubbles. A total of 15 specimens were prepared for each mix. After casting, the specimens were covered with a plastic sheet to prevent the evaporation of alkaline solution and excess water. The specimens were then cured in an oven for 48 h at $90°C$. The mix proportions for both the control (Mix-1) and rubberized geopolymer concrete (Mix-2) are presented in Table 4.1.

Elevated temperature exposure The specimens were heated in a muffle furnace designed for a maximum temperature of $1000°C$. The specimens were treated at $200°C$, $400°C$, $600°C$, and $800°C$, with a rate of heating of $4.4°C$/min starting from room temperature. The specimens were placed into the furnace for approximately 2 h after the desired treatment temperature was achieved. The specimens were then allowed to cool in air at room temperature, and analysed for weight loss, compressive strength, and density. The chemical changes in specimens after exposure were also examined using XRD, FTIR, and TGA-DTA analysis.

Table 4.1: Mix proportion (per m^3)

Mixes	Fly Ash	Aggregate			Rubber Fibre	NaOH	Sodium Silicate	Extra Water	Super-Plasticizer
	(kg)	20 mm (kg)	10 mm (kg)	Fine Sand (kg)	(kg)	(kg)	(kg)	(kg)	(kg)
M-1	446.43	731.25	487.5	656.25	0.00	51.02	127.55	22.32	8.93
M-2	446.43	731.25	487.5	629.34	26.90	51.02	127.55	22.32	8.93

4.3 Testing and Characterization of Microstructure of Rubberized Geopolymer Concrete

X-ray Powder Diffractometer Before and after exposure to high temperature, specimens were crushed to a powder with a typical grain size of 45 μm for XRD analysis. XRD was conducted using a PANalytical XPert Powder device. The diffracted intensities were recorded using an X-Celerator high-speed linear detector over a range of 5–65° 2θ with a step size and count time of 0.02° and 0.6 s/step, respectively. The analysis was carried out using Xpert HighScore software from PANalytical.

Fourier Transform Infrared Spectroscopy Analysis FTIR analysis was carried out using the KBr (potassium bromide) method. FTIR spectra with eight scans per sample were collected from 4000 cm^{-1} to 400 cm^{-1} with a resolution of 4 cm^{-1}.

Thermogravimetric analysis TGA was performed using a Perkin-Elmer Simultaneous Thermal Analyser (STA 6000) under isothermal conditions at 40° for 60 min to equilibrate the nitrogen environment (N_2 flowing at 200 ml/min). Thereafter, samples were heated to 900° at a rate of 10°/min under the same gaseous environment.

4.3.1 Compressive Strength

Rubberized and control geopolymer concrete cubes (100 mm size) containing 10% rubber fibres were cast. The specimens were tested for compressive strength at an age of 28 days and immediately after exposure to elevated temperature, as per IS 516:1959 [135]. Load was applied gradually at a rate of 140 kg/cm^2/min.

4.4 Results and Discussion

4.4.1 Visual Surface Appearance after Elevated Temperature

The changes that occur during the heating process include moisture loss, evaporation, and decomposition of chemical structure. As a result, hairline cracks developed in the rubberized geopolymer concrete at 800°C. Conversely, no cracks appeared in the control geopolymer concrete at elevated temperatures, as shown in Figure 4.1.

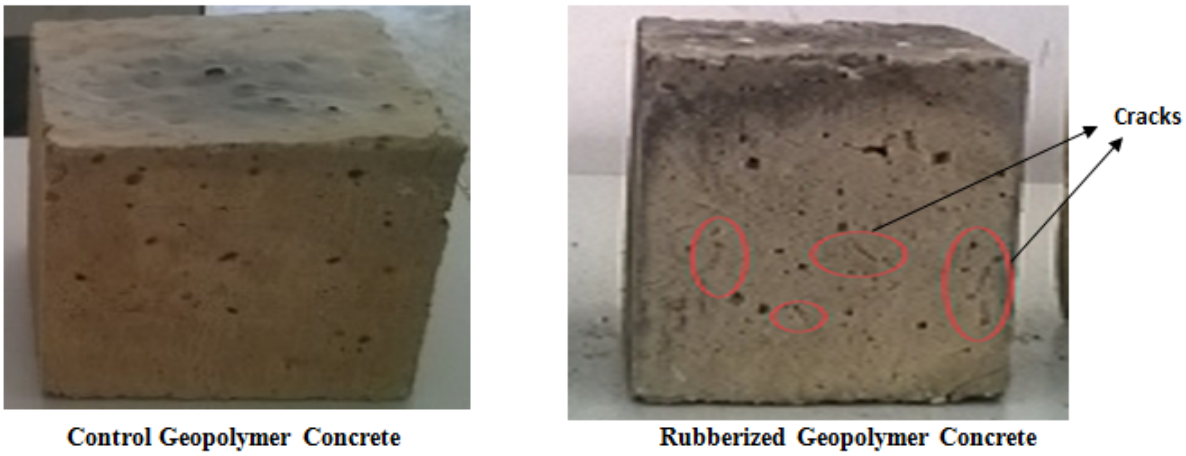

Figure 4.1: Hairline crack development in the specimens

4.4.2 Mass Loss

Weight loss due to exposure to elevated temperatures occurred during the heating process. The weight of both the control and rubberized geopolymer concrete specimens decreased with increasing temperature, as shown in Figure 4.2. As the elevated temperature increase, the control geopolymer concrete lost slightly less mass than the rubberized geopolymer concrete. Specifically, Figure 4.2 shows that, at 800°C, the mass loss in the control and rubberized geopolymer concrete was 15% and 17%, respectively.

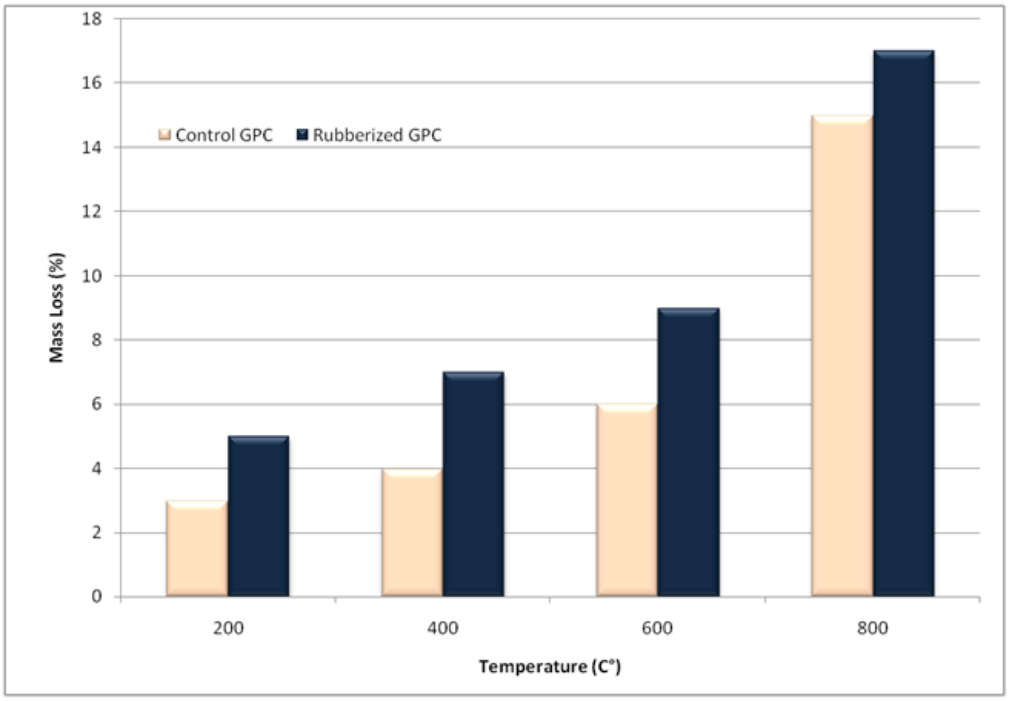

Figure 4.2: Mass loss of specimens subjected to elevated temperatures

4.4.3 Compressive Strength Reduction

It can be inferred from the Table 4.2 that the percentage reduction in compressive strength is higher for rubberized geopolymer concrete than the control geopolymer concrete at all temperatures. There are three reasons for this. First, the softer rubber particles are more prone to early cracking on the application of load, and this phenomenon may accelerate the cracking and failure of the specimen. Second, the density of the rubber is lower than that of the fine aggregate. It is clear that the inclusion of rubber fibres decreases the density of the geopolymer concrete. This may be because the rubber fibres entrap air about their jagged surface and have a lower specific gravity than the fine aggregate. Third, voids form around the rubber particles because of the poor compaction and bonding in these areas ref [164–171]. It can be inferred from Table 4.2 that the percentage reduction in compressive strength is higher for rubberized geopolymer concrete than the control concrete at all temperatures. The highest percentage reduction in compressive strength was observed for the rubberized geopolymer concrete at $600°C$. This may be attributed to the decomposition of rubber

particles at elevated temperatures, leading to the formation of voids in the concrete matrix. These voids enhance the pore pressure and accelerate the formation of cracks in the matrix. This results in poor residual strength in the specimen [172, 173]. Figure 4.3 indicates that the strength of both types of geopolymer concrete increased above 600°C, because the amorphous content increases with the polymerization of unreacted crystalline material [174]. As a result, there is no further strength loss in the geopolymer concrete (see Table 4.2). Figure 4.3 also illustrates that both the control and rubberized geopolymer concrete exhibit a similar reduction in strength.

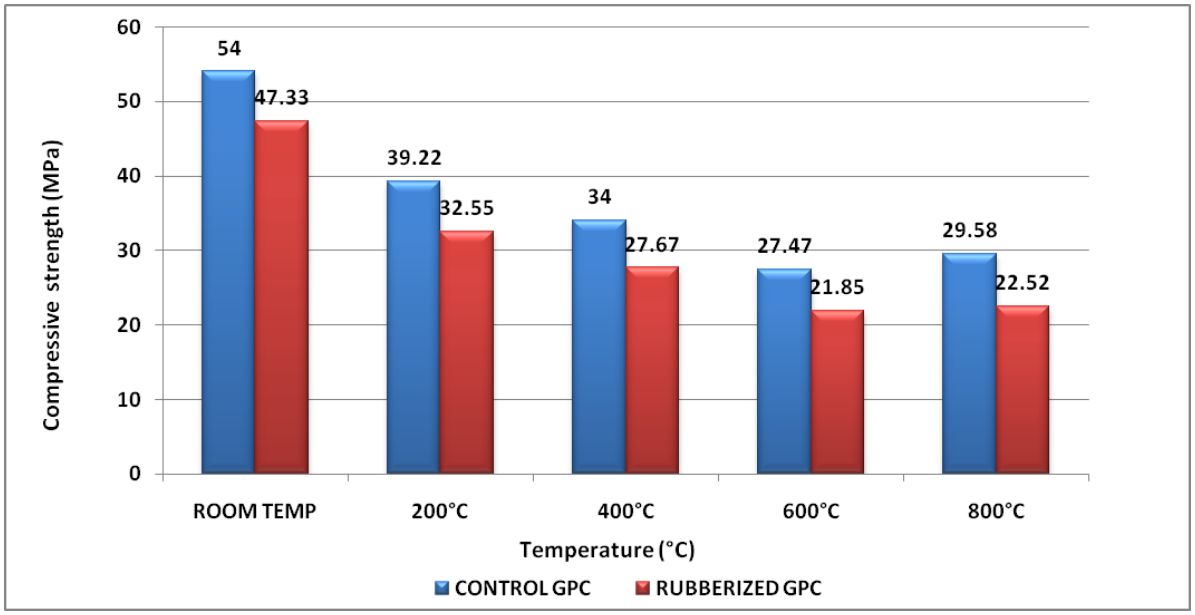

Figure 4.3: Compressive strength of control and rubberized geopolymer concrete specimens after exposure to elevated temperatures

Table 4.2: Compressive strength and density on exposure to elevated temperatures

Sr No.	Temperature (°C)	Compressive Strength N/mm^2		% Reduction of Compressive Strength N/mm^2		Density before Exposure kg/m^3		Density after Exposure kg/m^3	
		Control GPC	Rubberized GPC	Control GPC	Rubberized GPC	Control GPC	Rubberized GPC	Control GPC	Rubberized GPC
1	Room Temp	54	47.33	0	0	2392	2128	2063	1898
2	200°C	39.22	32.55	27.38	31.23	2365	2185	1964	1884
3	400°C	34.00	27.67	37.04	41.54	2385	2117	2105	1865
4	600°C	27.47	21.85	49.13	53.83	2409	2165	2050	1755
5	800°C	29.58	22.52	45.22	52.42	2355	2075	1889	1703

4.4.4 X-ray Powder Diffractometric Analysis

XRD was used to investigate the compositional transformations that occur in rubberized and control concrete samples when exposed to elevated temperatures.

Figure 4.4 shows that the intense peaks in the XRD spectra of geopolymer concrete reflect the presence of quartz and mullite in the ash and the effect of the activator when exposed to elevated temperatures. Mullite has a stable crystalline structure under ambient conditions. It retains its strength at elevated temperatures, and exhibits high temperature stability with little thermal expansion. [175, 176]. Semi-crystalline sodium aluminate silicate hydrate (N-A-S-H) gel was observed in specimens after exposure to 200°C.

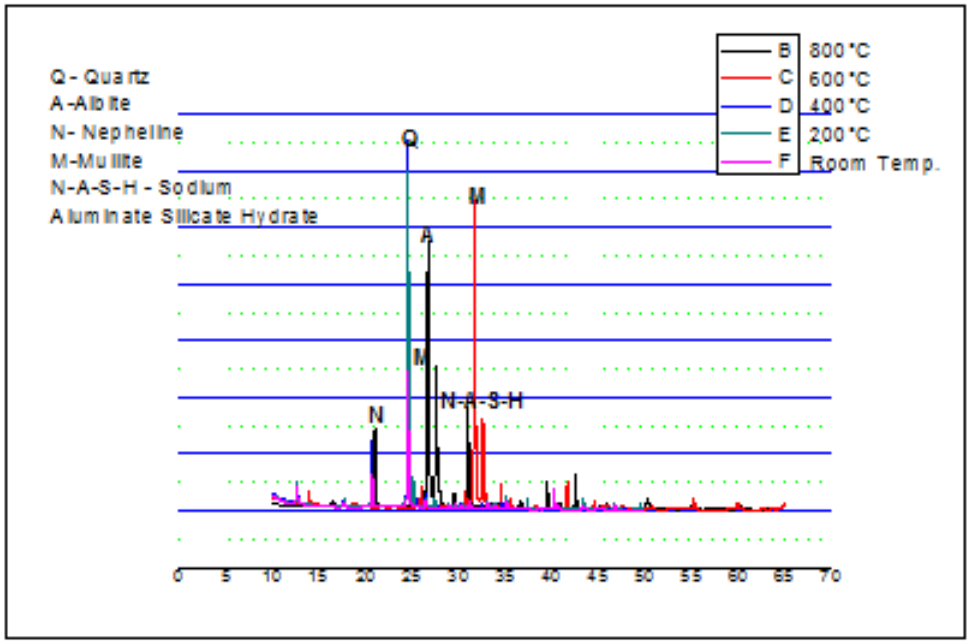

Figure 4.4: XRD spectra of GPC after various thermal treatments

In a previous study, Hussain *et al.* [176] reported the appearance of N-A-S-H (alumina silicate) gel in samples before and after thermal exposure to 200°C. The results of the current study are consistent with these findings. Zeolite was also formed as a by-product of this reaction. A crystalline phase of hydro-sodalite ($Na_4Al_3Si_3O_{12}OH$) formed during exposure to temperatures up to 400°C. The zeolite underwent recrystallization as nepheline ($NaAlSiO_4$) and albite ($NaAlSiO_8$) hydrous alumino-silicates after treatment at 600°C and 800°C [176, 177].

4.4.5 Fourier Transform Infrared Spectroscopy Analysis

FTIR spectra of the control and rubberized geopolymer concrete are shown in Figures 4.5 and 4.6, respectively. The spectra in Figure 4.5 exhibit major bands at approximately 3435, 1049, 777, and 458 cm^{-1}. Figure 4.6 shows similar bands occurring at approximately 3435, 1049, and 458 cm^{-1}. There are two common major bands in the control and rubberized geopolymer concrete, namely at 3435 cm^{-1} and 1049 cm^{-1}. The H-O-H band is located at 1049 cm^{-1} in both samples, which reflects the presence of water molecules. The H-O-H bond is formed after alkaline activation due to the presence of weakly bound water molecules [176].

The peaks at 3435 cm^{-1} and 1049 cm^{-1} correspond to stretching and bending of the OH bond, respectively. Similar results have been reported by Hussain et al. [176]. Na_2CO_3 was found to form in the control GPC at approximately 1049 cm^{-1} and 777 cm^{-1}. This is due to the carbonation of unreacted NaOH and Na_2SiO_3. Figures 4.5 and 4.6 indicate that the chain length decreases after treatment at 200°C because of the decrease in their bonding strength. Increasing the temperature from 200°C to 600°C does not reduce the chain length further, because all weakly bound water molecules are expelled at 200°C. At temperatures between 200°C and 600°C, there is a marginal decrease in peak intensity due to the occurrence of Si-O-Al and Si-O-Si bonds. However, beyond 600°C, absorption corresponding to vibrations in the Si-O-Si region occur due to the polymerization of unreacted materials [174].

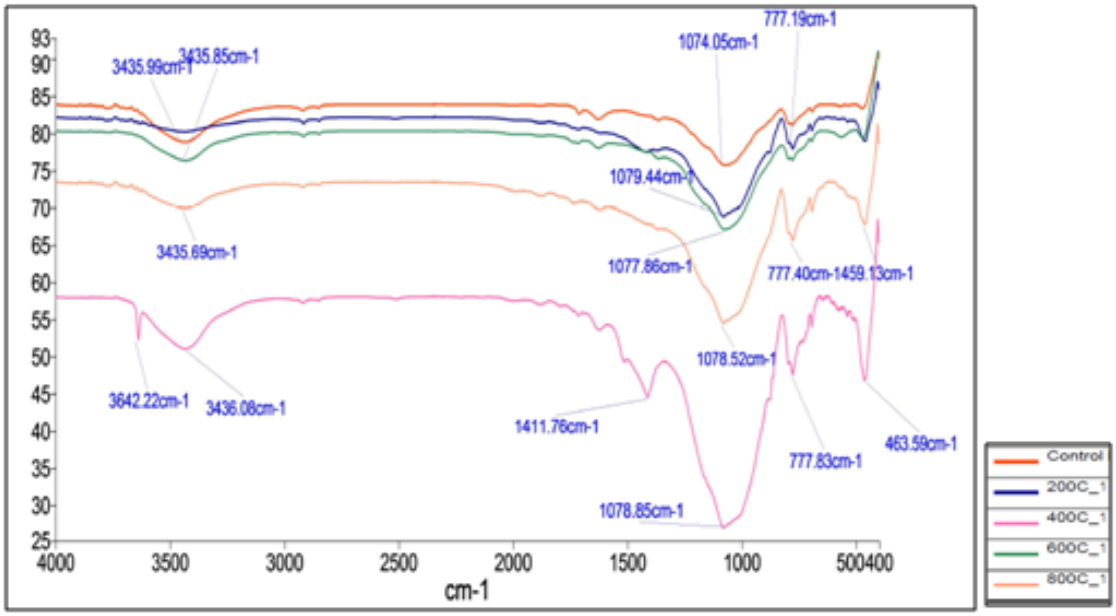

Figure 4.5: FTIR spectra of control GPC

N-A-S-H gel formation leads to an increase in the 1049 cm^{-1} peak intensity in both the control and rubberized GPC at all temperatures. This finding is confirmed by the XRD results in Figure 4.4. This gel remains in position because of the albite, which was observed in the XRD pattern shown in Figure 4.4 [176].

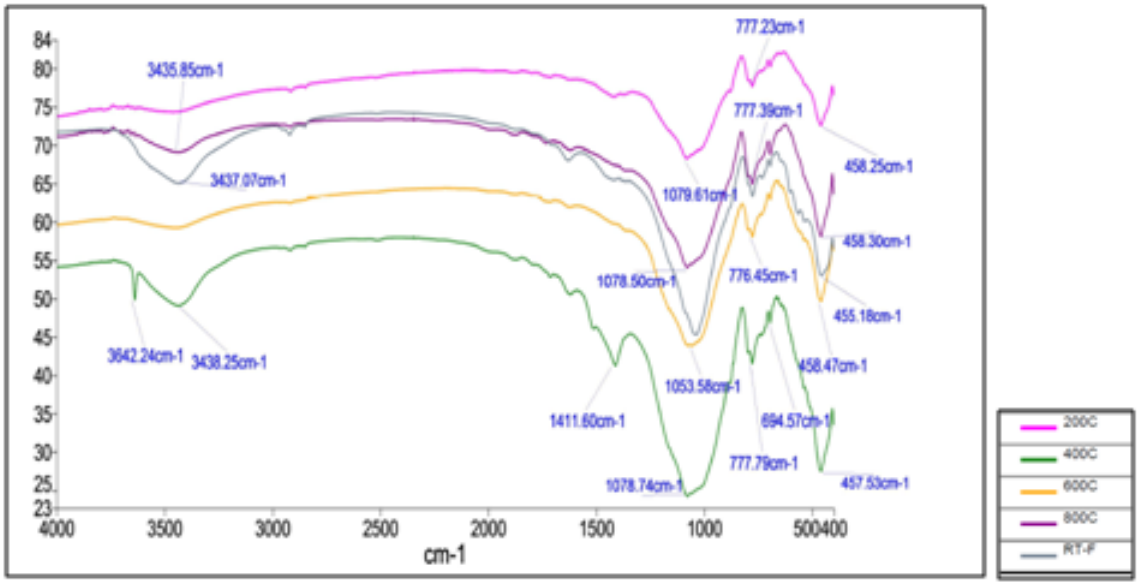

Figure 4.6: FTIR spectra of rubberized GPC

4.4.6 Thermogravimetric Analysis

TGA was carried out using a Perkin-Elmer simultaneous thermal analyser (STA 6000) to measure the mass loss of powder-like samples when heated from room temperature to 900°C.

The TGA and DTG curves of control geopolymer concrete shown in Figures 4.7 and 4.8 indicate that the maximum mass loss occurs at approximately 150°C. Beyond 150°C, the rate of mass loss remains relatively constant. Figure 4.7 shows a gradual reduction in mass with an increase in temperature. This loss is a result of moisture within the geopolymer concrete specimens rapidly migrating and changes in the chemical structure. These findings are consistent with the FTIR analysis as well as earlier reports [174, 178, 179], This effect causes surface and internal cracks to appear in the geopolymer specimens. A slightly higher rate of mass loss was observed at 750°C, which may be due to the formation of nepheline identified by the XRD spectra. The

TGA and DTG curves of geopolymer concrete exhibit similar behaviour, and have therefore been omitted.

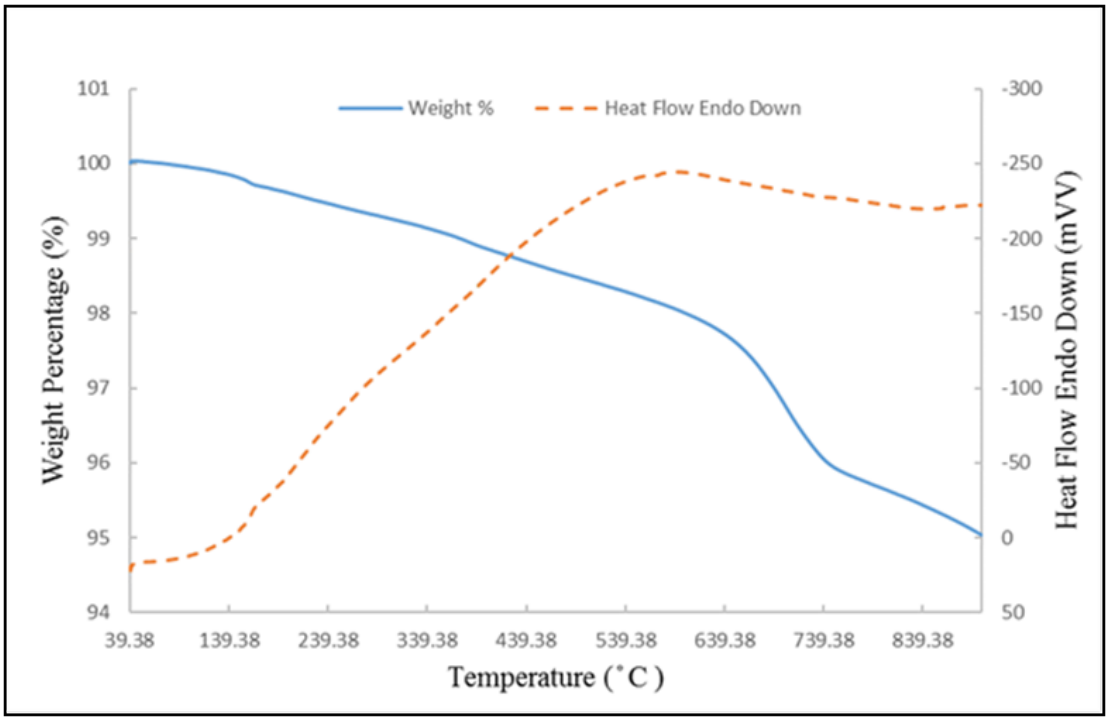

Figure 4.7: TGA curve of rubberized geopolymer concrete

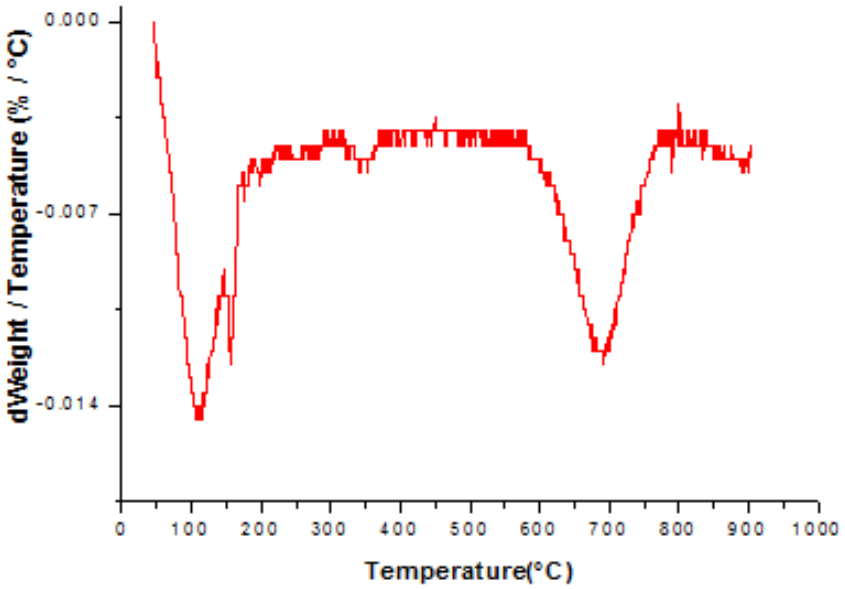

Figure 4.8: DTG curve of rubberized geopolymer concrete

4.5 Conclusion

The following conclusions can be drawn from the results in this chapter:

1. Elevated temperatures have a similar effect on both the control and rubberized geopolymer concrete.

2. The strength of the control and rubberized geopolymer decreases after thermal exposure up to 600°C. However, the compressive strength increases on exposure to temperatures greater than 600°C, and was observed to be higher at 800°C than at 600°C.

3. Hairline cracks were observed in rubberized geopolymer concrete after exposure to temperatures in excess of 600°C.

4. At elevated temperatures, N-A-S-H (alumina silicate) forms in both the control and rubberized geopolymer concrete. Zeolite forms as a secondary reaction product in both concretes; this is then converted into hydro-sodalite ($Na_4Al_3Si_3O_{12}OH$)

at elevated temperatures. The zeolite undergoes recrystallization as nepheline ($NaAlSiO_4$) and albite ($NaAlSiO_8$), similar to a hydrous alumina silicate, after exposure to 600°C and 800°C.

5. The FTIR signature of both types of geopolymer concrete shows minor changes in the region around 1049 cm^{-1} and 777 cm^{-1}, suggesting that both types of geopolymer concrete have good heat resistance.

Chapter 5

Fly ash based Geopolymer Mortar

5.1 Prelude

History has witnessed a continuous improvement and development in construction practices. Over the last century, the expense involved in the preparation of mortar and concrete has come to represent the majority of the total cost of a project. Driven by commercial and industrial demand to economize the construction process, a paradigm shift occurred in the technological advancement of mortar and concrete preparation. The inaccessibility of various important constituents of mortar and concrete, such as lime, made many construction projects economically unviable. Hence, various researchers investigated the replacement of OPC concrete and mortar by geopolymer concrete and mortar. This chapter focuses on carbonation and strength studies related to geopolymer mortar.

5.2 Requirements and Advantages of Geopolymer Mortar

Conventional mortar consists of a binder material cement, fine aggregate, and water, and is mainly used to fill the gaps between masonry or bricks. Mortar can be made of asphalt, cement, and mud. Cement is an important component of OPC and ordinary mortar. The manufacture of cement involves heating limestone to 1450°C in a kiln, a

process known as calcination. This process produces carbon dioxide while converting calcium carbonate into calcium oxide. In parallel, coal used to heat the kiln also emits carbon dioxide. Various studies have revealed that approximately one ton of carbon dioxide is emitted to produce one ton of cement [180, 181].

According to the literature, the global construction industry requires 2.6 billion tons of cement every year. Further, demand for cement is estimated to increase by around 25% over the next 10 years. As the fundamental material for the production of cement, natural reserves of limestone may face shortages in the next 25 years [181].

It is clear that the use of cement poses many challenges to our environment and atmosphere, and has the potential to disrupt the eco-system of the planet. International organizations such as the United Nations are pushing for reforms regarding climate change through the United Nations Framework Convention on Climate Change. The conference held in Paris is seen as a watershed moment in policy regarding climate change, with its stated intention to make a reduced carbon footprint legally binding in signatory countries. Hence, it is imperative that policy makers pay heed to the environmental challenges posed by cement production. It is vital to explore alternative methodologies that could replace the monopoly of cement as a binder material in the construction industry.

The use of geopolymers offers the best solution to the environmental challenges stated above. On the one hand, geopolymers use waste materials generated from thermal industries such as fly ash and blast furnace slag, while on the other hand, they can replace the use of cement as a binder material in the preparation of mortar. The main aim of the present chapter is to understand and investigate the performance of geopolymer mortar. Further, the performance of geopolymer mortar subjected to carbonation is thoroughly investigated. This chapter clarifies the possible mix composition of geopolymer mortar, and studies the influence of the mix composition on the mechanical strength, microstructure, and carbonation of geopolymer mortar.

5.3 Mix Proportion and Testing Method

An investigation of various parameters provides the platform for understanding the behaviour of geopolymer mortar. This enhances the likelihood of geopolymer mortar being used in various construction applications. Further, the influence of environmental degradation such as carbon dioxide exposure on the durability of the mortar enables the service life of the mortar to be estimated. In the present study, two experimental investigations were conducted. Series A examines the influence of mix proportions on the compressive strength of the mortar, whereas Series B studies the influence of mix proportions on the durability of the mortar against carbonation. This chapter discusses the test procedure and programme, and presents the experimental results and discussion.

5.3.1 Investigation of Compressive Strength

Series A examines the effect of mix proportions on the compressive strength of geopolymer mortar. This section presents the test methodology, test programme, results, and discussion.

5.3.2 Test Method

Preparation of mortar specimens

To prepare the geopolymer mortar specimens, fly ash and alkaline activating solution (NaOH and Na_2SiO_3) were blended in predefined proportions using a manual mixing technique. Further, the fine aggregate was mixed into the activated fly ash mix paste for a further 5 min. The prepared mortar was mixed up to a good consistency, and the prepared mortar was poured into steel moulds of length 50 mm, breadth 50 mm, and height 50 mm. The moulds were vibrated for 2 min to remove entrapped air, as shown in Figure 5.1. The specimens were preserved at room temperature for a duration of 300 min. The specimens were cured at a constant temperature of 60°C or 90°C for 24 h. After curing, the mortar samples were removed by unpacking the moulds and kept at room temperature shown in Figure 5.2.

Figure 5.1: Perspective view of the moulds

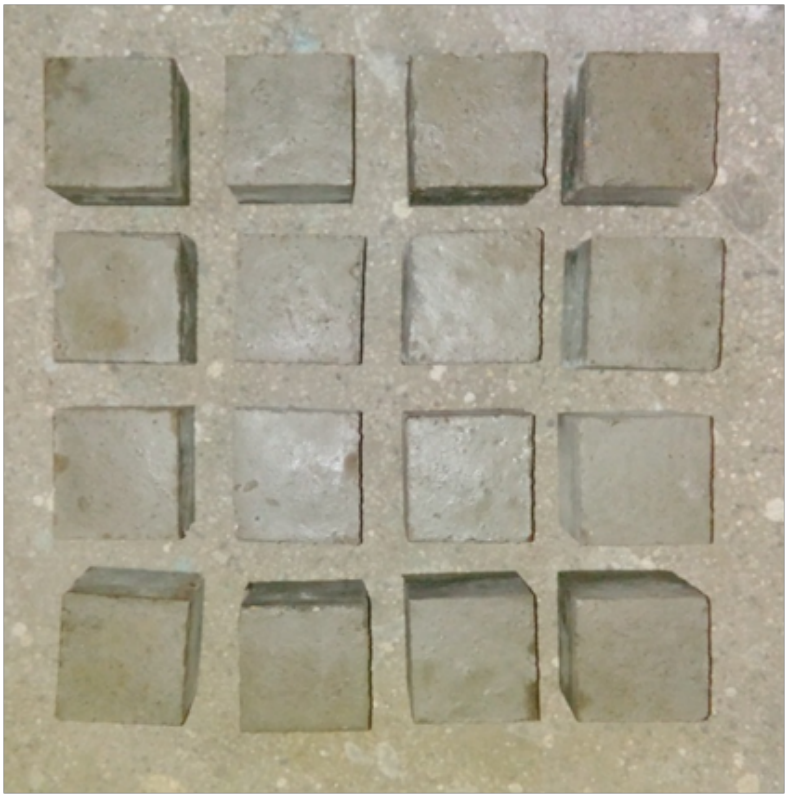

Figure 5.2: Perspective view of geopolymer mortar specimens

Testing procedure

The mortar samples obtained after curing were subjected to compression tests. Specimens were tested according to IS-2250 [182]. Three samples with an identical mix design were tested using machine CTM. The average compressive strength was computed from these samples. Further, crushed samples were obtained for further microscopic analyses. The crushed powder was used to analyse the mineralogical composition and structural arrangement.

5.3.3 Test Programme

Based on the literature, several parameter combinations of the alkaline activator to fly ash ratio, sodium silicate to sodium hydroxide ratio, curing time, and delay time were adopted for the mix compositions. The delay time refers to the time duration between pouring the mix into the moulds and the start of curing by heating. The value of the alkaline activator to fly ash ratio, sodium silicate to sodium hydroxide ratio, and delay time were set to 0.4, 1, and 5 h, respectively. In the present study, the NaOH concentration, aggregate to binder ratio, and curing temperature were varied while the above mentioned parameters were held constant. Table 5.1 summarizes the test programme for Series A. It is important to note that the test programme given in Table 5.1 was conducted twice: in Series A1, samples were cured for up to 7 days, whereas in series A2, the samples were cured for up to 28 days.

5.3.4 Results and Discussion

The results for series A are reported in terms of compressive strength. The compressive strength of each mix composition was computed by taking the average compressive strength obtained from the three samples with identical compositions. As discussed in Table 5.1, the present section shows the influence of mix composition parameters on the compressive strength of the mortar.

Table 5.1: Summary of the test programme adopted for Series A in the present study

Mixes	NaOH concentration	Aggregate to binder ratio	Curing temperature
S-1	14M	1:1	60^0C
S-2	14M	2:1	60^0C
S-3	14M	3:1	60^0C
S-4	11M	1:1	60^0C
S-5	11M	2:1	60^0C
S-6	11M	3:1	60^0C
S-7	8M	1:1	60^0C
S-8	8M	2:1	60^0C
S-9	8M	3:1	60^0C
S-10	14M	1:1	90^0C
S-11	14M	2:1	90^0C
S-12	14M	3:1	90^0C
S-13	11M	1:1	90^0C
S-14	11M	2:1	90^0C
S-15	11M	3:1	90^0C
S-16	8M	1:1	90^0C
S-17	8M	2:1	90^0C
S-18	8M	3:1	90^0C

5.3.5 Influence of NaOH Concentration on Compressive Strength

Figures 5.3 and 5.4 show the variation in compressive strength achieved after 7 days with respect to the concentration of NaOH. As can be seen, the compressive strength increases with the concentration of the alkali activator. The increase in compressive strength can be attributed to the greater amount of leaching of Si^{4+} and Al^{3+} ions. The leaching of Si^{4+} and Al^{3+} ions leads to the formation of alumino-silicate gel, which in turn provides compressive strength to the mortar sample. The maximum compressive strengths for the mortar cured at $60°C$ and $90°C$ are 30.53 MPa and 32.92 MPa, respectively. The maximum compressive strengths are given by the 14M concentration of the alkali activator.

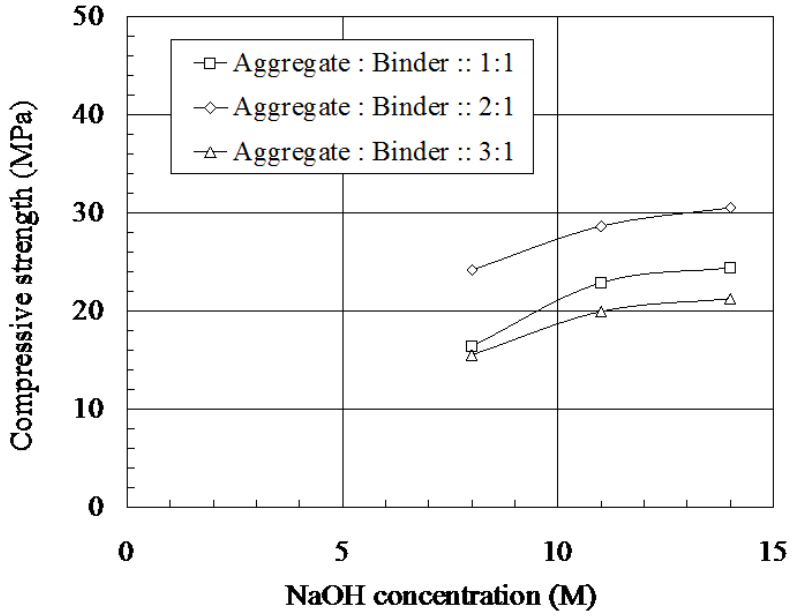

Figure 5.3: Variations in 7 days compressive strength of mortar with NaOH concentration (curing temperature (T_c) = $60°C$)

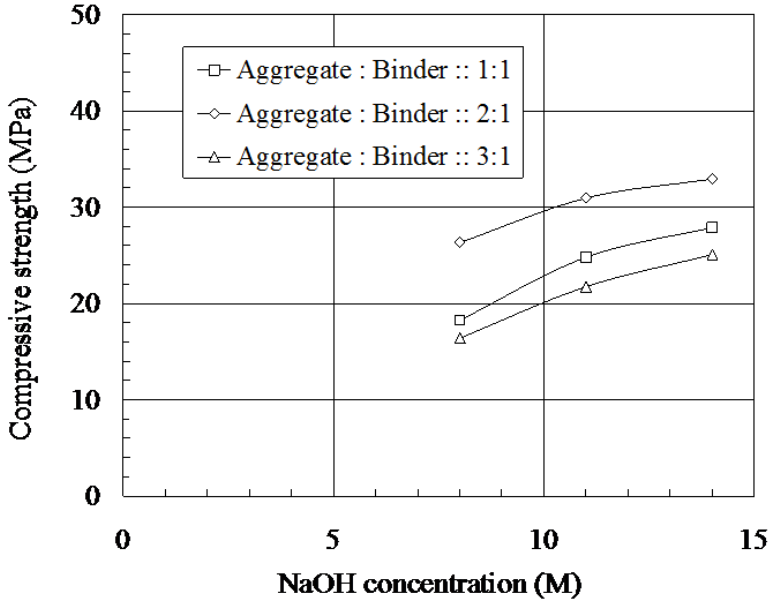

Figure 5.4: Variations in 7 days compressive strength of mortar with NaOH concentration (curing temperature (T_c) = $90°C$)

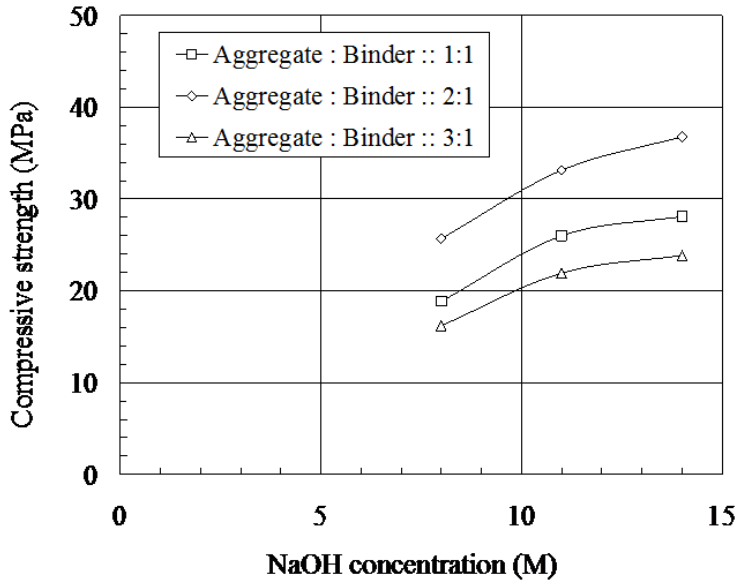

Figure 5.5: Variations in 28 days compressive strength of mortar with NaOH concentration (curing temperature (T_c) = $60°C$)

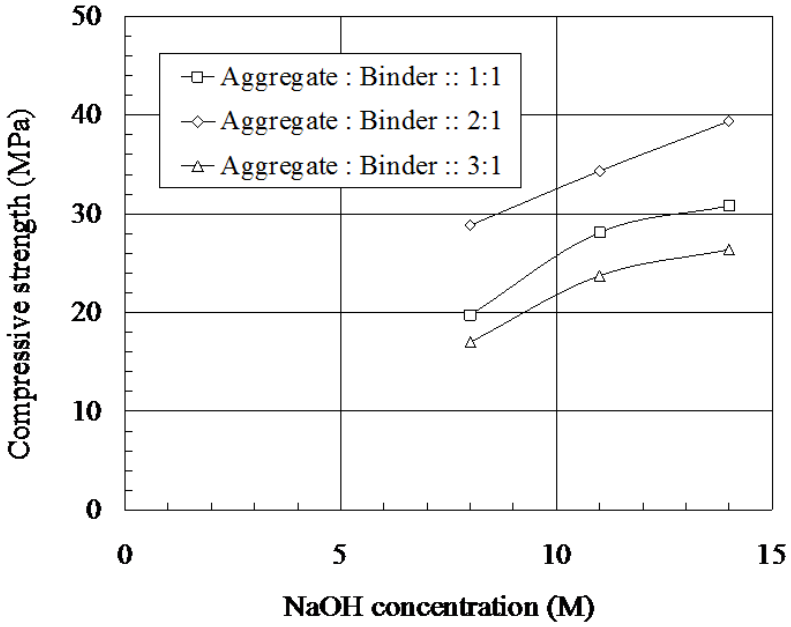

Figure 5.6: Variations in 28 days compressive strength of mortar with NaOH concentration (curing temperature (T_c) = $90°C$)

Figures 5.5 and 5.6 compare the variation in compressive strength (after 28 days) of the mortar cured at temperatures of $60°C$ and $90°C$ with respect to the concentration of NaOH. It can be observed that the compressive strength increases significantly with the addition of NaOH at increased concentrations (8M, 11M, and 14M). The increased compressive strength is a result of the higher dissolution of Si^{4+} and Al^{3+} ions, which results in the presence of more alumino-silicate gel within the matrix of the mortar. The alumino-silicate gel attains compressive strength when subjected to higher temperature. The increase in temperature (up to a certain extent) may help in achieving higher strength, which is evident from the higher compressive strength in the mortar cured at $90°C$ than in that cured at $60°C$.

5.3.6 Influence of Aggregate to Binder Ratio on Compressive Strength

Figures 5.7 and 5.8 depict the variation in the 7-day compressive strength of geopolymer mortar with respect to changes in the aggregate to binder ratio. For this purpose, various concentrations of NaOH were used. It can be seen that the compressive strength of the mortar increases as the aggregate ratio decreases from 3:1 to 2:1. Further, a decrease in aggregate content from 2:1 to 1:1 causes a decrease in compressive strength. The compressive strength of alkali-activated fly ash geopolymer mortar is governed by the strength of the binder (alkali-activated fly ash) and proper bonding between the fine aggregate and binder material. An increase in compressive strength at low aggregate to binder ratios can be attributed to proper bonding between the fine aggregate and geopolymer mortar. Further, a decrease in compressive strength following a decrease in aggregate content can be attributed to the increased porosity of the geopolymer mortar in the presence of a smaller fraction of fine aggregates.

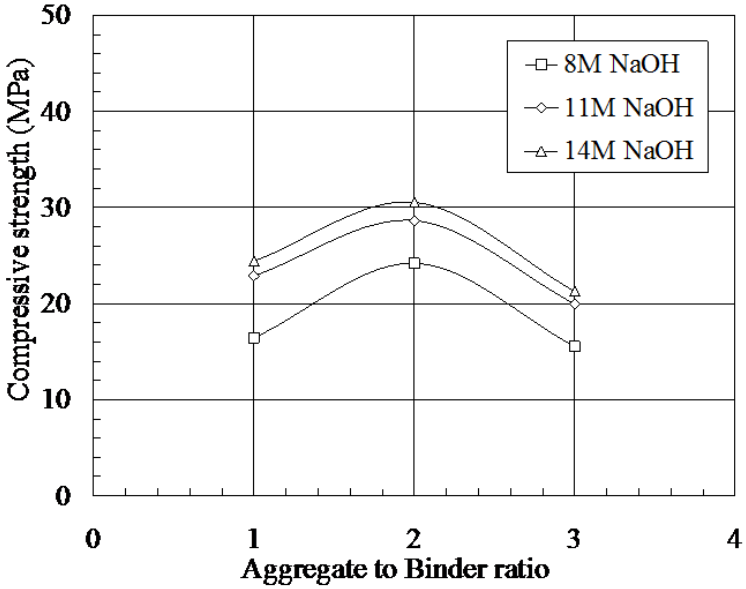

Figure 5.7: Variations in 7 days compressive strength of mortar with NaOH concentration (curing temperature (T_c) = $60°C$)

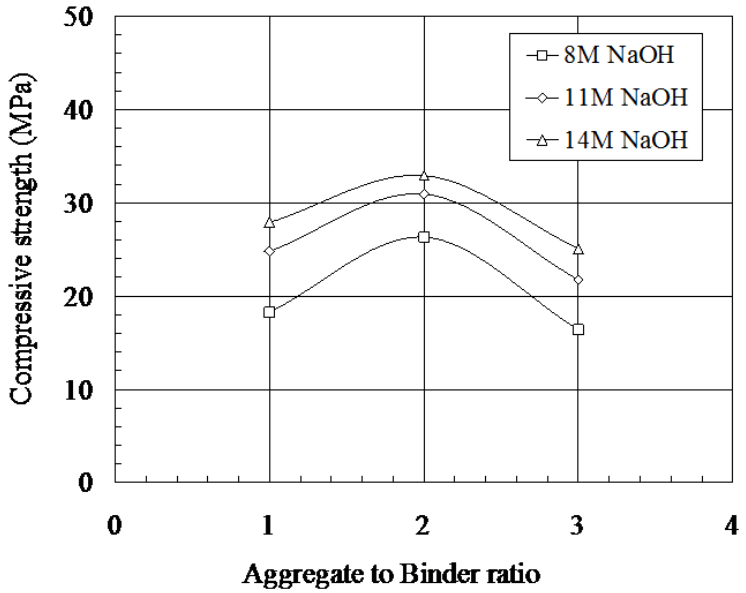

Figure 5.8: Variations in 7 days compressive strength of mortar with NaOH concentration (curing temperature (T_c) = $90°C$)

The influence of changes in the concentration of sodium hydroxide on the compressive strength of similar specimens was investigated. For each concentration of NaOH, an identical pattern of variation in compressive strength was observed with respect to the change in aggregate content. However, specimens prepared with high concentrations of NaOH possessed higher compressive strengths. This is because of the increased alkali activation of fly ash and proper leaching of Al^{3+} and Si^{4+} ions from fly ash to the geopolymer matrix.

Figure 5.8 demonstrates the variation of the 7-day compressive strength of geopolymer mortar with respect to the aggregate and concentration of NaOH for a curing temperature of $90°C$. The nature of this curve is identical for curing temperatures of $60°C$ and $90°C$. Maximum compressive strengths of 26.31 MPa, 30.93 MPa, and 32.92 MPa were obtained for NaOH concentrations of 8M, 11M, and 14M, respectively, at the optimum binder to sand ratio of 2:1.

Figures 5.9 and 5.10 demonstrate the variation in 28-day compressive strength with respect to the concentration of NaOH and aggregate to binder ratio for specimens cured at temperatures of $60°C$ and $90°C$. Maximum compressive strength was attained by mixing an aggregate-binder ratio of 2:1 for NaOH concentrations of 8M, 11M, and 14M. Higher compressive strength was observed for higher concentrations of NaOH, which signifies the importance of leaching phenomena in achieving good compressive strength.

Further, the influence of curing temperature on the compressive strength was also examined. It was found that the higher curing temperature resulted in higher compressive strength. This is because the geopolymer matrix hardens under heating.

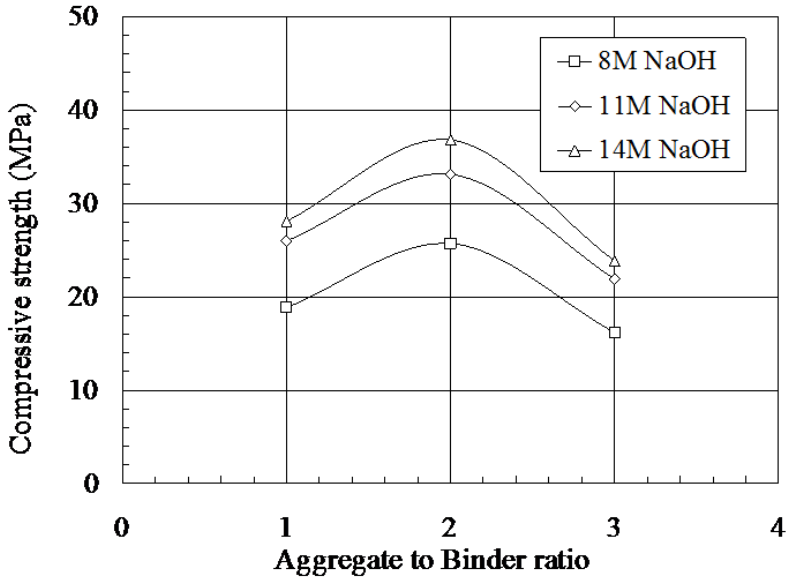

Figure 5.9: Variations in 28 days compressive strength of mortar with NaOH concentration (curing temperature (T_c) = $60°C$)

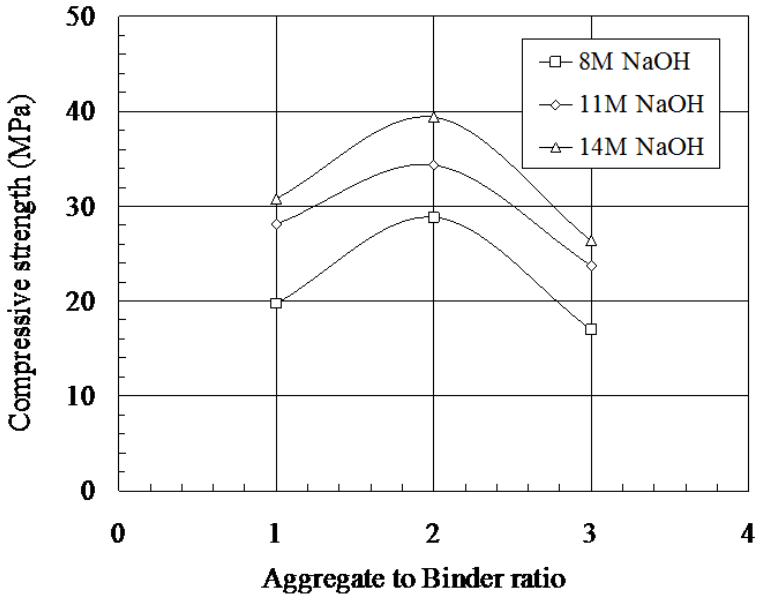

Figure 5.10: Variations in 28 days compressive strength of mortar with NaOH concentration (curing temperature (T_c) = $90°C$)

5.3.7 Influence on Microstructure of Geopolymer Mortar

Scanning Electron Microscopy

In the present study, a scanning electron microscope available at the Material Research Center, MNIT Jaipur, was used to investigate variations in the microstructure features of geopolymer mortar and unreacted fly ash. Figures 5.11, 5.12, and 5.13 show micrographs of the mortar made up of 14M NaOH using varying aggregate to binder ratios. Plenty of alumino-silicate gel was observed in the mortar made from an aggregate to binder ratio of 1:1. With aggregate to binder ratios of 2:1 and 3:1, the amount of gel present in the matrix of the mortar decreases. The micrographs are in agreement with the compressive strength results.

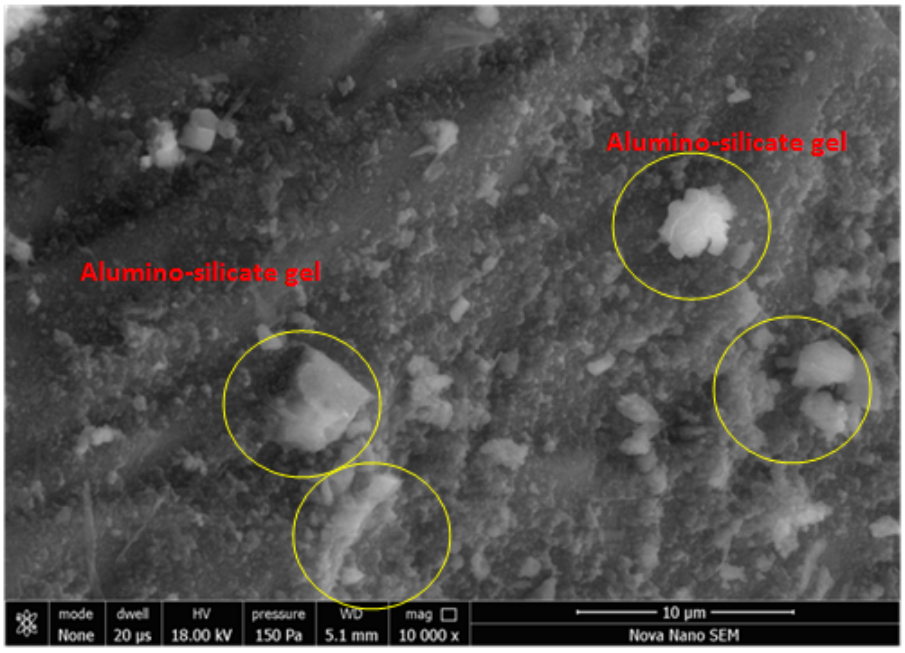

Figure 5.11: Micrograph of geopolymer mortar obtained from SEM (14M NaOH, aggregate to binder ratio = 1:1)

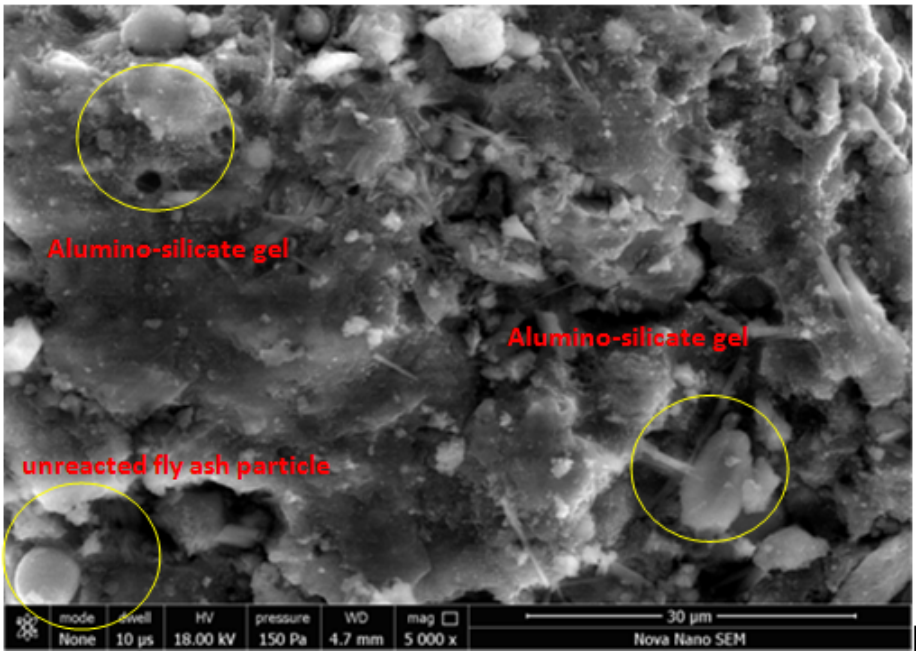

Figure 5.12: Micrograph of geopolymer mortar obtained from SEM (14M NaOH, aggregate to binder ratio = 2:1)

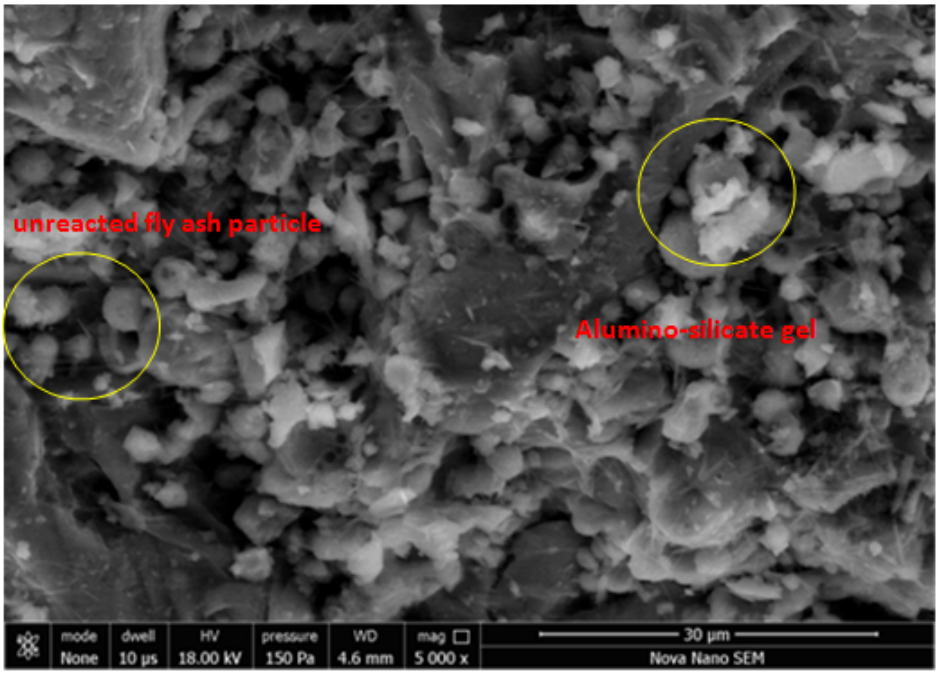

Figure 5.13: Micrograph of geopolymer mortar obtained from SEM (14M NaOH, aggregate to binder ratio = 3:1)

Figures 5.14, 5.15, and 5.16 show micrographs obtained from SEM for mortar made using sodium hydroxide of varying concentrations. The NaOH acts as a dissolution and leaching agent during the preparation of the mortar. Higher concentrations of NaOH accelerate the dissolution of fly ash particles into the matrix, which in turn become alumino-silicate gel. In the figures, the matrix of gel, fly ash, and fine aggregate around particles of the fly ash can be seen. It was observed that, in the case of mortar made up of 8M NaOH, a significant number of unreacted fly ash particles were present. The presence of unreacted fly ash particles indicates insufficient NaOH to dissolve all the fly ash particles and does not allow the mortar to achieve its potential strength. However, in the case of the mortar with 11M and 14M NaOH, there is a noticeable improvement in the dissolution of fly ash particles.

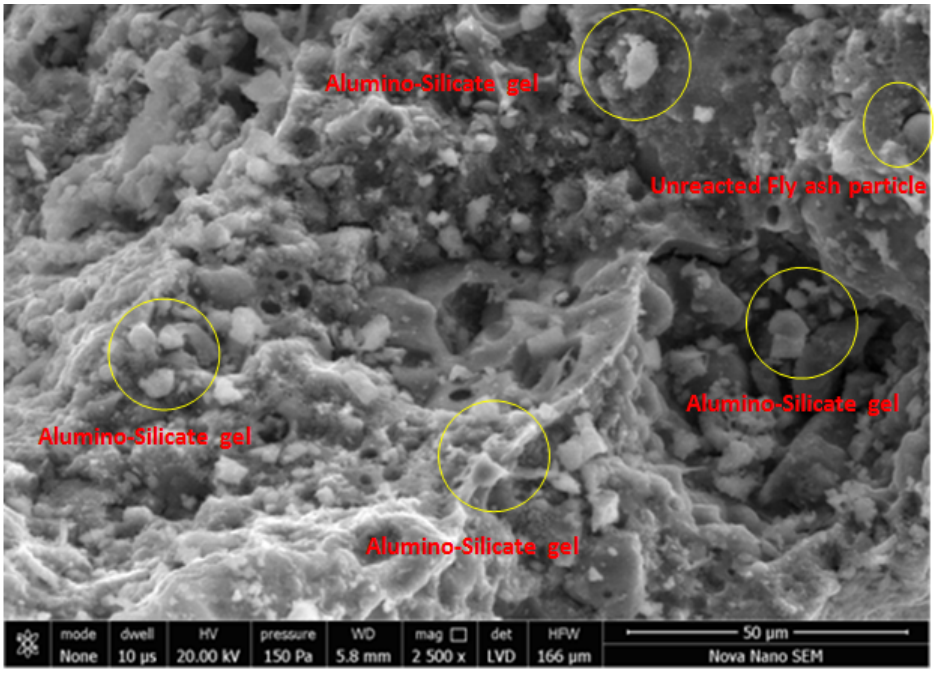

Figure 5.14: Micrograph of geopolymer mortar at 14M NaOH

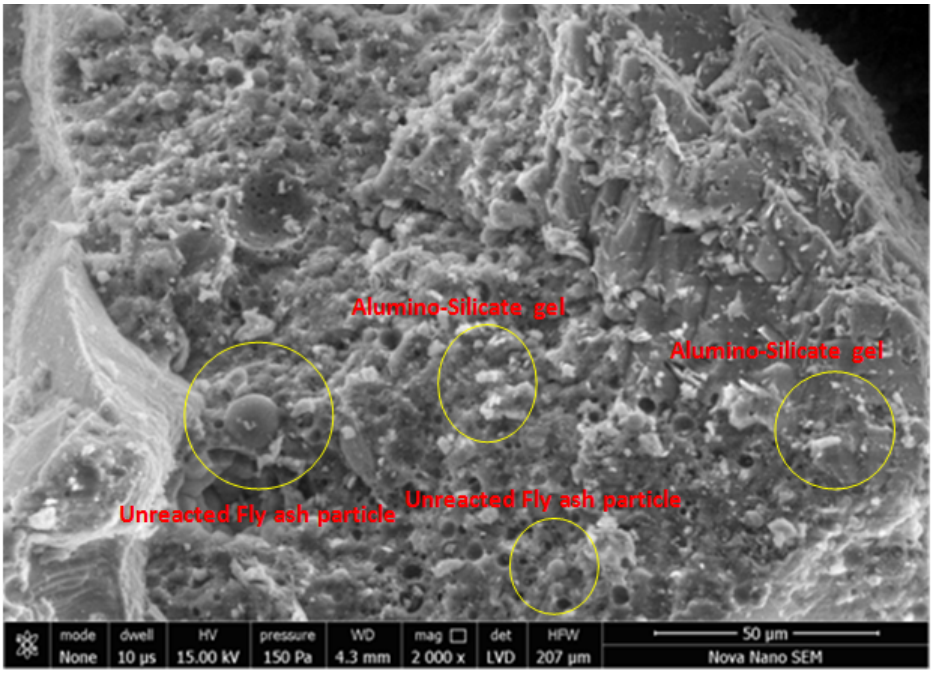

Figure 5.15: Micrograph of geopolymer mortar at 11M NaOH

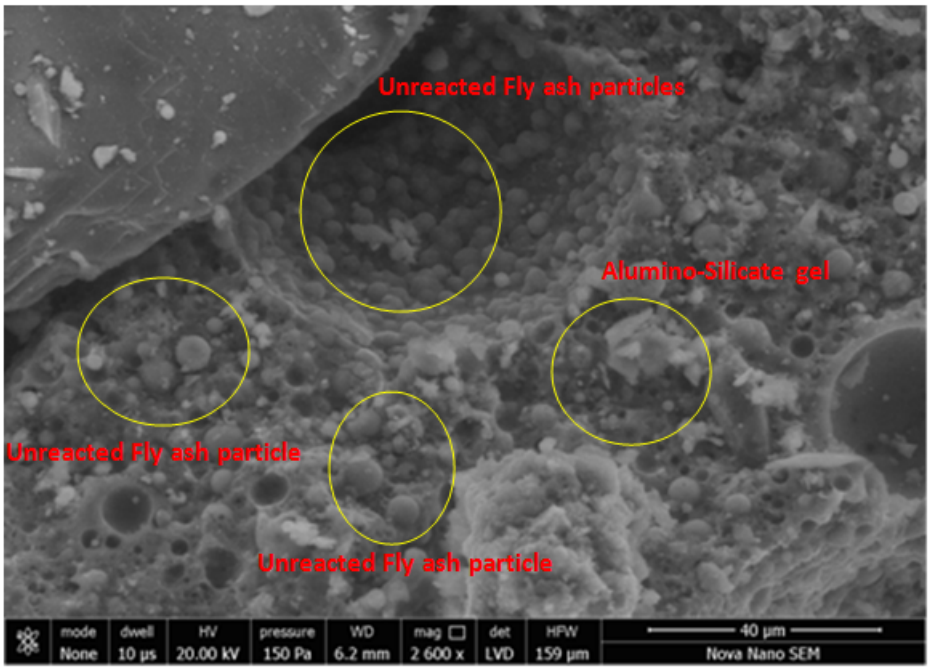

Figure 5.16: Micrograph of geopolymer mortar at 8M NaOH

X-ray diffractometry

XRD analyses were performed using a high-resolution powder X-ray diffractometer at the Material Research Center, MNIT Jaipur, with generator settings of 40 mA and 40 kV. The tests were conducted as per standard guidelines at room temperature of $25°C$. An angular range of 20°, step size of 0.03°, and wavelengths $\lambda = 1.5$ A° were adopted for the data acquisition. Further, the data obtained from the XRD were analysed using the PANalytical Xpert HighScore software. This software processes the data and removes background noise using in-built mathematical functions. The processed data are used for further identification of the peaks. The peaks are matched with standard minerals and available peaks are marked. The software automatically uses the standard data file provided by ICSD (International Chemical Data Service). In this section, the crystallography of the geopolymer mortar is studied and discussed.

Figures 5.17, 5.18, and 5.19 show the variation in geopolymer mortar with changes in the aggregate to binder ratio. Figure 5.17 shows a geopolymer mortar made up using 14M NaOH. The diffractogram of fly ash alone shows various minerals such as mullite (M), quartz (Q), and hematite (H). The presence of these minerals is in agreement with the chemical composition of the fly ash reported in earlier chapters. Further, under the geopolymerization process, the crystallography of the mortar changes. However, crystals present in the geopolymer mortar change with the mix composition. With an aggregate binder ratio of 1:1, the mortar possesses a sodalite (S) mineral. Aggregate binder ratios of 2:1 and 3:1 produce different minerals, respectively, namely i) sodalite and cristobalite (C) and ii) sodalite and zeolite (Z).

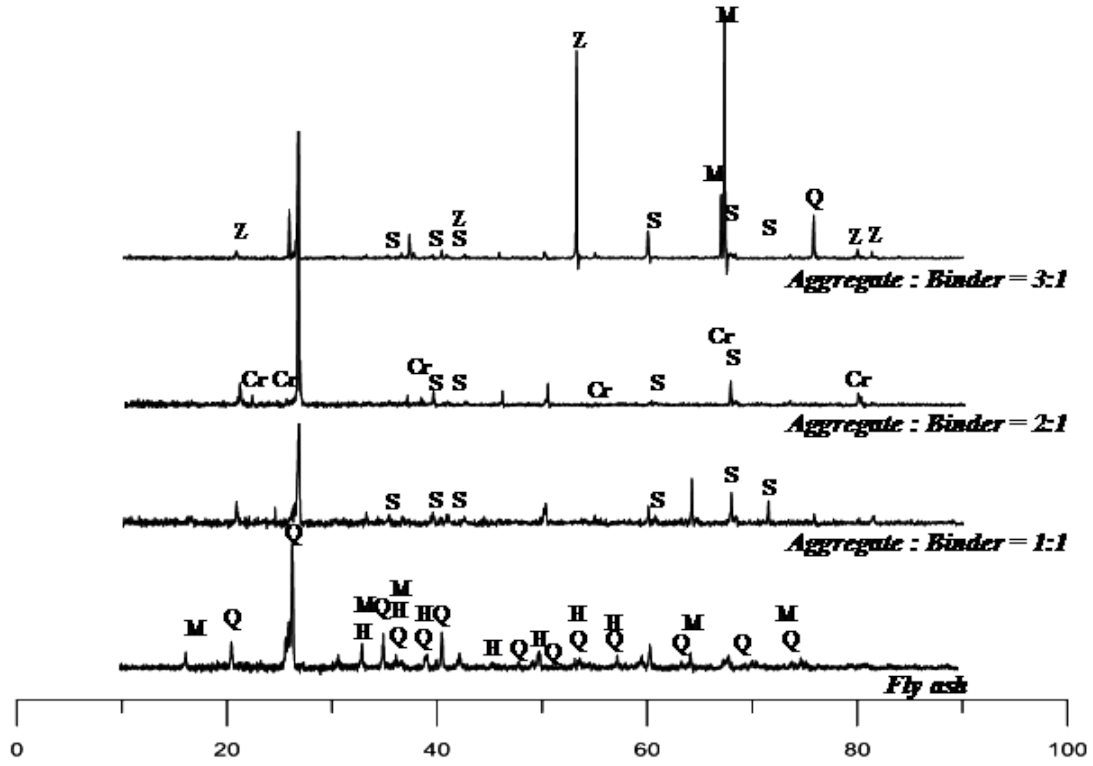

Figure 5.17: XRD of alkali-activated geopolymer mortar (14M NaOH)

Figure 5.18 shows the mortar made up using 11M NaOH. The change in crystallography due to the geopolymerization process is clearly visible. The diffractogram shows that different sets of crystals appear in the mortars at each aggregate to binder ratio (1:1, 2:1, and 3:1), namely i) sodalite and magnetite, ii) sodalite, magnetite, and hematite, and iii) sodalite, magnetite, and hematite, respectively. This demonstrates the influence of mix composition on the crystal structure of the mortar matrix.

Figure 5.19 depicts the geopolymer mortar given by 8M NaOH. The crystal structure is strongly influenced by the geopolymerization process. Note that mortar made up of each different aggregate binder ratio (1:1, 2:1, and 3:1) has a different set of crystals, namely i) sodalite, mullite, and magnetite, ii) sodalite, mullite, and hematite, and iii) magnetite, sodalite, and feldspar.

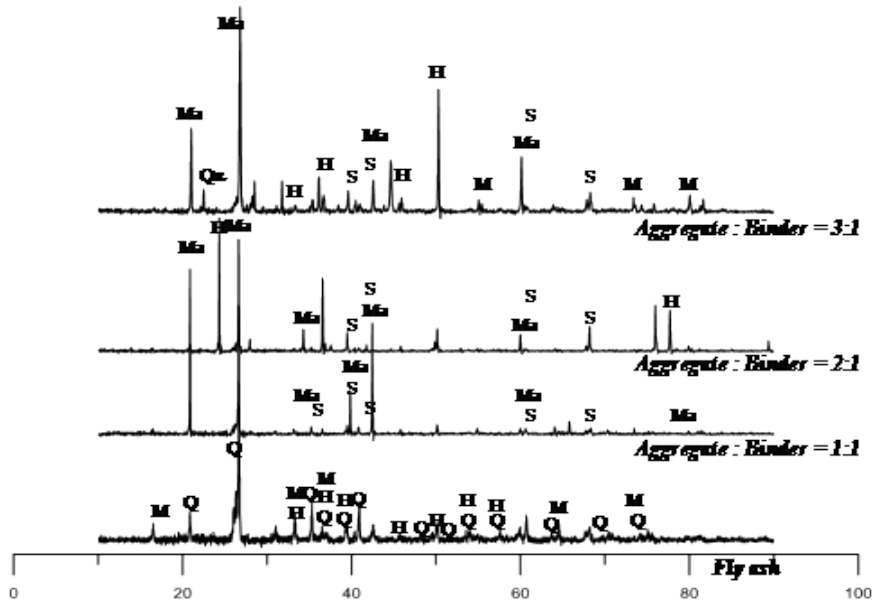

Figure 5.18: XRD of alkali-activated geopolymer mortar (11M NaOH)

Figures 5.20, 5.21, and 5.22 illustrate the variation of the geopolymer according to the influence of the NaOH concentration. It can be seen that, for mortar made up of higher concentrations of NaOH, sodalite is prominent in the matrix. The presence of sodalite is irrespective of the aggregate to binder ratio. At lower concentrations of NaOH, several minerals are found. For example, in mortar with an aggregate binder ratio of 1:1, for 8M and 11M NaOH, two set of minerals are found, namely i) hematite, magnetite, and sodalite, and ii) magnetite and sodalite.

Similarly, the mortar with an aggregate-binder ratio of 2:1 exhibits two sets of minerals, i) magnetite and sodalite with 8M NaOH and ii) magnetite and sodalite with 11M NaOH (see Figure 5.21). Further, the mortar with an aggregate-binder ratio of 3:1 has two groups of minerals, i) zeolite, magnetite, feldspar and sodalite with 8M NaOH and ii) magnetite, hematite, and sodalite with 11M NaOH.

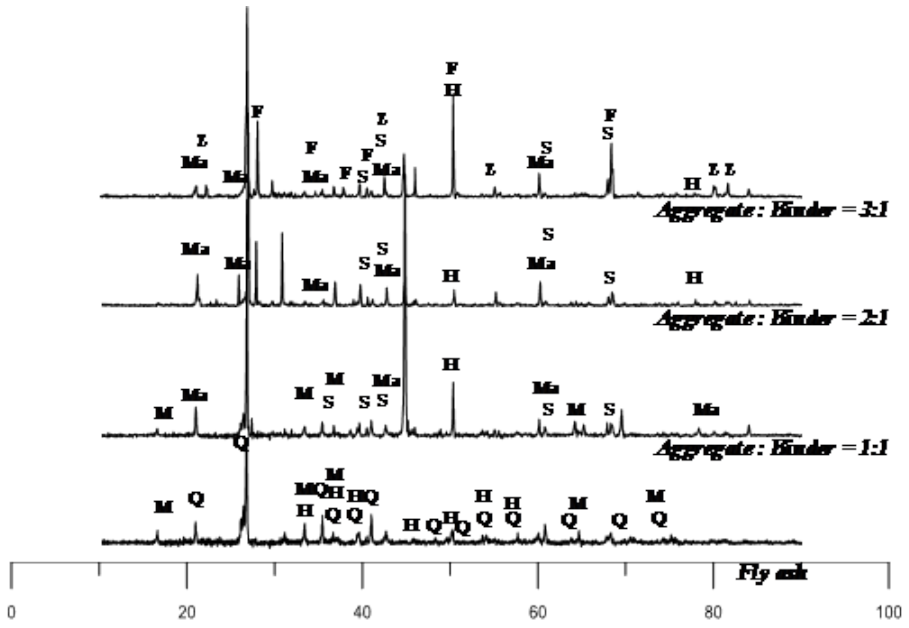

Figure 5.19: XRD of alkali-activated geopolymer mortar (8M NaOH)

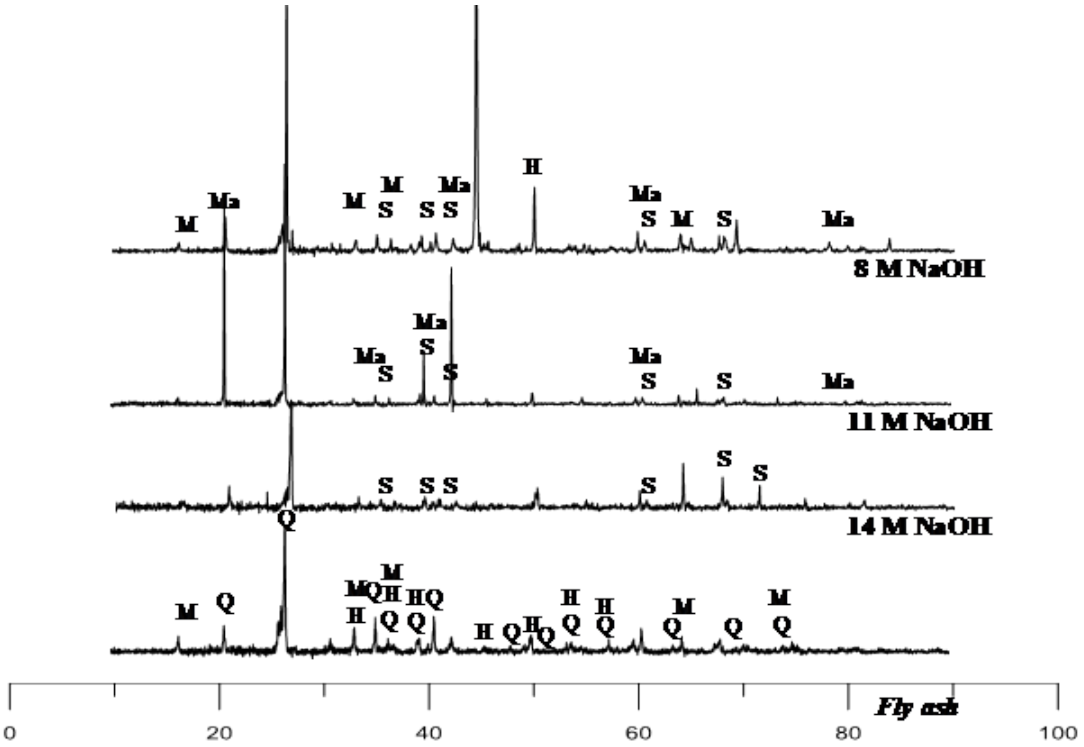

Figure 5.20: XRD of alkali-activated geopolymer mortar (aggregate to binder ratio = 1:1)

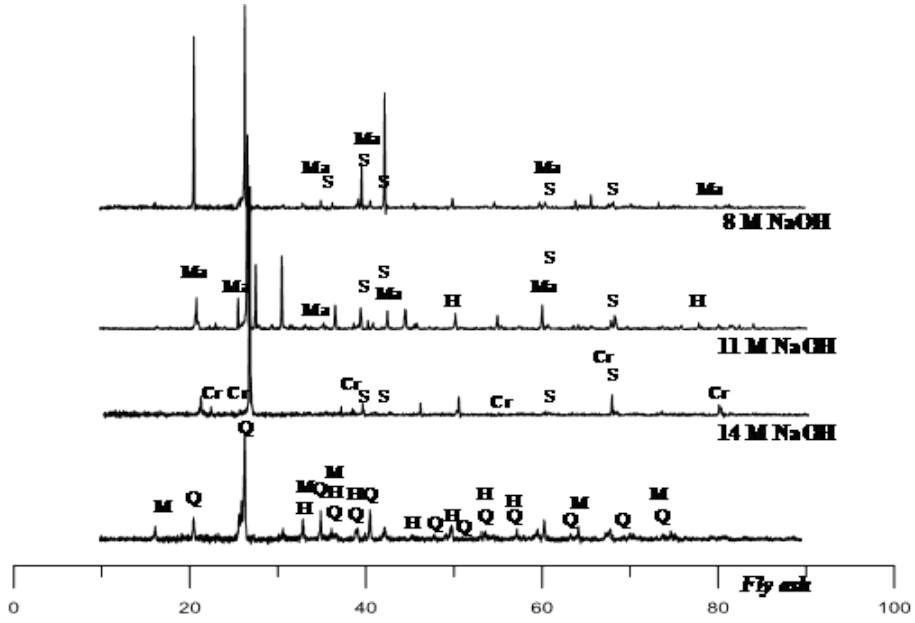

Figure 5.21: XRD of alkali-activated geopolymer mortar (aggregate to binder ratio = 2:1)

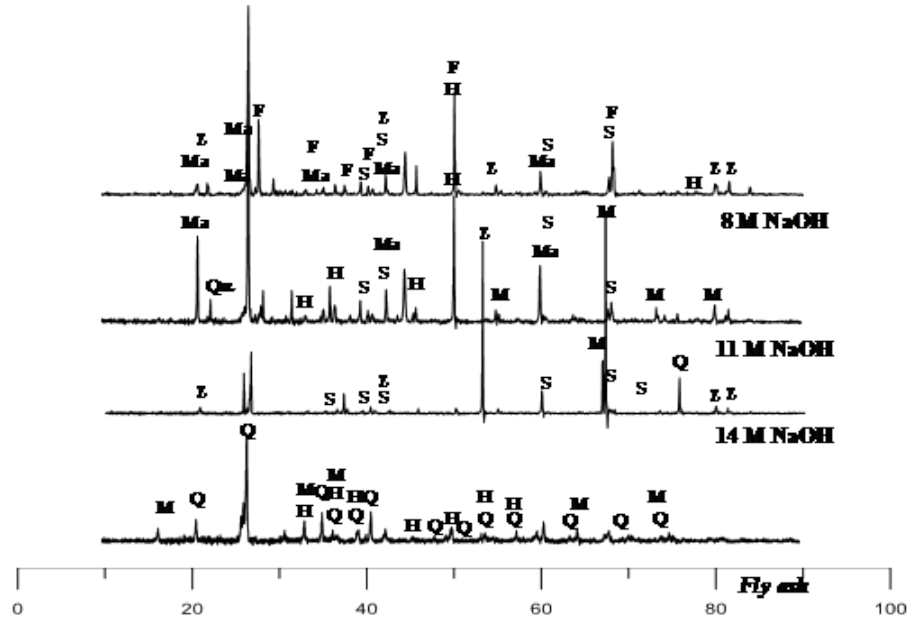

Figure 5.22: XRD of alkali-activated geopolymer mortar (aggregate to binder ratio = 3:1)

5.4 Investigation of the Apparent Porosity and Water Absorption of Geopolymer Mortar

The porosity of mortar is a vital and necessary property for predicting its durability and strength. In this study, the influence of the aggregate binder ratio and curing temperature on the apparent porosity of the geopolymer mortar was examined.

5.4.1 Test Method

The apparent porosity can be predicted indirectly by calculating the bulk density. However, being a porous matrix, such as indirect methodology may produce erroneous results. In view of the above, Montes *et al.* [183] proposed a novel methodology to measure the porosity of mortar and concrete using Archimedes principle. The apparent porosity n can be expressed in terms of weights as

$$n = \frac{(M_w - M_d)}{(M_w - M_s)} \times 100 \tag{5.1}$$

where,

M_w = Weight of specimen after immersion in water for 48 h

M_d = Weight of specimen after drying in an oven at $85°C$ for 24 h

M_s = Weight of specimen when suspended in water

In the present study, geopolymer mortar specimens were cast by mixing the various components in predefined proportions. The specimens had dimensions of 50 mm x 50 mm x 50 mm. After air curing the mortar specimens for a duration of 28 days, the samples were placed in an oven for drying. The dry weight was measured at 24 h periods until the difference between dry weights measured in two subsequent drying durations was less than 0.05%. This final dry weight is M_d. Further, the specimen was soaked in water for 48 h and its saturated surface dry weight was measured. This process was repeated at 24 h intervals to a tolerance of 0.05%. The final saturated

surface dry weight is M_w. Finally, the weight of the specimen was measured in suspension in the water, giving M_w. Finally, based on the above equation, the apparent porosity was calculated.

5.4.2 Test Programme

This test examined the effect of changes in the aggregate to binder ratio and curing temperature on the apparent porosity and water absorption capacity of the mortar. For this purpose, the test matrix in Table 5.2 was adopted. The average apparent porosity was calculated by measuring the apparent porosity of three specimens with identical compositions and curing conditions. The next section presents the results of all tests conducted to evaluate the apparent porosity and water absorption capacity of the specimens.

5.4.3 Results and Discussion

Figure 5.23 shows the variation in porosity with respect to the aggregate to binder ratio and curing temperature. It can be seen that the porosity initially decreases as the aggregate to binder ratio increases; after a certain point, porosity increases with further increases in the aggregate to binder ratio. The initial decrease in porosity can be attributed to the proper compaction of the fine aggregates and binder into the mortar matrix. An increase in the curing temperature helps the mortar to achieve a densified matrix, and lower porosity, which is evident from Figure 5.23.

Figure 5.24 shows the relation between average compressive strength, average porosity, and curing temperature. Note that the compressive strength of the alkali-activated geopolymer mortar is inversely proportional to average porosity. With an increase in temperature, at approximately constant porosity, the average compressive strength increases. The above relation can be fitted to a polynomial to obtain an empirical relation between the parameters. This relation could then be used to predict the average compressive strength of the geopolymer mortar.

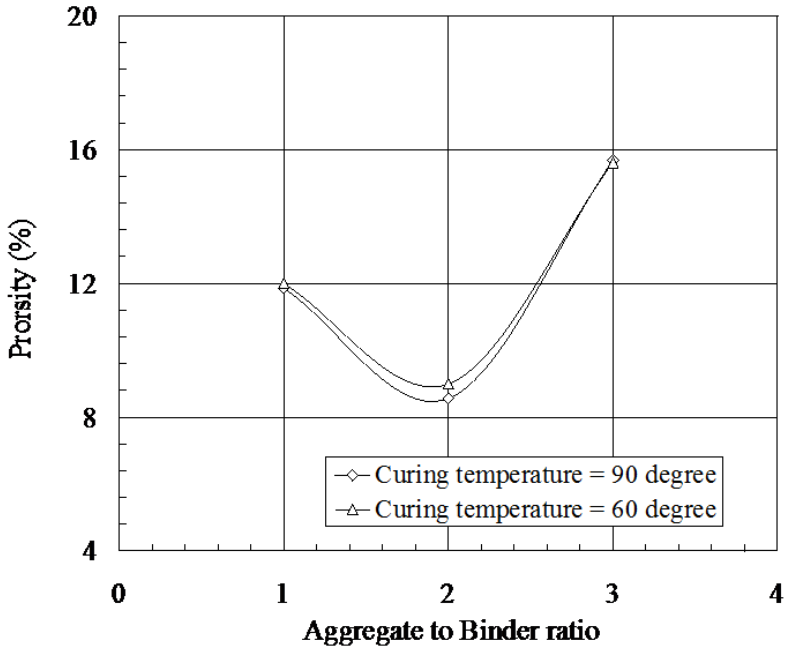

Figure 5.23: Variation of porosity with aggregate to binder ratio

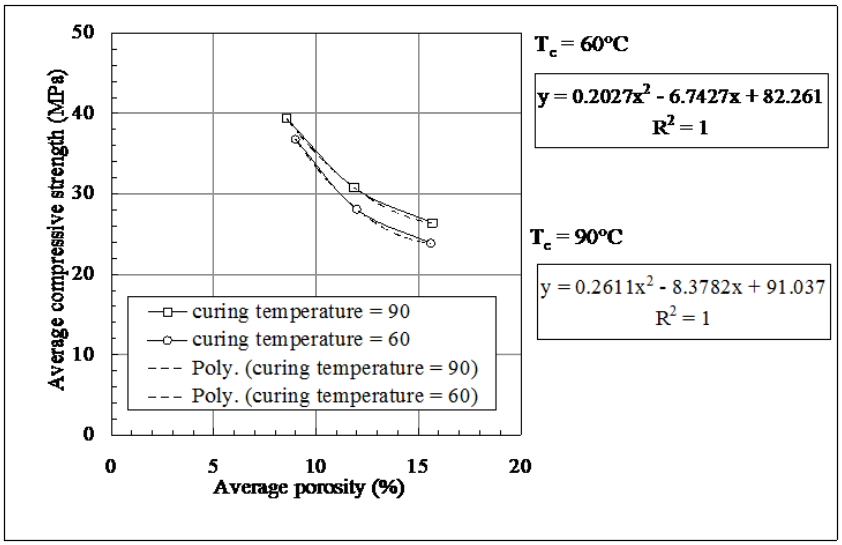

Figure 5.24: Relation between compressive strength and porosity

5.5 Investigation of the Carbonation of Geopolymer Mortar

According to the literature, the durability of mortar is significantly affected by exposure to CO_2. To understand the process of carbonation and the effect of the mortar mix composition on the carbonation process, a series of experiments was conducted. This section describes the test method and programme adopted in the present study, and presents the test results and discussion.

5.5.1 Test Method

The carbonation of the mortar specimens was conducted according to the CPC18 standard [140].

Preparation of mortar specimen

Pre-defined proportions of the various components were blended manually to achieve the mix composition. The paste was poured into moulds to prepare beam specimens as shown in Figure 5.25. The beam specimens had a length of 160 mm, breadth of 40 mm, and height of 40 mm. After curing at room temperature for 300 min, the beam specimens were placed in an oven for 24 h to achieve curing due to heating.

Test procedure

Accelerated carbonation tests were carried out in a chamber under specific experimental conditions: atmospheric pressure, temperature of $20 \pm 2°C$, relative humidity of $65 \pm 5\%$, and a constant concentration of CO_2. The concentration of CO_2 was maintained at 5% to allow for a reasonable test duration in the laboratory. The relative humidity was maintained at 65% using an ammonium nitrate saturated solution in the carbonation chamber. Specimens were placed into the carbonation chamber.

After air curing, the specimens were painted on four faces using two layers as explained

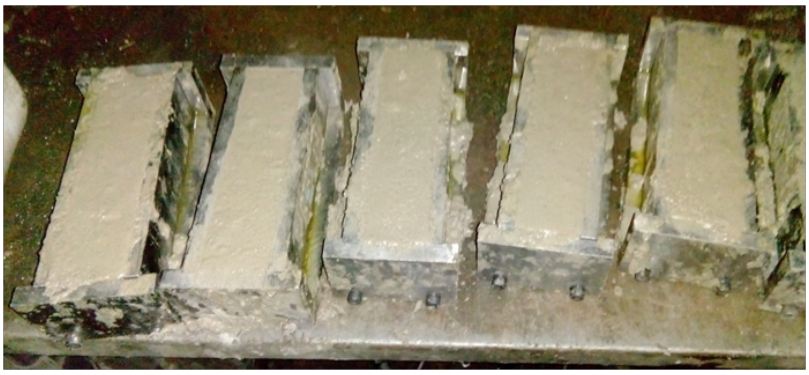

Figure 5.25: Casting of carbonation moulds

Figure 5.26: Preparation of carbonation moulds

in CPC18 [140] shown in Figure 5.26. The carbonation was quantified in terms of the variation in carbonation with depth. The carbonation depth can be used to compute the carbonation coefficient of the geopolymer mortar. To measure the carbonation depth, the beam specimens were split into two parts along their length after completion of the carbonation process. A phenolphthalein solution (prepared by mixing 1% phenolphthalein in 70% ethyl alcohol) was sprayed on the freshly broken surface. This solution is used to identify the change in pH of the freshly broken surface. In the presence of this solution, non-carbonated surfaces become pink, whereas carbonated surfaces remain colourless. The difference in the colour profile was then measured according to a predefined scale. Measurements of the carbonation depth were conducted according to CPC18 [140] guidelines. These guidelines recommend a certain methodology when the profile of the carbonation is undulating or curvy.

5.5.2 Test Programme

The test series for the carbonation experiments was termed Series B. A mix composition with a NaOH concentration of 14M was selected from Series A. Further, parameters for the aggregate to binder ratio and curing temperature were varied while the values of other parameters were held constant. Table 5.2 presents the test programme for series B and the corresponding parameter values.

Table 5.2: Summary of the test programme adopted for Series B in the present study

Mixes	NaOH concentration	Aggregate to binder ratio	Curing temperature
C-1	14M	1:1	$60°C$
C-2	14M	2:1	$60°C$
C-3	14M	3:1	$60°C$
C-4	14M	1:1	$90°C$
C-5	14M	2:1	$90°C$
C-6	14M	3:1	$90°C$

5.5.3 Results and Discussion

In this study, the influence of the aggregate to binder ratio and curing temperature on the carbonation process of geopolymer mortar was studied. For this purpose, several samples with the mix compositions stated in Table 5.2 were placed in the carbonation chamber. The samples were tested at specific times and the carbonation depth was measured according to CPC18 [140]. In the next section, the results of the carbonation tests are reported.

5.5.4 Influence on Carbonation Depth

Figures 5.27 and 5.28 depict the variation in carbonation depth with time and aggregate content in the geopolymer mortar. As can be seen from Figure 5.27, the carbonation depth increases with carbonation time. The carbonation depth was found to be smallest in samples with an aggregate binder ratio of 2:1. Note that the compressive strength test and porosity test indicated that the geopolymer made up of an aggregate

to sand ratio of 2:1 gave the maximum compressive strength and minimum porosity. Hence, the reduced amount of carbonation can be attributed to the decreased porosity and compact state of the geopolymer matrix. Similarly, the samples with an aggregate-binder ratio of 3:1 gave the maximum carbonation depths throughout the test. The higher amount of carbonation can be attributed to the increased porosity of the sample, as evident from the porosity test results reported in previous sections.

Figure 5.28 demonstrates the variations in carbonation depth with carbonation time for the samples cured at $90°C$. It can be seen that a marginal decrease in carbonation depth was achieved at the higher curing temperature. This can be attributed to the solidification of the gel under the elevated temperature, resulting in decrease in the porosity of the matrix. This decrease in porosity hinders the diffusion of CO_2 into the matrix of the geopolymer mortar. Based on the results of the carbonation

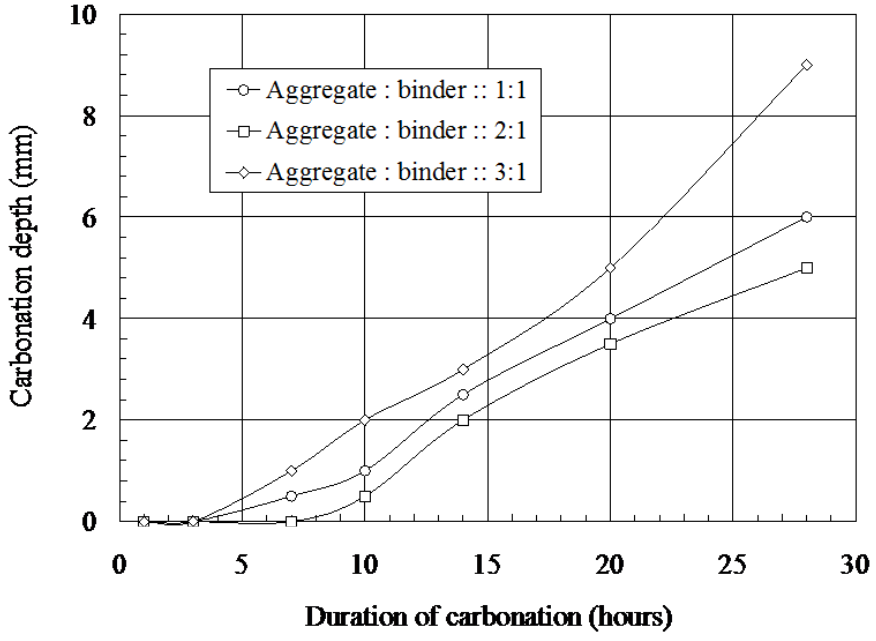

Figure 5.27: Variation of carbonation depth with carbonation time (h) (curing temperature $60°C$

experiments, it can be concluded that the durability of geopolymer mortar against carbonation can be improved by tuning the mix composition of the mortar. It was

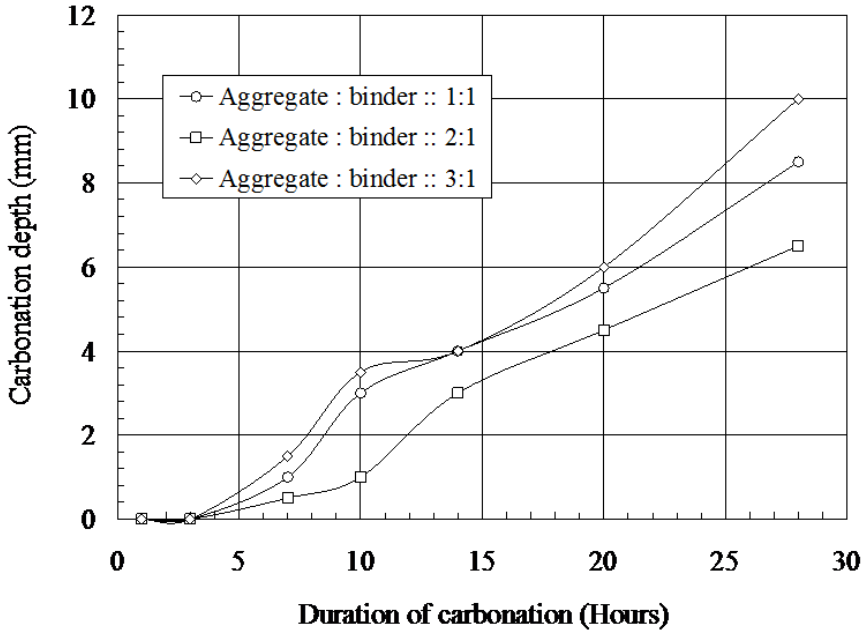

Figure 5.28: Variation of carbonation depth with carbonation time (h) (curing temperature $90°C$

found that the fine aggregate to binder ratio and curing temperature are vital mix composition parameters in dictating the durability of geopolymer mortar when subjected to carbonation.

5.5.5 Influence on Microstructure of Geopolymer Mortar under Carbonation

Figures 5.29 and 5.30 present SEM images of the mortar before and after the carbonation process. These allow us to compare the microstructure of the surface of the mortar during carbonation. It can be seen that small depressions in the external surface of the mortar are present before the carbonation; these may be due to uneven geopolymerization of the mortar. In Figure 5.30, it is interesting to note that the depression in the surface changed during carbonation. The carbonation caused the surface to deteriorate at the micro-level. As evident from the image, the deteriorated material was found in particulate form.

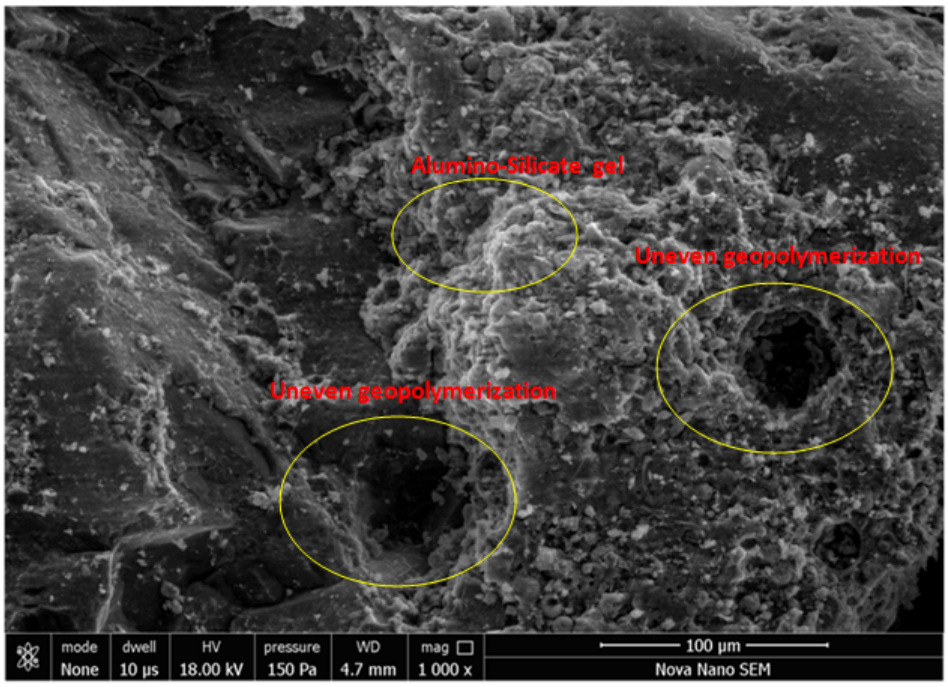

Figure 5.29: Micrograph of geopolymer mortar before carbonation

Figures 5.31, 5.32, and 5.33 show micrographs of the geopolymer mortar for aggregate to binder ratios of 1:1, 2:1, and 3:1. It can be seen that needle-type crystals form during the carbonation of the mortar. The formation of these crystals is most pronounced in the case of a 3:1 aggregate to binder ratio. The presence of different crystals can be further investigated with the help of XRD analysis.

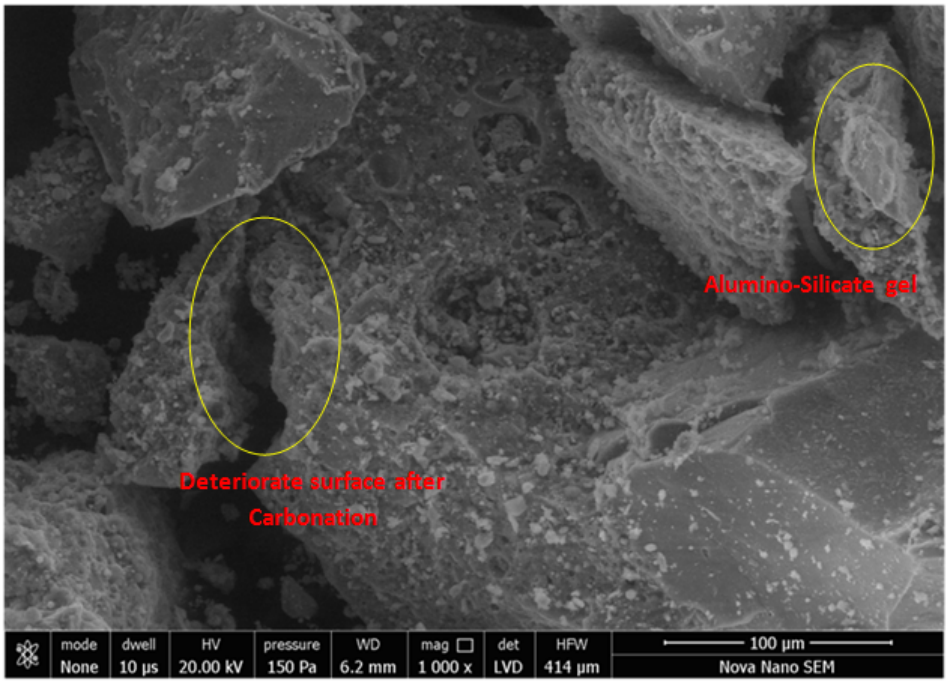

Figure 5.30: Micrograph of geopolymer mortar after carbonation

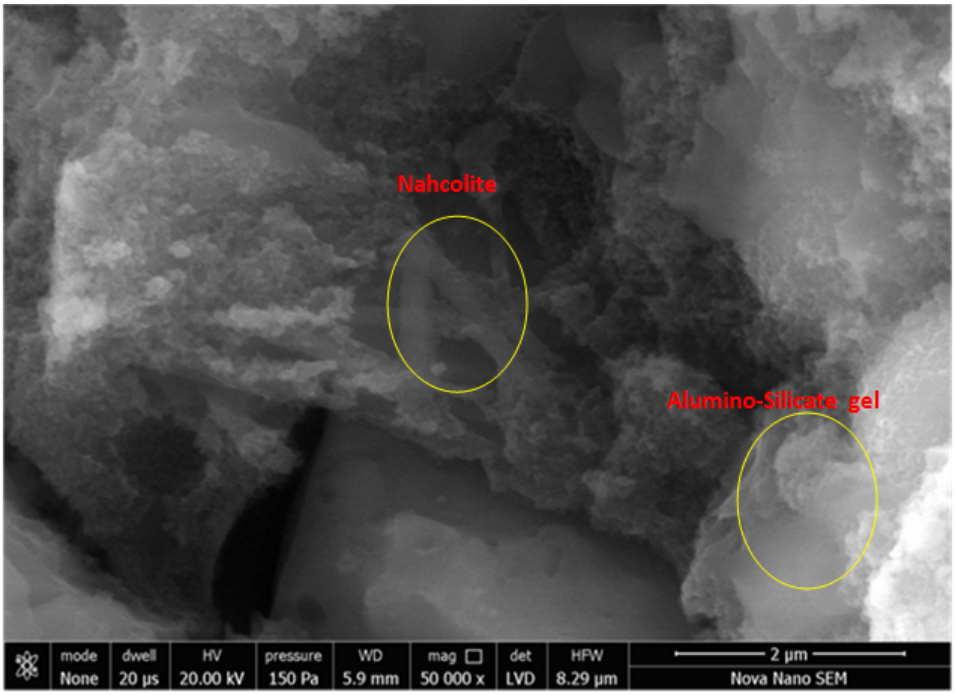

Figure 5.31: Micrograph of carbonated samples with an aggregate to binder ratio of 1:1

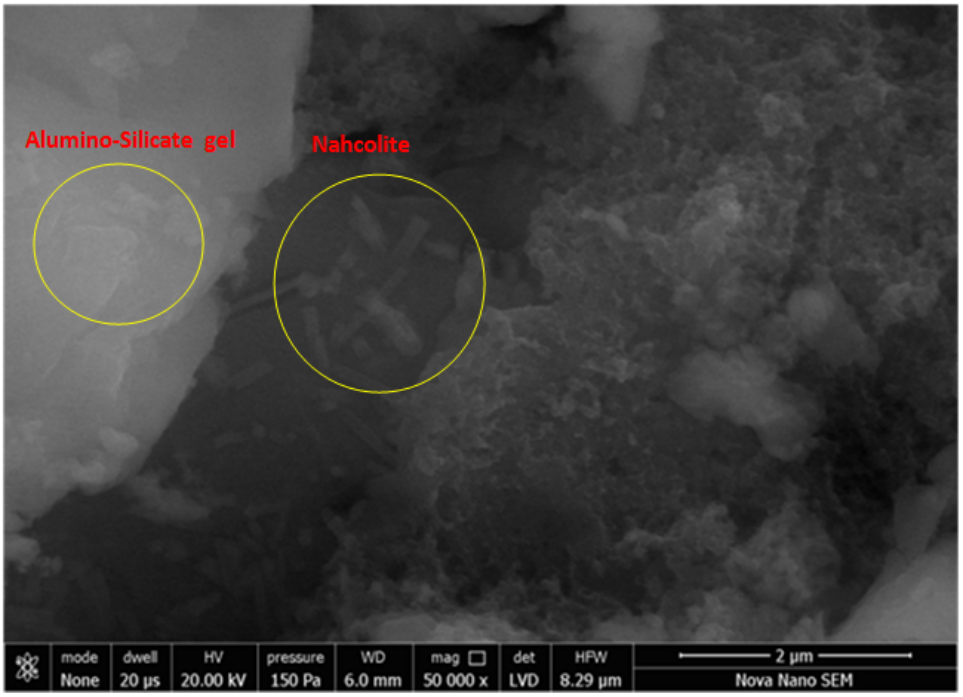

Figure 5.32: Micrograph of carbonated samples with an aggregate to binder ratio of 2:1

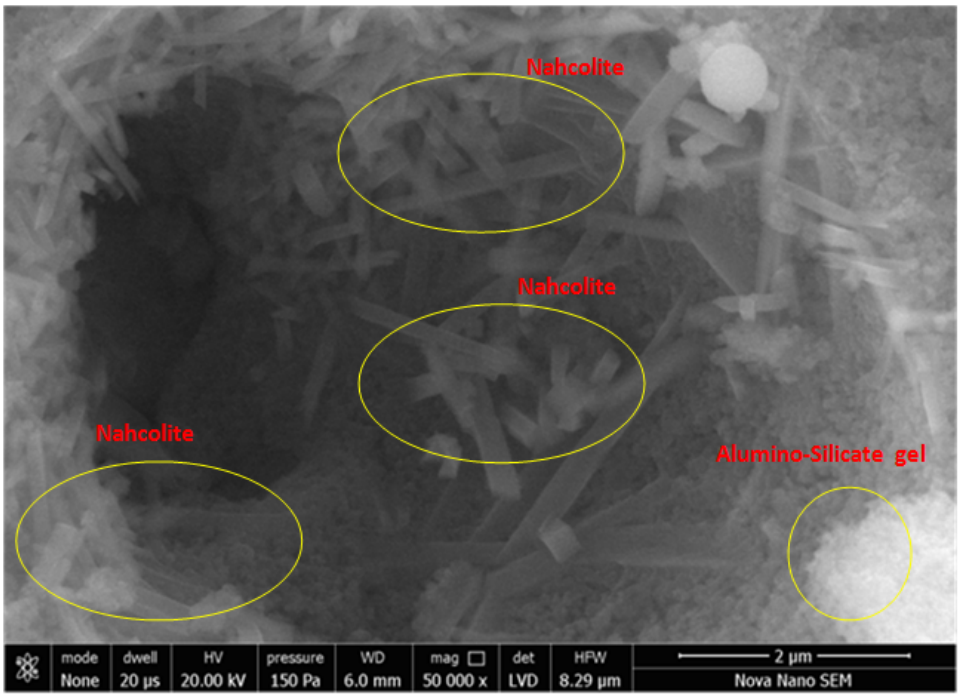

Figure 5.33: Micrograph of carbonated samples with an aggregate to binder ratio of 3:1

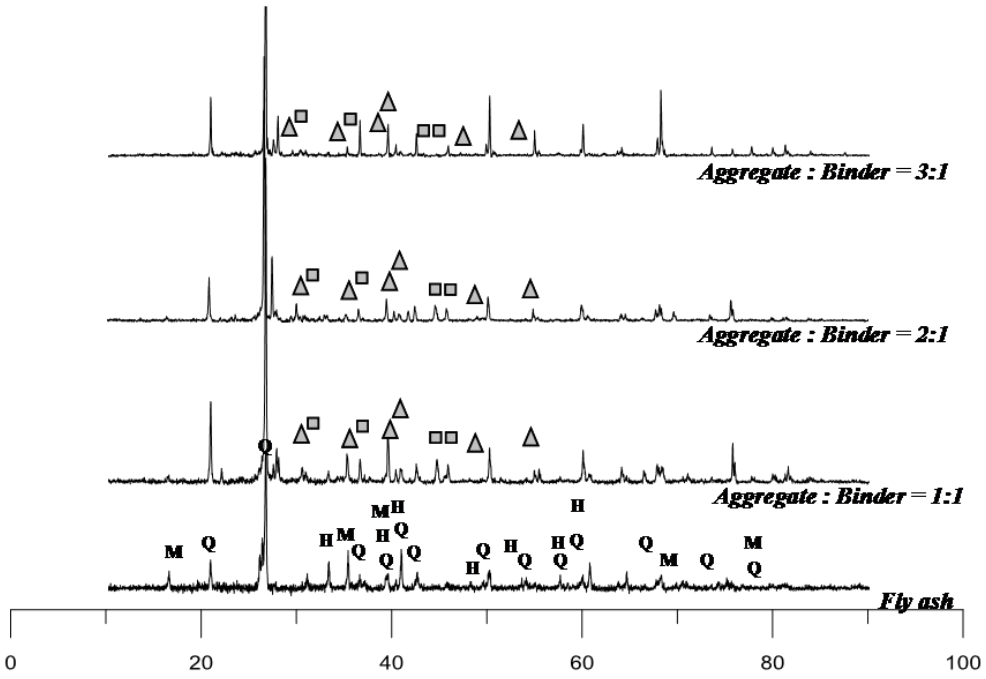

Figure 5.34: XRD pattern of carbonated geopolymer mortar (curing temperature $60°C$)

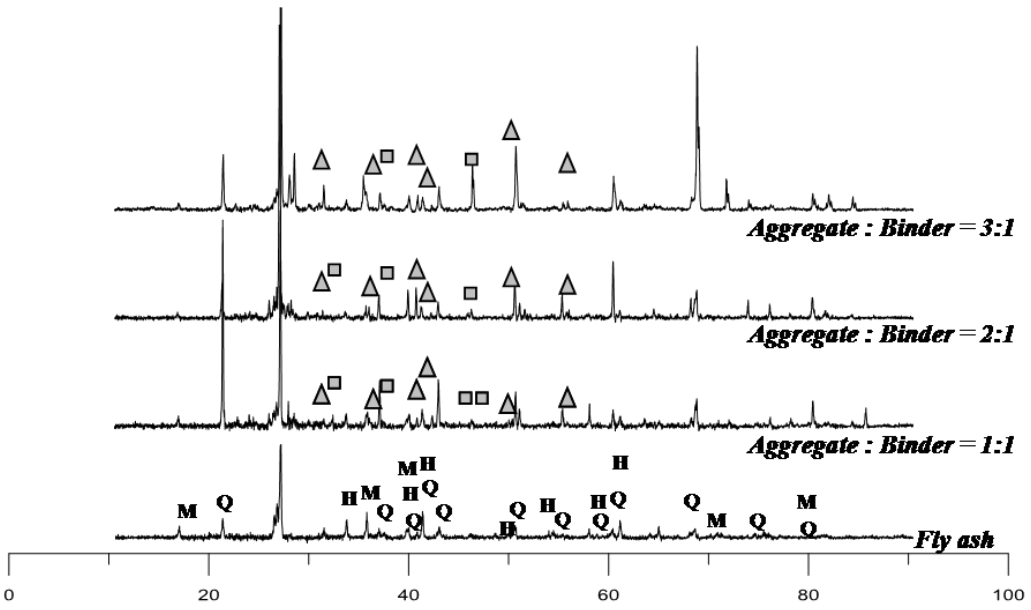

Figure 5.35: XRD pattern of carbonated geopolymer mortar (curing temperature $90°C$)

XRD images of carbonated geopolymer mortar were obtained for various aggregate-binder ratios (1:1, 2:1, and 3:1) and curing temperatures ($60°C$ and $90°C$). The carbonation process significantly changes the pore chemistry. In this study, with the help of diffractograms, changes in pore solution chemistry could be identified. For this purpose, a mineral named nahcolite (▲) was investigated. As shown in Figures 5.34 and 5.35, at the onset of carbonation, the pore solution chemistry changes and nahcolite (▲) is formed. In parallel, sodium carbonate hydrate (■) is also formed. During carbonation, under the prevalent thermodynamic and environmental conditions, nahcolite (▲) is the most favourable formation product. Similar observations were observed in mortars with various aggregate-binder mix compositions and curing temperatures.

5.6 Conclusion

From the results reported in this chapter, the following conclusions can be drawn:

1. NaOH helps in the dissolution of fly ash and its dissolution into the mortar matrix. Higher concentrations of NaOH influence the formation of aalumino-silicate gel that results in greater compressive strength.

2. An aggregate to binder ratio of 2:1 was found to be optimal, as this achieves a suitable compactness of the mortar, as evident from the porosity values.

3. The aggregate-binder ratio of 2:1 also achieved optimal performance against carbonation. This indicates the importance of an appropriate mix composition in ascertaining the performance of geopolymer mortar.

4. Diffractograms of various mortar specimens provided information about the crystals formed during geopolymerization of the mortar. The crystals formed during this process include sodalite, mullite, magnetite, hematite, zeolite, and feldspar. Similarly, during carbonation, visible changes in morphology were observed, with newly formed minerals such as nahcolite. SEM provided crucial information about changes in the surface features of the geopolymer mortar. Further, with the help

of micrographs, the presence of unreacted fly ash particles were observed in some of the samples. This indicates an insufficient concentration of NaOH to dissolve all of the fly ash.

Chapter 6

Sea Sand Effect on Geopolymer Composites

6.1 Prelude

In this Morden era, surge in global population which increases demand for resources i.e. fresh water. As countries around the world continue their development, a major role is played by infrastructure, which requires a huge amount of construction materials. Mortar and concrete are the most widely used materials in construction, and their manufacture has substantially increased the production of cement. In India, the second-largest producer of cement in the world, demand is expected to reach 550–600 million tonnes per annum by 2025. The main driver of demand is the housing sector, accounting for about 67% of total cement consumption in India.

Conventionally, OPC is used as a binder in concrete and mortar. However, there are many issues in using OPC as a mortar constituent. One major issue is its harmful environmental impact. Every ton of cement produced results in one ton of carbon dioxide being emitted into the atmosphere [50]; cumulatively, cement production is responsible for 7% of global CO_2 emissions.

Another major concern with conventional OPC-based mortar is its durability in adverse conditions. Studies have shown that OPC provides sufficient strength, but can deteriorate under severe environmental conditions, such as when exposed to acidic surroundings. Conventional OPC-based mortar also has long setting and hardening times. It can bear a load after curing for 7–10 days, which is a long time in a modern era that demands rapid construction. Moreover, huge amounts of water are required for the curing of mortar. All these concerns lead to an urgent need for a sustainable, eco-friendly mortar that performs well in adverse surroundings.

India is a major rice-producing country. The husk generated by milling the rice is mostly used as a boiler fuel for processing the paddy, producing energy through direct combustion and/or gasification. This produces about 20 million tons of rice husk ash each year, which poses a significant environmental threat to the land on which it is dumped. Thus, methods for making commercial use of this rice husk ash are attracting considerable attention.

In coastal areas, sand is available in meagre quantity and its transportation cost is huge. Nevertheless, sea sand is available in ample quantity in coastal areas. Past researchers found that sea sand can not be used in construction as fine aggregate due to salt and chloride present in sea sand which affect the hydration process in OPC Concrete. The situation is however divergent in case of geopolymer concrete. Since the geopolymerization process takes place in this case, hence salt and chloride content are not anticipate to have detrimental effect. The flyash is also expected to mitigate the harmful effects of the chloride present in sea sand. [111].

United Nations (UN) and World Metrological Organization (WMO) have predicted that 5 billion people will be in short of even drinking water. It is also said that in 2025 half of the humanity will live in the areas where fresh water is not enough [120]. One solution is to utilize sea water to substitute fresh water in concrete casting. Sea water is expected to be less harmful for the geopolymer composites.

This chapter reports the findings and analysis of compressive strength tests on geopolymer mortar with 100% replacement of cement with fly ash. Additionally, the fly ash was partially replaced by rice husk ash (0%, 10%, 20%, and 30% replacement) to observe the effect on compressive strength of geopolymer mortar. Each set of replacements was formed using four combinations of sand and water, namely normal sand, sea sand, normal water, and sea water, to investigate the variation in compressive strength in the geopolymer mortar. The chapter also presents the experimental results for mechanical properties such as split tensile strength and flexural strength for fly ash based geopolymer concrete prepared by sea water and sea sand as well as control geopolymer concrete.

6.2 Material Characterization and Mix Proportioning

6.2.1 Source Material

Fly ash was selected as the primary source material because of its high silica and alumina content, which is favourable for the process of geopolymerization. The secondary source material was chosen to be rice husk ash (RHA), as we wish to investigate the impact of replacing fly ash with RHA. The Particle size distribution and chemical component of rice husk ash is shown in Figure 6.1 and Table 6.1, respectively.

6.2.2 Alkaline Liquid

A mixture of sodium hydroxide (NaOH) and sodium silicate (Na_2SiO_3) was used as the alkaline activator. The liquid was prepared 24 h prior and kept undisturbed until casting.

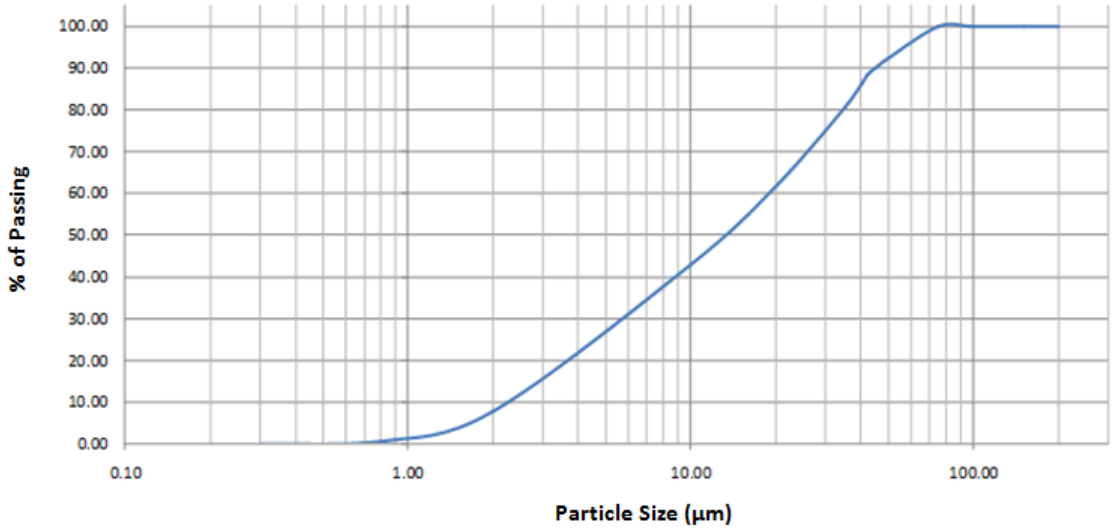

Figure 6.1: Particle size analysis of Rice husk ash

6.2.3 Mix Proportioning of Geopolymer Mortar and Concrete

Mix Proportioning of geopolymer mortar and geopolymer concrete are shown in Tables 6.2 and 6.3 ,respectively. For each of the Geopolymer mortar mixes (G-1, G-2, G-3, and G-4), different proportions of fly ash were replaced by RHA. In the following, G1/10 denotes the G1 mortar with 10% replacement of fly ash by RHA, and so on. For each of the geopolymer concrete mixes (GC-1, GC-2, GC-3 and GC-4), fly ash was used as source material. The following constituents for mix design were determined based on the results of the parameter study reported earlier in this thesis:

Rice husk based Geopolymer Mortar

- Ratio of alkaline liquid to fly ash by mass: 0.45
- Ratio of sodium silicate to sodium hydroxide: 2.5
- Concentration of sodium hydroxide solution: 14M
- Admixture dosage: 1%

Table 6.1: Properties of Rice husk ash

Sr. No.	Particulars	Unit	Rice husk ash Properties
1	Colour	-	Grey
2	Loss on ignition	%	5.96
3	SiO_2	%	86.32
4	C	%	5.58
5	CaO	%	0.62
6	Al_2O_3	%	0.35
7	Fe_2O_3	%	0.24
8	SO_3	%	0.42
9	MgO	%	0.51

- Additional water content: 5%
- Curing temperature: 60°C
- Curing time: 24 h
- Rest period: 0 days

Fly ash based Geopolymer Concrete

- Ratio of alkaline liquid to fly ash by mass: 0.4
- Ratio of sodium silicate to sodium hydroxide: 2.5
- Concentration of sodium hydroxide solution: 14 M
- Admixture dosage: 2%
- Additional water content: 5%
- Curing temperature: 65°C, 90°C
- Curing time: 48 h
- Rest period: 1 day

Table 6.2: Mix proportion for trial variables (per m^3)

Trial Mixes	Fly Ash (kg)	Rice husk ash (kg)	Fine Aggregate		NaOH (kg)	Sodium Silicate (kg)	Extra Water		Super-Plasticizer (kg)	Remarks
			River Sand (kg)	Sea Sand (kg)			Sea Water (kg)	Normal Water (kg)		
G1	527	0	–	1586	68	169	71.1	–	5.27	Sea Sand And Sea Water
G2	474.3	52.7	1586	–	68	169	–	71.1	5.27	River Sand and Normal Water
G3	421.6	105.4	–	1586	68	169	–	71.1	5.27	Sea Sand And Normal Water
G4	368.9	158.1	1586	–	68	169	71.1	–	5.27	River Sand And Sea Water

Table 6.3: Mix Proportion for Geopolymer Concrete (per m^3)

Trial Mixes	Fly Ash (kg)	Fine Aggregate		Coarse aggregate (kg)	NaOH (kg)	Sodium Silicate (kg)	Extra Water		Super-Plasticizer (kg)	Remarks
		River Sand (kg)	Sea Sand (kg)				Sea Water (kg)	Distilled Water (kg)		
GC-1	446.43	–	656.25	1218.75	51.02	127.55	22.32	–	8.93	Sea Sand And Sea Water
GC-2	446.43	656.25	–	1218.75	51.02	127.55	–	22.32	8.93	River Sand And Distilled Water
GC-3	446.43	–	656.25	1218.75	51.02	127.55	–	22.32	8.93	Sea Sand And Distilled Water
GC-4	446.43	656.25	–	1218.75	51.02	127.55	22.32	–	8.93	River Sand And Sea Water
GC-5	431.03	–	656.25	1218.75	55.42	138.55	21.55	–	8.62	Sea Sand And Sea Water
GC-6	431.03	656.25	–	1218.75	55.42	138.55	–	21.55	8.62	River Sand And Distilled Water
GC-7	431.03	–	656.25	1218.75	55.42	138.55	–	21.55	8.62	Sea Sand And Distilled Water
GC-8	431.03	656.25	–	1218.75	55.42	138.55	21.55	–	8.62	River Sand And Sea Water

Table 6.4: Seven day compressive strength of rice husk based geopolymer mortar

Ingredients	Mix Proportion	Compressive Strength (MPa)
Sea Sand and Sea water	G1/0	12.56
	G1/10	12.90
	G1/20	11.20
	G1/30	5.48
River Sand and Normal Water	G2/0	13.60
	G2/10	14.47
	G2/20	12.49
	G2/30	8.93
Sea Sand and Normal Water	G3/0	11.73
	G3/10	12.62
	G3/20	10.33
	G3/30	7.12
River Sand and Sea water	G4/0	12.49
	G4/10	13.44
	G4/20	11.41
	G4/30	8.69

6.3 Results and Discussion

6.3.1 Compressive Strength Test

As described above, 7 day and 28 day compressive strength tests were conducted. The results are presented in Table 6.4 and 6.6.

Table 6.5: Maximum 7 day compressive strength and percentage change (taking G2 as reference)

Mix Proportion	Compressive Strength (MPa)	Change in percentage
G1/10	12.90	10.85
G2/10	14.47	-
G3/10	12.62	12.78
G4/10	13.44	7.07

From Table 6.4 and 6.5, it is apparent that 10% replacement of fly ash with RHA gives the maximum 7 day compressive strength for all specimens. Table 6.5 presents the results for all combinations of sea sand, river sand, sea water, and normal water. From these, it is clear that, though the 7 day compressive strength decreases in the presence of salinity/impurity (in the form of sea water, sea sand, or both), these mixes are stronger than the conventional H1-type OPC mortar after 28 days, i.e. 10 MPa in all cases (except for the 30% replacement of all four combinations). This confirms that, as far as early and higher compressive strength gains are concerned, geopolymer mortar is superior to conventional OPC mortar.

Figure 6.2 shows the variation in compressive strength with sand and water type for various replacement percentages of fly ash with RHA. Similarly, Tables 6.6 and 6.7 tabulate the 28 day compressive strength results, confirming that 10% replacement of fly ash with RHA gives the maximum 28 day compressive strength for all specimens. Similar to Figures 6.3 shows the same variations for 28 day compressive strength.

Table 6.6: Twenty-eight day compressive strength test results (MPa)

Ingredients	Mix Proportion	Compressive Strength (MPa)
Sea Sand and Sea Water	G1/0	16.04
	G1/10	18.21
	G1/20	13.22
	G1/30	10.25
Normal Sand and Normal Water	G2/0	20.48
	G2/10	21.78
	G2/20	20.24
	G2/30	16.5
Sea Sand and Normal Water	G3/0	17.97
	G3/10	19.34
	G3/20	16.92
	G3/30	12.35
Natural Sand and Sea Water	G4/0	14.52
	G4/10	19.17
	G4/20	15.40
	G4/30	11.5

Table 6.7: Maximum 28 day compressive strength and percentage change (taking G2 as reference)

Mix Proportion	Compressive Strength (MPa)	Change in percentage
G1/10	18.21	16.40
G2/10	21.78	-
G3/10	19.34	11.23
G4/10	19.17	12.00

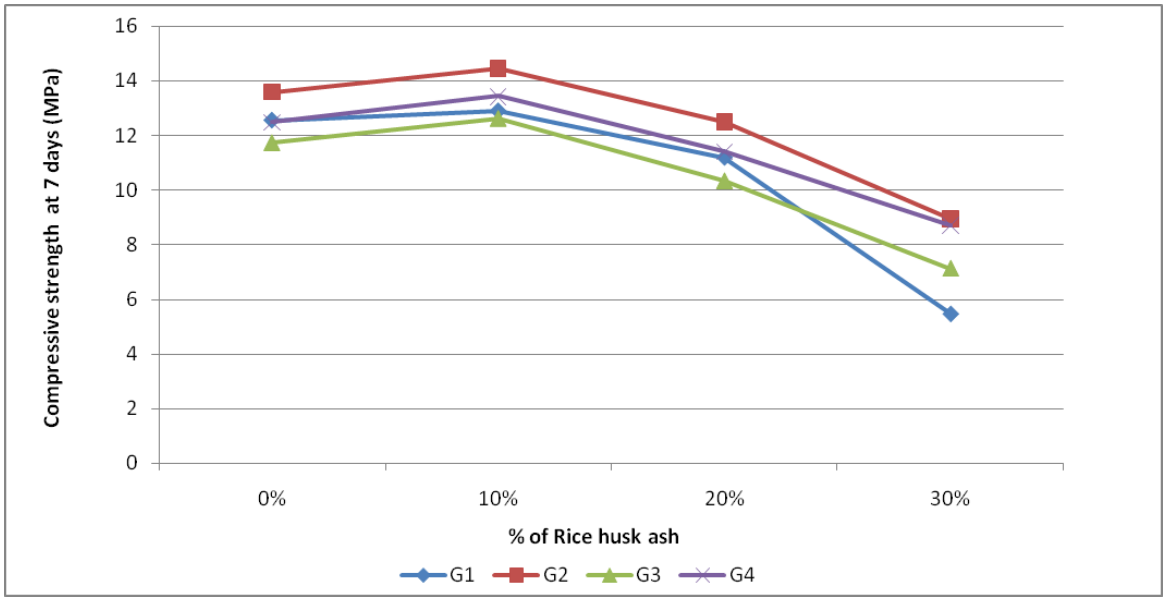

Figure 6.2: Seven day compressive strength variation

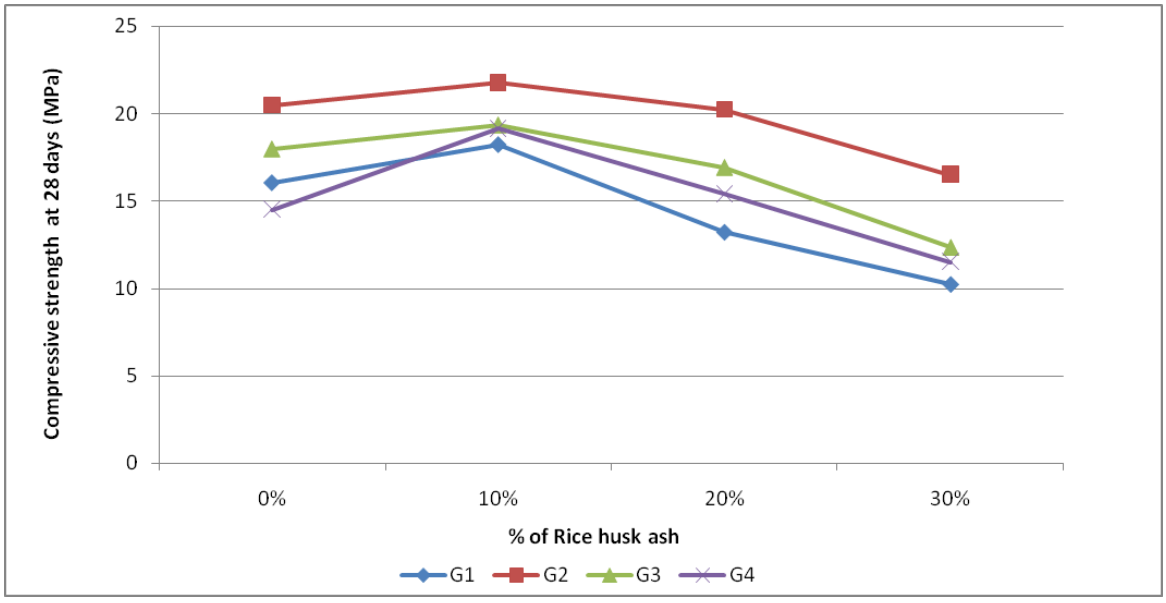

Figure 6.3: Twenty-eight day compressive strength variation

Figures 6.4 and 6.5 shows a graphical representation of compressive strength for all mixes of fly ash based geopolymer concrete at 3, 7 and 28 days. Figures show that increase in compressive strength with the increase in the age of the geopolymer concrete at 65°C and 90°C curing temperature for all mixes. A significant change in compressive strength was observed in geopolymer composites fabricated with seawater and sea sand. The compressive strength of geopolymer concrete increase as the curing temperature increased was observed. Similar observations were shown by past research [120].

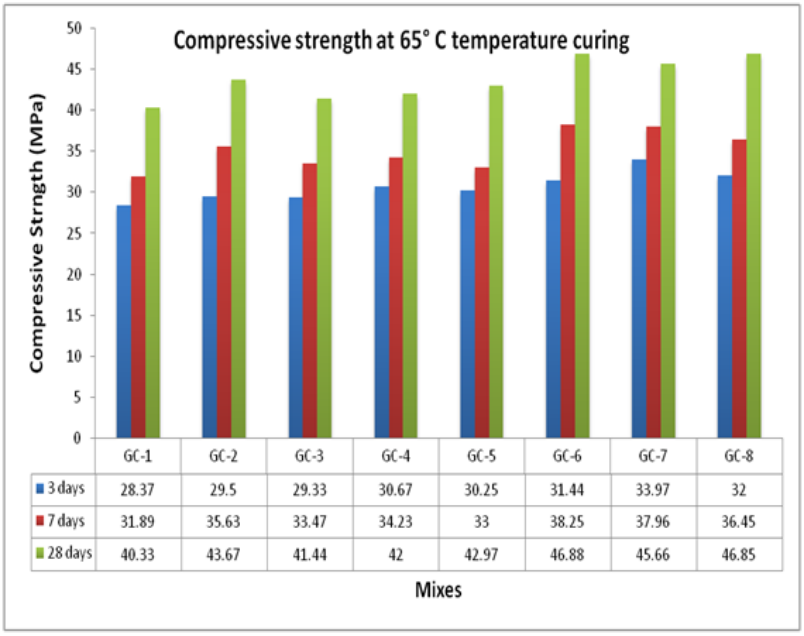

	GC-1	GC-2	GC-3	GC-4	GC-5	GC-6	GC-7	GC-8
3 days	28.37	29.5	29.33	30.67	30.25	31.44	33.97	32
7 days	31.89	35.63	33.47	34.23	33	38.25	37.96	36.45
28 days	40.33	43.67	41.44	42	42.97	46.88	45.66	46.85

Figure 6.4: Compressive strength of geopolymer concrete at 65 $^{\circ}C$ curing temperature

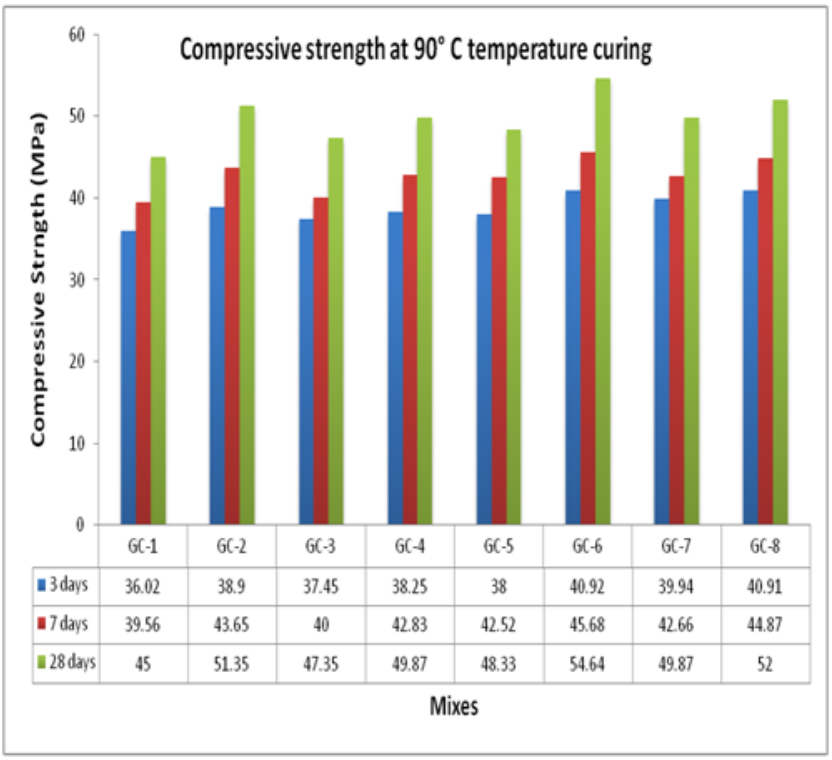

	GC-1	GC-2	GC-3	GC-4	GC-5	GC-6	GC-7	GC-8
3 days	36.02	38.9	37.45	38.25	38	40.92	39.94	40.91
7 days	39.56	43.65	40	42.83	42.52	45.68	42.66	44.87
28 days	45	51.35	47.35	49.87	48.33	54.64	49.87	52

Figure 6.5: Compressive strength of geopolymer concrete at 90 °C curing temperature

6.3.2 Split Tensile Strength Test

The split tensile strength of geopolymer concrete, using sea sand as partial replacement of river sand and sea water were determined at the ages 3, 7, 28 days. Figures 6.6 and 6.7 show the split tensile strength of geopolymer concrete from 65 °C and 90 °C curing temperature. Split tensile strength of geopolymer concrete with sea water and sea sand is considerably lesser than the control geopolymer concrete at the ages of 3, 7 and 28 days. As the curing temperature was increased as 65 °C to 90 °C, the strength was also increased for all mixes.

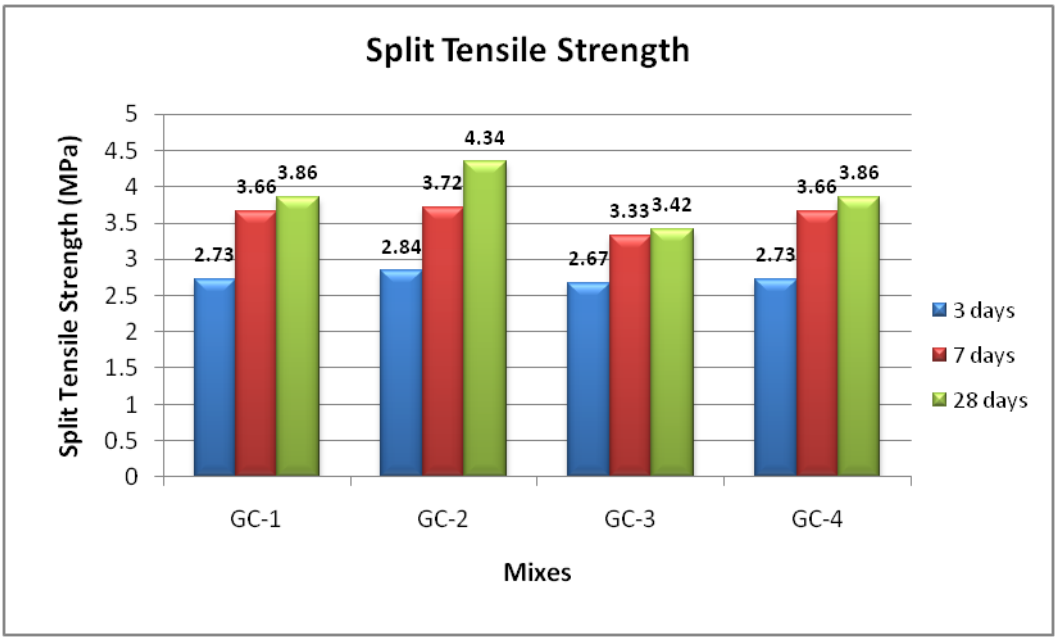

Figure 6.6: Split tensile strength of geopolymer concrete at $65°C$ curing temperature

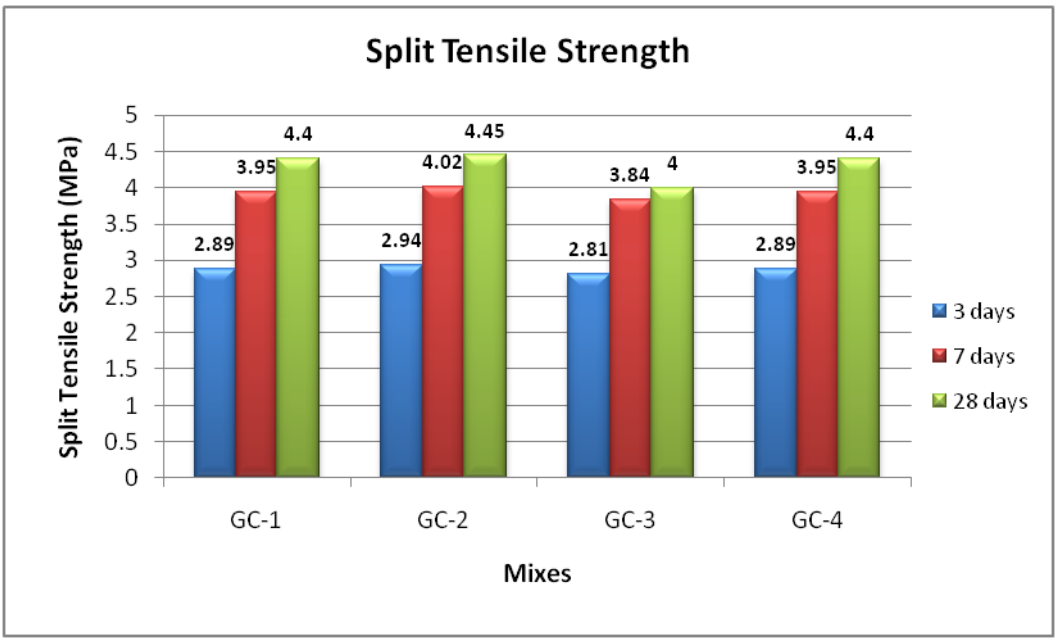

Figure 6.7: Split tensile strength of geopolymer concrete at $90°C$ curing temperature

6.3.3 Flexural Strength Test

The flexural strength of geopolymer concrete, using sea sand as partial replacement of river sand and sea water were determined at the ages 3, 7, 28 days. Figures 6.8 and 6.9 show the flexural strength of geopolymer concrete from 65 °C and 90 °C curing temperature. Flexural strength of geopolymer concrete with sea water and sea sand is considerably lesser than the concrete geopolymer concrete at the ages of 3, 7 and 28 days. As the curing temperature was increased from 65 °C to 90 °C, the strength was also increased for all mixes.

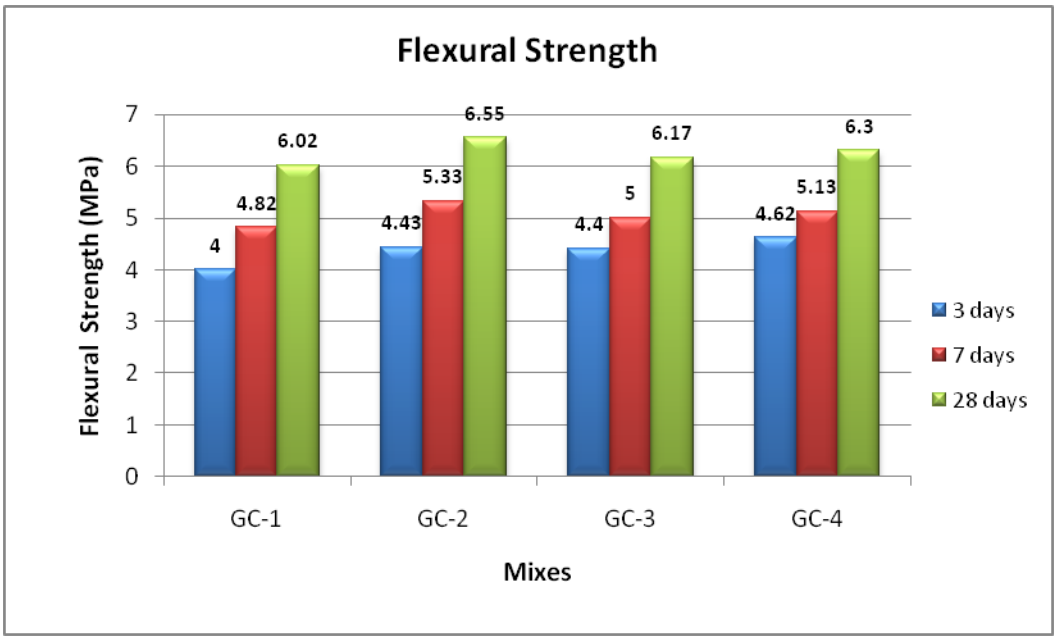

Figure 6.8: Flexural strength of geopolymer concrete at 65°C curing temperature

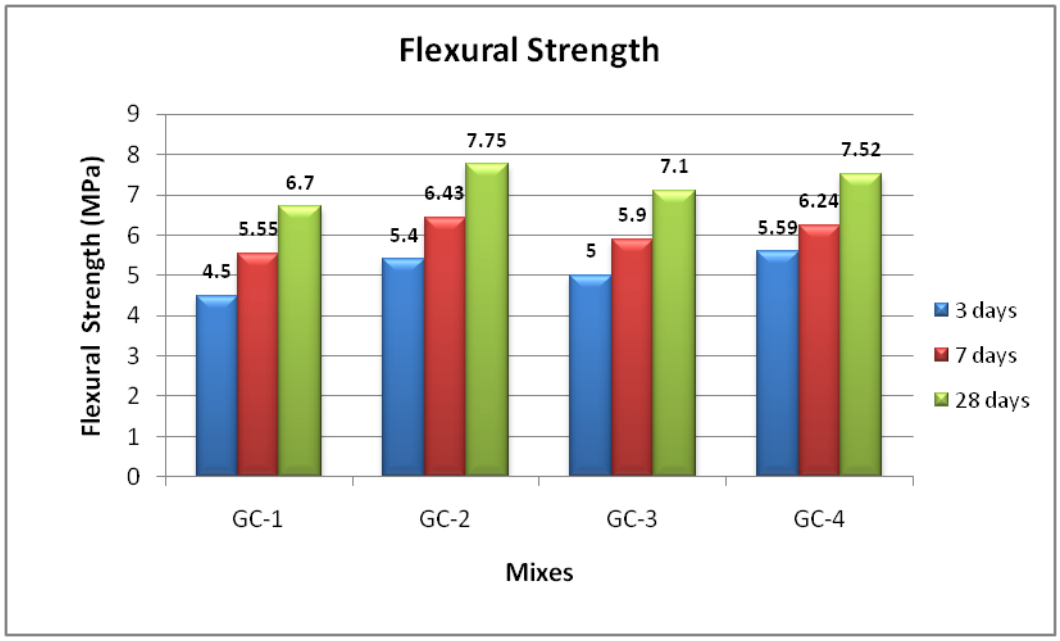

Figure 6.9: Flexural strength of geopolymer concrete at 90°C curing temperature

6.4 Conclusion

The following conclusions can be drawn from the results in this chapter:

1. The replacement of 0%, 10%, and 20% of fly ash with RHA in fly ash-based geopolymer mortar resulted in higher 7 day compressive strength than the 28 day compressive strength of corresponding conventional H1-type cement mortar, i.e. 10 MPa. This verifies the high and early strength gain of geopolymer mortars; hence, geopolymer-based mortar should be used in construction works where speed of building is important.

2. Geopolymer mortar performs satisfactorily when it has saline material as its constituents, i.e. using sea water instead of normal water, sea sand instead of river sand, or both sea sand and sea water instead of river sand and normal water. In all such combinations, the resulting 7 day compressive strength was again higher than the 28 day compressive strength of the corresponding conventional H1-type OPC mortar (10 MPa).

3. It also confirms the feasibility of using locally available sea sand and sea water

in geopolymer mortar for coastal area construction, as the compressive strength of all four combinations are in a comparable range and well above the H1 quality mortar.

4. A significant decrease in compressive strength, Flexural strength and Split tensile strength were observed in geopolymer composites fabricated with seawater and sea sand.

Chapter 7

Conclusions and Recommendations

7.1 Prelude

This chapter concludes the investigation and comparison of the strength, durability, and elevated temperature performance of rubberized geopolymer concrete concrete, ordinary geopolymer composites, and OPC concrete. This research also examined the use of rice husk ash in geopolymer mortar made with sea water and sea sand. The current research contributes to the body of knowledge on the durability of rubberized and control geopolymer concrete. This research first examined the use of rubber tyre fibres in geopolymer concrete and sea water/sea sand in geopolymer composite. The preparatory study was useful in determining the dominant parameters for further appraisal in this research. The Taguchi method was used to develop a mix design for rubberized geopolymer concrete. This method enhanced our ability to select the optimum parameters, thus avoiding an unnecessary increase in the number of experiments. The compressive strength, flexural strength, and split tensile strength of mixtures with the optimum selected parameters were studied over a period of 365 days. The elastic modulus, abrasion resistance, and pull-off strength of geopolymer concrete were studied for a period of 28 days. This research study also evaluated the durability performance of various concrete mixtures, such as the water permeability, carbonation resistance, shrinkage resistance, corrosion resistance, sorptivity resistance, acid resistance, salt resistance, and sulfate resistance. The microstructure

of geopolymer composites was also investigated. The main conclusions and findings are stated in the following section.

7.2 Conclusions

7.2.1 Parameter Study

- The Taguchi method is a highly beneficial optimization technique for determining which geopolymer concrete mixtures to focus on, thus helping to reduce the number of experiments.

- The eight factors considered by the Taguchi method were the curing time, Na_2SiO_3/NaOH ratio, alkaline liquid/fly ash ratio, plasticizer, rest period, water content, NaOH concentration, and curing temperature. Each factor was considered at three levels.

- Orthogonal arrays, L_{27} (3^{13}), were developed by the Taguchi method. Primary tests were conducted to specify the range of each factor. The compressive strength was evaluated in a total of 27 trial mixes of rubberized geopolymer concrete (T1–T27).

- The curing temperature, NaOH concentration, and sodium silicate to sodium hydroxide ratio (Na_2SiO_3/NaOH) were found to be the main contributory factors in maximizing the compressive strength of concrete. They were ranked as 1, 2, and 3, respectively, by the ANOVA method. It was observed that augmented values of these factors increased the compressive strength of rubberized geopolymer concrete.

- An increase in curing time 48 h to 72 h reduced the strength of the concrete because of the additional water evaporation. The optimum value of each factor in rubberized geopolymer concrete was determined using the Taguchi method.

- The maximum compressive strength for rubberized geopolymer concrete was obtained at an alkaline solution/fly ash ratio of 0.35, silicate to sodium hy-

droxide ratio (Na_2SiO_3/ NaOH) of 2.5, NaOH concentration of 14M, curing temperature of 90°C, curing time of 48 h, water content of 20%, rest period of 1 day, and superplasticizer content of 2%.

7.2.2 Strength Performance

- The compressive strength, flexural strength, and split tensile strength of geopolymer concrete improves with age in geopolymer concrete.
- An increase in the percentage of waste rubber tyre decreases the compressive strength of geopolymer concrete.
- It can be found that the compressive strength of OPC concrete decreases as waste rubber fibres are introduced.
- The compressive strength of OPC concrete is less than that of geopolymer concrete.
- Geopolymer concrete exhibits higher tensile strength than OPC concrete. This is because of the good bonding between the geopolymer paste and aggregate.
- For all mixes, as the compressive strength increases, the tensile strength also increases. The highest split tensile strength was observed in concrete with 30% rubber fibres after 365 days.
- The flexural strength of geopolymer concrete is higher than that of OPC concrete.
- The flexural strength of geopolymer concrete varies from 6.45–9.97 MPa, whereas that of OPC concrete ranges from 5.35–6.86 MPa.
- The modulus of elasticity of geopolymer concrete varies from 20–31.5 GPa, while that of OPC concrete ranges from 18–27.5 GPa.
- An increase in the rubber fibre content decreases the homogeneity of geopolymer and OPC concrete, which results in a decrease in the modulus of elasticity.

- Geopolymer concrete has better pull-off strength than OPC concrete. Rubber fibre geopolymer and OPC concrete have poor pull-off strength, because there is less bonding between the paste and aggregate, which results in a weaker surface layer than in the control geopolymer and control OPC concrete.

7.2.3 Durability Performance

- The depth of wear for all mixes was within permissible limits. It can be concluded from abrasion results that rubber tyre fibres could be used with fly ash or cement as regular flooring tiles or even heavy-duty floor tiles.

- The water penetration depth increases as the rubber fibre content is increased. The water penetration is lower in geopolymer concrete than in OPC concrete.

- The continuous chemical reaction between fly ash and alkaline solution results in a change in porosity and creates denser pores of geopolymer concrete.

- Minimum and maximum water penetration of 31.2 mm and 35.7 mm were observed in geopolymer concrete. The increase in permeability can be attributed to the increased porosity of the concrete evident with the higher levels of rubber fibres.

- In OPC concrete, the minimum and maximum water penetration was observed to be 38.03 mm and 42.8 mm, respectively.

- Geopolymer concrete has lower sorptivity (0.09–0.164 mm/min$^{0.5}$) than OPC concrete (0.113–0.203 mm/min$^{0.5}$) after 28 days. This is because the strong reaction between the alkaline solution and source material in geopolymer concrete results in few capillary pores, whereas OPC concrete has many capillary pores due to the hydrating of the cement. This is because of the fineness of Fly ash results in better packing, reducing voids and capillary. The formation of geopolymeric products such as N-A-S-H is a rapid process which is realised within 3 days whereas in OPC concrete the formation of C-S-H continues throughout the lifetime leaving higher voids and capillaries than geopolymer concrete. The

values of DIN also support the formation of lower voids/pores in geopolymer concrete than control concrete

- The macrocell current for rubberized concrete mixes was more than that for the control concrete at all the ages. For OPC concrete, current exceeded 10 μA at 8^{th} month to 12^{th} month for all mixes. It can be shown that the inclusion of waste rubber fiber increases the probability of early initiation of corrosion in both type of concrete.

- The half cell potential of waste rubber fiber geopolymer and OPC concrete was higher than that for the control geopolymer and OPC concrete mix at the ages. More negative than -350 mV potential was recorded at 10^{th} month to 12^{th} month in rubberized geopolymer concrete whereas, In rubberized OPC concrete the potential became more negative than -350 mV at 9^{th} month to 12^{th} month.

- The drying shrinkage increased with the increase in the rubber fiber content as well as increase in time for both the cases. The increase in porosity due to rubber particles which lead to decrease the rate of shrinkage.

- The carbonation depth for any replacement level of fine aggregate by rubber fiber decreased with increase in rubber content.

- The excellent salt resistance of geopolymer concrete (both control as well as rubberized) as compared to the OPC concrete (both rubberized as well as geopolymer).

7.2.4 Fly ash based Geopolymer Mortar Performance

Conclusions from Compressive Strength Tests

- NaOH helps the dissolution of fly ash and its dissolution into the mortar matrix. Higher concentrations of NaOH lead to the formation of a gel that increases the compressive strength.

- The influence of the aggregate to binder ratio was investigated, and the optimum ratio for maximum compressive strength was identified. In the present study,

an aggregate to binder ratio of 2:1 was found to be optimal, as this ensures suitable compactness of the mortar, as evident from the porosity values.

- The porosity and water absorption capacity of the geopolymer mortar was found to be dependent on the curing temperature and aggregate-binder ratio. Further, the porosity and compressive strength of the geopolymer mortar were found to be interlinked. Their relationship can be described by an empirical equation.

Conclusions from Carbonation of the Geopolymer Mortar

- The carbonation depth was found to increase at lower curing temperatures. This highlights the importance of the curing temperature to arrest the possible degradation of mortar when subjected to carbonation, which in turn influences the long-term performance of the mortar.

- Similarly, an aggregate-binder ratio of 2:1 was found to give the best performance against carbonation. This indicates the importance of an appropriate mix composition to ascertain the performance of geopolymer mortar.

Conclusions from XRD and SEM Analysis

- Diffractograms of the various mortar mixtures provide information about the crystals formed during geopolymerization of the mortar. The crystals formed during this process are sodalite, mullite, magnetite, hematite, zeolite, and feldspar.

- Similarly, during carbonation, a visible change in morphology was observed, with the addition of nahcolite crystals.

- SEM indicate the presence of unreacted fly ash particles was observed in some of the samples. This indicates an insufficient concentration of NaOH to dissolve all of the fly ash.

7.2.5 Geopolymer Composites Performance against Sea Sand and Sea Water

- The replacement of 0%, 10%, 20% and 30% of fly ash with rice husk ash in geopolymer mortar resulted in higher 7 day compressive strength than the 28 day compressive strength of corresponding conventional H1-type cement mortar, i.e. 10 MPa. This verifies the high and early strength gain of geopolymer mortars; hence, geopolymer-based mortar should be used in construction works where speed is important.

- Of all the mixes, the 10% replacement of fly ash with rice husk ash gave the best performance, as it not only makes sustainable use of waste rice husk ash, but also increases the compressive strength as compared to regular fly ash-based mortar or any other percentage replacement.

- Geopolymer mortar performs satisfactorily when made with saline material such as sea water instead of normal water, sea sand instead of river sand, or both sea sand and sea water instead of river sand and normal water. In all combinations, the resulting 7 day compressive strength was again higher than the 28 day compressive strength of corresponding conventional H1-type OPC mortar (10 MPa).

7.2.6 Thermal Properties

- Elevated temperatures had a similar effect on both the control and rubberized geopolymer concrete.

- The strength of the control and rubberized geopolymer decreased after thermal exposure of up to 600°C, but increased at higher temperatures.

- Hairline cracks were observed in rubberized geopolymer concrete after exposure to temperatures in excess of 600°C.

- At elevated temperatures, N-A-S-H (alumina silicate) formed in both the control and rubberized geopolymer concrete. Zeolite formed as a secondary reaction

product in both concretes, before converting into hydro-sodalite ($Na_4Al_3Si_3O_{12}OH$) at elevated temperatures. The zeolite then underwent recrystallization as nepheline ($NaAlSiO_4$) and albite ($NaAlSiO_8$), similar to a hydrous alumina silicate, after exposure at 600°C and 800°C.

- The FTIR signature of both types of geopolymer concrete showed minor changes in the region around 1049 cm^{-1} and 777 cm^{-1}, suggesting that both types of geopolymer concrete have good heat resistance.

7.3 Recommendations

- The packing density method could be used to reduce the porosity of geopolymer concrete.
- Geopolymer concrete may be used for reinforced cement concrete structures.
- Detailed microstructure studies should be conducted to identify the changes that occur in geopolymer concrete.
- Fly ash or slag can be replaced by other source materials, i.e. rice husk ash, silica fume, metakeoline or a combination of different source materials.
- Investigations should be carried out on different alkaline activators with different molarities.
- The strength of geopolymer concrete could be investigated by employing different curing methods.

Appendix A

Publications

a. Luhar S.B., Chaudhary S., Dave U.V., *Effect of different parameters on the compressive strength of rubberized geopolymer concrete*, Proceedings of the 5th Nirma University International Conference on Engineering, Nirma University, Ahmedabad, 26-28 November 2015, CRC Press, Pp:77-86.

b. Luhar S.B., Chaudhary S., *Effect of Elevated Temperatures on Rubberized Geopolymer Mortar*, Proceedings of the International Conference on Recent Innovations in Engineering and Technology, Gandhi Institute of Engineering and Technology Odisha, 05-06 November 2016, Pp:79-86.

c. Luhar S.B., Chaudhary S., Dave U.V., *Effect of Different Type of Curing On Fly Ash and Slag Based Geopolymer Concrete*, Proceedings of the International Conference on Recent Innovations in Engineering and Technology, Gandhi Institute of Engineering and Technology Odisha, 05-06 November 2016, Pp:69-78.

d. Luhar S.B., Chaudhary S., *Strength and Carbonation Study on Fly Ash Based Geopolymer Mortar*, Proceedings of the 7th International Conference of Asian Concrete Federation Vietnam, 30 October-02 November 2016.

e. Luhar S.B., Chaudhary S., Dave U.V., *A brief review on geopolymer concrete*, Proceedings of the 5th Nirma University International Conference on Engineering, Nirma University, Ahmedabad, 26-28 November 2015.

References

[1] Mehta P.K., *Concrete: Microstructure, Properties, And Materials* , McGraw Hill Education, New York, 2014.

[2] Akan M.A., Dhavale D.G., Sarkis J., *Greenhouse gas emissions in the construction industry: An analysis and evaluation of a concrete supply chain*, Journal of Cleaner Production , 2017, Pp:1195-207.

[3] Singh G., *Strength and Durability Studies of Concrete Waste Foundry Sand*, Department of civil engineering, Thapar university, Panjab, India, 2012.

[4] Cement production Worldwide Page [Internet], www.statisa.com.

[5] Cement production in India Page [Internet], www.statisa.com.

[6] Wallah S.E., Rangan B.V., *Low-calcium fly ash-based geopolymer concrete: Long term properties, Reserch Report GC3*, Faculty of engineering, Curtain university, perth, Australia, 2006.

[7] Talha M.J., *Properties of ambient cured blended alkali activated cement concrete* , Materials Science and Engineering, 2017, Pp:1-10.

[8] Provis J.L, Deventer V., *Geopolymer- Structures, Processing, Properties and Industrial Applications*, Woodhead Publishing , Australia, 2009.

[9] Davidovits J., *Global Warming effect on cement and aggregate industries*, Worlds resource review, Vol. 6, 1994, Pp:263-278.

[10] Nanthagopalan P., Santhanam M., *Fresh and hardened properties of self-compacting concrete produced with Manufactured sand*, Cement and Concrete Composites, Vol. 33, 2011 , Pp:353-358.

[11] Xie Z., Xi Y., *Hardening Mechanism of an Alkaline-Activated Class F Fly Ash* , Cement and Concrete Research, Vol.31, 2001, Pp:1245-1249.

[12] Palomo, A., Grutzeck M.V., Blanco M.T., *Alkali-Activated Fly Ashes, A Cement for the Future*, Cement and Concrete Research, Vol.29, 1999 ,Pp 1323-1329.

[13] Zosin, A. P., Priimak, T. I., Avsaragov, K. B., *Geopolymer materials based on magnesia-iron slags for normalization and storage of radioactive wastes*, Atomic Energy, 85, 1998, 510-514.

[14] Malhotra V.M., *Making concrte greener with fly ash*, ACI concrete International, 21, 1999, Pp:61-66.

[15] ACI Committee Report 232, *Use of fly ash in concrete*, 1996 , ACI 232.2R-96.

[16] Bhanumathidas N, Kalidas N, *Fly ash for sustainable development*, Ark Communications, Chennai.

[17] Sumajouw D. J. ,Hardjito D,Wallah S.E. *Fly ash-based geopolymer concrete: study of slender reinforced columns*, Journal of Material Science, 2007, Pp:3124-3130.

[18] Disposal of fly ash at site page [Internet], www.downtoearth.org.in.

[19] Davidovits J., *Geopolymer Chemistry and Applications*, Geopolymer Institute, 2008.

[20] Mustafa A., Kamarudin A.M., H., Bnhussain M., Khairul N., Rafiza A.R., Zarina, Y., *Microstructure of different NaOH molarity of fly ash-based green polymeric cement*, J. Eng. Technol. Res. 2011, Pp:4449.

[21] Davidovits J., *Environmentally Driven Geopolymer Cement Applications*, Geopolymer Conference, Melbourne, Australia, 2002.

[22] Davidovits J., *Global warming Impact on the cement and aggregate industries*, World Resource Review, 1994, Pp:263-278.

[23] Davidovits J., *Properties of geopolymer cements*, First international conferance on alkaline cements and concretes, Ukrain, 1994, Pp:131-149.

[24] Davidovits, J., *Soft Mineralurgy and Geopolymers*, The Geopolymer 88, First European Conference on Soft Mineralurgy, Compiegne, France, 1988.

[25] Davidovits, J.,*Geopolymer Chemistry and Properties*, The Geopolymer 88, First European Conference on Soft Mineralurgy, Compiegne, France, 1988.

[26] Davidovits, J., *Geopolymers: Inorganic Polymeric New Materials*, Journal of Thermal Analysis, 1991, Pp:1633-1656.

[27] Jaarsveld V., Deventer V., Lukey, G. C., *The effect of composition and temperature on the properties of fly ash- and kaolinite-based geopolymers*, Chemical Engineering Journal, 2002, Pp:63-73.

[28] Chanh N.V., Trung D.B., Tuan D.V.,*Recent Research Geopolymer Concrete*, The 3rd ACF international conferance,Vietnam, 2008.

[29] Davidovits, J., *Geopolymers of the First Generation: SILIFACE-Process*, The Geopolymer 88, First European Conference on Soft Mineralurgy, Compiegne, France, 1988.

[30] Davidovits, J., *Geopolymeric Reactions in Archaeological Cements and in Modern Blended Cements*, The Geopolymer 88, First European Conference on Soft Mineralurgy, Compiegne, France, 1988.

[31] Barbosa V.F., MacKenzie K.J.,Thaumaturgo C., *Synthesis and characterisation of materials based on inorganic polymers of alumina and silica: sodium polysialate polymers*, International Journal of Inorganic Materials, 2000, Pp:309-317.

[32] Xu H., Deventer, J. S., *The geopolymerisation of alumino-silicate minerals*,International Journal of Mineral Processing, 2000, Pp:247-266.

[33] Jaarsveld V., Deventer V., Lorenzen, L., *The potential use of geopolymeric materials to immobilise toxic metals: Part I. Theory and applications*, Minerals Engineering, 1997, Pp:659-669.

[34] Palomo A., Grutzeck M.,Blanco M.T. *Alkali-activated fly ashes A cement for the future*, Cement And Concrete Research, 1999, Pp:1323-1329.

[35] Cheng T. W., Chiu, J. P., *Fire-resistant geopolymer produced by granulated blast furnace slag*, Minerals Engineering, 2003, Pp:205-210.

[36] Fernndez A., Palomo, A., *Characterisation of fly ashes Potential reactivity as alkaline cements*, Fuel, 2003 , 2259-2265.

[37] Gourley, J. T., *Geopolymers; Opportunities for Environmentally Friendly Construction Materials* Conference: Adaptive Materials for a Modern Society, Sydney, 2003.

[38] Davidovits, J. , *Geopolymers Inorganic polymeric new materials*, Journal of Thermal Analysis, 1991, Pp:1633-1656.

[39] Wallah S.E., Rangan B.V., *Low-calcium fly ash-based geopolymer concrete: Long term properties*, Curtain university, perth, Australia, 2006.

[40] Abdullah. M, Hussin.K, Bnhussain M.,Ismail N., Ibrahim W., *Mechanism and Chemical Reaction of Fly Ash Geopolymer Cement- A Review*, International Journal of Pure and Applied Sciences and Technology, 2011, Pp:35-44

[41] Comrie D., Paterson, J., Ritchey D., *Geopolymer Technologies in Toxic Waste Management*, The Geopolymer 88, First European Conference on Soft Mineralurgy, Compiegne, France, 1988.

[42] Balaguru P., Kurtz S., Rudolph J, *Geopolymer for Repair and Rehabilitation of Reinforced Concrete Beams*, The Geopolymer Institute, 2002.

[43] Gourley, J. T. , *Geopolymers; Opportunities for Environmentally Friendly Construction Materials*, The Materials 2003 Conference: Adaptive Materials for a Modern Society, Sydney,2003.

[44] Gourley J. T., Johnson G. B., *Developments in Geopolymer Precast Concrete*, The International Workshop on Geopolymers and Geopolymer Concrete, Perth, Australia ,2005.

[45] Davidovits, J., *30 years of successes and failures in geopolymer applications.* Market trends and potential breakthroughs. In proceedings of Geopolymer 2002 Conference, October 28-29, Melbourne, Australia, 2002.

[46] *Report on scrap the market USA*, Rubber manufactures association 2005.

[47] Evans J.J, *Rubber Tire Leachates in the Aquatic Environment*, Reviews of Environmental Contamination and Toxicology, Springer New York, 1997.

[48] Atul A.P., Yogesh M. B.,Patil D.Y., Amol A. W., Jitendra D. D.,*Comprehensive Literature Review on use of Waste Tyres Rubber in Flexible Road Pavement*,International Journal of Engineering Research and Technology, 2015, Pp:685-689.

[49] Rubber tire waste at site page [Internet], www.minipakr.com.

[50] Luhar S., *Fly Ash and Slag Based Geopolymer Concrete: Experimental Facts*, LAP Lambert Academic Publishing, 2016.

[51] Zaher K. K., Fouad M. B., *Rubberized Portland Cement Concrete*, Journal of Materials in Civil Engineering, 1999, Pp:206-13.

[52] Guneyisi E., Gesoglu M., Ozturan T., *Properties of rubberized concretes containing silica fume, Cement and Concrete Research*, 2004, Pp:2309-2317.

[53] Reda T., Dieb A. S., Wahab M. A., Hameed M. E., *Mechanical, fracture, and microstructural investigations of rubber concrete*, Journal of Materials in Civil Engineering, 2008 , Pp:640-649.

[54] Batayneh M., Marie I., Asi I., *Promoting the use of crumb rubber concrete in developing countries*, Waste Management, 2008, Pp:2171-2176.

[55] Son K.S., Hajirasouliha I.,Pilakoutas, K., *Strength and deformability of waste tyre rubber filled reinforced concrete columns*, Construction and Building Materials, 2011, Pp:218226.

[56] Ozbay E., Lachemi M., Sevim U.K., *Compressive strength, abrasion resistance and energy absorption capacity of rubberized concretes with and without slag*, Material and Structures, 2011, Pp:1297-1307.

[57] Grinys A., Sivilevicius H., Daukys, M., *Tyre rubber additive effect on concrete mixture strength*, Journal of civil engineering and management, 2012, Pp:393-401.

[58] Xue J.,Shinozuka M., *Rubberized concrete: A green structural material with enhanced energy-dissipation capability*, Construction and Building Materials, 2013, Pp:196-204.

[59] Onuaguluchi, Obinna, Panesar, Daman K., *Hardened properties of concrete mixtures containing pre-coated crumb rubber and silica fume*, Journal of Cleaner Production, 2014, Pp:125-131.

[60] Li G., Stubblefield M.A., Garrick G., Eggers J., Abadie C., Huang B. *Development of waste tire modified concrete*, Cement and Concrete Research, 2004, Pp:2283-2289.

[61] Ganjian E., Khorami M., Maghsoudi A.A. *Scrap tyre rubber replacement for aggregate and filler in concrete*, Construction and Building Material, 2009, Pp:1828-1836.

[62] Benazzouk A., Douzane O., Langlet T., Mezreb K., Roucoult J.M., Queneudec, M., *Physico-mechanical properties and waste absorption of cement composites containing shredded rubber wastes*, Cement and Concrete Composites, 2007, Pp:732-740.

[63] Turatsinze A.,Garros M. *On the modulus of elasticity and strain capacity of self-compacting concrete incorporation rubber aggregates*, Resources, Conservation and Recycling, 2008, Pp:1209-1215.

[64] Turki M., Ben N.I., Makni M., Rouis J., Sa K., *Mechanical and damage behaviour of mortar-rubber aggregates mixtures: experiments and simulations*, Material and Structure, 2009, Pp:1313-1324

[65] Najim, Khalid B., Hall M. R.,*Mechanical and dynamic properties of self-compacting*, Construction and Building materials, 2012, Pp: 521-530.

[66] Haolin S.,Jian Y.,Tung-Chai L.,Gurmel S. G., Samir D., *Properties of concrete prepared with waste tyre rubber particles of uniform and varying sizes*, Journal of Cleaner Production , 2015, Pp:2088-2096.

[67] Gesoglu, Mehamet, Guneyisi, Erhan, *Strength development and chloride penetration in rubberized concretes with and without silica fume*, Material and Structure, 2007, Pp:953-964.

[68] Sukontasukkul P., Chaikaew, C., *Properties of concrete pedestrian block mixed with crumb rubber*, Construction and Building Materials, 2006, Pp:450-457.

[69] Dubravka B., Ana B., Marijana S., *Durability Properties of Concrete with Recycled Waste Tyres*, International conference on durability of building materials and components, Belgium, 2017.

[70] Su H., *Properties of concrete with recycled aggregates as coarse aggregate and as-received/surface-modified rubber particles as fine aggregate in Civil Engineering*, University of Birmingham, 2015, Pp: 228.

[71] Turatsinze, A., and Garros, M., *On the modulus of elasticity and strain capacity of self-compacting concrete incorporation rubber aggregates*, Resources, Conservation and Recycling, 2008, Pp:1209-1215.

[72] Bravo, Miguel, Brito, Jorge, *Concrete made with used tyre aggregate: durability-related performance*, Journal of Cleaner Production,2012, Pp:4250.

[73] Nguyen T., Toumi A., Turatisnze A., Tazi F., *Restrained shrinkage cracking in steel fibre reinforced and rubberized cement based mortars*, Material and Structure, 2012, Pp:899-904.

[74] Sukontasukkul, Piti, Tiamlom, Koshi, *Expansion under water and drying shrinkage of rubberized concrete mixed with crumb rubber with different size*, Construction and Building Material. 2012, Pp:520-526.

[75] Yung H., Yung L. C., Hua L.,*A study of the durability properties of waste tire rubber applied to self-compacting concrete*, Constrution and Building Material, 2013, Pp:665-672.

[76] Uygunoglu, Tayfun, TopcU., Ilker B.,*The role of scrap rubber particles on the drying shrinkage and mechanical properties of self consolidating mortars*,Constrution and Building Material, 2010, Pp:1141-1150.

[77] Akhras.A, Nabil, Samadi, Mohammed M., *Properties of tire rubber ash mortar*, Cement and Concrete Composite, 2004, Pp:821-826.

[78] Dong, Qiao, Huang, Baoshan, Shu, Xiang, *Rubber modified concrete improved by chemically active coating and silane coupling agent*, Construction and Building Material, 2013, 48,Pp:116- 123.

[79] Azevedo F., Pacheco T., Jesus, C., Aguiar B., Canoes A.F.,*Properties and durability of HPC with tyre rubber wastes*, Construction and Building Material,2012, Pp:186-191.

[80] Raghvan D., Huynh H., Ferraris C.F.,*Workability, mechanical properties and chemical stability of a recycled tyre rubber-filled cementitious composites*, Journal of Material Science, 1998, Pp:1745-1752.

[81] Hardjito D., Wallah S. E., Sumajouw D. M. J., Rangan B. V. *Fly Ash Based Geopolymer Concrete*, Australian Journal of Structural Engineering, 2005(a), Pp:77-86.

[82] Lloyd N.A., Rangan B.V.,*Geopolymer Concrete with Fly Ash*, Second international conference on sustainable construction materials and technologies, Italy, 2010.

[83] Panias D., Giannopoulou I.P.,Perraki.T,*Effect of synthesis parameters on the mechanical properties of fly ash-based geopolymers*,Colloids Surfaces A: Physicochem. Eng. Aspects, 2007, Pp:246-254.

[84] Sofi M., Deventer J., Mendis .P, Lukey G. C.,*Engineering Properties of Inorganic Polymer Concretes (IPCs)*, Cement and Concrete Research, 2007, Pp:251-257.

[85] Rangan B,V., Wallah, S.E., Low Calcium fly Ash Based Geopolymer concrete: long- Term Properties, Research Report GC2, Faculty of Engineering Curtin University of Technology, Perth, 2006.

[86] Fernandez J., Palomo A. ,*Characterization of Fly Ash: Potential Reactivity Alkaline Cements*, Fuel, 2003, Pp:2259-2265.

[87] Neville, A. M.,*Properties of Concrete* (Fourth and Final ed.). Essex, England: Pearson Education, Longman Group, 2000.

[88] Hardjito D., Wallah S. E., Sumajouw D. M., Rangan B. V., *Introducing Fly Ash-Based Geopolymer Concrete: Manufacture and Engineering Properties.*, Our World in Concrete and Structures International Conference, Singapore,2005(b).

[89] Bakharev T., Durability of geopolymer materials in sodium and magnesium sulfate solutions,Cement And Concrete Research, 2005(a), Pp:1233-1246.

[90] Thokchom S, Ghosh P, Ghosh S, Performance of Fly ash Based Geopolymer Mortars in Sulphate Solution, Journal of Engineering Technology Review, 2010, Pp:36-40.

[91] Cheema D.S., Lloyd N.A., Rangan B.V., *Durability of Geopolymer Concrete Box Culverts- A Green Alternative*, Proceedings of the 34th Conference on Our World in Concrete and Structures, Singapore, 2009.

[92] David W. L.,Patnaikuni, Adam.A, Molyneaux.T, *Strength, sorptivity and carbonation of geopolymer concrete*, Challenges, Opportunities and Solutions in Structural Engineering and Construction, 2009.

[93] Anurag M., Deepika, Namrata, Manish, Nidhi and Durga, *Effect of concentration of alkaline liquid and Curing time on strength and water absorption Of geopolymer concrete*, ARPN journal of engineering and applied science, 2008, Pp:14-18.

[94] Song, S., Jennings H. M.,*Pore solution chemistry of alkali-activated ground granulated blast-furnace slag*, Cement and Concrete Research,1999, Pp:159-170.

[95] Sathia R, Babu K.G., Santhanam M, *Durability study of low calcium fly ash geopolymer concrete*, The 3rd ACF International Coference ACF, Vietenam,

[96] Bakharev T., Sanjayan J. G., Cheng, J. B., *Resistance of alkali-activated slag concrete to acid attack*, Cement and Concrete Research, 2003, Pp:1607-1611.

[97] Song X. J., Marosszeky M. M., Munn R., *Durability of fly ash-based Geopolymer concrete against sulphuric acid attack*, International Conference on Durability of Building Materials and Components, Lyon, France, 2005.

[98] Roy, D. M., *Alkali-activated cements Opportunities and Challenges*, Cement and Concrete Research, 1999, Pp:249-254.

[99] Olivia, M., Nikraz, H.R., *Corrosion performance of embedded steel in fly ash geopolymer concrete by impressed voltage method*, Sustainable practice in mechanics of structures and materials, 2011.

[100] Rashad A.M, Zeedan S.R., *The effect of activator concentration on the residual compressive strength of alkali- activated fly ash paste subjected to thermal load*, Construction and Building Materials, 2011, Pp:3098-3107.

[101] Kong D.L.Y.,Sanjayan J.G., *Damage behavior of geopolymercomposites exposed to elevated temperatures*, Cement and Concrete Composites, 2008, Pp:986-991.

[102] Kong D.L.Y.,Sanjayan J.G., *Effect of elevated temperatures on geopolymer paste, mortar and concrete*, Cement and Concrete Research, 2010, Pp:334-339.

[103] Pan.Z., Sanjayan J.G., Rangan B.V, *An investigation of the mechanisms for strength gain or loss geopolymer mortar after exposure to elevated temperature*, Journal of Material Science,2009, Pp:1873-80.

[104] Ranjbar.N, Mehrali.M, Alengaram U.J, Metselaar, Jummat M.Z, *Compressive strength and microstructural analysis of fly ash/ palm oil fuel ash based geopolymer mortar under elevated temperatures*, Construction and Building Materials, 2014, Pp:114-121.

[105] Kong D.L.Y.,Sanjayan J.G.,Crentsil K.S.,*Factors affecting the performance of metakaolingeopolymers to elevated temperatures*,Journal of Material Science, 2008, Pp:824-831.

[106] Pan.Z., Sanjayan J.G., Collins F., *Effect of transient creep on compressive strength of geopolymer concrete for elevated temperature exposure*, Cement and Concrete Research, 2014, Pp:182-189.

[107] Hussain M.W., Bhutta M.A.R, Azreen M., Ramadhansyah P.J., Mirza J., *Performance of blended ash geopolymer concrete at elevated temperature*, Materials and Structures, 2015, Pp:709-720.

[108] T Bakharev, *Thermal behavior of geopolymers prepared using class F fly ash and elevated temperature curing*, Cement and Concrete Research, 2006, Pp:1134-1147.

[109] Omar A.A, Bakri A.M, Kamarudin H., Nizar I.K., Saif A.A., *Effect of elevated temperatures on the thermal behaviour and mechanical performance of fly ash geopolymer paste, mortar and lightweight concrete*, Construction and Building Materials, 2014, Pp:377-387.

[110] Zhang Y, Sun W, Li Z, *Infrared spectroscopy study of structural nature of geopolymeric products*, J. Wuhan Univ. Technol, 2008, Pp:522527.

[111] Shinde B.H.,Kadam K.N, *Strength properties of fly ash based geopolymer concrete with sea sand* , American journal of engineering research , 2016, Pp:129-132.

[112] Khan M. A., Padmakaran.P, Amritphale S. D., *Potential Application of Sea Sand and Sea Water as Advanced Geopolymeric Material: Novel Initiative of the Millennium*, India international science festival, 2015.

[113] Limbra J., Etxeberria M., Agullo L.,Molina D., *Mechanical and Durability properties of concrete made with dredged marine sand*, Construction and building materials, 2011, Pp:4167-4174,

[114] Karthikeyan M., Nagarajan.V, *Chloride analysis of sea sand for making concrete*, National Academy Science Letters, 2016.

[115] Karthikeyan M., Nagarajan V., *Feasibility study on utilization of marine sand in concrete for sustainable development*, Indian journal of Geo marine sciences,2016, Pp:313-318.

[116] Liu W., Cui H., Dong Z., Xing F., Zhang H.,Lo T.Y., *carbonation of concrete made with dredged marine sand and its effect on chloride binding*, Construction and Building Matetials, 2016, Pp:1-9.

[117] Katano K., Takeda N.F., Ishizeki Y., Iriya K., *Properties and Application of Concrete Made with Sea Water and Un-washed Sea Sand*, Third International conference on Sustainable Construction Materials and Technology, Obayashi Corporation, Japan, 2013.

[118] Ming C., Mao J.Z., Guang D., Ben L., *Experimental study on mechanical properties of marine sand and sea water concrete*, International conference on mechanics and civil engineering ,2014.

[119] Hunguang Y., Yan L., Henglin L., Quan G., *Durablity of Sea sand containing concrete: effects of chloride ion penetration*, Mining science and Technology, 2011, Pp:123-127.

[120] Nishida T., Otsuki N., Ohara H., Garba Z.M., Nagata T., *Some considerations for the applicability of sea water as mixing water in concrete*, 3rd international conference Sustainable construction materials and technologies,Japan, 2013.

[121] Mohammed T.U., Hamada H., Yamaji T., *Performance of sea water mixed concrete in the tidal environment*, Cement and concrete research, 2004, Pp:593-601.

[122] Sun W., Liu J., Dai Y., Yan,J, *Study on the influence of chloride ions content on the sea sand concrete performance*, American journal of civil engineering, 2016, Pp:50-54.

[123] Olivia M., Nikraz H., *Properties of fly ash geopolymer concrete designed by Taguchi method*, Material and Design, 2012, Pp:191198.

[124] Nazari A. *Compressive strength of geopolymers produced by ordinary Portland cement: Application of genetic programming for design*,Materials and Design, 2013, Pp:356-366.

[125] Nazari A., Khanmohammadi H., Amini M., Hajiallahyari H., Rahimi A., *Production geopolymers by Portland cement: Designing the main parameters effects on compressive strength by Taguchi method*, Material and Design, 2012, Pp:41-49.

[126] Mijarsh M. J. A., Johari M. A. M., Ahmad Z. A., *Synthesis of geopolymer from large amounts of treated palm oil fuel ash: Application of the Taguchi method in investigating the main parameters affecting compressive strength*, Construction and Building Materials, 2014, Pp:473-481.

[127] Bagheri A., Nazari A., *Compressive strength of high strength class C fly ash-based geopolymers with reactive granulated blast furnace slag aggregates designed by Taguchi method*, Materials and Design, 2014, Pp:480-490.

[128] Richi S., Nazari A., Zaarei D., Khalaj G., Bohlooli H., Kaykha M. M., *Compressive strength of ash-based geopolymers at early ages designed by Taguchi method*, Materials and Design, 2012, Pp:443-449.

[129] IS: 3812-1981, *Specification for fly ash for use as pozzolana and admixture*, Bureau of Indian Standards, New Delhi, 1981.

[130] ASTM C618-03, *Standard Specification for Coal Fly Ash and Raw or Calcined Natural Pozzolan for Use in Concrete*, 2003.

[131] IS: 2386-1963, *Methods of test for aggregate for concrete*, Bureau of Indian Standards, New Delhi, 1963.

[132] IS: 383-1970, *Specification for Coarse and Fine aggregate from natural sources for concrete*, Bureau of Indian Standards, New Delhi, 1970.

[133] IS 4031(Part 6):1988, *Methods of physical tests for hydraulic cement: Part 6 Determination of compressive strength of hydraulic cement*,Bureau of Indian Standards, New Delhi, 1988.

[134] IS 1199: 1959, *Methods of sampling and analysis of concrete*, Bureau of Indian Standards, New Delhi, 1959.

[135] IS: 516- 1959, *Methods of tests for strength of concrete*, Bureau of Indian Standards, New Delhi, 1959.

[136] IS: 5816-1999, *Splitting tensile strength of concrete method of test*, Bureau of Indian Standards, New Delhi, 1999.

[137] ASTM C1583 - 04, *Standard Test Method for Tensile Strength of Concrete Surfaces and the Bond Strength or Tensile Strength of Concrete Repair and Overlay Materials by Direct Tension (Pull-off Method)*, 2004.

[138] DIN 1048, *Testing Concrete. Water Permeability, Part 5*, Section 36, German Standards, 1991.

[139] ASTM C1585 - 04, *Standard Test Method for Measurement of Rate of Absorption of Water by Hydraulic-Cement Concretes*,2004.

[140] RILEM Committee TC56, *Measurement of hardened concrete carbonation depth -CPC 18*, Materials and Structures, 1988, Pp:453-455.

[141] ASTM G109 - 07, *Standard Test Method for Determining Effects of Chemical Admixtures on Corrosion of Embedded Steel Reinforcement in Concrete Exposed to Chloride Environments*, 2013.

[142] ASTM C876 - 15, *Standard Test Method for Corrosion Potentials of Uncoated Reinforcing Steel in Concrete*, 2015.

[143] ASTM C1556 - 11,Standard Test Method for Determining the Apparent Chloride Diffusion Coefficient of Cementitious Mixtures by Bulk Diffusion, 2016.

[144] IS- 1237:2012, *Cement Concrete Flooring Tiles - Specification* ,Bureau of Indian Standards, New Delhi, 2012.

[145] Roy, R., *A primer on the Taguchi method*, Society of Manufacturing Engineering, New York, USA, 2009.

[146] IS 10262- 2009, *concrete mix proportioning - guidelines*, Bureau of Indian Standards, New Delhi, 2009.

[147] Rangan B.V., *Mix design and production of fly ash based geopolymer concrete*, Indian Concr Journal, 2008, Pp:7-15.

[148] Provis J.L.,Deventer J.S.J., *Geopolymers, structure, processing, properties and industrial applications*, Oxford: Woodhead Publishing Limited; 2009.

[149] Fernandez J.A., Palomo A., Lopez H.C.,*E*ngineering properties of alkali-activated fly ash concrete, ACI Materials Journal. 2006, Pp:106-112.

[150] Shetty M.S., *Concrete Technology: Theory and Practice*, S. Chand, 2008.

[151] Olivia M., *Durability Related Properties of Low Calcium Fly Ash Based Geopolymer Concrete*,Curtin University of Technology, 2011.

[152] Sofi M., Deventer J.S.J, Mendis P.A, Lukey G.C., *Engineering properties of inorganic polymer concretes (IPCs)*, Cement and Concrete Research. 2007, Pp:251-257.

[153] Lee W.K.W, Deventer J.S.J., *The interface between natural siliceous aggregates and geopolymers*, Cement and Concrete Research, 2004, Pp:195-206.

[154] Pacheco T.F., Castro G.J., Jalali S., *Investigations about the effect of aggregates on strength and microstructure of geopolymeric mine waste mud binders*, Cement and Concrete Research, 2007, Pp:933-941.

[155] Vicroads, *Test methods for the assessment of durability of concrete- Technical Note*, [Internet]. Melbourne: Vicroads; 2007.

[156] Papworth F., Grace W., *Designing for concrete durability in marine environs*, Concrete 85 Conference: The Performance of Concrete and Masonry Structures ,Brisbane, 1985.

[157] Olivia M., *Durability Related Properties of Low Calcium Fly Ash Based Geopolymer Concrete*,Curtin University of Technology, 2011.

[158] Bakharev T., *Durability of geopolymer materials in sodium and magnesium sulfate solutions*, Cement and Concrete Research, 2005, Pp:1233-1246.

[159] Rilem Technical Committee 32-RCA, *Seawater attack on concrete and precautionary measures*, Materials and Structures, 1985, Pp:223-226.

[160] Tikalsky P. J., Carrasquillo, R. L., *Influence of Fly Ash on the Sulfate Resistance of Concrete*, ACI Materials Journal, 1992, Pp:69-75.

[161] Lea F. M., Hewlett P. C., *The Chemistry of Cement and Concrete*, Edward Arnold, London, 1970.

[162] Neville A. M., Dilger W. H., Brooks J. J., *Creep of plain and structural concrete*, Construction Press, Loandon, 1983.

[163] Reda T. M., El-Dieb A.S., Wahab M.E., Abdel H., *Mechanical, fracture and micro structural investigations of rubber concrete*, Journal of Materials in Civil Engineering, 2008,Pp:640-649.

[164] Guneyisi E., Gesoglu M., Ozturan T., *Properties of rubberized concretes containing silica fume*, Cement and Concrete Research, 2004, Pp:2309-2317.

[165] Gupta T., Chaudhary S., Sharma R.K., *Mechanical and durability properties of waste rubber fibre concrete with and without silica fume*, Journal of Cleaner Production, 2016, Pp:702-711.

[166] Khaloo A.R., Dehestani M., Rahmatabadi P., *Mechanical properties ofconcrete containing a high volume of tire-rubber particle*, Waste Management, 2008, Pp:2472-2482.

[167] Yilmaz A., Degirmenci N., *Possibility of using waste tire rubber and fly ash with Portland cement as construction materials*, Waste Management, 2009, Pp:1541-1546.

[168] Benazzouk A., Mezreb K., Doyen G.,Goullieux A., Queneudec M., *Effect of rubber aggregates on the physico-mechanical behavior of cementrubber composites-influence of the alveolar texture of rubber aggregates*, Cement and Concrete Composites, 2003, Pp:711720.

[169] Wong S.F., Ting S.K., *Use of recycled rubber tires in normal-and high-strength concretes*, ACI Materials Journal, 2009, Pp:325-332.

[170] Khatib Z.K., Bayomy F.M., *Rubberized Portland cement concrete*, Journal of materials in civil engineering, 1999, Pp:206-213.

[171] Eldin N.N., Senouci A.B., *Rubber-tire particles as concrete aggregate*, Journal of materials in civil engineering, 1993, Pp:478-496.

[172] Gupta T., Siddique S., Sharma R.K., Chaudhary S., *Effect of elevated temperature and cooling regimes on mechanical and durability properties of concrete containing waste rubber fibre*, Construction and Building Materials, 2017, Pp:35-45.

[173] Marques A.M., Correia J.R., Brito J., *Post-fire residual mechanical propertiesof concrete made with recycled rubber aggregate*, Fire Safety Journal, 2013, Pp:4957.

[174] Josheph B., *Behaviour of Geopolymer Concrete Exposed to Elevated Temperatures*, thesis, Cochin University of Science And Technology, Kochi, 2015.

[175] Pan Z., Sanjayan J.G., Rangan B.V., *An investigation of the mechanisms for strength gain or loss of geopolymer mortar after exposure to elevated temperature*, Journal of Material Science, 2009, Pp:1873-1880.

[176] Hussain M.W., Bhutta M.A.R., Azreen M., Ramadhansyah P.J., Mirza J., *Performance of blended ash geopolymer concrete at elevated temperature*, Materials and Structures, 2015, Pp:709-720.

[177] Rashad A.M., Zeedan S.R., *The effect of activator concentration on the residual compressive strength of alkali- activated fly ash paste subjected to thermal load*,Construction and Building Materials, 2011,Pp:3098-3107.

[178] Xin. J., Huang C., *Fire risk analysis of residential buildings based on scenario clusters and its application in fire risk management*, Fire Safety Journal, 2013, Pp:72-78.

[179] Yao D, Dai J G, Shi C J *Mechanical properties of alkali-activated concrete: A state-of-the-art review* Construction and Building Materials, Pp:68-79.

[180] Thokchom S., Ghosh P., Ghosh S., *Performance of fly ash based geopolymer mortars in sulphate solution*, Journal of Engineering Science and Technology Review,2010, Pp:36-40.

[181] Bosoga A., Masek O., Oakey, E. J.,CO_2 *Capture Technologies for Cement Industry*, Energy Procedia,2009, Pp:133-140.

[182] IS:2250 -1981, *Code Of Practice for Preparation and Use of Masonry Mortars*, Bureau of Indian Standards, New Delhi,1981.

[183] Montes F., Valavala S., Haselbach M., *A new test method for porosity measurements of Portland cement pervious concrete*, Journal of ASTM International, 2005.

[184] Mehta A., Siddique R., *Strength, permeability and micro-structural characteristics of low-calcium fly ash based geopolymers*, Construction and Building Materials, 2017, Pp:325-34.

[185] Dassekpo J.M., Zha X., Zhan J., *Synthesis reaction and compressive strength behavior of loess-fly ash based geopolymers for the development of sustainable green materials*, Construction and Building Materials, 2017, Pp:491-500.

[186] Wardhono A., Gunasekara C., Law D., Setunge S., *Comparison of long term performance between alkali activated slag and fly ash geopolymer concretes*, Construction and Building Materials, 2017, Pp:272-79.

[187] Mehta A., Siddique R., *Sulfuric acid resistance of fly ash based geopolymer concrete*, Construction and Building Materials, 2017, Pp:136-43.

[188] Karthik A., Sudalaimani K., Kumar V., *Investigation on mechanical properties of fly ash-ground granulated blast furnace slag based self curing bio-geopolymer concrete*, Construction and Building Materials, 2017, Pp:338-49.

[189] Mehta A., Siddique R. Singh B.P., Aggoun S., agd G., Hunek D.B., *Influence of various parameters on strength and absorption properties of fly ash based geopolymer concrete designed by Taguchi method*, Construction and Building Materials, 2017, Pp:817-24.

[190] Mehta A., Siddique R., *Properties of low-calcium fly ash based geopolymer concrete incorporating OPC as partial replacement of fly ash*, Construction and Building Materials, 2017, Pp:792-807.

[191] Sanjayan J.G., Nazari A., Chen L., Nguyen G.H., *Physical and mechanical properties of lightweight aerated geopolymer*, Construction and Building Materials, 2015, Pp:236-44.

[192] Wongsa A., Zaetang Y., Sata V., Chindaprasirt P.,*Properties of lightweight fly ash geopolymer concrete containing bottom ash as aggregates*, Construction and Building Materials, 2016, Pp:637-43.